



National Library
of Canada

Bibliothèque nationale
du Canada

Canadian Theses Service

Services des thèses canadiennes

Ottawa, Canada
K1A 0N4

CANADIAN THESES

THÈSES CANADIENNES

NOTICE

The quality of this microfiche is heavily dependent upon the quality of the original thesis submitted for microfilming. Every effort has been made to ensure the highest quality of reproduction possible.

If pages are missing, contact the university which granted the degree.

Some pages may have indistinct print especially if the original pages were typed with a poor typewriter ribbon or if the university sent us an inferior photocopy.

Previously copyrighted materials (journal articles, published tests, etc.) are not filmed.

Reproduction in full or in part of this film is governed by the Canadian Copyright Act, R.S.C. 1970, c. C-30. Please read the authorization forms which accompany this thesis.

AVIS

La qualité de cette microfiche dépend grandement de la qualité de la thèse soumise au microfilmage. Nous avons tout fait pour assurer une qualité supérieure de reproduction.

S'il manque des pages, veuillez communiquer avec l'université qui a conféré le grade.

La qualité d'impression de certaines pages peut laisser à désirer, surtout si les pages originales ont été dactylographiées à l'aide d'un ruban usé ou si l'université nous a fait parvenir une photocopie de qualité inférieure.

Les documents qui font déjà l'objet d'un droit d'auteur (articles de revue, examens publiés, etc.) ne sont pas microfilmés.

La reproduction, même partielle, de ce microfilm est soumise à la Loi canadienne sur le droit d'auteur, SRC 1970, c. C-30. Veuillez prendre connaissance des formules d'autorisation qui accompagnent cette thèse.

THIS DISSERTATION
HAS BEEN MICROFILMED
EXACTLY AS RECEIVED

LA THÈSE A ÉTÉ
MICROFILMÉE TELLE QUE
NOUS L'AVONS REÇUE



National Library
of Canada

Bibliothèque nationale
du Canada

0-315-24850-5

Canadian Theses Division / Division des thèses canadiennes

Ottawa, Canada
K1A 0N4

PERMISSION TO MICROFILM — AUTORISATION DE MICROFILMER

- Please print or type — Écrire en lettres moulées ou dactylographier

Full Name of Author — Nom complet de l'auteur

William Charles Swayze Pick

Date of Birth — Date de naissance

1958-01-29

Country of Birth — Lieu de naissance

CANADA

Permanent Address — Résidence fixe

2007 137 Ave
Edmonton, Alberta
T5Y 1L1

Title of Thesis — Titre de la thèse

Characterization of Pt-Ir/Alumina
Catalysts by X-ray Diffraction

University — Université

University of Alberta

Degree for which thesis was presented / Grade pour lequel cette thèse fut présentée

Master of Science

Year this degree conferred — Année d'obtention de ce grade

1984

Name of Supervisor — Nom du directeur de thèse

Dr. S.E. Wanke

Permission is hereby granted to the NATIONAL LIBRARY OF CANADA to microfilm this thesis and to lend or sell copies of the film.

The author reserves other publication rights, and neither the thesis nor extensive extracts from it may be printed or otherwise reproduced without the author's written permission.

L'autorisation est, par la présente, accordée à la BIBLIOTHÈQUE NATIONALE DU CANADA de microfilmer cette thèse et de prêter ou de vendre des exemplaires du film.

L'auteur se réserve les autres droits de publication; ni la thèse ni de longs extraits de celle-ci ne doivent être imprimés ou autrement reproduits sans l'autorisation écrite de l'auteur.

Date

October 11 / 1984

Signature

William C. Pick

THE UNIVERSITY OF ALBERTA

Characterization of Pt-Ir/Alumina Catalysts by X-ray
Diffraction

by



William C.S. Pick

A THESIS

SUBMITTED TO THE FACULTY OF GRADUATE STUDIES AND RESEARCH
IN PARTIAL FULFILMENT OF THE REQUIREMENTS FOR THE DEGREE
OF MASTER OF SCIENCE

Department of Chemical Engineering

EDMONTON, ALBERTA

Fall 1984

THE UNIVERSITY OF ALBERTA

RELEASE FORM

NAME OF AUTHOR William C.S. Pick
TITLE OF THESIS Characterization of Pt-Ir/Alumina
Catalysts by X-ray Diffraction
DEGREE FOR WHICH THESIS WAS PRESENTED MASTER OF SCIENCE
YEAR THIS DEGREE GRANTED Fall 1984

Permission is hereby granted to THE UNIVERSITY OF ALBERTA LIBRARY to reproduce single copies of this thesis and to lend or sell such copies for private, scholarly or scientific research purposes only.

The author reserves other publication rights, and neither the thesis nor extensive extracts from it may be printed or otherwise reproduced without the author's written permission.

(SIGNED)

William C. Pick

PERMANENT ADDRESS:

2007 139 Ave
Edmonton, Alberta
T5Y 1L1

DATED October 9 1984

THE UNIVERSITY OF ALBERTA
FACULTY OF GRADUATE STUDIES AND RESEARCH

The undersigned certify that they have read, and recommend to the Faculty of Graduate Studies and Research, for acceptance, a thesis entitled Characterization of Pt-Ir/Alumina Catalysts by X-ray Diffraction submitted by William C.S. Pick in partial fulfilment of the requirements for the degree of Master of Science.

Richard E. Utter
.....

Supervisor

David T. Lynch
.....

Reg. Eade
.....

Date *October 9, 1984*
.....

ABSTRACT

In this work, several new X-ray diffraction (XRD) techniques were developed to study the metal crystallites supported on non-amorphous materials. The purpose of this study was to determine the effect of atmosphere and heat treatment on supported metal catalysts. Properties studied were phases present, average crystallite size, and particle size distributions. XRD patterns were measured for alumina supported 1 and 4 wt. % Pt, 1 wt. % Ir, and 1% Pt-1% Ir. Methods were developed to analyze XRD patterns.

A new numerical technique involving point-by-point subtraction of a weighted support profile from the catalyst profile allowed detailed analysis of the metal crystallites on the alumina. Due to relatively large noise-to-signal ratio in many of the profiles, a new profile fitting function was developed. This technique was numerically shown to accurately represent the input data for continuous length distribution functions. Numerical techniques were also used to show that the lower limits of reliable crystallite detection, using both the Scherrer and Fourier analysis, correspond roughly to 2 nm particles. It is possible to obtain information about particles below this size, but the accuracy is significantly reduced. Complex interactions between the particle shape and particle size in the observed X-ray profiles makes determination of reliable crystallite size distributions difficult.

It was shown that the area weighted average crystallite length determined by Fourier analysis of X-ray peaks is correlated to particle diameter determined by chemisorption. It is probable that the stoichiometry of absorption is slightly greater than $H/M=1.0$, but owing to the relationship between particle shape and size distribution in the observed profile a unique determination of the stoichiometry is not possible. Perhaps the most valuable information which was obtained using the techniques developed here is the semi-quantitative analysis of the metal profiles of the bimetallic catalyst. Significant differences in crystal structure result from treatments in different atmospheres. Oxygen treatment at elevated temperatures causes separation of the two (Pt and Ir) phases while hydrogen treatment does not. Crystallite growth is much more rapid in oxygen than in hydrogen.

Table of Contents

Chapter	Page
1. INTRODUCTION	1
2. LITERATURE SURVEY	5
2.1 Introduction	5
2.2 Techniques of Study	6
2.3 Previous Studies of Metal Crystallites in Catalysis	9
2.4 X-ray Diffraction	14
3. X-RAY DIFFRACTION THEORY	16
3.1 Introduction	16
3.2 X-ray Diffraction Peak Intensities	17
3.3 Peak Broadening	23
3.3.1 Instrumental Broadening	24
3.3.2 Size-Shape Broadening	27
3.3.3 Strain Broadening	30
3.4 Fourier Techniques	32
3.4.1 Principles	32
3.4.2 Length Distributions from Fourier Coefficients	37
3.4.3 Numerical Techniques in Fourier Analysis	43
4. NUMERICAL STUDIES	50
4.1 Introduction	50
4.2 Pure Profiles	51
4.3 Observed Profiles	59
4.4 Conclusions from the Numerical Study	66
5. EXPERIMENTAL	68
5.1 Catalyst Heat Treatment	69

5.2	Sample Preparation	72
5.3	X-ray Diffraction	73
5.4	The Standard Sample	74
6.	DATA ANALYSIS	76
6.1	Removing the Support Profiles	76
6.2	Angle Dependent Factors	79
6.3	Fraction of Metal Detected	80
6.4	Error Analysis	83
6.5	Limits of Detectability	90
7.	RESULTS	95
7.1	Introduction	95
7.2	Phase Studies	95
7.3	Strain-Shape Effects	99
7.4	Particle Size	104
7.5	The Length Distribution Function	108
7.6	Summary of Results	111
8.	CONCLUSIONS	113
8.1	Future Work	114
9.	NOMENCLATURE	116
10.	REFERENCES	124
11.	APPENDIX A: Plots of Raw Data	127
12.	APPENDIX B: Catalyst Analyses	139
12.1	Program RXRAY	166
12.1.1	User Documentation	166
12.1.2	FORTTRAN Program RXRAY	168
12.2	Program XRM D	170
12.2.1	User Documentation	170

12.2.2	FORTTRAN Program XRMD	173
12.3	Program XRDAV	176
12.3.1	User Documentation	176
12.3.2	FORTTRAN Program XRDAV	178
12.4	Program XINTG	180
12.4.1	User Documentation	180
12.4.2	FORTTRAN Program XINTG	184
12.5	Program XFIT	187
12.5.1	User Documentation	187
12.5.2	FORTTRAN Program XFIT	193
12.6	Program XPROF	197
12.7	Program XPURE	200
12.8	Program XNUMT	206
12.9	Program XFOR	210
12.10	Program XNOIS	211
12.11	Program XLDFE	213
12.12	Subroutines Used	214
12.12.1	Subroutine PEAK	215
12.12.2	Subroutine FOR	216
12.12.3	Subroutine WIND1	217
12.12.4	Subroutine ALIGN	218
12.12.5	Subroutine CNTRD	219
12.12.6	Subroutine RREAD	220
12.12.7	Subroutine INIT	221
12.12.8	Subroutine MACHP	222

12.12.9	Subroutine ALINE	223
12.12.10	Subroutine NEWPK	225
12.12.11	Subroutine DETLO	226
12.12.12	Subroutine VOLDF	227
12.12.13	Subroutine ARADF	229
12.12.14	Subroutine SAVE1	231
12.12.15	Subroutine NEWX	233
12.12.16	Subroutine FIT	234
12.12.17	Subroutine BSOLV	237
12.12.18	Subroutine FUNC	241
12.12.19	Subroutine DIST	242
12.12.20	Subroutine PROF	245
12.12.21	Subroutine ESTB	246
12.12.22	Subroutine READP	249
12.12.23	Subroutine NURNG	250

List of Tables

Table	Page
4.1 Accuracy of Several Methods of Determining Average Length from Numerically Generated Pure X-ray Profiles of Dirac Delta Type Length Distribution Functions	54
4.2 The Effect of Broadening the Length Distribution Function on the Accuracy of Several Methods of Determining Average Length from Pure XRD Profiles	55
4.3 The Accuracy of Various Methods of Measuring the Average Length for Several Continuous Input Length Distribution Functions	56
4.4 A Comparison of Different Methods of Correcting Observed Profiles for Instrument Broadening	61
4.5 Average Lengths Calculated from Complete Fourier Analysis of XRD Peaks Compared to the Input Average Lengths	66
5.1 Supports Studied	69
5.2 Bimetallic Catalysts Studied	70
5.3 Monometallic Catalysts Studied	71
6.1 Determination of Parameter 'Y' in Equation 6-1	83
7.1 Size-Strain Analysis of Catalyst HP-3	102
7.2 Average Crystallite Sizes for 1% Ir/Alumina Catalysts	105
7.3 Average Crystallite Sizes for Monometallic Pt/Alumina Catalysts	106

List of Figures

Figure	Page
3.1 Graphical Determination of $\langle La \rangle$	36
4.1 Pure XRD Profiles for Different VLDF's	52
4.2 Fourier Analysis of a Numerically Generated Pure XRD Profile	58
4.3 Fourier Analysis of a Numerically Generated XRD Profile For a Log-Normal Volume Weighted Length Distribution Function	63
4.4 Fourier Analysis of a Numerically Generated XRD Profile for a Linear VLDF	64
4.5 Fourier Analysis of a Numerically Generated XRD Profile for an Input VLDF of Unisized Spherical Crystallites	65
6.1 Three Typical X-ray Diffraction Patterns	77
6.2 A Comparison of Random Noise to Observed Noise	85
6.3 Auto-correlation Coefficients of Random and Observed Noise	86
6.4 Effect of Sample Packing on XRD Noise	87
6.5 Effect of Heat Treatment on the Support XRD Pattern	89
6.6 Analysis of Typical XRD Peak	94
7.1 Influence of Heat Treatment in a Reducing Atmosphere on the Bimetallic Pt-Ir/Alon Catalyst	96
7.2 Influence of Heat Treatment in an Oxidizing Atmosphere (Followed by Reduction) on the Bimetallic Pt-Ir/Alon Catalyst	98
7.3 Influence of Heat Treatment in an Oxidizing Atmosphere (Without Reduction) on the Bimetallic Pt-Ir/Alon Catalyst	100
7.4 Strain-Shape Analysis of Catalyst HP-3	103

Figure		Page
7.5	Comparison of D _p with <La>	107
7.6	Area and Volume Weighted LDF's for Catalyst HP-3	110
11.1	Support Profiles	128
11.2	Profiles of 4% Pt/Alon Catalysts	129
11.3	Profiles of 1% Pt+1% Ir/Alon Catalysts	130
11.4	Profiles of 1% Pt+1% Ir/Alon Catalysts - II	131
11.5	Profiles of 1% Pt/Alon Catalysts	132
11.6	Profiles of 1% Pt/Alon Catalysts - II	133
11.7	Profiles of 1% Ir/Alon Catalysts	134
11.8	Profiles of 1% Ir/Alon Catalysts - II	135
11.9	Profiles of 1% Ir/Alon Catalysts - III	136
11.10	Standard and Support Profiles Used	137
11.11	Profiles for Size-Strain Analysis of Catalyst HP-3	138

1. INTRODUCTION

Catalytic naphtha reforming is one of the world's highest volume heterogeneously catalyzed reactions. The primary purpose of the process is to produce high octane gasolines and aromatic chemical feedstocks from lower octane naphthas. Important by-products include hydrogen and low molecular weight hydrocarbons. Catalytic reforming has become increasingly important in recent years as pollution control considerations have forced refiners to use less tetraethyl lead for octane enhancement.

Until the late 1960's, North American refiners relied almost exclusively on dual functional catalysts composed of (typically less than 1%) platinum supported on high surface area (typically 100-200 m²/g) η - or γ -alumina. These catalysts have high initial activity but deactivate over a period of several months.

The main short term deactivation is due to extensive coke formation which reduces the number of available active sites on the alumina. Catalysts deactivated by coking and sulphur poisoning are regenerated by burning off these compounds. Operating with an excess of H₂ in the reactor feed slows the rate of coking. It is believed [1] that coke precursors on the alumina are broken down by atomic hydrogen which spills-over from the metal. Unfortunately, due to the thermodynamics of the reaction, the large pressure of

hydrogen required to significantly reduce coking shifts the products away from the desired reformat to lower molecular weight (cracked) compounds.

Bimetallic reforming catalysts are a significant improvement on these alumina supported platinum catalysts. The bimetallic catalysts show initial activity similar to that of the older catalysts, but catalyst deactivation is much slower than monometallic platinum. Perhaps the main advantage of bimetallic catalysts is that they allow operation at much lower hydrogen partial pressure. More flexible operation is possible - higher yields can be traded off against longer periods between catalyst regeneration.

After several of these cycles, catalyst activity cannot be completely returned. This is due to increased average metal particle size, or sintering. (The increase in particle size results in fewer surface atoms, since the total number of metal atoms does not change.) The sintered catalysts can be regenerated by a carefully controlled oxy-chlorination procedure. The details of this procedure are available for Pt-Al₂O₃ catalysts but are generally proprietary for bimetallic catalysts.

The first commercial units using bimetallic reforming catalysts began operation in 1967. Chevron's Rheniforming® process involved a catalyst containing approximately equal loading of rhenium and platinum (about 0.5% of each) on an alumina support. Other corporations soon developed other bimetallic and multi-metallic reforming catalysts. The

subject of this study is one of the most commercially important reforming catalysts: bimetallic platinum and iridium supported on alumina which was developed by the Exxon Research Company.

There is controversy in the literature about the mechanism whereby the bimetallic catalysts show increased resistance to deactivation. It is not even clear what form the iridium metal takes; isolated metal atoms, small Ir clusters, amorphous and heterogenous platinum-iridium alloys have all been proposed. There is also no agreement on the mechanism of sintering; particle and atomic surface migration as well as gas phase and intrasupport migration have all been postulated.

Further improvements in these catalysts are hindered by a lack of understanding of the nature of metal on the support. The purpose of this work was to develop X-ray diffraction techniques to extract the following information about bimetallic Pt-Ir on γ -alumina reforming catalysts:

1. The nature of the supported metal both in fresh and aged catalysts.
2. The effect of atmosphere and temperature history on the metal crystallites.
3. Information about the rate and mechanism of catalyst sintering:
 - a. Average particle sizes as functions of the time-temperature-atmosphere history.
 - b. Particle size distributions (which will give

evidence to substantiate one or the other of the two main sintering theories - particle or atomic migration).

2. LITERATURE SURVEY

2.1 Introduction

In order to understand how Supported Metal Catalysts (SMC's) and specifically bimetallic SMC's function, knowledge of several physical properties of the metal on the support is necessary.

Since chemical reactions occur on active sites on the metal surfaces, it is important to know the number of sites available for reaction. For most catalysts, the number of active sites is directly proportional to the number of metal atoms exposed to the surface (the ratio of active sites to surface metal atoms is often very close to 1). The ratio of metal atoms on the surface to the total number of metal atoms is called dispersion. The dispersion of real catalysts must lie in the range:

$$0 < \text{dispersion} < 1.$$

If one knows (or assumes) something about the shape of the metal particles, area-average particle size can be directly related to the dispersion. In order to study sintering, it is valuable to know not only the average particle size, but also the range of particle sizes which exists in a catalyst sample. This is extremely important when comparing the results of average particle size obtained by different methods since the number weighted, area weighted, and volume weighted average particle sizes may be significantly different, and since each method of measuring

dispersion has different lower limits of detection for metal particles.

Another important physical property in the study of bimetallic catalysts is the composition of the metal particles. Specifically, it is important to know whether Pt and Ir exist as separate entities, as completely homogeneous alloys, or as has been suggested (Sinfelt et al. [2]) heterogeneous crystallites in which the particles have one metal concentrated near the core, and are richer in the other metal near the exterior of the particle.

Since aged catalysts behave much differently than fresh catalysts it is generally believed that these properties change significantly as a result of heat treatment. Two important parameters in heat treatment are of course the temperature and length of time that the catalyst is heat treated. The atmosphere in which the catalyst is heated also makes a significant difference to the final character of the catalyst. It appears that the main difference is whether the atmosphere is reducing (such as occurs when the catalyst is in operation) or oxidizing (as during decoking operations).

2.2 Techniques of Study

Several methods are used to characterize the metal crystallites on supported metal catalysts. The low loading (and resulting high dispersion) of metal on reforming catalysts makes study of the metals extremely difficult.

Previous investigations [3-16] of these catalysts used primarily chemisorption, electron microscopy, and X-ray diffraction.

Chemisorption provides information about the total number of surface metal atoms in a catalyst by measuring the amount of gas adsorbed on a sample. Typically, either carbon monoxide or hydrogen is adsorbed in static or pulsed flow conditions. For noble metals, it is usually assumed that 1 hydrogen atom or 1 carbon monoxide molecule is adsorbed per surface metal atom. However, measured stoichiometries of between 0.8:1 and 2.0:1 have been reported depending primarily on the type of apparatus used, the gas used, and the metal adsorbing the gas [3]. It is also believed that metal-support interactions (MSI) and particle shape may influence the stoichiometry of adsorption. By assuming a typical particle shape, area weighted average particle size can also be calculated. Although these results are very reproducible, they probably are only relative rather than precise measures of average particle size. Chemisorption does not provide any information about the composition of bimetallic noble metal crystallites, or about the size distribution of the particles. However, there is no lower limit to the size of particles which can be detected - since even an individual surface metal atom will adsorb the gas. (Note however that the adsorption stoichiometry may not be the same for individual atoms as for the metal atoms on the surface of

large crystallites.)

Electron microscopy is a measurement technique which allows direct measurement of average particle size and the particle size distribution function. Through the use of electron diffraction, some semi-quantitative information about the nature of relatively large crystallites can also be determined. No information about the oxidation state of the metal can be determined, however. Particle sizes for particles greater than 1.5 nm in diameter are quite reliable, but reliability decreases significantly for particles smaller than this (see Flynn et al. [4]). Average particle sizes calculated using transmission electron microscopy are biased upwards due to the fact that small particles may not be detected due to interference by the support material. Further, average metal particle sizes are also biased upwards because, for example, 1000 small particles have about the same number of atoms as a single particle of 10 times the diameter. Thus, whether or not a single particle in 1000 is counted can make a 50% difference to the calculated volume average particle size.

X-ray diffraction does not show the same limitations as the other methods. All particles greater than about 2.0 nm are measured. Again, precision decreases dramatically for particles smaller than this. Owing to the large number of particles which are irradiated, results are much more repeatable than with electron microscopy, and estimates of average particle size should be more accurate. The angle at

which peaks occur gives information about the composition of the metal particles. The integrated area under the peaks indicates how much of the metal is being detected. The shapes of the peaks give information about the average particle size, and in some cases, the particle size distribution function can be determined.

2.3 Previous Studies of Metal Crystallites in Catalysis

X-ray diffraction techniques were used as early as 1962 (Adams et al. [5]) to study metal crystallites in supported metal catalysts. This work studied 2.5% Pt on silica gel and compared the results using hydrogen adsorption, electron microscopy, and X-ray diffraction. They pointed out that each method yields average metal particle sizes with different weightings; electron microscopy weights by number of particles, chemisorption by surface area of the particles, and X-ray diffraction weights by the volume of the crystallites. They found the volume average particle sizes to be about 3.5 nm, with 10%-20% difference in average diameter between the three methods. The investigators assumed no internal strain in the crystallites, and concluded that they were unable to distinguish particle shape information from experimental error.

Pope et al. [6] made the first attempt to deal with metal in crystallites of sizes below the lower limit of detectability. This work investigated 5-20% Pd on graphitic carbon. They used an internal standard method (adding a

known amount of MgO and comparing the ratio of the area of the MgO (200) peak to the area of the Pd(111) peak) to estimate the amount of Pd which was 'X-ray amorphous', that is, in undetectably small crystallites. Defining a as:

$$a = (\text{Area Pd (111)}) / (\text{Area MgO (200)}) \quad 2-1$$

they found a_m (measured value) to be below 0.85 of a , (theoretical) for all standards made with Pd black, and they showed significant reduction in the area ratio as the average size of the Pd crystallites was increased. They also showed that the ratio decreased as X-ray wavelength increased. This implied that some microabsorption effect is responsible.

The magnitude of this effect is much larger than the predictions of any theory known to this author. Fifteen percent reduction in area corresponds, for example using Taylor's method [18] to a particle size about 50 times larger than was observed. Applying this factor of 50 to the observed length, and using the particle absorption factor method suggested by Taylor gives accurate predictions of a for mechanical mixtures of Pd black crystallites between 19 and 56 nm. However, the observed a 's were more than 20% larger than this simple 'model' predicts for 2 of the 7 reported catalysts with relatively large crystallites. Note that points below Taylor's line are easily explained by assuming 'X-ray amorphous' palladium. Slight excursions

above or below the line can be explained by broad length distribution functions with complicated distributions such as bi- or multimodal.

Smith [7] used Fourier analysis to study 10% Pd on silica and carbon. This high loading permitted the author to determine that strain was negligible (since at least two orders of reflection were distinguishable). He reported slightly higher values of surface area (only about 5%) for X-ray diffraction than for chemisorption, but saw the close agreement as coincidental.

Pausescu et al. [8] and van Nordstrand et al. [9] studied Pt on alumina using the zero-strain hypothesis. The first group used phosphoric acid to remove the support from 0.35% Pt on $\gamma\text{-Al}_2\text{O}_3$. The authors found this step to be necessary because the crystallographic similarity between metal and support means that peaks overlap. They used Fourier techniques and applied an iterative procedure to correct for errors in the length distribution function due to the errors in the tails of the peak and Fourier series cut-off effects. The procedure caused length distribution functions to show bimodality which this author believes to be spurious.

Van Nordstrand et al. [9] used the simple Scherrer equation to correlate particle sizes for Pt on alumina. They studied the Pt(311) peak because it lies in the area of least variation in the Al_2O_3 profile. With results from a mixture of 10 nm Pt black particles in concentrations from

0.1% to 0.7% Pt, they numerically generated profiles for particle sizes from 3.5 nm (their stated 'lower limit of detectability') up to 15 nm. They found that fresh reforming catalysts (0.65% Pt) contained no metal particles greater 3.5 nm in diameter.

Sashital et al. [10] studied 1.1 to 2.0% Pt on SiO_2 gel with XRD. They showed platinum particles to be free from microstrain until the particles approached the gel pore size. They also found that the metal exists in metallic particles with no significant change in the lattice parameters (that is the change was less than 0.1%) even in the presence of oxygen. They found the particles to be relatively free of stacking faults and microtwins. (This result has been assumed in this study). They also found, except for very large crystallites, that the particles were essentially equiaxed. The lower limit of detectability was reported to be about 2.5 nm although length distribution functions are reported down to 1.0 nm.

Ganesan et al. [11] used single peak analysis to study very heavily loaded (in the order of 50%) NiO on alumina and silica. Extremely slow step scans (500 s/step) were performed. They incorrectly attributed the reason that the Scherrer equation gives sizes 1.5 to 2.0 times larger than the various Fourier sizes to problems with the accuracy of the Scherrer equation, rather than to the differences in weighting between the two methods. (The Scherrer equation gives volume weighted means and their Fourier method gives

area weighted means.) They found significant microstrain in catalysts with particles as small as 1.8 nm and they found that microstrain becomes more significant as size increases. It is not possible to use their single peak method for catalysts of low loading because of the accuracy required in the tails of the peaks.

Many of the definitive works on the subject of Pt-Ir catalysts have been by the Exxon Research and Engineering Company, notably by Sinfelt and his co-workers. In 1979 they [16] were able to show the existence of large (2.7 nm to 4.9 nm) Pt-Ir clusters in catalysts of from 5%-20% Pt and Ir on SiO_2 . They later pointed out [2] that the bulk metal at these conditions shows Pt-Ir immiscibility between 7% and 99% Ir, and so postulated significant metal-support interactions (MSI) to account for this apparent contradiction. They also found that following treatment at elevated temperatures (above 500°C) in oxygen, large IrO_2 crystallites are found, which can be converted to large crystallites of Ir upon reduction in hydrogen. Sinfelt et al. [2] postulated on the basis of some results using Extended X-ray Absorption Fine Structure (EXAFS), that the clusters are not homogeneous, but contain Pt-rich and Ir-rich regions. Further, since Pt has a lower surface energy than Ir, Pt would tend to concentrate near the surface of the particle, leaving an Ir-rich 'core'.

There are several limitations apparent in previous investigations of both Pt and Pt/Ir reforming catalysts.

Most investigators have studied catalysts with relatively high metal loading in order to produce intense X-ray profiles. However, metal crystallite sizes and size distributions probably depend strongly on the metal loading, and thus the catalysts studied should be as close as possible to the metal loading of operational catalysts.

The other major limitations of previous work is the use of support corrections. Most investigators have used amorphous supports such as silica. However, alumina has a crystallographic structure similar to that of platinum, and this similarity has been suggested as the source of metal support interactions which probably alter the rate and possibly the nature of the sintering [9]. Two previous investigations [8,9] have used alumina supports but in the first of these, the support was removed by acid and the second was aimed only at achieving weight average sizes (and not size distributions) and so more investigation is warranted in this area.

The emphasis of this work is to use XRD to study Pt-Ir/Alumina catalysts of low loading with special interest in particle size and particle size distribution.

2.4 X-ray Diffraction

An interesting phenomenon which has been dealt with theoretically [17], but which has been only lightly treated by investigators in the field of catalysis is the relationship between the Length Distribution Function (LDF)

which can be derived from X-ray peak profiles, and the practically important Particle Size Distribution Function (PSDF). X-ray profiles are broadened due to incomplete interference of waves interacting within metal crystallites. If the distance travelled by incident X-ray beams within a metal crystallite depends on the position within the particle, then the X-ray profile will be broadened not only by the size of the particle, but also by the shape. It is thus possible to have fairly complex LDF's due not only to the PSDF but also to the particle shape.

3. X-RAY DIFFRACTION THEORY

3.1 Introduction

The theory of X-ray diffraction is presented by several authors (for example Taylor[18], Cullity [19], Klug and Alexander [20], and Zachariassen [21]). and will not be given in detail here. Several key equations and concepts are outlined however for reference in later sections.

X-ray diffraction is most easily explained by the concept of 'Bragg Reflection' from the planes of atoms in a crystal. These planes are normally described by their Miller indices, in general denoted by (hkl) in this work. The equation which describes this reflection is:

$$n\lambda = 2d \sin(\theta_x)$$

3-1

where λ is the X-ray wavelength, d is the distance between the (hkl) planes, θ_x is the angle between the surface of the sample and the incident X-ray beam, and n is the order of the reflection (for example $n=1$ for the (111) peak, and $n=2$ for the (222) peak).

If a sample of a crystalline substance is ground to a fine powder and is placed at the Bragg angle, θ_x , to a parallel beam of monochromatic X-rays, and an X-ray counter is placed at the same angle away from the sample, X-rays will be detected. If the same procedure is carried out at

angles very close to the exact Bragg angle, destructive interference of the X-ray beam will result in no detectable beam. If the incident and receiving angles are varied from low to high angles, a profile of sharp peaks will result. The combination of the location of these peaks and their intensity provide a characteristic 'fingerprint' for any crystalline phase. Normally only one or a few of these peaks are examined using X-ray diffraction to study supported metal catalysts, since a great deal is known in advance about the chemical composition of the catalyst. A considerable amount of work (for example, Sinfelt et al. [16]) has been done using only the Bragg equation to indicate which species are present in bimetallic Pt/Ir catalysts. The location of the peak centroid (in terms of angle, or given the X-ray wavelength, in terms of the more general planar spacing) indicates the metal crystallite composition. The presence of two (hkl) peaks corresponding to lattice parameters 0.39240 nm (Pt) and 0.38390 nm (Ir) indicate separate platinum and iridium rich clusters, whereas a single peak corresponding to lattice parameters midway between the two indicates that the bulk of the crystals are bimetallic alloys.

3.2 X-ray Diffraction Peak Intensities

All materials absorb X-rays. The rate of absorption varies with distance into a sample of material, x , and is proportional to the intensity of the X-rays at that point,

I, that is:

$$dI/dx = -\mu I$$

3-2

where μ , the linear X-ray absorption coefficient, is a constant.

The mass absorption coefficient, μ/ρ , for any element is constant for a given X-ray wavelength, regardless of its physical or chemical state. These have been tabulated (see Cullity [19], for example) for the commonly used wavelengths and given the density and composition of a sample, its X-ray absorption properties can be calculated. This is useful because it allows calculation of the thickness of a sample which will give essentially the same X-ray intensity as one of infinite thickness. The intensity of X-ray peaks increases with the sample thickness but within a very short distance (normally much less than 2 mm) the peaks are within 0.1% of the maximum intensity. Knowledge of X-ray absorption characteristics is also required to accurately remove support profiles from catalyst profiles in order to study the peaks due to metal crystallites.

Another important property of X-rays is the superposition principle, that is, the wave amplitudes of X-ray beams (when phase differences are taken into account) are additive. In combination with the known relation between X-rays and their depth of penetration, the diffraction profile of the support may be subtracted from

the profile of the combined support and dispersed metal catalyst to give the profile of the metal crystallites. This principle also makes it possible to use Stokes method to separate the broadening effects due to the X-ray diffraction machine from those due to crystallite size and strain.

Crystallite sizes and size distributions can also be extracted from the X-ray line profiles. Large crystallites exhibit very narrow peaks, broadened to a finite width due to instrumental non-idealities. As the crystallites are reduced in size, the peaks are broadened due to incomplete constructive interference at the exact Bragg angle, and incomplete destructive interference at angles very close to the Bragg angle. It is possible to show (see for example Taylor [18]) that the total area under the profile is proportional to the number of irradiated unit cells if all else is held constant. (That is, the area is independent of crystallite size.) This allows the estimation of the amount of finely dispersed, non-crystalline metal.

This area is called the integrated intensity, and is proportional to the total diffracted energy per unit length of diffraction line. It is given for pure substances by Cullity [19], as:

$$I_d = T_1 \cdot T_2 \cdot T_3 \quad 3-3a$$

where:

$$T_1 = I_0 A \lambda^3 / (32 \pi r) \quad 3-3b$$

$$T_2 = \left[\frac{\mu_0 e^2}{4\pi m V} \right]^2 \left[\frac{\exp(-2M)}{2\mu} \right] \quad 3-3c$$

$$T_3 = |F|^2 P \left[\frac{1 + \cos^2(2\theta)}{\sin^2 \theta \cos \theta} \right] \quad 3-3d$$

I_0 = incident energy, J/s·m²

A = irradiated area, m²

r = diffractometer circle radius, m

μ_0 = conversion factor, $4\pi \times 10^{-7}$ kg·m·C⁻²

e = charge of an electron, C

m = mass of an electron, kg

V = volume of a unit cell, m³

$\exp(-2M)$ = temperature factor

μ = linear absorption coefficient, m⁻¹

F = structure factor (equal to atomic number at $\theta=0$)

P = multiplicity factor

For mixtures of 2 or more phases the intensity of the (xyz) peak of substance i is given by Taylor [7]

$$I_{xyz i} = K_{xyz i} \cdot \tau_i \cdot (\rho_m C_i / \mu_m \rho_i) \quad 3-4a$$

where:

ρ_m = density of the sample, kg/m³

C_i = weight fraction of component i

μ_m = linear absorption coefficient of the sample

ρ_i = density of pure component i (without voids)

$$\begin{aligned} \tau_i &= \text{particle absorption factor} \\ &= 1/v_i \int_0^{v_i} \exp(-x(\mu_i - \langle \mu \rangle)) dv_i \end{aligned} \quad 3-4b$$

v_i = average volume of particles of component i

$\langle \mu \rangle$ = mean absorption coefficient of the sample if it had no voids

μ_i = linear absorption coefficient of component 'i' in the solid particles

x = total path length of the radiation in the particles

K_{xyz} = constant containing the other factors from Equation 3-3.

Taylor [18] performed the integration for spherical particles and lists values of the particle absorption factor for several values of θ and $R_i(\langle \mu \rangle - \mu_i)$ where R_i is the average particle radius.

In the study of catalysts, it is frequently observed that the integrated intensities are not constant, but gradually increase as the dispersion is decreased, remain constant for particles from about 5 to 100 nm in diameter, and then decrease as the particle size is increased beyond this 'maximum intensity' range.

The first observation is easily explained in terms of broadening. When a peak is broadened (due to small particle sizes), the maximum intensity is gradually decreased, and the intensity at angles relatively far removed from the

exact Bragg angle is increased slightly. Eventually, the intensity of a significant fraction of the profile becomes smaller than the background noise. This results in the erroneous removal of some of the profile during smoothing. Accuracy can of course be improved by using slower scans, but there are practical limits to the length of time available for experimentation. Also, extremely small particles are not crystalline but amorphous and thus do not show peaks in XRD regardless of how slow scans are used. This problem is very important in work dealing with catalysts of low loading (1 - 4% metal on support). When the support is slightly crystalline, large and uneven background intensities result and the relative size of these errors is increased.

The observation that peak intensity decreases as the particle size is increased above about 50 nm cannot be explained by the phenomenon of extinction which occurs when crystal size approaches 10 micrometers. The only plausible explanation is then microabsorption which is the result of the non-homogeneous nature of the catalyst sample. Equation 3-4 uses the factor τ , to quantify this phenomenon. For example, for the (111) reflection from a 200 nm particle ($R_p \approx 100$ nm) of platinum ($\mu_p \approx 4250 \text{ cm}^{-1}$) in a two phase mixture of 1% Pt in Al_2O_3 ($\langle \mu \rangle \approx 160 \text{ cm}^{-1}$), the intensity of the metal reflection is about 95% of what would be calculated using the average absorption coefficient. This type of analysis is valuable to demonstrate that the

particle size for Pt black reference samples have crystallites greater than 100 nm in length.

3.3 Peak Broadening

Under 'ideal' conditions, X-ray diffraction peaks are exceedingly sharp. Several factors can cause peak broadening. The area of the peak is preserved during broadening, so there is a decrease in maximum intensity corresponding to the increase in peak breadth. Several causes of this effect are collectively known as instrumentation factors. The resulting instrumental broadening is due primarily to the fact that the beam is not truly monochromatic and is not truly parallel.

There are other causes of X-ray line broadening which are useful in the study of crystals. Broadening can be caused by extremely small particle sizes, by internal strain (and lattice distortions) and by concentration gradients within crystals. The observed X-ray profile is the convolution of all broadening effects, so theoretically at least, it is possible to separate the effects.

It can be shown that for crystals less than about 100 nm in diameter, size broadening is inversely proportional to the crystal size. By examining several peaks it is possible to distinguish between strain broadening and size broadening. This is because size broadening is independent of which peak is examined but strain broadening increases with the Bragg angle. For the case of bimetallic

crystallites, concentration gradients within the crystals also cause broadening of the profiles. A homogeneous interatomic alloy of Pt and Ir (which are atoms of similar atomic size and identical face centred cubic crystal structure) would show some broadening due only to the slightly imperfect lattice spacing because of the slightly different metal atom sizes.

3.3.1 Instrumental Broadening

There are several causes of instrumental broadening, which can be grouped as causing symmetrical and asymmetrical broadening. Symmetrical broadening is due primarily to the fact that the X-ray source is not a point but has finite width, and thus is passed through a slit which allows passage of slightly non-parallel beams, and through a finite receiving slit. Residual imperfections between the alignment of the incident beam, the sample, and the receiving arm of the goniometer have also been shown (Klug and Alexander [20]) to produce symmetrical broadening.

Asymmetrical broadening is due to the flat (rather than slightly curved) sample, so-called vertical (actually horizontal in the goniometer used here) beam divergence, and absorption of the beam by the sample. However, the largest asymmetrical effect is broadening due to a non-monochromatic incident beam.

X-rays are normally generated by impinging high voltage electrons onto a metal anode. Electrons of these target

atoms are excited by the beam, and when they return to their ground state, they emit X-rays. These X-rays are most intense at a few frequencies, and through use of appropriate filters, an approximately monochromatic beam can be generated. The most intense X-rays appear as a doublet of wavelengths, denoted $K\alpha_1$ - $K\alpha_2$. (For the copper anode used in this study, the $K\alpha_1$ wavelength = 1.54056 nm, and $K\alpha_2$ = 1.54439 nm.) The intensity of $K\alpha_1$ is about twice that of $K\alpha_2$. Some monochromators can eliminate broadening due to this effect but this method was not used here.

Examination of the Bragg equation (Equation 3-1) with knowledge of the shape of the sine function indicates that for small incident angles, $K\alpha$ broadening will be small, but as θ_x approaches 90° , broadening can be quite large. (The effect for standard profiles of the (311) peak of Pt is large enough to cause a double image of the peak.)

It has been noted that this broadening is often the largest source of asymmetries in the X-ray profiles, and thus it is useful to correct for it before other corrections are made. It is possible to show that Fourier techniques can be directly used to correct for $K\alpha$ broadening. However, the high angle peaks also have the least intensity and thus are the least amenable to Fourier analysis. Numerous other methods are available, for example Langford [22] lists four. Since curve fitting techniques are used here to reduce counting errors, curve fitting is also used to remove $K\alpha$ broadening. This technique assumes that the two incident

beams cause two overlapping peaks of identical shape with intensity ratios of 2:1, and separated by a constant amount as given by the Bragg equation for the different wavelengths. (The methods mentioned by Langford make the same assumptions.)

In order to analyze broadening for size, strain, and shape of crystallites, the other instrumental effects must also be removed. Fourier methods are the most accurate for this purpose, but since very detailed information about peak shape is needed, simpler but less rigorous methods are used for most work.

The breadth of the profile may be calculated as the width at 1/2 of the peak height, $B_{1/2}$, or by the more theoretically sound integrated width defined by:

$$B_i = \frac{\text{Peak Area}}{\text{Maximum Peak Height}}$$

3-5

If one assumes that the form of the line profile is a Gaussian distribution function, (i.e. has the general form of $f(x) = a \cdot \exp(-bx^2)$ where $x = \theta - \theta_x$) then the instrument broadening can be separated from the broadening due to other factors by:

$$(B^m)^2 = (B^s)^2 + B^2$$

3-6

where B is the width of the pure diffraction profile, B^m is the measured width of the diffraction profile, and B^s is the width of a profile produced by a sample of crystallite size known to be greater than about 100 nm and with no internal strains. If the line profile more closely approximates the Cauchy function, then

$$B^m = B^s + B$$

3-7

One compromise between these two possibilities which is recommended by Delhez et al., [23,24] is to approximate the line profile by the Voigt function, which is the convolution of the Cauchy and the Gaussian error functions. Delhez et al. [24] give empirical formulae for the half breadths and integral breadths of the pure profile given the half breadth and integral breadths of the machine and size broadened profiles, assuming that both can be approximated by the Voigt function. The method is recommended only if the peak is very well defined.

A simpler compromise is given by Taylor who suggests that the geometric mean of the result of Equations 3-6 and 3-7 be used to determine B .

3.3.2 Size-Shape Broadening

Many references on X-ray diffraction develop the theory of how particle size information can be extracted from peak shapes. For a sample composed entirely of identical

particles of constant depth in the (hkl) direction, Taylor's results [18] can be written as:

$$I(s) = K \sin^2(\pi N s) / \sin^2(\pi s) \quad 3-8$$

$$-1/2 < s < 1/2$$

where:

$$s = n(2d \sin(\theta)/\lambda - 1) \quad 3-9$$

and:

θ = actual angle $\theta_x \pm \Delta\theta$

N = total number of reflecting planes in the (hkl) direction

and the other symbols are as defined for Equation 3-1.

The value of K depends on the usual factors (air pressure, Bragg angle, concentration of the sample, and the apparatus) as well as the size of the particles.

For a sample composed of N_p different discrete lengths, each of volume fraction V_i , and average distance perpendicular to the reflecting planes, L_i , the results of Delhez et al. [24] can be written as:

$$I(s) = k \sum_{i=1}^{N_p} \frac{V_i \sin^2 \pi N_i s}{L_i \sin^2 \pi s} \quad 3-10$$

where k is not a function of the particle size or shape.

Early techniques used to extract information about crystallite sizes involved comparison of the size and shape

of the diffraction profile of a catalyst with those of mechanical mixtures containing known quantities of metal of known average particle size (van Nordstrand et al. [9]). Later investigators (Pausescu et al., [8]) leached the alumina support away by acids and examined the residual powder using standard powder techniques. This method has the disadvantage that the acid almost certainly changes the nature of the smallest crystallites (many are probably washed away with or dissolved in the acid solution). Other investigators [2,5,6,10-16] have used silica supports (which being amorphous do not show diffraction patterns, but which do not show bifunctional catalytic activity and which likely exhibit very different metal-support interactions than alumina supported catalysts).

Several authors [2,5] have used the simple Scherrer equation which relates the width of an XRD peak to an apparent crystallite size. If B is the pure breadth (corrected for instrument broadening as described earlier) due only to size effects, expressed in radian units, then the volume average crystallite thickness, $\langle L_v \rangle$, is given by the Scherrer equation, as:

$$\langle L_v \rangle = (K, \lambda) / (B \cdot \cos \theta)$$

3-11

where K is a constant approximately equal to unity; and which depends on the definition of B . $\langle L_v \rangle$ is the thickness normal to the X-ray beam, i.e. for an (hkl) peak, it is the

product of the average number of (hkl) planes and the distance d , between each (hkl) plane. As such, it is a function of both the crystallite size and shape. Note that this definition is somewhat different than other definitions (e.g. Klug and Alexander [20]) which include shape effects in the Scherrer constant, K .

The crystallite length distribution function can be extracted from the shape of the peaks by a method due to Stokes [25,26]. The method relies on the superposition principle and the discrete Fourier transform.

3.3.3 Strain Broadening

Previous authors (e.g. Păulescu [8]) assumed no strain in dealing with particle size distributions, or, owing to the fact that second order reflections usually cannot be measured accurately enough for multiple order Fourier analysis of supported noble metal catalysts, single profile analysis techniques have been used (e.g. Ganesan et al. [11]). This method requires precise knowledge of the profile shape and a number of assumptions about the nature of the strains. These shortcomings can lead to erroneous results, especially when dealing with catalysts with low metal loadings.

It has been hypothesized that strain in low loading catalysts should be very small due to the lack of physical distortion of the metal in relatively large pores. However, metal-support interactions may contribute to strain. Strain

broadening can be separated from size broadening because the former is much more strongly influenced by the Bragg angle than the latter. Spherical particles show no angle dependence of size broadening, other shapes have only slight (and irregular) dependence.

The simplest equation relating strain to the breadth of the pure profile was developed by Stokes and Wilson [22,26]. If there are no size broadening effects:

$$B \cdot \cot(\theta_x) = 5.0 \langle e^2 \rangle^{1/2} \quad 3-12$$

where $\langle e^2 \rangle^{1/2}$ is the root mean square strain.

If both strain and size broadening occur in the same sample, two equations for the two limiting peak shapes have been developed. If the peaks are nearly Cauchy in shape, then:

$$B \cdot \cos(\theta_x) = B_{s,z} + B_{s,n} \cdot \sin(\theta_x) \quad 3-13$$

where $B_{s,z}$ is the breadth due to size broadening, and $B_{s,n}$ is the breadth due to strain broadening. If, however, the peaks are more nearly Gaussian, then:

$$B^2 \cos^2(\theta_x) = B_{s,z}^2 + (B_{s,n}^2 \sin^2 \theta_x) \quad 3-14$$

Langford [22] gives detailed procedures on how to use the known relationship between the width at half-height, the

integral breadth, and the Voigt function to extract the fraction of the breadth which is due to each of the Cauchy and Gaussian profiles for peaks that do not approach either of the two extremes. Although $B_{1/2}$ and B_1 are known quite accurately for the first few peaks, it was found that they are not known precisely enough for the (311) and (222) peaks for the method to be of practical use here. However, plotting the left hand sides of Equations 3-13 and 3-14 against $\sin(\theta_x)$ and $\sin^2(\theta_x)$ respectively allows for approximate determination of strain and size broadening.

It is important to note that shape effects can also greatly influence the broadening of different (hkl) peaks. For this reason, it is important to plot at least two orders of the same peak (for example (111) and (222)) in the manner described above so that shape effects are not accidentally labelled as strain effects.

3.4 Fourier Techniques

3.4.1 Principles

In order to extract the most detailed information about crystallites from the observed and standard profiles, deconvolution of the various broadening effects is necessary. The method was developed by Warren and Averbach [25] and relies on the superposition principle and the discrete Fourier transform. Under ideal conditions, Fourier techniques can be used to examine the concentration

gradients, internal strain, particle size distribution function and particle shapes. Unfortunately, it is not possible in practice to separate all of these effects when they occur simultaneously as may be the case in bimetallic catalysts.

The broadened profile, $h(s)$, observed as the result of small crystallite size or non-uniform strain is actually the convolution of 2 profiles, the 'pure' peak, $f(s)$, and the peak due to instrument broadening, $g(s)$. (Recall that 's' is defined in Equation 3-9.)

$$\begin{aligned} h(s) &= \int_{-\infty}^{\infty} g(a)f(s-a)da \\ &= \int_{-\infty}^{\infty} f(a)g(s-a)da \end{aligned} \quad 3-15$$

The Fourier Transform, $F(j)$, of a function $f(s)$, is defined as:

$$F(j) = (1/\sqrt{2\pi}) \int_{-\infty}^{\infty} f(s) \cdot \exp(2\pi isj) ds \quad 3-16$$

It can be numerically approximated by the discrete Fourier Transform:

$$F(j) \cong (1/\sqrt{2\pi}) \sum_s f(s) \cdot \exp(2\pi isj) \cdot (\Delta s) \quad 3-17a$$

$$= \frac{\Delta s}{\sqrt{2\pi}} \left[\sum_s f(s) \cdot \cos(j\omega_j) + i \sum_s f(s) \cdot \sin(j\omega_j) \right] \quad 3-17b$$

$$= Fr(j) + i \cdot Fi(j) \quad 3-17c$$

where:

$$\omega_j = (2\pi s)/(s_{mx} - s_{mn}) \quad 3-18$$

and s_{mx} and s_{mn} correspond to the value of s at the maximum angle, θ_{mx} , and minimum angle, θ_{mn} , respectively. The Fourier transform is useful because the convolution in Equation 3-15 can be rewritten as a product or a quotient of the Fourier transform such as:

$$F(j) = H(j)/G(j) \quad j = 0, 1, \dots, J \quad 3-19$$

$$J = K/2 - 1$$

for K observations of s . Since F , G , and H are composed of real and imaginary parts, the transform of the pure profile is given by:

$$Fr(j) = \frac{Hr(j)Gr(j) + Hi(j)Gi(j)}{Gr(j)^2 + Gi(j)^2} \quad 3-20$$

$$Fi(j) = \frac{Hi(j)Gr(j) - Hr(j)Gi(j)}{Gr(j)^2 + Gi(j)^2} \quad 3-21$$

The pure peak can be reconstructed using:

$$f(s) = (1/\sqrt{2\pi}) [\sum_j Fr(j) \cos(j\omega_j) + i \sum_j Fi(j) \sin(j\omega_j)] \quad 3-22$$

It is not normally necessary to reconstruct the pure peak, however, as most particle size information can be extracted from the discrete Fourier transform of the pure diffraction profile ($F(j)$). If the transforms are generated about $s=0$ =peak centroid, and there are no non-uniform strains in the crystals, the imaginary coefficients, $F_i(j)$, are small and may be assumed to be zero. If all strains are small, then the coefficients of 2 orders of a diffraction peak (for example (111) and (222) peaks) will be the same and an area weighted average column length, $\langle La \rangle$ is given by:

$$\langle La \rangle = j_1 \cdot a \quad 3-23$$

where j_1 is given by:

$$\lim_{j \rightarrow 0} \frac{dFr(j)}{dj} = -1/j_1 \quad 3-24$$

'a' is defined by:

$$\lambda = 2a(\sin(\theta_{mx}) - \sin(\theta_{mn})) \quad 3-25$$

Figure 3.1 shows how j_1 can be determined graphically. The real Fourier coefficients of the pure profile are plotted against Fourier number (dotted curve in Figure 3.1). If the area of the standard and measured profiles are the same, $Fr(0)=1.0$. The solid curve is given by drawing the tangent to the Fourier coefficient curve as $j \rightarrow 0$. The intercept of this tangent with the abscissa gives the value of ' j_1 ' as given in Equation 3-24.

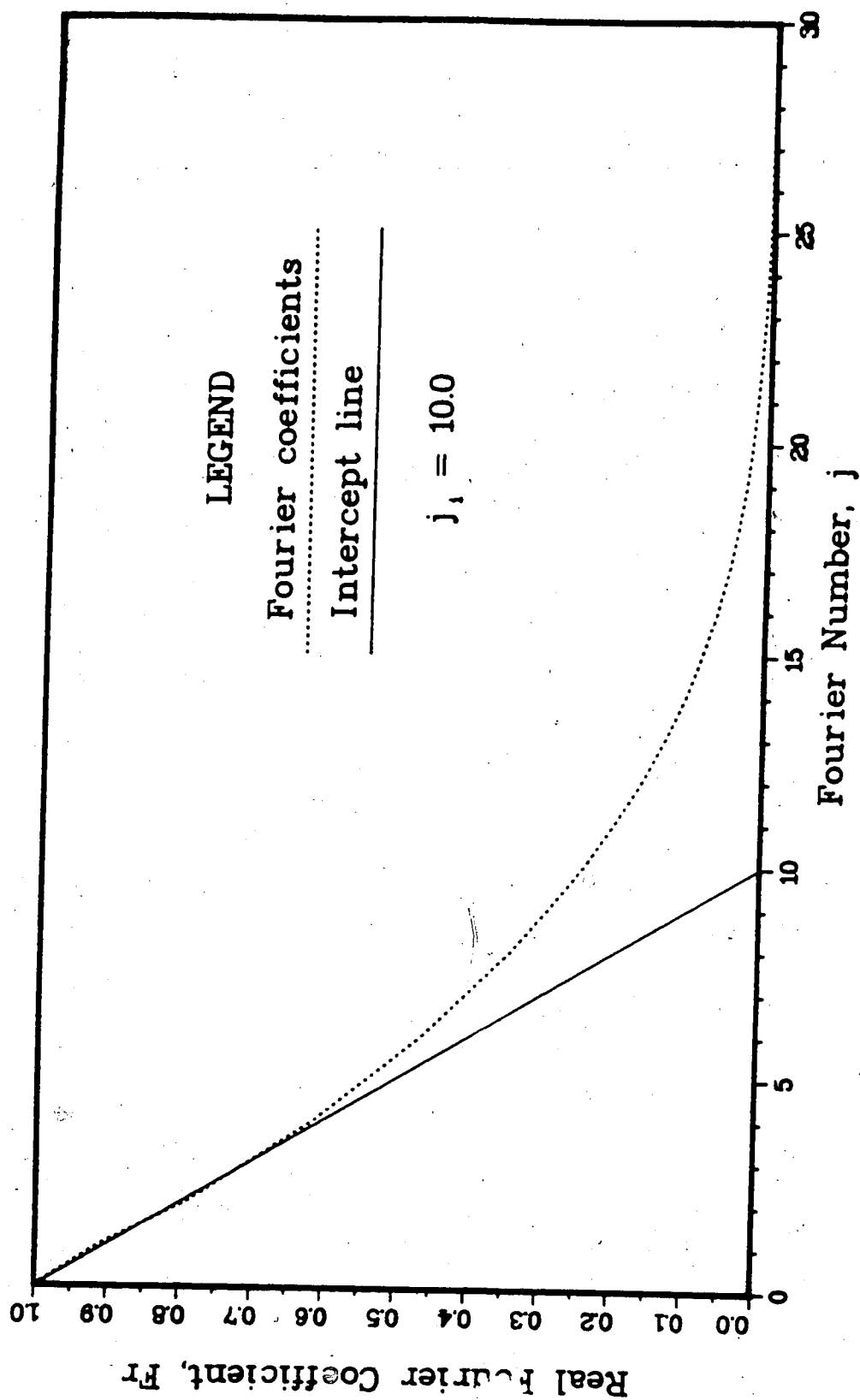


FIGURE 31 Graphical determination of $\langle La \rangle$
(111) peak of catalyst HP-3

3.4.2 Length Distributions from Fourier Coefficients

The length distribution function (LDF) as given by Fourier analysis of X-ray data is considerably different from the particle size distribution functions (PSDF) which are the result of electron microscopy. X-ray diffraction measures the lengths of columns of unit cells perpendicular to the reflecting planes. Within a single crystallite, there is normally a range of column lengths; small lengths near the edge, and long columns near the middle in the case of spherical crystallites. This means that, if all particles are identical, (that is a Dirac delta function PSDF) the LDF as observed by X-ray diffraction may be quite complex and broad.

It is possible to extract several different weightings of these LDF's. Area weighting means that the LDF is weighted according to the area of the reflecting planes of that length (that is to the X-ray silhouette of the crystallite). Volume weighting refers to the product of this area and the length of the column. It necessarily follows that the volume weighted average length is larger than the area weighted average length.

The column length distribution function can be determined from the second derivative of these Fourier coefficients. The area weighted length distribution function (ALDF) is given by:

$$Pa(L) = \frac{1}{Ca} \frac{d^2 Fr(j)}{dj^2} \quad 3-26$$

where Ca is a constant which is determined from:

$$\int_0^{\infty} Pa(L) dL = 1.0 \quad 3-27$$

$$\text{and } L = a \cdot j \quad 3-28$$

Another average particle length which should be identical to $\langle La_1 \rangle$ is:

$$\langle La_2 \rangle = \frac{\sum Pa(L) \cdot L}{\sum Pa(L)} \quad 3-29$$

A volume weighted length distribution (VLDF) function is given by:

$$Pv(L) = \frac{j}{Cv} \frac{d^2 Fr(j)}{dj^2} \quad 3-30$$

where Cv is determined from:

$$\int_0^{\infty} Pv(L) dL = 1. \quad 3-31$$

Another volume weighted average length is given by:

$$\langle Lv_2 \rangle = \frac{\sum Pv(L) \cdot L}{\sum Pv(L)} \quad 3-32$$

It is also possible to evaluate a number average particle length and length distribution function by:

$$P_n(L) = (1/(C_n \cdot j^2)) \frac{d^2 Fr(j)}{dj^2} \quad 3-33$$

and:

$$\langle L_n \rangle = \frac{\sum P_n(L) \cdot L}{\sum P_n(L)} \quad 3-34$$

Some discussion about the different weighting factors used in comparing catalyst particle sizes is in order. Experts in the field of catalysis (for example Adams et al. [5]) refer to number weighted average particle sizes obtained by electron microscopy, surface area weighted average particle sizes obtained by chemisorption and volume weighted average particle sizes obtained by X-ray diffraction. It has been noted (e.g. Smith [17]), that except for extremely narrow particle size distributions, these weightings would not be expected to give the same result. X-ray diffraction allows for determination of these three weightings. However, 'area' weighting refers not to the surface area of the particles, as in chemisorption, but to the projected area perpendicular to the reflecting planes. If the shape of the particles does not change as the particle size increases, these two 'area' weighting factors should give equivalent results. If, however, the shape changes, (for example from raft-like to more 3-dimensional in character), these two are not equivalent.

The ratio of volume weighted ($\langle Lv_1 \rangle$ or $\langle Lv_2 \rangle$) to the area weighted ($\langle La_1 \rangle$ or $\langle La_2 \rangle$) is an indication of the range of particle sizes.

It is useful to note that a relatively broad width of the length distribution function may be the result of particle shape and not of a range of particle sizes. Smith [17] showed that spherical particles have an area weighted particle size distribution function of:

$$Pa(L) = 2L/D \quad 3-35$$

and an average length of:

$$\langle La \rangle = 2D/3 \quad 3-36$$

The effect of the particle shape on average particle size was first quantitatively examined by Wilson and Stokes. (See Taylor [18] for a table of the value of Scherrer constant for several particle geometries. In this case, shape effects are incorporated into the constant rather than in $\langle Lv \rangle$ as is done in this work.) The ratio of $\langle Lv \rangle / \langle La \rangle$ for unisized spheres is 1.125. Taylor [18] shows that $\langle Lv \rangle / \langle La \rangle$ of up to 1.4 may be due solely to such simple particle shapes as tetrahedra, thus great care should be used in relating $\langle Lv \rangle / \langle La \rangle$ to the breadth of the particle size distribution.

The combined effect of the shape and the particle size distribution to the length distribution function was also studied by Stokes and Wilson and expanded by Smith [17] who showed that the observed profile, $Pa(L)$ is the integral of the particle size distribution function, $Ps(D)$, with the shape distribution function corresponding to the particle size, $f(L,D)$ where L refers to the observed length and D refers to the characteristic length of the particles:

$$Pa(L) = \int_{D_0}^{\infty} f(L,D) \cdot Ps(D) dD \quad 3-37$$

where D_0 is the smallest characteristic length which can have columns of length L . (For example taking D as the diameter of a sphere, $D_0=L$.)

Combining the results due to Smith with the assumption that the particle shapes are constant as the particles grow gives different results for the final relation between $Pa(L)$ and $Ps(D)$ depending on the assumed shape. For all reflections on spherical crystallites:

$$\frac{d}{dL} \left[\frac{Pa(L)}{L} \right] = -k \cdot Ps(L) \quad 3-38$$

Combining this result with Equation 3-26 shows that the particle size distribution can be extracted from the third derivative of the Fourier coefficients - which are unfortunately, very difficult to determine.

For cubic crystallites (with crystallite axes oriented with the units cells) the relationship is even more complex

because it is highly dependent on the order of the reflection. For reflections of the type (h00):

$$P_a(L) = L \cdot P_s(L)$$

3-39

and for reflections of the type (hhh):

$$\frac{d^2 P_a(L)}{dL^2} = k_1 P_s(k_2 L)$$

3-40

(Note that this reflection requires a fourth derivative of the Fourier coefficients to establish the particle size distribution).

All reflections of tetrahedra follow the same general behaviour as Equation 3-40.

Although evaluation of Equations 3-38 to 3-40 is not possible, several generalities can be extracted. For spherically shaped crystallites, all area weighted length distributions must pass through the origin, reach a maximum and decline to zero again, regardless of the nature of the particle size distribution. If all crystallites are tetrahedra, the length distribution function must start at some finite value at 'zero' length, and steadily decline to zero with increasing length. The (h00) reflections of the cubic crystallites behave generally as spherical crystallites, and the (hhh) reflections behave as tetrahedra.

3.4.3 Numerical Techniques in Fourier Analysis

Fourier methods must be used with great care. Three of the most important potential pitfalls are error multiplication, aliasing, and information leakage. Numerical methods have successfully been applied to reduce the effects of these phenomena.

Error multiplication occurs because $F(j)$ is determined by dividing two very small numbers when j gets large. (Recall that $F(j)=H(j)/G(j)$, see Equation 3-17.) Because of the shape of the peaks, as j tends to infinity, $H(j)$ and $G(j)$ must both tend to zero. The information about G as $j \rightarrow 0$ is mostly obtained in the region near the peak maximum, while as $j \rightarrow \infty$, the tails of the peak determine the nature of G . As G tends to zero (i.e. as $j \rightarrow \infty$) very small changes in $g(s)$ in the peak tails can cause very large changes in $G(j)$ and even larger variations in $F(j)$ because $H(j)$ is also small. Since the LDF is determined by the second derivative in $F(j)$, some smoothing technique must be used. One generality which can be extracted from the equations is that the variance of the Fourier coefficients increases with harmonic number as a result of random variations in X-ray counting statistics. Several methods are used to deal with this problem each having advantages and disadvantages.

1. *Smoothing the oscillation profiles:*

This has the disadvantage of hiding details in the profiles, and as will be shown subsequently, these details are crucial if particle size distribution

information is to be extracted.

2. *Smoothing the distribution function:*

The errors are regarded as being part of the profile, and the resulting length distribution curve is smoothed. This method is only possible when there are very small variances in the background and thus was found to be inappropriate in this investigation.

3. *Curve fitting:*

This method has several advantages for this work. Relatively large errors can be eliminated if a suitable smoothing function is used. Two close peaks may also be separated (although distribution information is probably not precise, particle length data can be determined quite accurately). The principle disadvantage of this method is that the nature of the smoothing function distorts the particle length distribution. Previous investigators have used the following smoothing functions:

a. *The von Laue function:* [23]

$$f = K_1 \sin^2 ks / (ks)^2 \quad 3-41$$

This function forces the length distribution function into a very narrow distribution, and owing to its oscillatory nature, it does not describe the observed profile very well. The function does not allow for asymmetries in the profile.

b. *The Cauchy Profile:*

$$f = K_1 / (1 + ks^2) \quad 3-42$$

This is a much better approximation to the observed size broadened profile (Klug and Alexander [16], Delhez et al. [23]) but does not describe the shape of the lower portion of the profile well. It also does not deal with asymmetries in the profile, and does an especially poor job describing the unbroadened 'standard' profile.

c. *Vogel [27] modified Cauchy profile:*

$$f = \frac{K_1}{(1 + K_2(2\theta - 2\theta_0)^2)^t} \quad 3-43$$

where $2\theta_0$ and t are also adjustable parameters. This profile is an excellent function if the length distribution function is known to be log-normal (Vogel et al. [27]). This function also does not describe the asymmetries in the observed profile, and it forces the length distribution function into the log-normal form with a characteristic long tail regardless of the true distribution.

d. *Modified Voigt profile:*

The Voigt profile, the convolution of the Gaussian distribution function and the Cauchy profile has been suggested by several authors (e.g. Delhez et al [24]) In order to retain the character of this profile, but to simplify calculation and allow for asymmetries in the profile, the following function was eventually chosen in this work to describe the profiles:

$$f = F_1(2\theta) + F_2(2\theta)$$

3-44

where:

$$F_1(2\theta) = \frac{b_1}{[1 + ub_2(2\theta - 2\theta_0)^2]^t}$$

$$F_2(2\theta) = b_3 \exp(-ub_4(2\theta - 2\theta_0))$$

and $u = 1.0$ for all $2\theta \geq 2\theta_0$

$u = b_5$ for all $2\theta < 2\theta_0$

Here, $2\theta_0$, b_1 , b_2 , b_3 , b_4 , and t are adjustable parameters. This function also has the advantage of being able to regenerate bimodal length distribution functions.

3

Aliasing occurs when steps of Δs (or $\Delta 2\theta$) which are large relative to the breadth of the peak are used. Information is lost during the transform, and two possible peak shapes could give the same Fourier coefficients. Instead of falling off to zero as the Fourier frequency (j) increases, aliased transforms decrease, then gradually increase to unity as the Fourier frequency is increased. (See Delhez et al. [23]). The effect is essentially avoided if steps of $\Delta 2\theta < 0.1 B^m$ are used.

Information leakage is the result of performing the Fourier analysis over a relatively narrow band of s (or a small range of angles in 2θ). As Bloomfield [28] points

out, truncating the series before its natural frequency results in significant information "leakage". The natural frequency for X-ray diffraction analysis corresponds to the range

$$-0.5 < s < 0.5$$

Solving for θ_{mx} and θ_{mn} using Equation 3-9 and substituting into Equation 3-25, we see that the natural Fourier frequency corresponds to a distance

$$a = d = \text{interplanar spacing}$$

No resolution is possible below this level.

Leakage changes the shape of the Fourier coefficient versus frequency (j) curve, by smoothing abrupt changes in the slope, and by causing oscillations in the Fourier coefficients about 0.0 for high frequencies. This problem becomes increasingly significant as the size of the peak tails cut off is increased.

Looking at a relatively narrow band of data, (say about 6 to 12 ° of 2θ) amounts to looking at the data through a rectangular (or boxcar) window. For small particle sizes, (where a significant portion of the area is cut off) leakage can be quite large, but this effect can be reduced by hanning, or tapering the data by applying the split bell cosine window, $u(k)$ to the data $hm(k)$, i.e.:

$$h(k) = u(k) \cdot hm(k)$$

$$u(k) = 0.5 * (1 - \cos(\pi(J+k-0.5)/M)) \quad k = -J, \dots, -J+M-1$$

$$= 1. \quad \text{for } k = -J+M, \dots, J-M \quad 3-46$$

$$= 0.5 * (1 - \cos(\pi(J-k+0.5)/M)) \quad k = J-M+1, \dots, J$$

where

$h(k)$ = the hanned data

$hm(k)$ = the measured data

k = the data points, $-J < k < J$

K = total number of data points, $K = 2J+1$

J = number of the maximum Fourier coefficient

(including the zeroth coefficient, there are $J+1$
Fourier Coefficients)

M = the number of hanned data points at each end of the
window

This window has the effect of reducing the oscillations to essentially zero for Fourier frequencies greater than $(J-M)$ and also makes the Fourier coefficient versus frequency curves more closely approximate the curve taken from the natural range at lower frequencies. Tukey (in [28]) recommended that

$$0.1 < 2M/K < 0.2$$

and the lower limit of 0.1 hanning was used in this investigation.

One possible solution to the problem of leakage which was not investigated would be to apply a final baseline correction rather than applying hanning. This correction would force the peak to zero at θ_{mn} and θ_{mx} by subtracting a straight line from $[\theta_{mn}, f(\theta_{mn})]$ to $[\theta_{mx}, f(\theta_{mx})]$ from the fit profile.

4. NUMERICAL STUDIES

4.1 Introduction

Because of the complex relationship between particle size and length distribution functions, the several forms of broadening and the measured X-ray profiles, and because of the extensive data manipulation required to separate these effects, computer techniques are essential in the analysis of experimental data. Some method of smoothing the profiles is also necessary before Fourier analysis can be performed, and this too is usually done using computer algorithms.

The numerical methods used are complicated, and programs are so long that even the most detailed scrutiny of source code cannot be relied upon to trace all errors. The only feasible way to verify that the methods are accurate is therefore to use test programs to simulate experimental data closely, and then apply the numerical methods to these artificial data. Many other useful results can be obtained using these numerical methods, not the least of which is a much more thorough understanding of X-ray diffraction phenomena.

The procedure used was first to numerically generate pure X-ray diffraction profiles from different assumed length distribution functions. Scherrer and Fourier analysis was carried out on these to test the accuracy of the numerical methods, since several approximations are used in the analysis of the data.

The second step was to combine these size broadened pure profiles with instrument profiles. This was accomplished using Fourier techniques. These were deconvoluted and the resulting length distribution function was extracted.

Noise equivalent in magnitude to that which occurs experimentally was then added. The 'noisy' profiles were then fit using the 7 parameter modified Voigt function. The smoothed functions were then unfolded (using the same Fourier techniques as were used on the experimental data) and the resulting length distribution function was compared to the initially assumed LDF.

4.2 Pure Profiles

The first check of the numerical method was to generate the pure diffraction profiles resulting from several assumed length distributions and apply the Scherrer and Fourier techniques to recover the average length and length distribution functions.

Figure 4.1 shows the pure profiles for 3 different length distribution functions each with $\langle L_v \rangle = 10$ nm. Note that most of the LDF information is stored near the base of the peak, while the width at half height is approximately constant indicating that the volume average particle size is the same for all three LDF's.

The profiles were generated using program XPURE.
(Copies of all computer programs are in Appendix C.)

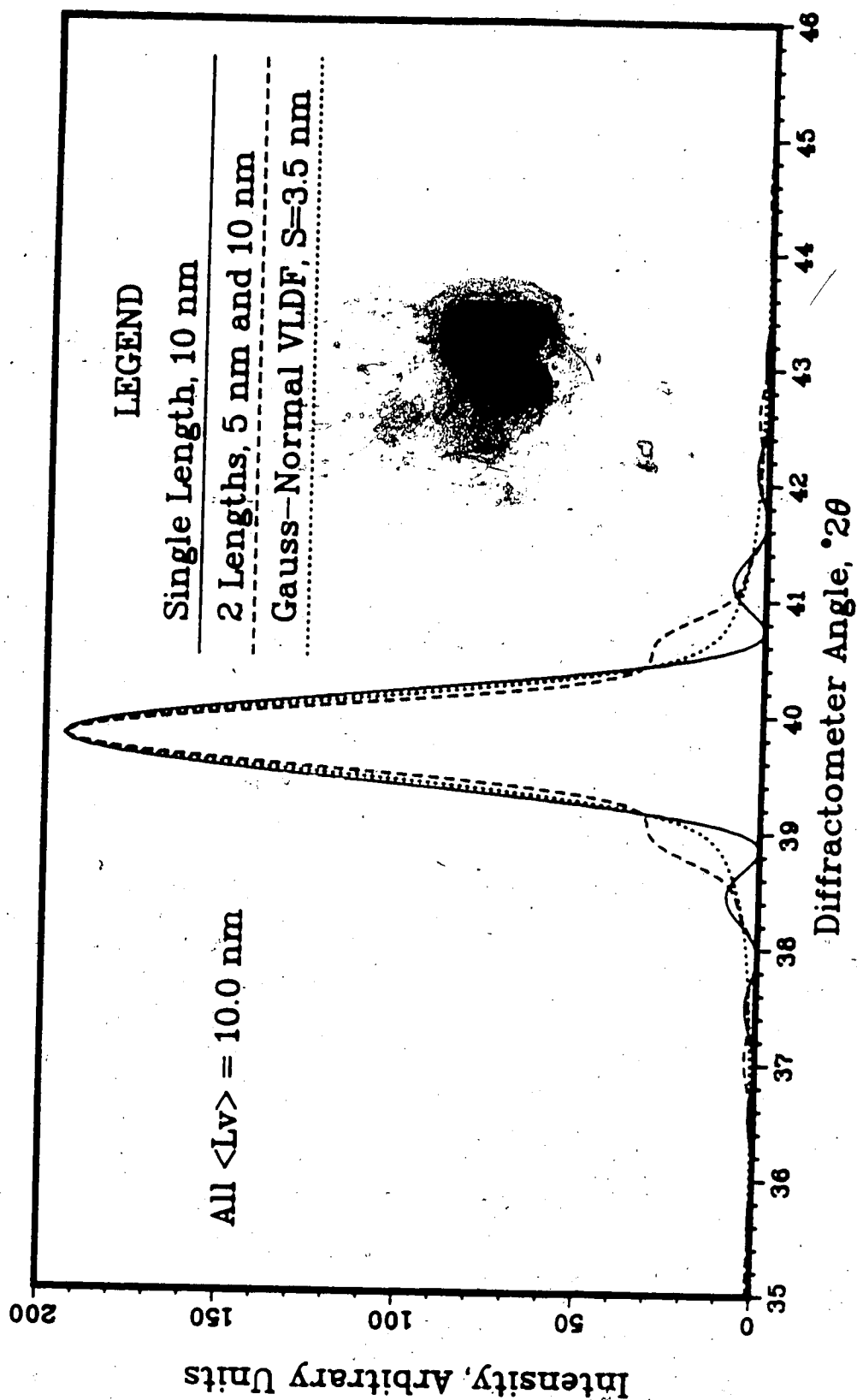


FIGURE 4.1 Pure XRD Profiles for Different VLDFs

Because of the superposition principle, the integrated area of the pure profile is proportional to the volume of metal observed. (In this development, the volume of metal observed remains constant as the particle size changes, which is equivalent to assuming constant metal loading. All of the metal is assumed to exist as crystallites.) The program uses Equation 3-10 to weight discrete column lengths according to an assumed mass-fraction. Profiles were generated with data points at every 0.05° of 2θ to match the precision of the experimentally collected data. Profiles were generated for a range of 20° of 2θ around the Pt (111) peak at $2\theta=39.8^\circ$.

Profiles were generated for particles of unisized cubes oriented with the (111) plane parallel to the reflecting planes for cubes with sides of length 1, 2, 5, 10, 20, and 50 nm. Using the Scherrer equation and the measured half-breadth (found by linear interpolation along the profile), and the integrated breadth (integrated over 20° of 2θ using program XINTG) were compared. A summary of these results appears as Table 4.1.

For single length input functions, the half-breadth calculation of average size was within 1% of the true size, but the average size calculated by the integral breadth method gradually increased with respect to the true size as the particle size was decreased. The calculated average size about 10% larger than the actual size for the 1 nm cubes, indicating one of the dangers of using X-ray

Table 4.1 Accuracy of Several Methods of Determining Average Length from Numerically Generated Pure X-ray Profiles of Dirac Delta Type Length Distribution Functions

Length (nm)	Scherrer $\langle L_v \rangle_{1/2}$ $K_s=0.89$ (nm)	Scherrer $\langle L_v \rangle_1$ $K_s=1.0$ (nm)	Fourier $\langle L_v \rangle$ (nm)	Fourier $\langle L_v \rangle / \langle L_a \rangle$ (ideal=1.0)
50	50.33	50.08	50.00	0.996
20	20.05	20.08	20.12	1.003
10	10.03	10.08	10.12	1.01
5	5.01	5.08	5.13	1.02
2	1.99	2.09	2.17	1.13
1	0.99	1.09	1.41	1.00

techniques for such small particle sizes. The errors were due to truncation of the peak tails, and much larger errors are expected in practice since it is extremely difficult to distinguish between a level background and the long peak tails due to the noise in the data and especially overlap with other peaks.

Profiles were also generated for several bimodal length distribution functions for volume average length of 5 nm and 10 nm. The results for these simulations are given in Table 4.2: Here, it can be seen that while similar increases in

Table 4.2 The Effect of Broadening the Length Distribution Function on the Accuracy of Several Methods of Determining Average Length from Pure XRD Profiles

Length ¹ (nm)	True <Lv>/<La>	Scherrer <Lv> _{1/2} (nm)	Scherrer <Lv> _i (nm)	Fourier <Lv> (nm)	Fourier <Lv>/<La>
10	1.00	10.03	10.08	10.12	1.01
5 15	1.33	12.69	10.11	10.16	1.36
1 19	5.26	18.40	10.43	11.38	3.06
5	1.00	5.01	5.08	5.13	1.02
2.5 7.5	1.33	6.35	5.10	5.18	1.39
1 9	2.78	8.41	5.38	5.74	2.20
0.5 9.5	5.26	9.21	6.97	5.26	1.29

¹Dirac delta length distributions. All lengths are equally volume weighted. (For example, "5 15" indicates 1/2 of the volume is 5 nm particles, 1/2 is 15 nm, for a volume average length of (5+15)/2=10 nm.)

error occur for <Lv>_i as the size is decreased, the length calculated by the half-height width shows much higher errors for broad particle size distributions than for narrow distributions. Particle sizes are always overestimated owing to the fact that the long tails are inadequately counted by measuring the width at half height.

Table 4.3 shows the results for several continuous LDF's. One common function used to approximate the particle size (or length) distribution function is the log-normal distribution function, given by:

$$P_v(L) = L \cdot \exp[-uL'] / C_v$$

Table 4.3 The Accuracy of Various Methods of Measuring the Average Length for Several Continuous Input Length Distribution Functions

LDF Type	True <Lv>	Ratio ¹	Scherrer <Lv> _{1/2}	<Lv> ₁	Fourier <Lv>	Ratio ¹
Log-normal	4.45	1.28	5.27	4.56	4.64	1.20
Gauss-normal	5.00	1.21	5.57	5.10	5.18	1.19
Sphere	5.00	1.13	5.35	5.09	5.16	1.13
Linear	3.85	1.60	5.23	3.98	4.17	1.40

¹Ratio=<Lv>/<La>

where C_v is defined as in Equation 3-30 and s , t and u are adjustable parameters.

The log-normal input function in Table 4-3 was produced using $s=3.5$, $t=1.0$, and $u=1.0$ in Equation 4-2. The Gauss-normal distribution function is for a standard deviation of 1.75 nm. The single sphere is the length distribution function for spherical particles 6.67 nm in diameter (i.e. $\langle L_v \rangle = 5.0$ nm). The linear function decreases from 1 nm to 10 nm.

Fourier analysis to determine both $\langle L_v \rangle$ and $\langle L_a \rangle$ was also performed on these artificially generated profiles. The program XNUMT was used to perform the Fourier analysis. The program uses steps of constant $\Delta \theta$ rather than steps

of constant Δs as is strictly correct to perform the Fourier transforms. (The derivation is given by Equations 3-8, 3-9, and 3-12 to 3-21.) Because real data has a constant baseline for only a few degrees of 2θ , and because of the length of time required to perform the Fourier transform for very long series, the Fourier analysis is performed only over the range of:

$$\theta_{mx} - \theta_{mr} = 12^\circ \text{ of } 2\theta.$$

Tables 4.1, 4.2 and 4.3 also show the results of Fourier analysis of these profiles. Error in the calculated average particle size increases from about 2% for 10.0 nm particles to as much as 40% for 1 nm lengths. The theoretical minimum observable size possible from a Fourier analysis of 12° of 2θ is about 0.8 nm. The average of $\langle La_1 \rangle$ and $\langle La_2 \rangle$ were used to determine $\langle La \rangle$ in the measured ratio: $\langle Lv \rangle / \langle La \rangle$ which also appear in these tables. These are both accurate to within 5% for average lengths greater than 3.0 nm.

Figure 4.2 shows an artificially generated length distribution function, and the LDF regenerated by taking the Fourier coefficients in steps of constant $\Delta 2\theta$ over a range of 12° of 2θ compared to the input function. The errors introduced by using these steps instead of steps of constant Δs are negligible. The negative initial VLDF (at lengths less than 2.0 nm) is due to truncating the peak at 12° of 2θ and the extension of the observed VLDF beyond the input VLDF is due to leakage.

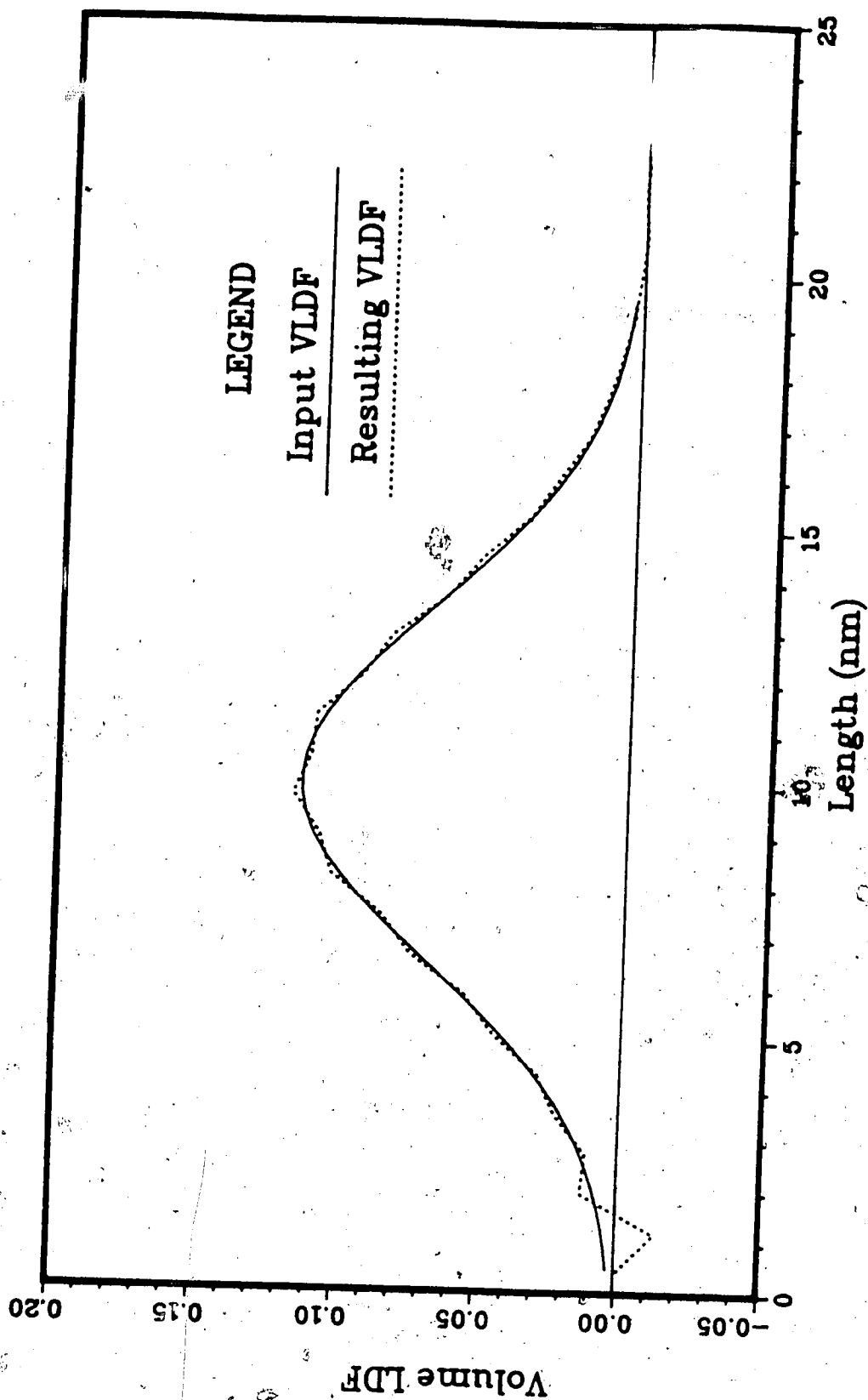


FIGURE 4.2 Fourier Analysis of a Numerically Generated Pure XRD Profile

4.3 Observed Profiles

The next step in the simulation was to numerically produce peaks which would be observed for these length distributions. The pure profiles were combined with the machine profile generated from a 7 parameter MVP fit of the measured machine profile. This resulted in the Fourier coefficients of the 'simulated observed' profiles. The inverse Fourier transform was then performed to produce the profiles.

The normalized coefficients for the machine profile were generated by program XFOR. In order to eliminate aliasing (which results in unstable oscillations in the Fourier coefficients at high frequencies) the machine profile was generated over a range of 2.5° of 2θ and mathematically expanded to the broader range using the method described by Klug and Alexander [20].

Program XNUMT performs the folding; given the Fourier coefficients of the machine profile, $G(j)$, and of the pure profile $F(j)$, the coefficients of the observed profile are given by the complex product:

$$H(j) = F(j) * G(j) \quad j=0,1,\dots,J$$

4-2

The observed profiles were then generated from these Fourier coefficients.

The methods of correcting for instrument broadening when using the Scherrer equation were tested using these numerically produced 'observed' profiles. (Since the fitting procedure corrects for $K\alpha$ broadening in the observed and standard peaks, this effect is not taken into account here.) Table 4.4 shows a comparison of the results obtained by correcting for instrument breadth using the 3 procedures given in Section 3.3.1. The Gaussian form of the correction is most accurate for all sizes and LDF's but there is some evidence that Taylor's geometric mean may be better for particle sizes larger than 10 nm. The accuracy of the method does not appear to be affected as the LDF becomes broader for a given average length.

Noise of zero mean and different standard deviations was added to the observed profiles using program XNOIS. The profile was then fit to the 7 parameter MVP function (Equation 3-44) using program XFIT. The program uses a Marquardt algorithm which was developed by W. Ball [31] and modified for this program. It is important to note that there are always at least two local minima in the best fit parameters corresponding to $b_1 \approx 0$ and $b_3 \approx 0$. These may or may not be the best parameters. For this reason, the program starts from the point:

$$b_1 = b_3 = (\text{peak height})/2.$$

Table 4.4 A Comparison of Different Methods of Correcting Observed Profiles for Instrument Broadening¹

LDF Type -----	True <Lv> _i ----- (nm)	Pure <Lv> _i ----- (nm)	Cauchy <Lv> _i ----- (nm)	Gauss <Lv> _i ----- (nm)	Taylor <Lv> _i ----- (nm)
Delta	10.0	10.08	12.21	9.67	10.87
Log-normal	4.45	4.56	5.09	4.56	4.82
Gauss-normal	5.00	5.10	5.76	5.09	5.41
Delta	5.00	5.08	5.75	5.08	5.41
Delta	2.00	2.09	2.31	2.19	2.25

¹ Scherrer constant, $K_s=1.0$, Breadth of standard profile $B_s=0.0040$ radians

The last step was to unfold the fit profile with the machine Fourier coefficients (Equations 3-20 and 3-21) to give the pure coefficients. The two main length distribution functions (area weighted and volume weighted) were then regenerated from these pure coefficients. These operations are performed by program XPROF.

The MVP fitting function (3-44) forces the length distribution function into a relatively broad form with either unimodal or bimodal nature. Because of the particle shape contribution to the length function, and because electron microscopy has shown that there is a range of

particle sizes, this is not a serious restriction on the length distribution function.

Figures 4.3 to 4.5 show several distributions with solid lines and with the length distribution functions extracted using the procedure described above in dotted lines. The LDF's have average lengths approaching the lower limit of detectability of XRD. These average sizes are similar to those in the catalysts studied. Figure 4.3 shows the result for a log-normal volume weighted input function. The parameters in Equation 4-2 are $s=3.5$, $t=u=1.0$. Note the excellent fit. Figure 4.4 shows the results for a linearly decreasing input function. The fit is poor at small lengths, owing to the sharp discontinuity in the VLDF. Figure 4-5 shows the poor fit which results from fitting the profile due to unisized 6.6667 nm spheres. Again, the MVP does not handle discontinuities well. It should be noted however that such discontinuities are not likely to occur in real catalysts.

The resulting area and volume average lengths are quite accurate for all of the input LDF's, even when approaching the lower limit of detectability (as in the linear profile). At worst, the error in $\langle L_v \rangle$ is about 5%, and in $\langle L_a \rangle$ is about 20%. The ratio of $\langle L_v \rangle / \langle L_a \rangle$ which is used to approximate the breadth of the LDF (and indirectly the particle size distribution) in the real catalysts is about 10% too low in the worst case. These results are summarized in Table 4.5.

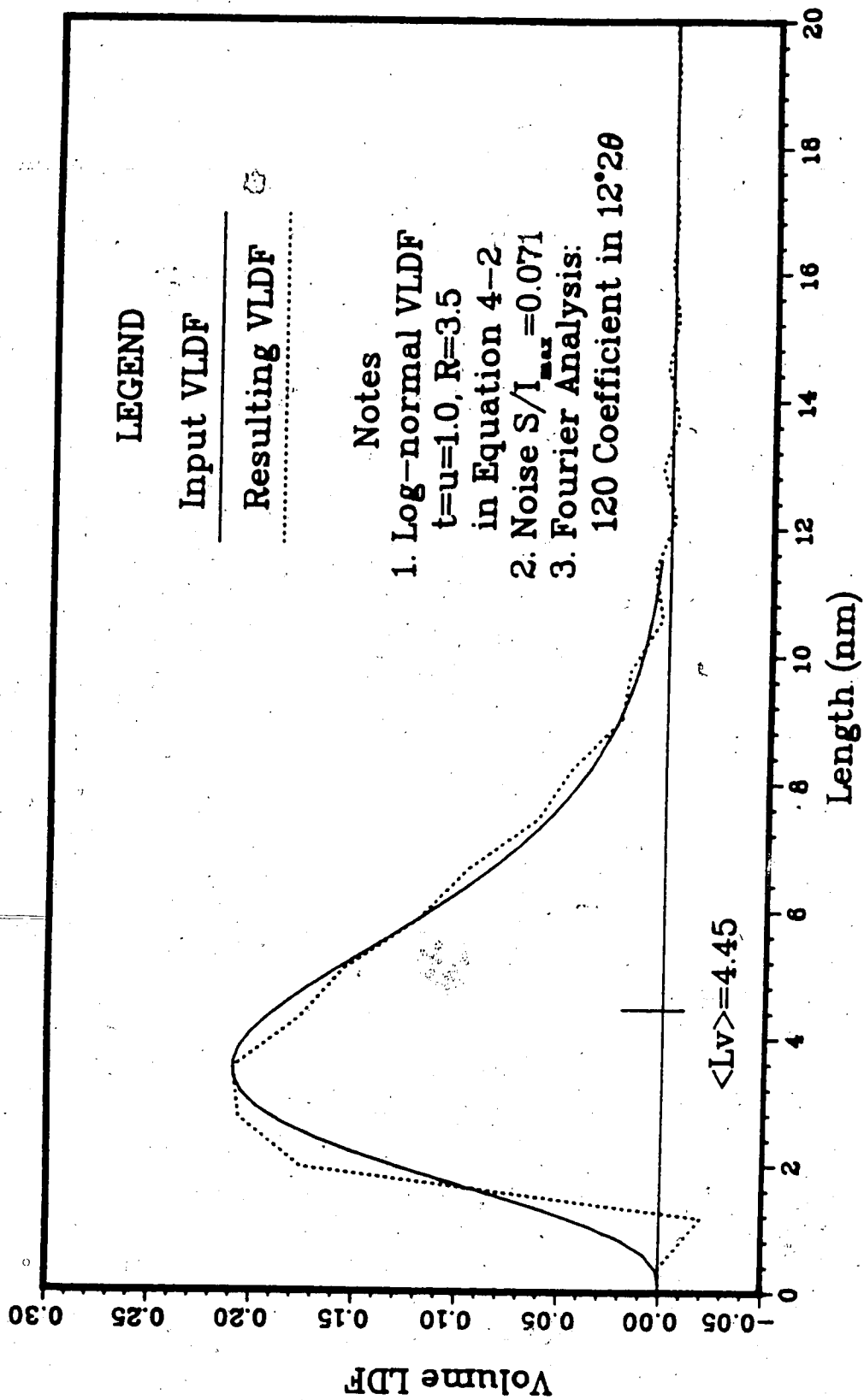


FIGURE 4.3 Fourier Analysis of Log-normal Volume Weighted Length Distribution Input Function

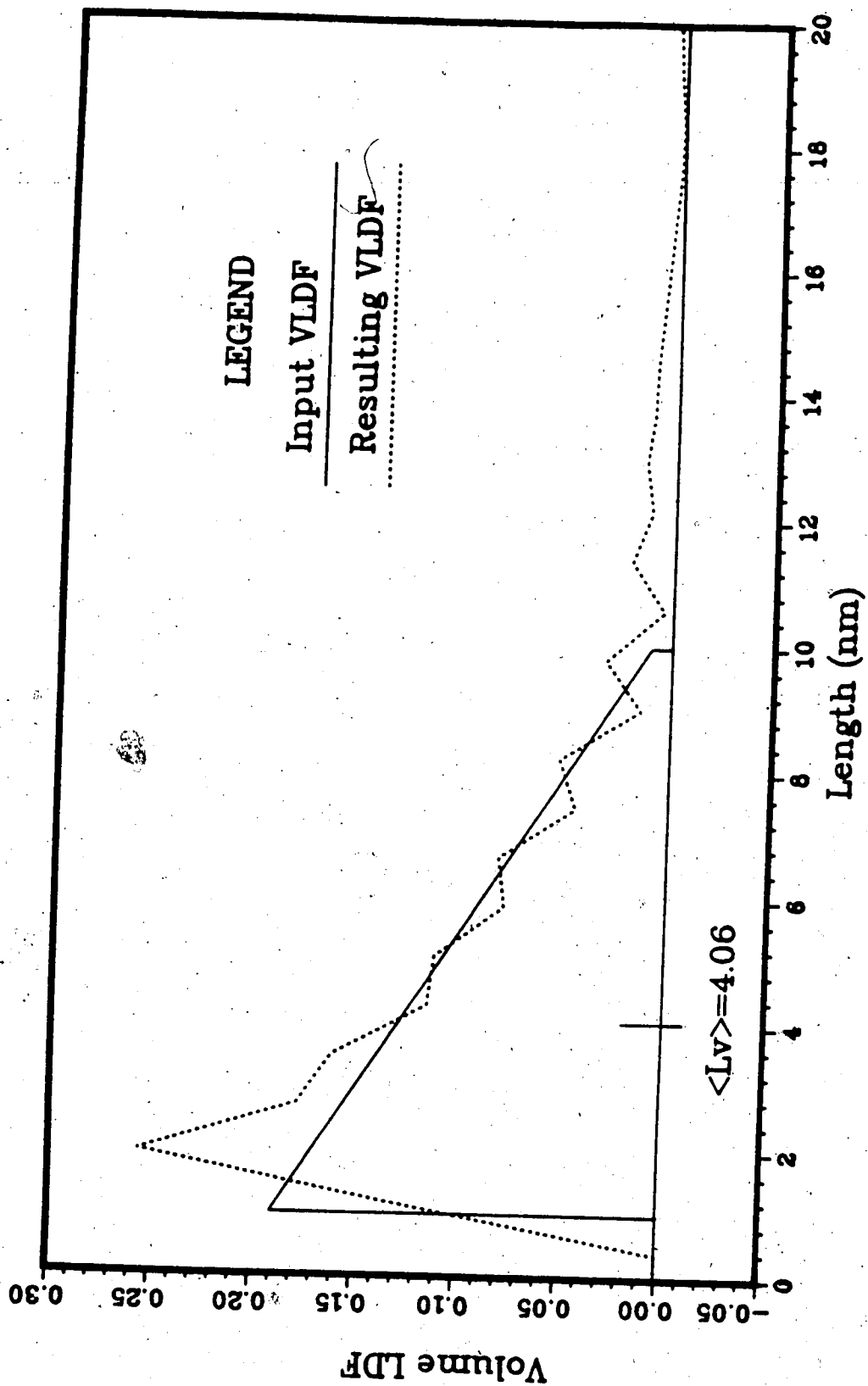


FIGURE 4.4 Fourier Analysis of Linear Volume Weighted Length Distribution Input Function

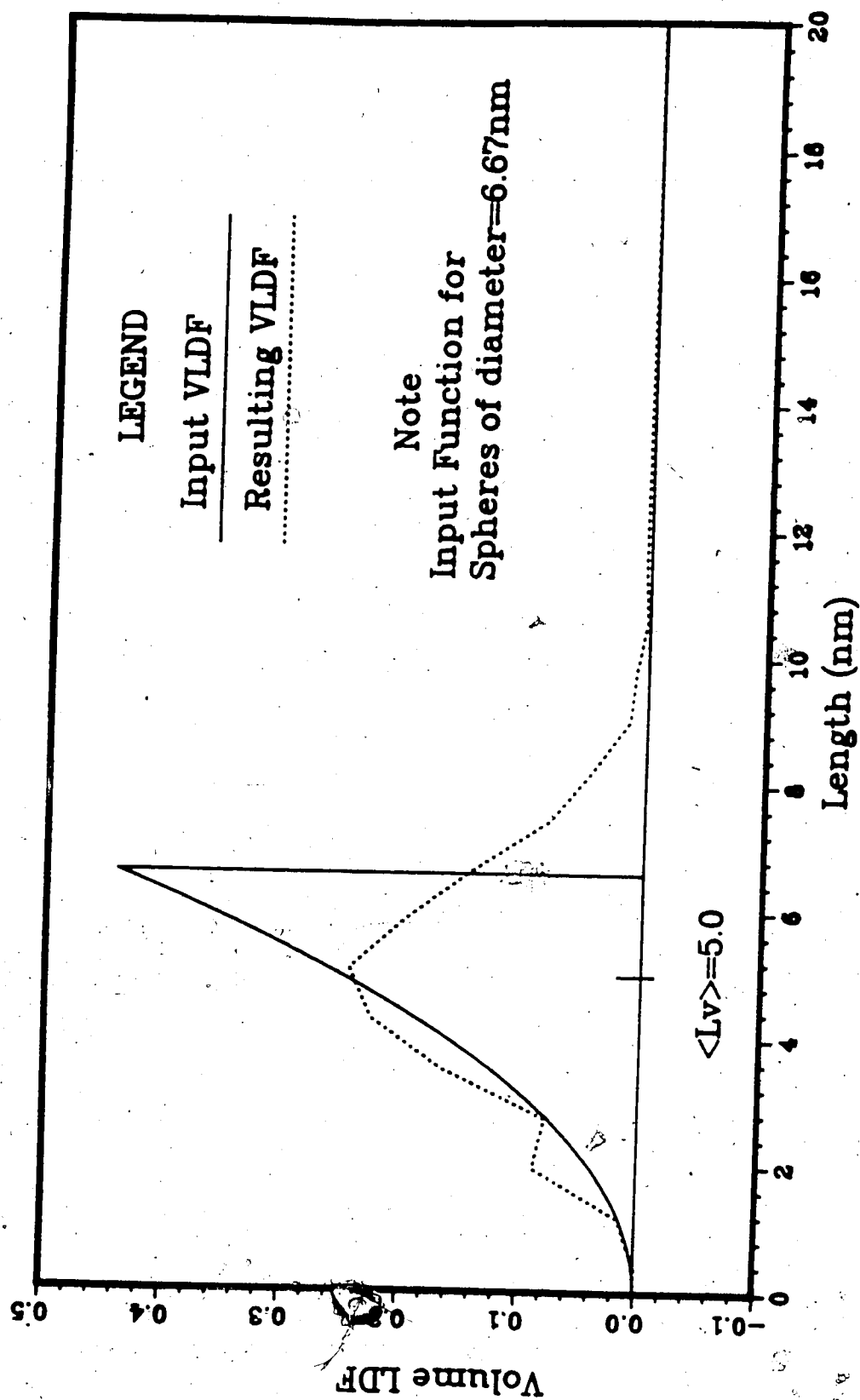


FIGURE 4.5 Fourier Analysis of VLDF for Spherical Particles

Table 4.5 Average Lengths Calculated from Complete Fourier Analysis Compared to the Input Average Lengths

VLDF Type	TRUE		FOURIER		Ratio ¹
	<Lv> (nm)	<La> (nm)	<Lv> (nm)	<La> (nm)	
-----	-----	-----	-----	-----	-----
Log-normal	4.45	3.49	4.57	3.84	0.932
Gauss	5.00	4.12	4.23	3.67	0.949
Sphere	5.00	4.44	5.03	4.53	0.989
Linear	3.85	2.41	4.06	2.85	0.892

$$^1\text{Ratio} = \frac{\langle Lv \rangle / \langle La \rangle \text{ (Fourier)}}{\langle Lv \rangle / \langle La \rangle \text{ (True)}}$$

4.4 Conclusions from the Numerical Study

Numerical study of artificially generated pure diffraction profiles point out several important facts. First, the integral breadth gives greater accuracy in using the Scherrer equation than does the width measured at half height. The results of the two methods approach each other as the distribution functions becomes narrower, and width at half height loses its accuracy as the LDF becomes broader.

The accuracy of both methods decrease dramatically for lengths less than about 2 nm.

Fourier analysis using steps of 0.05° of 2θ over an angular breadth of 12° of 2θ was found to give accurate results (within 5-10%) for area and volume weighted average lengths down to about $\langle L_v \rangle \approx 2.0$ nm. Errors increased significantly below this size ($\langle L_v \rangle$ is overestimated by about 40% at 1 nm and completely unreliable at 0.5 nm). For broad LDF's, significant errors are expected between the true LDF and the LDF resulting from Fourier analysis of the peak for lengths less than about 2 nm.

The techniques for analyzing observed profiles resulted in similar errors at short lengths. The curve fitting methods gave very good results for such realistic LDF's as log-normal and Gauss-normal, but caused significant leakage of any LDF with abrupt changes in shape (such as Dirac delta function LDF's). Another effect of the numerical method is that the observed LDF's can show no more than uni- or bi-modality (tri- and multimodality is hidden in the smoothed information). In general, precision in the observed LDF decreases as the true LDF becomes more complex.

5. EXPERIMENTAL

The experimental procedures involved heat treatment, sample preparation, and X-ray diffraction runs. Heat treatment of the catalysts in different atmospheres was performed to determine the effects on the supported metal. It is possible that the support might also be affected by the heat treatments so heat treatments were also performed on the support material alone. The exact shape of the support profile is important because it is removed from the catalyst profile by a weighted subtraction technique which will be explained subsequently. Table 5.1 shows the supports studied with their heat treatments. Table 5.2 gives the bimetallic catalysts and Table 5.3 contains the monometallic catalysts studied.

All the catalysts were prepared by impregnation followed by reduction in flowing hydrogen (see Graham et al. [29] for details). Also included are the results for average particle sizes determined by chemisorption. Recall that one must assume particle shape (here hemispheres are assumed) and adsorption stoichiometry (here 1 H atom/exposed metal atom) to calculate these average diameters.

Table 5.1 Supports Studied (All Alon γ -Alumina)

Identification	Pre-Treatment	Heat Treatment			Reduction ¹
		Atm	Temp °C	Time h	
A1	2 cm ³ 0.8N HCl/g Alon	-	-	-	Yes
A3-1 ²	0.05N HCl/g Alon	-	-	-	Yes
A3-2 ³	" "	-	-	-	Yes
A3-3 ⁴	" "	-	-	-	Yes
A9	distilled water	-	-	-	No
A11	" "	O ₂	800	16	Yes
A12	" "	H ₂	800	72	Yes

¹Reduction is defined as 2 h in flowing H₂ at 500° C following heat treatment

²First Packing

³Re-run with the same packing as A3-1

⁴Re-run after re-packing the sample

5.1 Catalyst Heat Treatment

Heat treatments were carried out in flowing oxygen and hydrogen in a Lindberg model 51748 laboratory furnace equipped with a Thermoelectric Selectrol temperature controller. Approximately 1 g of catalyst sample was broken into a coarse powder. The catalyst was then placed in a quartz U-tube with quartz wool plugs to prevent carry-over of fines.

Flowing gas was introduced into the U-tube at a controlled rate of from 1-2 ml/s (at STP). This purge was continued for about 10 minutes to ensure that the sample was superficially degassed. (Any chemisorbed oxygen should form

Table 5.2 Bimetallic Catalysts Studied (All catalysts 1%Pt+1%Ir supported on Alon)

Identification	Heat Treatment ¹		Reduction	Chemisorption Diameter ² (nm)
	Atm	Temp °C Time h		
PI-16		fresh ³	Yes	3.0
PI-2	O ₂	300 16	Yes	3.0
PI-8	O ₂	500 16	Yes	2.9
PI-12	O ₂	600 16	Yes	
PI-18	O ₂	800 16	No	0
PI-19	O ₂	800 16	Yes	
PI-14	H ₂	650 16	Yes	
PI-17	H ₂	800 16	Yes	

¹Reduction is defined as 2 h in flowing H₂ at 500°C following heat treatment.

²Chemisorption diameter assumes an adsorption stoichiometry of H/M=1.0 and hemispherical shape.

³All samples pre-reduced at 500°C before subsequent reduction.

water in the presence of H₂ at the elevated temperatures of the heat treatment, and should be quickly desorbed.) The samples were then heated to 100° - 150° C for at least 1 hour to desorb water. The temperature was then set. The temperature was controlled to within ±5°C for all treatments at temperatures above 300°C.

After the heat treatment, the furnace was opened and cooling occurred. Gas was left flowing until the furnace temperature was well below 200°C. After oxygen treatment, samples labelled "reduced" were elevated to 500° C in flowing hydrogen for 2 hours following this treatment. As

Table 5.3 Monometallic Catalysts Studied

Identification	Composition	Heat Treatment ¹		Chemisorption Diameter ² (nm)
		Atm Temp °C	Time h	
HP-2	4% Pt/Alon	O ₂ 600	16	9.5
HP-3	"	O ₂ 600	16	15.
HP-6	"	O ₂ 750	16	75.
HP-7	"	fresh ³		4.5
AP-1	1% Pt/Alon	fresh ³		2.6
AP-6	"	O ₂ 500	16	1.9
AP-8	"	O ₂ 600	1	2.4
AP-9	"	O ₂ 600	16	2.4
AP-10	"	O ₂ 800	16	20.
AP-11	"	H ₂ 650	16	2.8
AP-13	"	H ₂ 650	16	4.7
AP-14	"	H ₂ 800	1	4.0
AP-16	"	H ₂ 800	16	-
AI-13	1% Ir/Alon	fresh ³		2.1
AI-2	"	O ₂ 300	16	2.0
AI-4	"	O ₂ 400	16	7.9
AI-5	"	O ₂ 500	1	6.4
AI-8	"	O ₂ 600	16	11.0
AI-8 ⁴	"	O ₂ 600	16	11.0
AI-15 ⁵	"	O ₂ 800	16	-
AI-16	"	O ₂ 800	16	-
AI-12	"	H ₂ 650	16	3.0
AI-14	"	H ₂ 800	16	-

¹All samples reduced after heat treatment except where noted (Reduction is defined as 2 hr in flowing H₂ at 500 C following heat treatment.)

²Chemisorption diameter assumes an adsorption stoichiometry of H/M=1.0 and hemispherical shape.

³All samples pre-reduced at 500 C before subsequent heat treatment.

⁴Run before re-alignment

⁵Run after re-alignment

⁶Not reduced after heat treatment

can be seen, the majority of the samples were reduced. Samples were stored in air after removal. In some cases, small quantities of quartz wool were later detected in the samples but quartz peaks never appeared in the measured X-ray diffraction profiles.

5.2 Sample Preparation

Approximately 0.5 g of catalyst sample was placed in a small mortar and ground to pass through a 60-120 micron screen. It should be noted that the alumina particles are much smaller than this (in the order of 30 to 80 nm). The grinding is necessary to provide a smooth diffraction surface, to allow random orientation of the crystallites, and to reduce microabsorption rather than to reduce crystal size.

A new sample holder was developed because use of existing methods produced inadequate intensity, reproducibility to allow subtraction of the profiles. The new sample holder consisted of a stainless steel block 0.5 cm (3/8") thick into which a disc shaped hole 1.905 cm (3/4") in diameter was machined to a depth of 0.203 cm (0.08"). The cavity was filled with 0.45 ± 0.02 g of catalyst (weighed to the nearest milligram). Alternating tamping and filling ensured equal density throughout the sample. The surface was smoothed using hand pressure and a rotating glass microscope slide. Once compressed, the sample could be easily handled.

5.3 X-ray Diffraction

A Philips type PW1730/10 X-ray generator equipped with a PW1050/70 vertical goniometer was used. The X-ray tube (Philips type PW 233/20) had a copper anode and a nickel filter which eliminated the $\text{CuK}\beta$ X-rays from the incident beam. The diffracted beam was passed through an AMRAY Model E3-202 GVW-7794 graphite monochromator to reduce the background radiation before detection with a Philips PW1965/60 proportional detector. An incident slit width of 1.0° and a receiving slit width of 0.1° were used.

The results were obtained using a step scan of 0.05° of 2θ counting 100 s/step. (Due to the extremely narrow peaks, 'infinite' particle size standards were determined using 0.01° steps.) The detector was interfaced with the Chemical Engineering Hewlett-Packard 1000 computer system and data was stored on discs with magnetic tape back-up.

Data was stored as 'angle-intensity' pairs, in the form of an integer number (100 times the angle in degrees of 2θ) and a real number of intensity in counts/second calculated by dividing the integer total number of counts by the time per step. This operation was performed by program RXRAY. Transmission errors resulted in 0 to 5 bad points (out of 280 data points) in the raw data; These were always easily identifiable by a missing digit. The points were manually corrected by interpolation between neighbouring points and labelled in the data file with an "I" after the correction.

Scans were carried out initially over a wide range of angles (typically 34° to 50° of 2θ). This allowed verification of the accuracy of the subtractions by examination of the background far removed from the peaks. For face centred cubic metals, the most intense X-ray peaks correspond to the (111) Miller indices, but the Pt and Ir peaks overlap with the (222) peak of the η -alumina. The (311) metal peak is smaller, but does not interfere with any alumina peak. Using the method described in Data Analysis, the support peak could be eliminated by performing a point-by-point subtraction of the support profile (appropriately weighted) from the catalyst profile. It was found that the Pt(111) and the Ir(111) peaks gave the best signal to noise ratio defined as:

$$S/N = \frac{\text{Maximum Peak Intensity}}{\text{Std. Dev. in Background Intensity}} \quad 5-1$$

For this reason, only the (111) and (200) peaks were intensively studied for most of the samples. Except for repeatability checks, only one run was made on each catalyst sample.

5.4 The Standard Sample

In order to correct observed peaks for instrument broadening effects, standard profiles (from metal with negligible size and strain broadening) must be generated.

The ideal standard has the same peak location, X-ray absorption characteristics as the catalysts to be studied, has particle sizes greater than 200 nm, and has no internal strains. These characteristics were obtained by mixing 1% platinum black (produced by the Matheson, Coleman, and Bell Laboratory Supply Co.) with Alon. This mixture was heated to 700°C for 1 hour in flowing H₂ to relieve any internal strains in the platinum. This mixture has identical X-ray absorption characteristics and peak locations to 1% Pt/Al₂O₃ catalysts.

X-ray diffraction was performed using step scans of 0.01° of 2θ/step, each step being 100 s long. This was necessary because the peaks were so narrow that significant information losses (especially peak height) resulted from steps of 0.05° of 2θ. Taylor's microabsorption equation (Equation 3-4) was used and the area of the Pt (111) peak for the standards of 0.42 radian·count/s compared to about 0.75 radian·count/s for the catalyst samples to estimate that the standard crystallites are about 2000 nm in diameter.

6. DATA ANALYSIS

Data generated by the step scans were gathered and stored using program RXRAY and were manipulated using several computer programs. The first objective of this data analysis was to eliminate the support profile effects from the catalyst profile to give the metal profile. The next step was to quantify the fraction of metal detected. Extensive error analysis was also performed, and attempts were made to quantify the lower limit of detectability.

Particle size and length distribution information was extracted from some of the profiles.

Several runs using pure support material were averaged to eliminate deviations due to surface irregularities and to reduce noise due to counting statistics. Averaging was performed by program XRDAV which matches angles to perform point-by-point averaging of intensities.

6.1 Removing the Support Profiles

For catalyst samples, the most important correction required in order to study the metal profile is to remove the effect of the support profile from the catalyst profile. Figure 6.1 shows 3 typical XRD patterns. (The profiles are separated vertically by 5 c/s for clarity.) Profile 'A' is of pure Alon support material, profile 'B' is due to a fresh 1% Pt-1% Ir catalyst and profile 'C' is the result of a heavily sintered Pt-Ir catalyst. The expected centroids of the Pt and Ir (111) and (200) peaks appear at the top of the

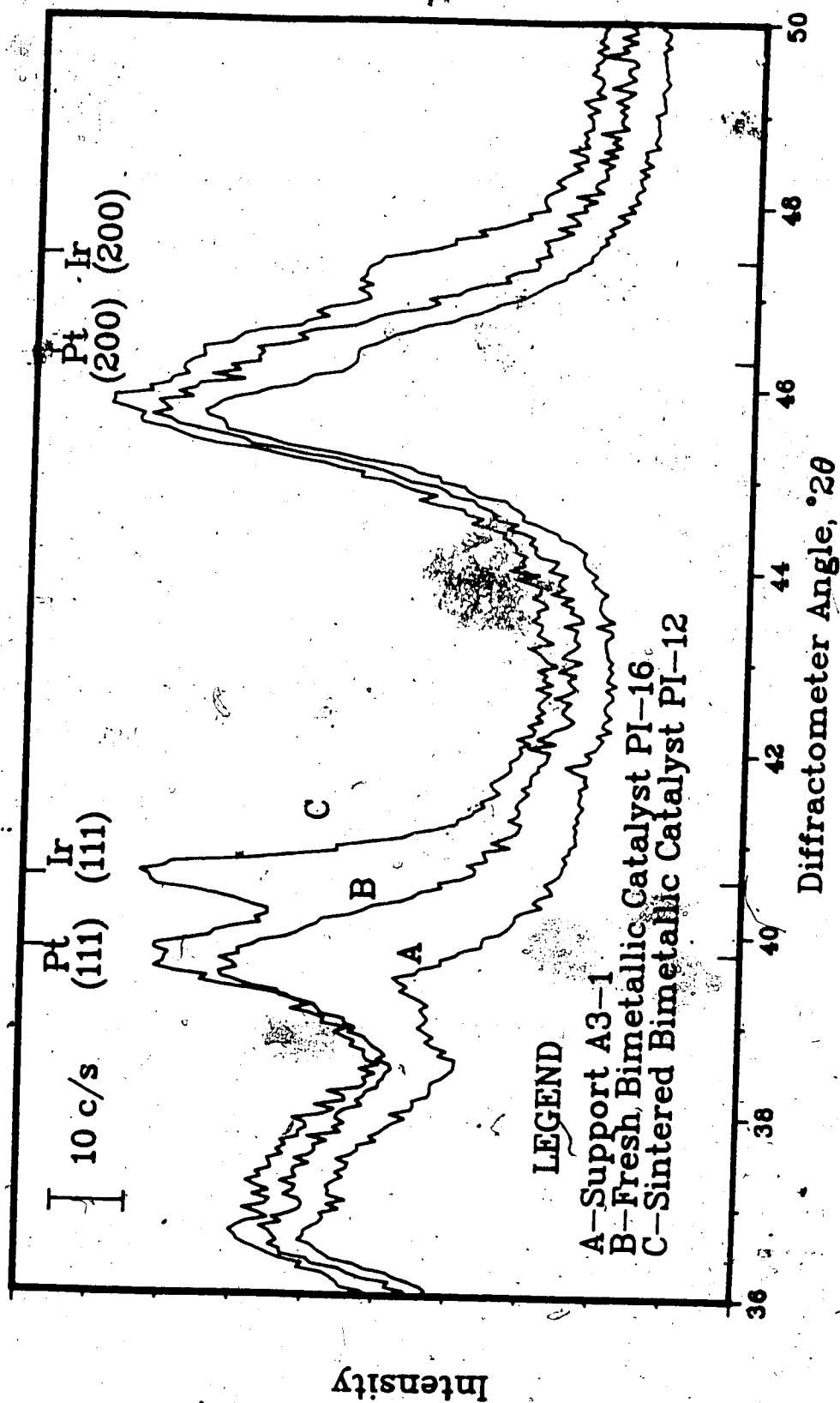


FIGURE 6.1 Three Typical X-ray Diffraction Patterns

figure. It is very difficult to analyze the metal peaks in these patterns because of the overlap of the alumina (222) peak with the Pt and Ir (111) peaks, and of the alumina (400) peak with the Pt and Ir (200) peaks.

The technique used to correct for this overlap is a weighted point-by-point subtraction of the profile due only to the support material from the profile for the catalyst. Using Equation 3-4 and the fact that the linear absorption coefficient of Pt is almost 10 times as large as that of the alumina in the sample imply that the ratio of the alumina peak intensities in the catalyst are less than those in the pure alumina.

Recognizing that K_{xyz} , the mixture density, ρ_m , the density of the support, ρ_i , are constant, the only differences between the catalyst sample and the support sample are the average absorption coefficient, μ_m , the support particle absorption factor, τ_i , and the concentration of the support, C_i . For a 1% - 2% metal catalyst, $C_i = 0.985 \pm 0.005$ and $\tau_i \approx 1.01$ (assuming that the alumina particles are about 0.1 mm in diameter). The product of these two terms is very close to unity. The ratio of the support peak intensities in the catalyst to those in the standards should then be very nearly the ratio of the linear absorption coefficient in the standard to that in the catalyst. If the peaks have the same shape in both the catalyst and the standard, using a weighting of 0.950 to remove the alumina profile from 1% metal catalysts and 0.907

for 2% catalysts should give good baselines for the metal profiles. This was verified.

It was noted, however, that the baselines after these weighted subtractions were not zero within the noise levels observed. Application of a linear baseline correction (as recommended by Delhez et al. [24]) of 0-2 counts/second produced baselines much closer to zero intensity. (The baselines were in almost all cases higher at the lower end of the 2θ scale.) This correction is probably required because of differences in water adsorbed on the alumina surfaces between runs. There was also some instrumental drift which may account for some of the non-zero baselines.

6.2 Angle Dependent Factors

There are several so-called angle dependent factors which should be eliminated in a rigorous analysis of X-ray profiles (see for example Delhez et al. [23,24]). These are collectively termed the Lorentz-Polarization factors and they appear in square brackets in the term T_3 in Equation 3-3. However, Delhez et al. [23] point out that these effects are negligible for $2\theta < 30^\circ$. It was found that these effects are small for the (111) metal peaks and so the correction was not made for peaks in this work.

6.3 Fraction of Metal Detected

The amount of metal detected by XRD can to a large degree be quantified. The program XINTG uses the trapezoidal rule to determine the integrated areas of the peaks. (More precise methods were not used because of the large number of data points, and relatively large variances of the baselines.) After the area in the region of the (111) peaks of Pt and Ir was corrected for catalyst X-ray absorption coefficient, and metal concentration (again using Equation 3-4), this area was compared with the average result for several mono-metallic catalysts with particle sizes in the range of 8-50 nm. This ratio is an indication of the fraction of metal detected.

The following procedure was used to determine K_{111} in Equation 3-4 (where λ refers to either Pt or Ir). Equation 3-4 can be re-written in terms of a factor, Y' :

$$Y' = K_{111} \tau_l = I_{111} \frac{\mu_m \rho_l}{\rho_m C_l}$$

6-1

using values of $(\langle \mu \rangle - \mu_l) = 4100 \text{ cm}^{-1}$ and $R=0$ and $R=50 \text{ nm}$ (corresponding roughly to monatomic metal and to particles of about 100 nm in diameter, the upper limit of the sensitivity of crystallite size determination by X-ray line broadening), and an incident angle of about 20° the microabsorption particle factor from Taylor ranges from 1.0 to 0.972.

Within experimental accuracy, τ_i for the metal can be taken as unity for all catalysts studied (but not for the Pt black standards). The right hand side of Equation 6-1 should thus be constant if all the metal present in the catalyst is detected. Noting that:

$$\begin{aligned}\mu_m &= (\mu/\rho)_m \cdot \rho_m \\ &= [(\mu/\rho)_s C_i + (\mu/\rho)_i (1-C_i)] \rho_m\end{aligned}\tag{6-2}$$

where subscript s refers to the support, m to the mixture and i to the metal. It can be shown that Equations 6-1 and 6-2 reduce to the equation developed by Nandi et al. [13] for the ratio of the intensities of the peaks of 2 catalysts with different loadings of the same metal on a given support. Their equation also assumes that $\tau_i \approx 1.0$. We can now define a new variable, Y, by:

$$\begin{aligned}Y &= I_{111} (\mu/\rho)_m a / C_i \\ &[=] \text{radian} \cdot \text{count} \cdot \text{cm}^2 / (\text{s} \cdot \text{g})\end{aligned}\tag{6-3}$$

where the factor $(\mu/\rho)_m$ is independent of the sample density, and is a function only of the concentration of components in the sample. The factor 'a' is used to correct for instrumental changes. Since profiles run after the

diffractometer maintenance in January 1983 were about 14% more intense than those run before that date, the factor is set at 1.0 and 0.86 for runs made before and after that date respectively.

In order to check the hypothesis that τ is indeed unity, the parameter γ is tabulated with $\langle L_v \rangle$ as determined by the Scherrer equation for 11 catalysts in Table 6.1. The areas were determined by integrating the γ parameter modified Voigt function over the range $-0.5 < s < 0.5$. These functions were determined by fitting metal profiles of appropriate width using the Marquardt algorithm in program XFIT. This technique proved much less sensitive to differences in baseline corrections than direct integration. The metal profiles to be fit were generated by point-by-point subtraction of the appropriately weighted support profiles from the catalyst profiles, followed by a linear baseline correction of the resulting metal profile to 50° of 2θ .

When the fact that catalyst AI-16 may well have experienced loss of metal due to vaporization of IrO_3 is considered, all 8 of the points where $\langle L_v \rangle$ is greater than 10 nm lie within 20% of the average. The average value of γ is $\gamma = 2110$ c/s with a 95% confidence interval of 161 c/s.

Three catalysts with very small crystallites show significant reduction in integrated area. (AP-16, AP-11, and AP-14 show 19%, 24%, and 40% reduction, respectively.) This is easily explained (as did Pope et al. [6]) by

Table 6.1 Determination of the parameter Y in Equation 6-1.

Catalyst	<L _v > (nm)	Area (c/s)	Time ¹	Y	Used ²
AI-4	12.5	0.780	a	2240	Yes
AI-5	10.2	0.644	a	1850	Yes
AI-8	14.9	0.653	b	2180	Yes
AI-8	11.4	0.733	a	2110	Yes
AI-16	25.7	0.527	b	1760	No
HP-2	11.0	2.214	b	2110	Yes
HP-3	10.8	2.193	b	2094	Yes
HP-6	21.7	1.895	b	1810	Yes
AP-10	28.9	0.866	a	2488	Yes
AP-14	4.6	0.376	b	1256	No
AP-11	2.9	0.481	b	1606	No
AP-16	3.8	0.512	b	1710	No

Note: All catalysts reduced 2hr at 500 C in H₂ after treatment.

¹ 'a' indicates run after re-alignment in January 1983, 'b' indicates run before re-alignment.

² Used in determining the average value of Y

assuming that about 1/5, 1/4, and 2/5 of the metal atoms respectively are in crystallites below the lower limit of detectability (about 2 nm).

6.4 Error Analysis

Errors were studied by comparing 2 runs of support material (Alon) with the same treatment. Unscaled profiles for several different heat treatments were subtracted point-wise using program XRM. The resulting profiles were integrated and standard deviations were calculated over both short regions (10 points, or 0.5° of 2θ) and over the whole profile. The difference between two profiles A3-1 and A3-3

appears in Figure 6.2, along with a profile generated by GAUSN, a Hewlett-Packard routine which produces noise of similar standard deviation (1.5 c/s) and zero mean.

The auto-correlation coefficients of these two profiles are plotted in Figure 6.3. The k-th autocorrelation coefficient of a time series is defined for a series of N terms, each with magnitude I_t , by:

$$C_k = \frac{1}{N-k} \sum_{t=1}^{N-k} (I_t - \langle I \rangle)(I_{t+k} - \langle I \rangle) \quad 6-4$$

Note that C_0 is ordinary variance. The large value of C_0 followed by small coefficients for all other k's indicate that the noise is truly random. Large coefficients for the second and third coefficients followed by a decline would indicate deviations in alignment from run to run. If coefficients are large up to say the seventh to tenth coefficient, then noise is not random but there are in fact significant peaks.

Several runs were made on support profiles to determine the source of this random noise. Figure 6.4 shows two subtracted profiles, one being the difference between two runs made without repacking the sample, the other with repacking the sample holder. The noise is essentially random in both cases but $S=1.45$ for the repacking, while $S=0.76$ for the runs without repacking. If the two sources of error, the variation in the X-ray intensity and the variation due to sample packing are independent and random,

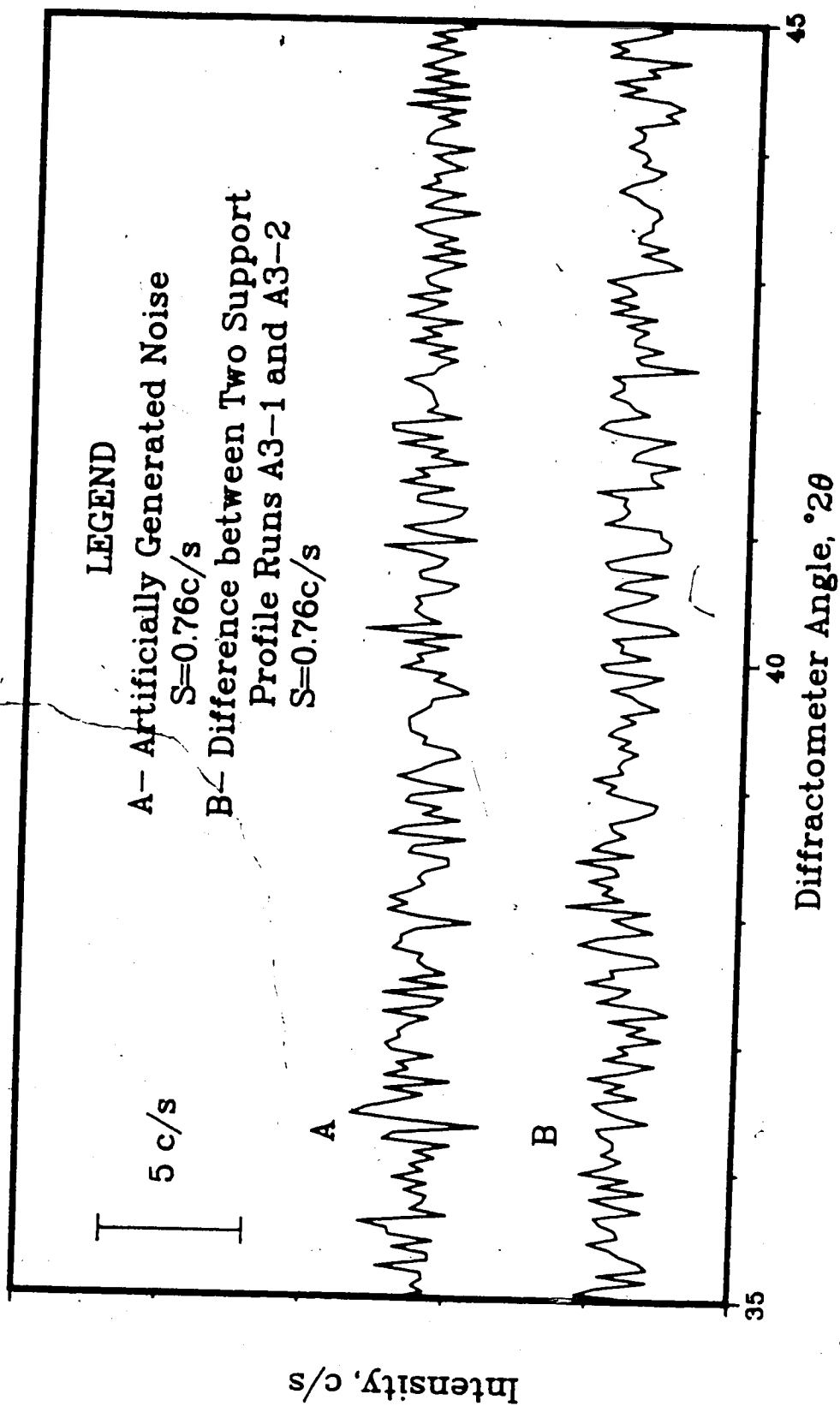


FIGURE 6.2 Comparison of the Difference between Two XRD
Runs and Random Noise

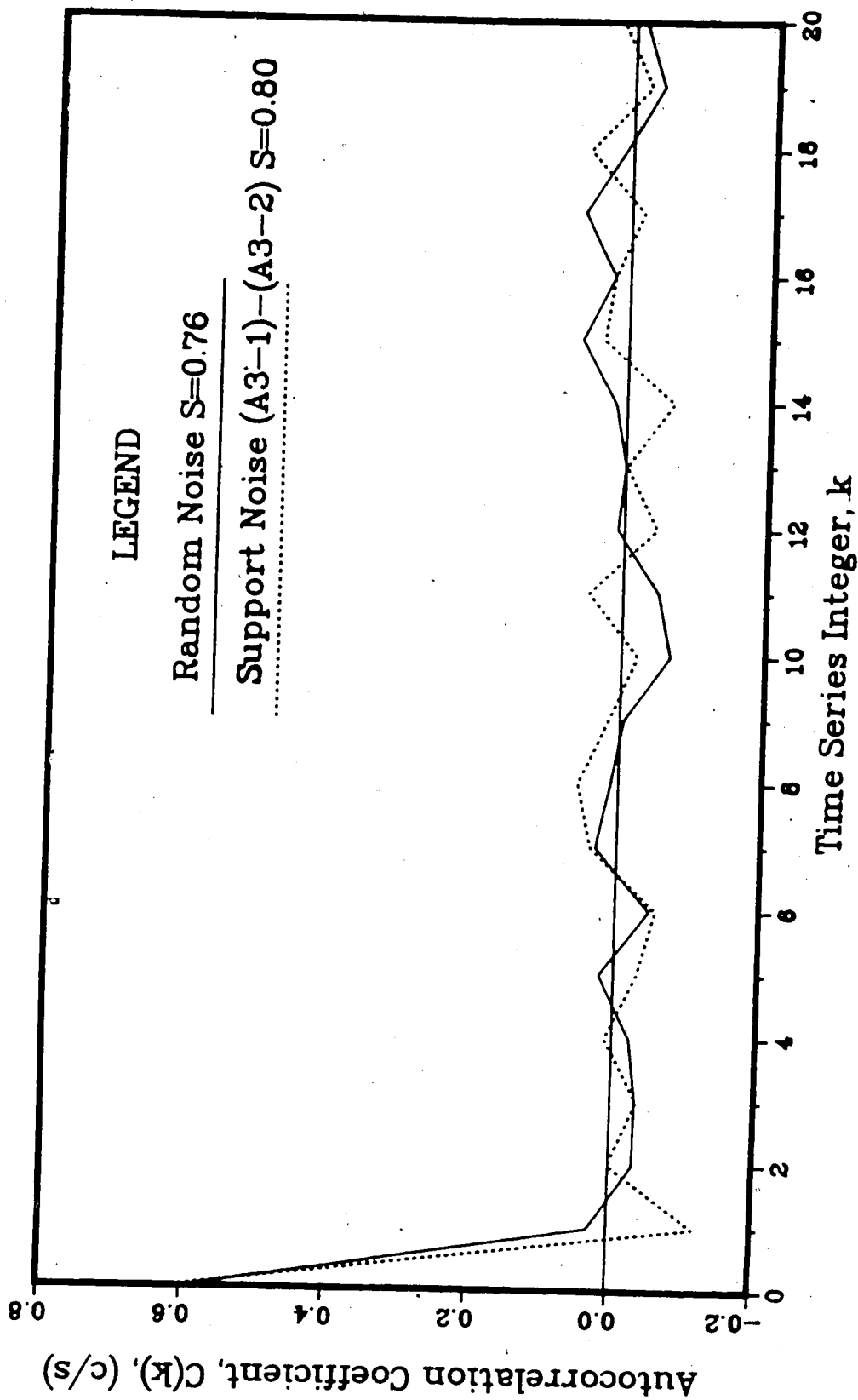


FIGURE 6.3 Comparison of Autocorrelation Coefficients for Support Profile Noise and Artificially Produced Noise

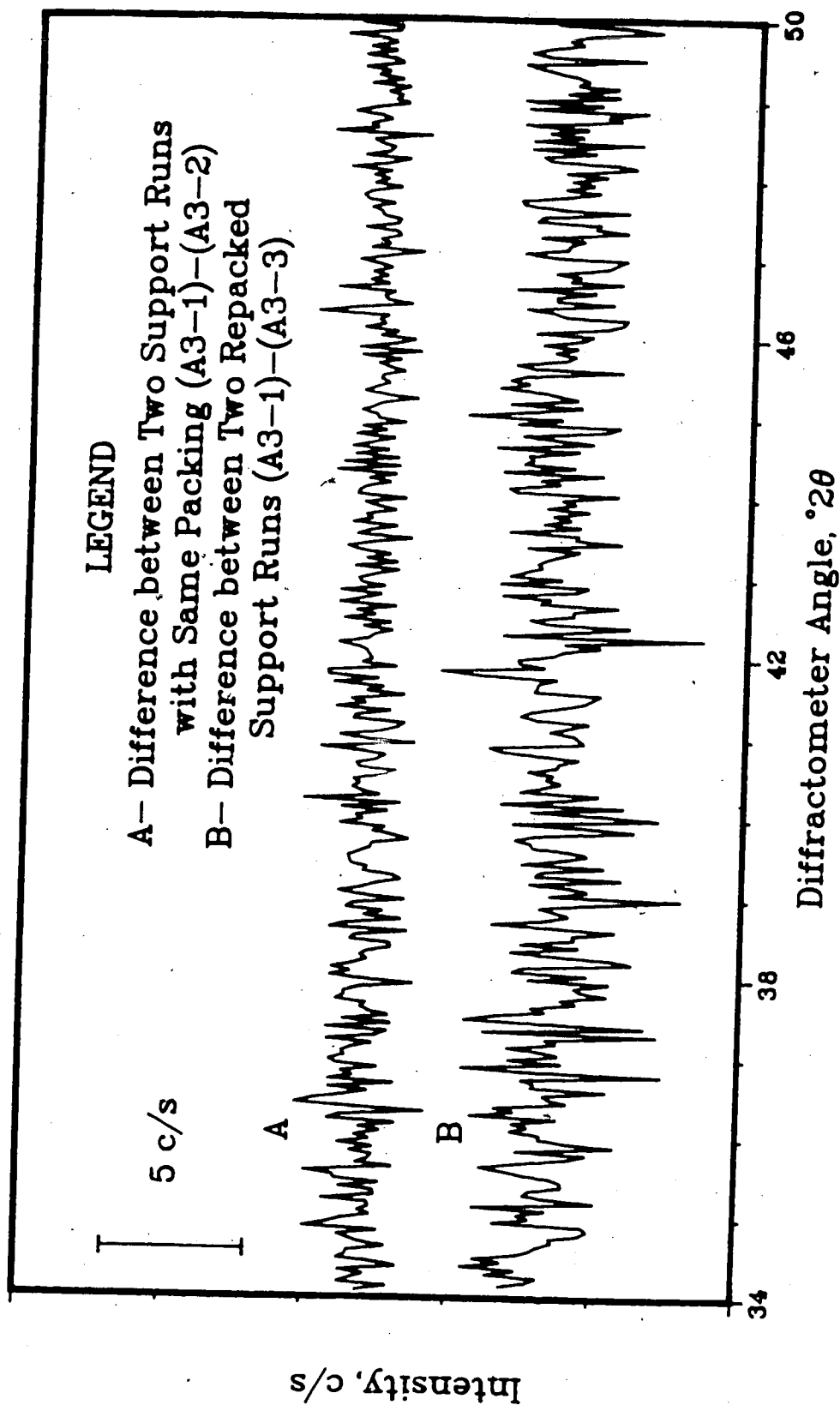


FIGURE 6.4 Effect of Sample Packing on Noise in XRD Profiles

variances are additive (that is total observed variance for repacking is the sum of squares of the contributing standard deviations). The deviation due to packing is thus $S=1.23$. Only marginal error reduction is possible from slower scan rates (which correspond to re-running without repacking). Significant improvements in the signal to noise ratio can be made using two or three repacked runs on each of the support and catalyst samples.

A significant source of systematic error is the change in the support crystal structure with heat treatment. Figure 6.5 shows the effect of heat treatment on the support pattern. The (311), (222) and (400) peaks of the alumina are noticeably sharpened by the heat treatment. The atmosphere has relatively little effect on this change. Fortunately, the majority of this effect occurs at temperatures at or below 500°C , and relatively little change occurs above this temperature. Subtractions were made using heat treated supports where possible. However, peaks of 3-4 c/s were sometimes observed in the subtracted profiles. It is assumed that the heat treatment is the source of these deviations, possibly with some added effect due to the interaction between the supported metal and the support. This may be due to changes in the support crystallinity, or to epitaxial growth of the metal. It is important to note that the location of these small 'peaks' is not fixed, but appears to move from about 36.5° of 2θ (the expected location for all γ -alumina (222) peaks) to about 38.0° of 2θ

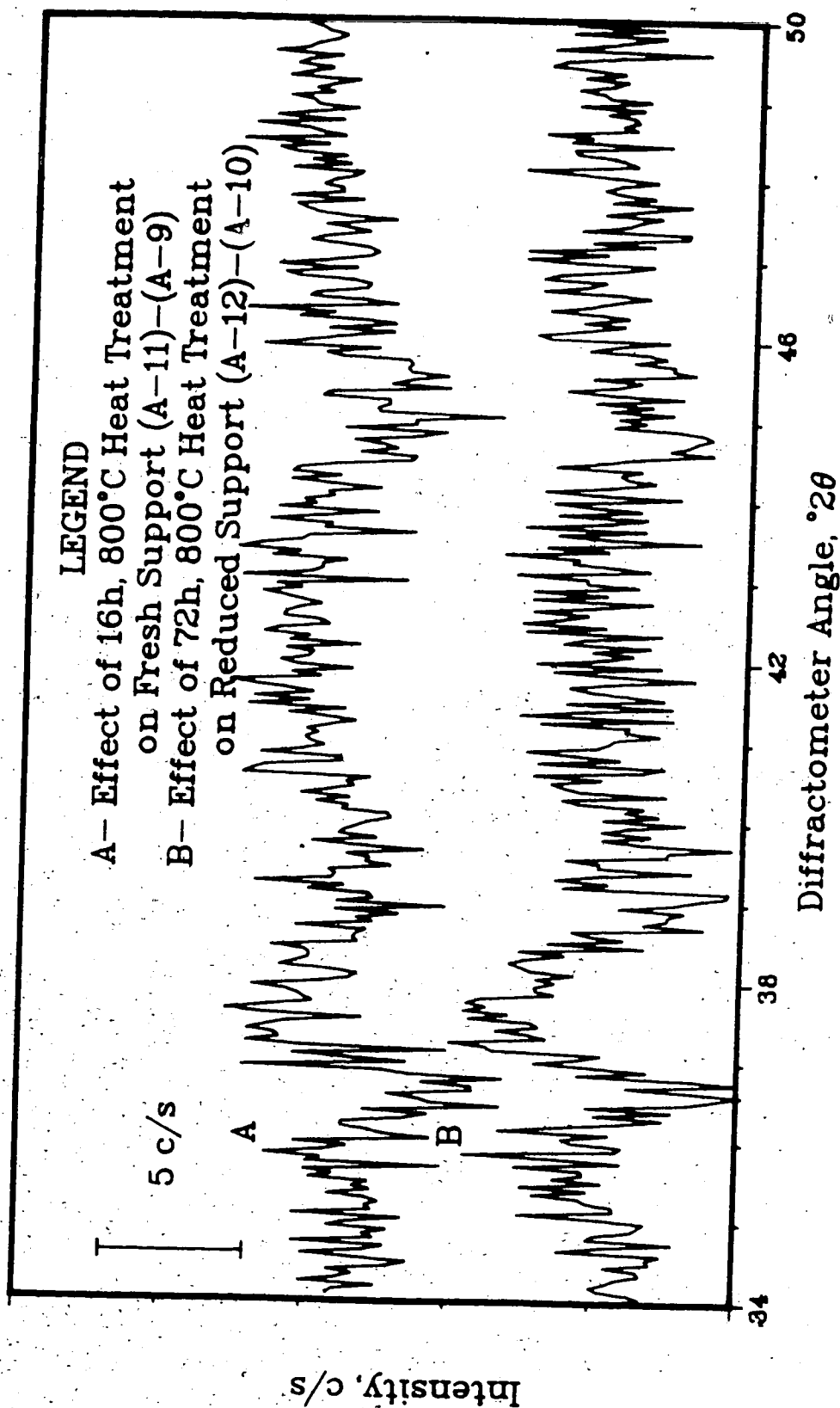


FIGURE 6.5 Effect of Heat Treatment on Support Patterns

which is about midway between the Al_2O_3 (222) and (311) peaks. The intensity is variable from 0-4 c/s and is poorly correlated with the heat treatment.

Because of the proximity of the alumina (222) peak to the Pt(111) peak, peaks with very low intensity must be analyzed with care. Since the alumina (311) peak grows larger than the (222) peak, this is a useful tool to distinguish between metal and support peaks for very small metal peaks.

6.5 Limits of Detectability

There are two major sources of error which contribute to the lower limit of detectability. The first source of error is random variation in the profile due to X-ray quanta counting statistics. This results in noisy backgrounds and in uncertainty about the height of the X-ray tails. For the purpose of this work, the lower limit of 'significant profile intensity' due to statistical variations is taken to occur when the 75% confidence interval for 10 raw data points about the fit curve crosses zero intensity. Recalling that the 75% confidence interval is given by:

$$C_{75} = 1.15S/\sqrt{N}$$

6-5

where:

$$N = 10$$

$$S \cong 1.5 \text{ c/s}$$

Substitution into Equation 6-5 gives $C_{7.5} = 0.55$ c/s. Thus any information about length distribution functions derived from the peak tails less than 0.5 c/s intensity is very imprecise at best. This value can be improved upon by using longer step times and repacking samples followed by profile averaging.

The other principle source of uncertainty relates to the fitting function. Owing to the strong emphasis placed on the intense regions of the peak, (since fits are made about the centroid of the peak for only a few degrees around the peak) the tails give very little information to the fit. Relatively large errors (easily of the order of 50% of the profile height at 3° of 2θ from the centroid) do not add significantly to the sum of the squares of the errors. For this reason, a lower limit of significant profile intensity due to the parameter fit could be defined as some fraction, say 1% of the maximum peak height.

It is frequently stated, (for example Ganesan et al. [11] and Sashital et al. [10]) that the first two or three Fourier coefficients are not used in determining the length distribution function due to errors in the baseline. The Fourier analyses carried out about 12° or 24° of 2θ give information in increments of about 0.78 and 0.39 nm respectively. This means that at best, the lower limit of detectability is $2a = 0.8$ nm (see equation 3-25) for a Fourier period of 24° of 2θ .

However, as Delhez [23] points out, this is due to incorrect baseline correction, causing the well-known 'hook' effect in the Fourier coefficients. In this condition the second derivative of the Fourier coefficients is initially negative. (This would correspond to a negative LDF which is not possible.) The correction normally made for this condition is linear extrapolation of $Fr(j)$ to $j \rightarrow 0$ from the point where $dFr(j)/dj \approx 0$. This amounts to 'zeroing' the LDF for very small lengths. It immediately defines the lower limit of detectability. Because of the fit function, this zeroing was rarely required for catalyst metal profiles.

There are also limits imposed by numerically evaluating the second derivative. The difference formula used in this work used 4 points to calculate the second derivative. It was observed that this method produced less oscillatory behaviour than the simple central difference formula (which uses only 3 points) at high frequencies. It has the disadvantage of smoothing some of the information in the profile over 4 Fourier numbers rather than 3. The formula used was:

$$\frac{d^2 Fr(j+1/2)}{dj^2} \approx \frac{Fr(j-1) - Fr(j) - Fr(j+1) + Fr(j+2)}{2} \quad 6-6$$

This imposes a lower limit of detectability of $L=1.5a$ which

corresponds to 0.6 nm for a Fourier range of 24° of 2θ . Note, however, that in almost all cases, the two previously mentioned lower limits of detectability are at larger lengths than the limit imposed by the numerical method. This means that although we can calculate LDF's down to $L=1.5a$, they are of questionable value.

Figure 6.6 and Equations 3-21 and 3-25 give a geometric justification for the rule of thumb that the first three Fourier coefficients should not be included in any length distribution analysis. The lower limit of the narrow period, $R, \approx 6^\circ$ gives a lower limit of detectability of about 1.6 nm. It also demonstrates that for catalysts with large particle sizes, much higher lower limits of detectability should be used than for similar loading with smaller particle sizes. A final reason that small metal clusters cannot be detected is that they lose metallic character as the number of atoms in a cluster is reduced. There is controversy in the literature about exactly when this occurs, but it is clear that when a cluster is smaller than the lattice parameter of a unit cell (0.392 nm for Pt, 0.384 nm for Ir) X-ray diffraction no longer obeys the normal laws. It is possible that metal clusters exist on support surfaces in layers as thin as 1 atomic layer. These would not be detectable using XRD.

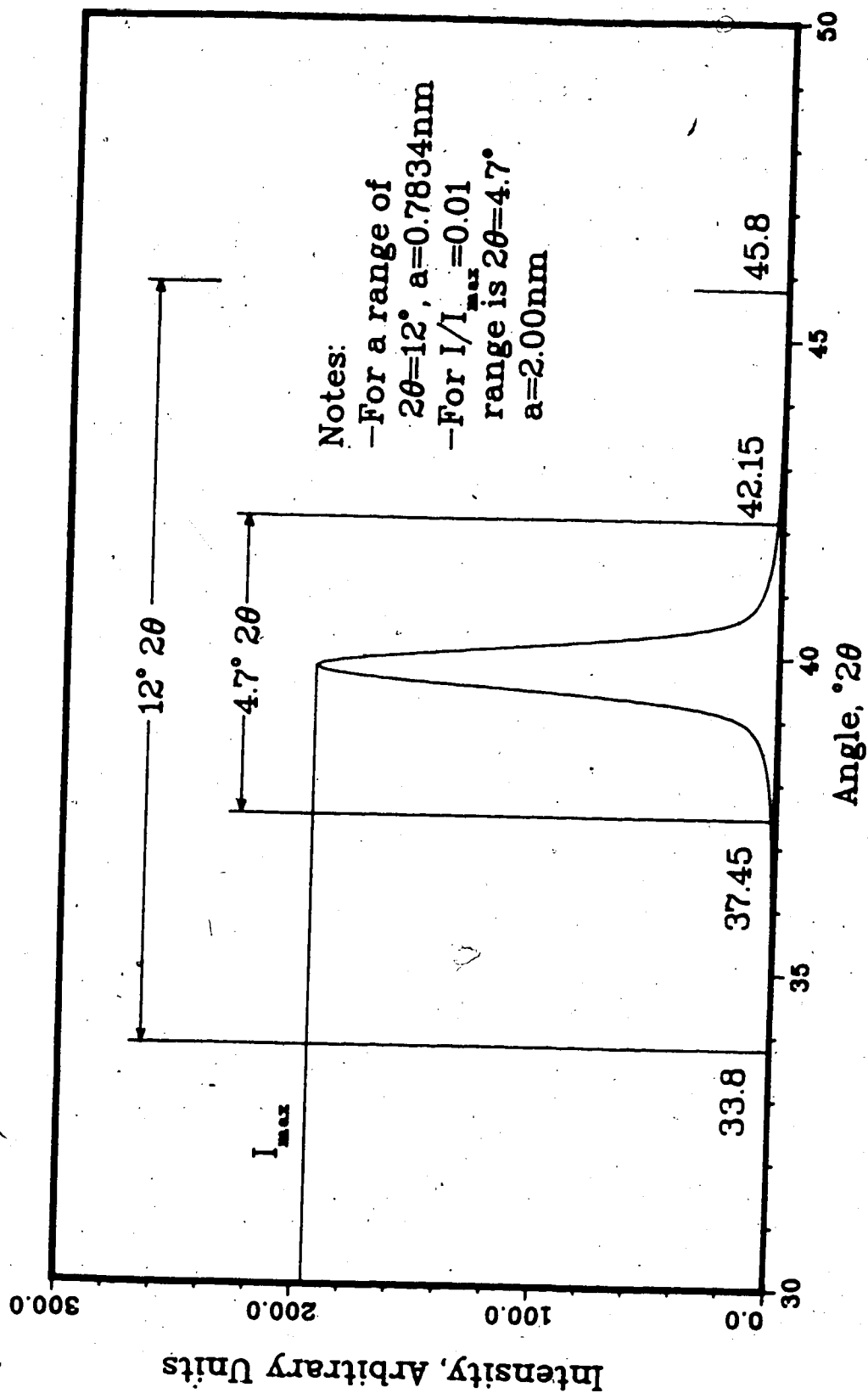


FIGURE 6.6 Lower Limit of Detectability

7. RESULTS

7.1 Introduction

Many different insights were drawn from the X-ray diffraction data. These have been arranged in order of decreasing certainty.

The effect of heat treatment on particle size and the nature of the alloys which exist in bimetallic catalysts was investigated qualitatively. It is very difficult to be quantitative about this because the broadening effects due to concentration gradients within the metal particles are superimposed on the size broadening effects. The next section deals with quantitative average sizes - weighted both by area and by volume. The possibility of strain broadening, and the effects of shape on apparent particle lengths is given for one catalyst. The ratio of these weighted average sizes gives information about the breadth of the PSDF. The LDF was also extracted for several of the heavily loaded catalysts and it, in combination with some assumptions about the typical particle shape gives much more detailed information about the PSDF.

7.2 Phase Studies

Figure 7.1A shows the influence of heat treatment in a reducing atmosphere (flowing H_2) on the bimetallic Pt-Ir catalyst. The support profile has been removed by the point-by-point subtraction procedure described in 'DATA

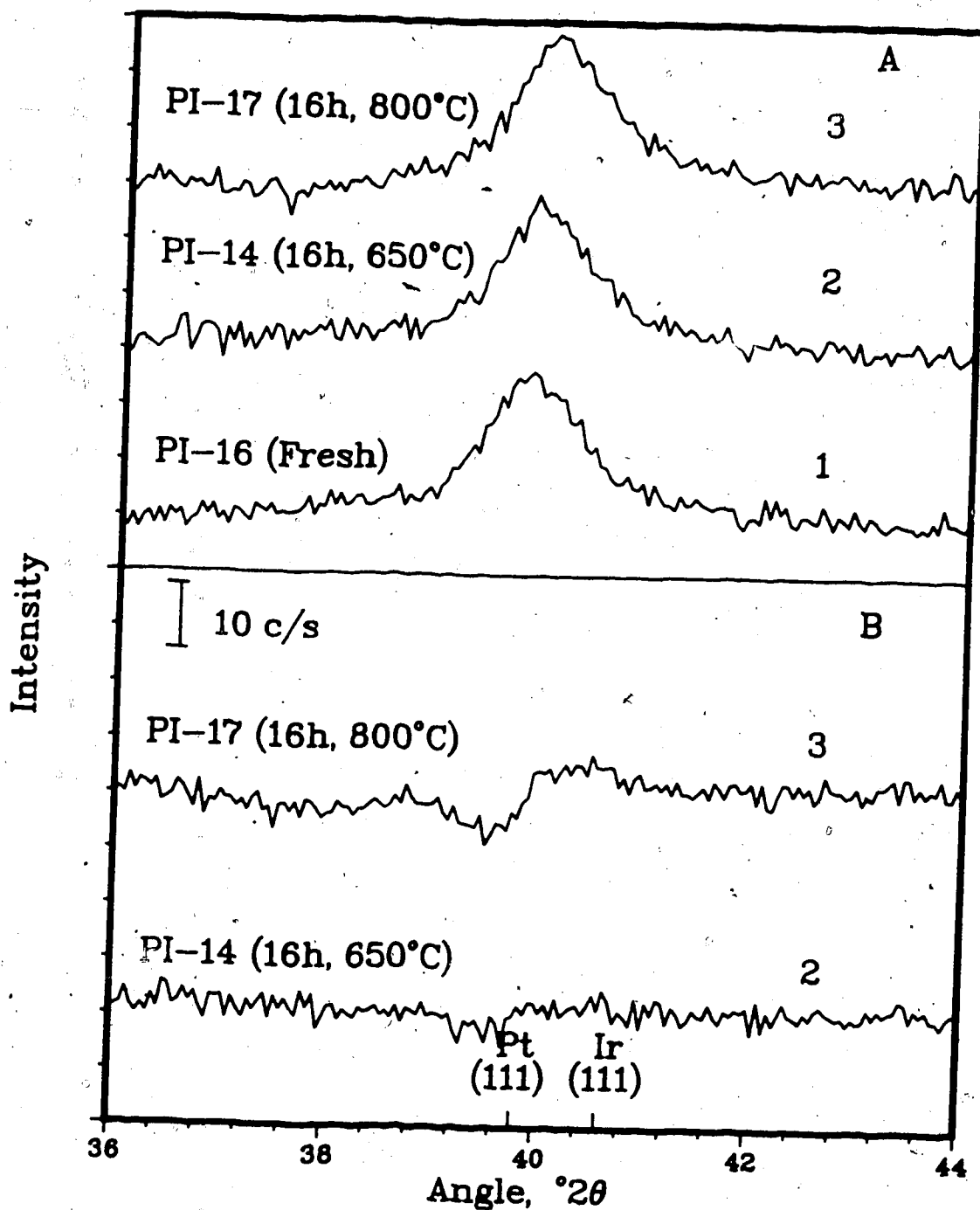


FIGURE 7.1 Influence of Hydrogen Treatment on XRD Patterns for 1%Pt-1%Ir/Alon
 A) Alon Pattern Subtracted from the Indicated Catalysts
 B) PI-16 Pattern Subtracted

ANALYSIS'. The peak corresponding to the (111) metal plane shows that the fresh catalyst has strong platinum character. However, as the temperature of heat treatment increases, the peak moves toward the location of the Ir(111) peak. This is more clearly shown in Figure 7.1B which is the (unscaled) point-by-point subtraction of the fresh catalyst profile from the profile of the heat treated catalyst. The decrease in intensity of profile 7.1B (3) at about 39.8° of 2θ and slight increase in intensity of this profile at about 40.5° of 2θ are clear indications of this shift.

Figure 7.2A shows the effect of heat treatments in an oxidizing atmosphere. (All of these samples were reduced in hydrogen at 500°C for 2 hours after the heat treatment in flowing oxygen.) The oxidizing heat treatments show much larger changes than those treated in reducing atmospheres. The effect is also opposite: instead of becoming more homogeneous, the Pt-rich and Ir-rich clusters tend increasingly to separate with increasing temperature. The effect appears to be much greater on the iridium than on platinum at 500°C and 600°C . Figure 7.2B shows these changes more clearly by showing the point-by-point subtraction of the fresh catalyst profile from the other profiles. Essentially no effect is observed after 16 hours in O_2 at 300°C , but for 500°C , large Ir clusters have formed while the platinum-like particles have reduced in size. Upon treatment at higher temperatures, both types of crystallites increase in size. However, at 800°C , the

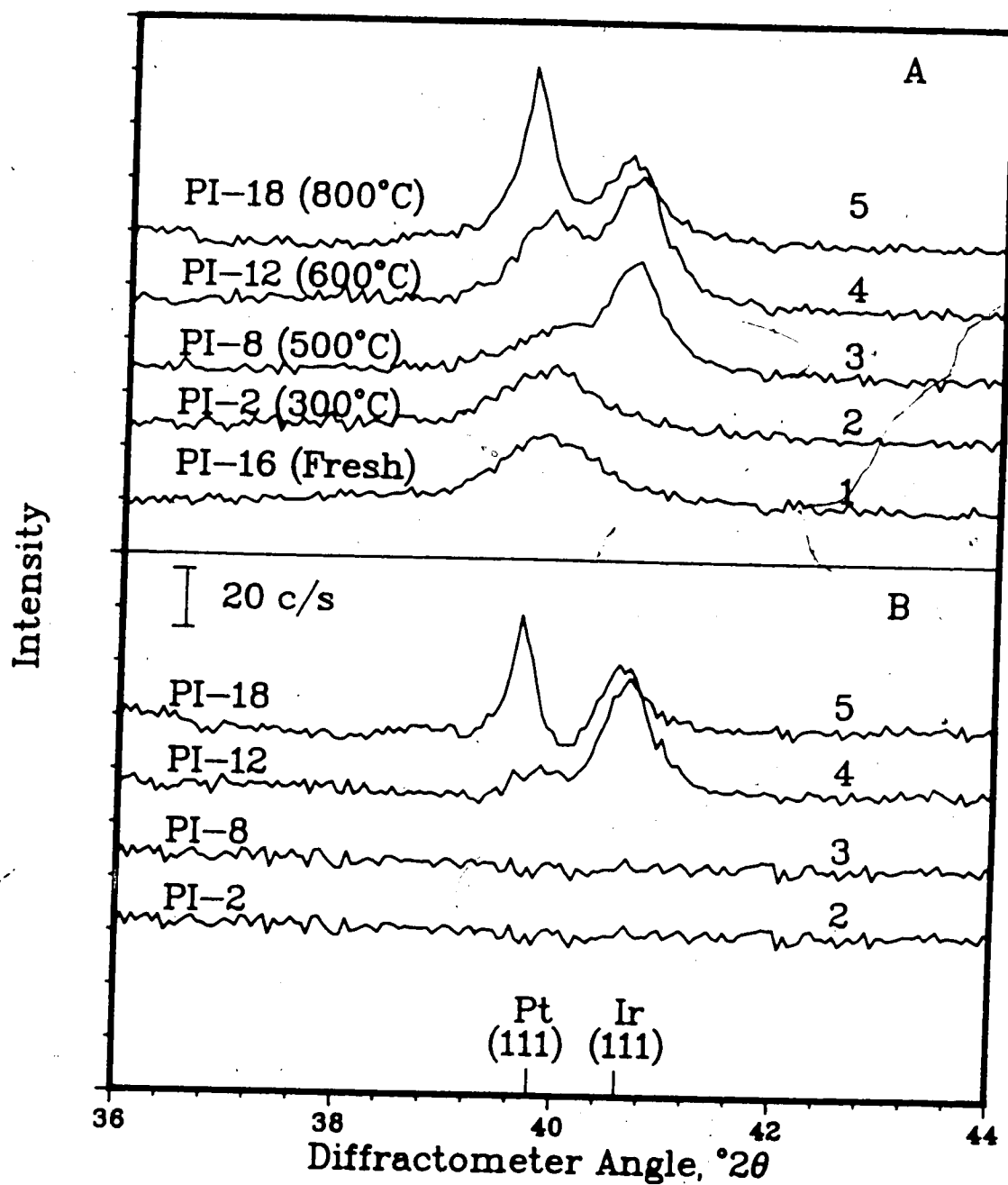


FIGURE 7.2 Influence of 16h Oxygen Treatment with Reduction on XRD Patterns for 1%Pt-1%Ir/Alon

A) Alon Pattern Subtracted from the Indicated Catalysts

B) PI-16 Pattern Subtracted

intensity of the peaks from the iridium-like profiles is smaller than at lower temperatures. This is probably due to the evaporation of Ir as IrO_3 . Solid IrO_2 has a significant vapour pressure of IrO_3 at these temperatures in the presence of oxygen (Schaefer [31]).

A final group of subtracted profiles is shown in Figure 7.3. These profiles are the result of three catalysts treated at 800 °C for 16 hr in flowing oxygen, but not reduced after heat treatment. Profile 7.3B is due to a 1% Pt catalyst which shows the large Pt crystallites which are the result of this treatment. Profile 7.3C is from a 1% Ir catalyst. Note that no Ir metal is detectable, but that peaks occur in the location of IrO_2 crystals. Figure 7.3A shows that the bimetallic catalyst looks very much like the separate (and independent) sum of the other two catalysts: Pt exists as large Pt crystallites, Ir exists as large IrO_2 crystallites.

7.3 Strain-Shape Effects

In order to show that internal strain is negligible, a 4% Pt catalyst (HP-3) was chosen for multiple peak analysis. This relatively high loading was necessary in order to reduce the relative errors for the higher order peaks such as the (311) and (222) peaks which have low intensities. The peaks were first fit with the 7 parameter modified Voigt function, and the integral breadths were compared. Three

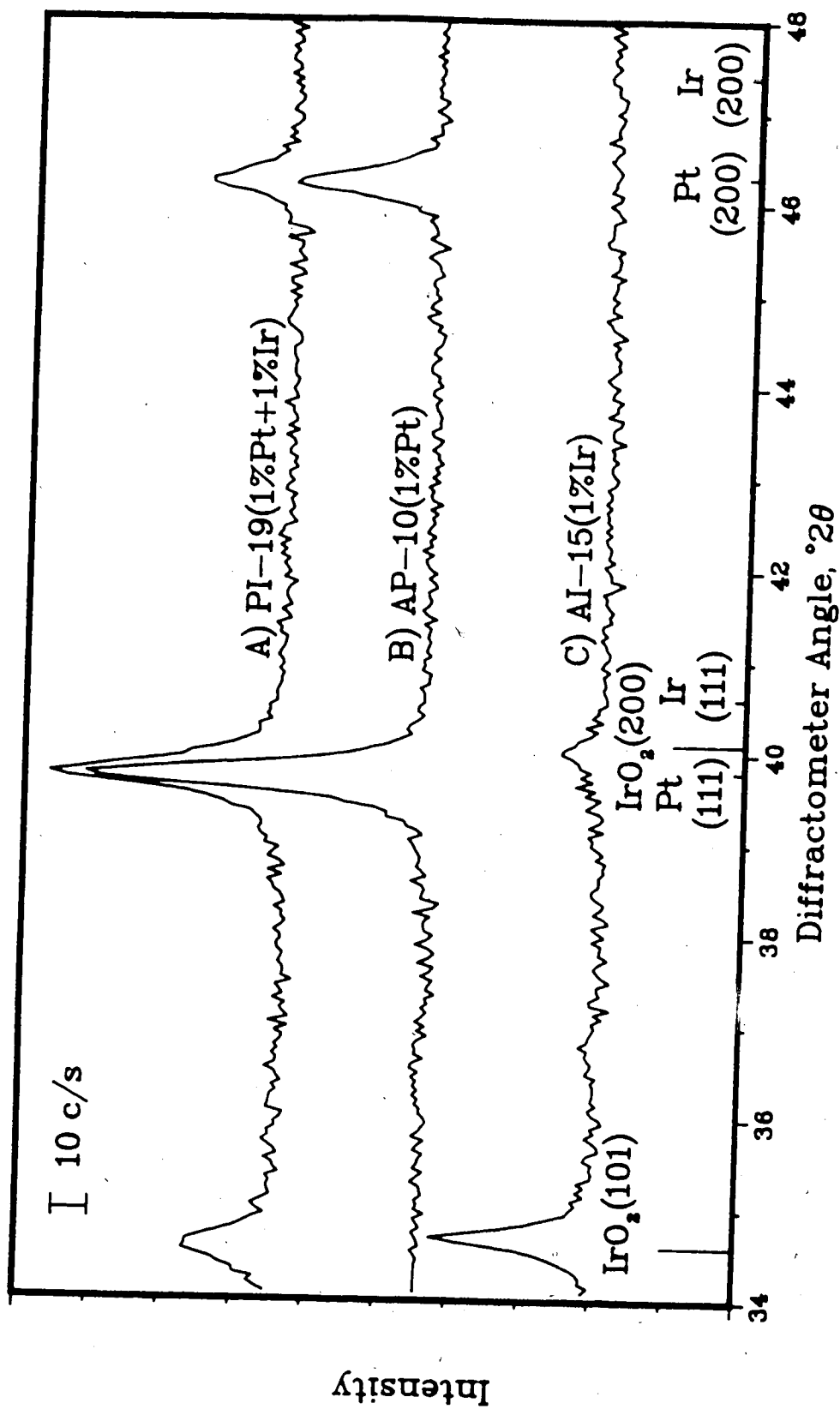


FIGURE 7.3 Influence of 800°C 16h Oxygen Treatment with No Reduction on XRD Patterns for Alon Supported Catalysts

numerical runs were made on the (220) peak, using different assumptions about the background, and although considerably different MVP (Modified Voigt function Parameters) resulted from each run, the height, half-width, and integral breadth were always within 0.5% of the average value. The Cauchy and Gaussian proportion of the breadths had large deviations (in the order of 20%), so Delhez's method for removing the machine broadening from the peaks was not used.

The apparent volume average lengths for the first 5 reflections of catalyst HP-3 appear in Table 7.1. The profiles were corrected as pure Cauchy and as pure Gaussian (Equations 3-7 and 3-9) and the geometric average pure integral breadth was used in the column titled 'Taylor'.

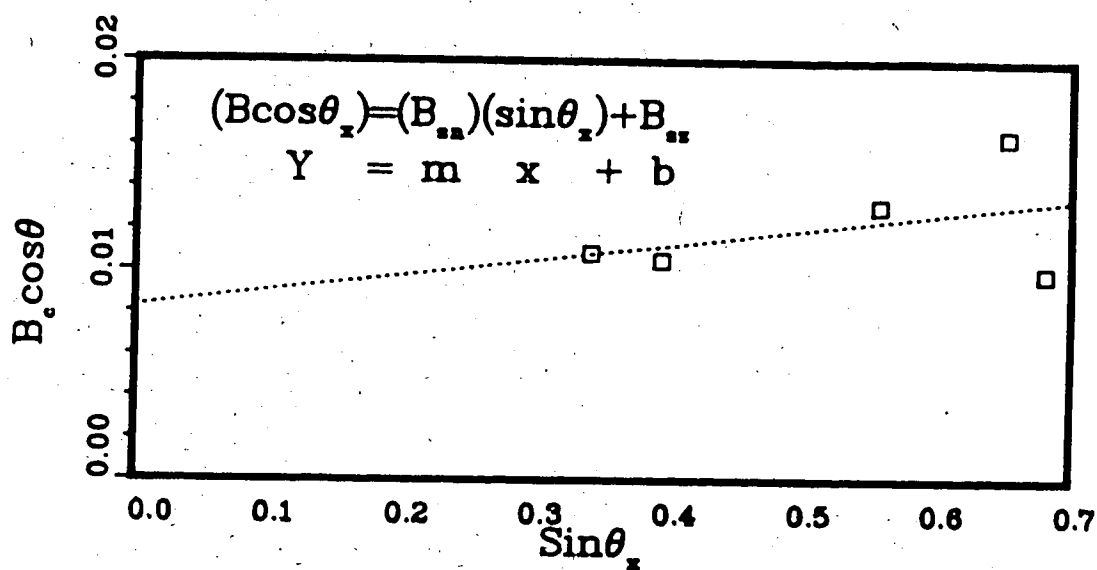
The ratio of maximum length to minimum length is about 1.2. The Scherrer constant for different shapes shows a maximum ratio of about 1.4 for tetrahedral geometry (Taylor, [18]). The relative magnitude of the Scherrer constant, K_s , is not the same as that calculated for tetrahedra by Stokes and Wilson, however, this depends on the plane which is chosen to be the base of the prism. It is clear from the results, especially of the (111) relative to the (222) peaks, that there is only slight (if any) systematic increase in the breadth of the peaks with increasing order and thus microstrain in the Pt crystallites is negligible. Further shape studies were not carried out because of the large number of planes possible and thus the complexity of the problem.

Table 7.1 Size-Strain Analysis of Catalyst HP-3

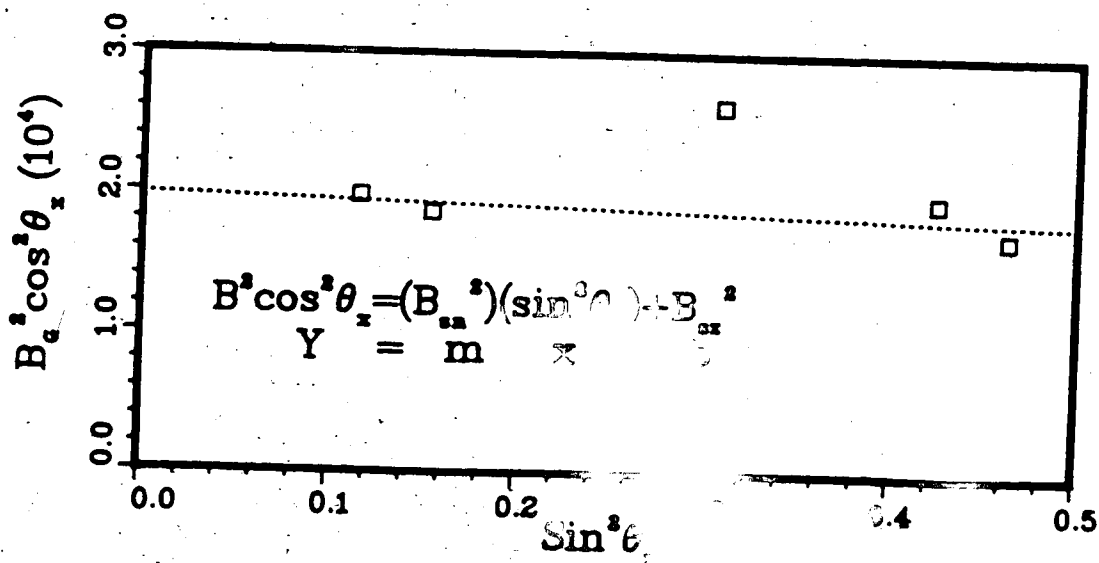
Peak -----	Breadth B^m (radians) -----	Length by different Methods <L _v >nm		
		Cauchy -----	Gaussian -----	Taylor -----
(111)	0.01549	14.3	11.0	12.5
(200)	0.01532	14.7	11.3	12.9
(220)	0.01998	11.8	9.5	10.6
(311)	0.02259	12.8	9.4	11.0
(222) ¹	0.01852	15.6	11.8	13.5

¹ Estimated $B^s = 5.0 \times 10^{-3}$ radians (large relative error expected)

Figure 7.4 expresses the same results in a different manner. This figure shows plots of Equations 3-13 and 3-14 as described in Section 3.3.2. One of the main conclusions of Chapter 4 (Numerical Studies) is that the Gaussian correction is more accurate than the Cauchy correction. Since the slope of the least squares fit of the data in Figure 7.4 (B) is nearly zero, we can conclude that there is no strain in the crystallites. Recall that the ordinate intercept is related to size broadening as given by Equations 3-13 and 3-14.



A) Cauchy Form of Correction



B) Gaussian Form of Correction

FIGURE 7.4 Strain Shape Analysis of Catalyst HP-3

7.4 Particle Size

The average length information extracted for monometallic Ir and Pt catalysts appear in Table 7.2 and 7.3 respectively. Figure 7.5 shows the area average length plotted against the average diameter determined by chemisorption. Chemisorption results were obtained from Graham [29] and Fiederow et al. [32]. With some notable exceptions, the ratio of $\langle La \rangle$ to D_p is about constant $D_p \geq 2.0$ nm. Note that relative deviations are larger at small particle sizes. This indicates that the stoichiometry and particle shape are probably constant (or at least any changes are self-compensating) for these particles. Also plotted are the expected curves for several different assumed stoichiometries and particle shapes. Assuming a stoichiometry of $1.0 < H/M < 2.0$, spherical, hemispherical, and cubic particles all fit the observations, while tetrahedra have $\langle La \rangle$ too short relative to D_p to be possible. If randomly oriented hemispherical particles are assumed, then the stoichiometry is $H/M=1.64$. It is important to note that the metal concentration is not known very accurately. This may cause additional errors in the interpretation of these results.

One area which is interesting to explore is the points which do not fit the curve. These 3 points are all monometallic platinum catalysts treated in O_2 above $600^\circ C$. One possible explanation is that there is some change in the absorption stoichiometry at least partially responsible for

Table 7.2 Average Crystallite Sizes for Monometallic $\text{Ir}/\text{Al}_2\text{O}_3$ Catalysts (All lengths in nm)

Catalyst	Fraction Detected	$\langle L_{a_1} \rangle$	$\langle L_{a_2} \rangle$	$\langle L_{v_1} \rangle$	$\langle L_{v_2} \rangle$	L.L.D. ¹ (nm)	$\langle L_{v_2} \rangle / \langle L_{a_1} \rangle$
AI-13	0.7	1.5	1.4	1.7	1.64	0.6	1.15
AI-2	0.85	1.0	0.8	1.0	1.20	0.6	1.22
AI-4	>0.95	6.0	5.8	10.9	11.8	1.2	1.92
AI-5	>0.95	5.2	5.6	9.1	9.5	1.2	1.72
AI-8'	>0.95	8.2	8.4	11.4	13.3	1.2	1.49
AI-16	0.85	9.2	8.2	14.9	12.9	1.2	1.60
AI-12	0.50	5.9	5.1	20.2	14.0	1.2	3.10
AI-14	0.72	2.7	2.7	2.7	3.1	1.2	1.07
		2.0	2.1	2.4	2.5	1.2	1.20

¹L.L.D.=Lower Limit of Detectability=1.5a, where a is defined by Equation 3-25

Table 7.3 Average Crystallite Sizes for Monometallic 1%Pt/Al₂O₃ and 4%Pt/Al₂O₃ Catalysts

Catalyst	Fraction Detected	$\langle L_a \rangle$	$\langle L_a \rangle$	$\langle L_v \rangle$	$\langle L_v \rangle$	L.L.D. ¹ (nm)	$\langle L_v \rangle / \langle L_a \rangle$
AP-1	0.54	1.7	1.4	3.4	3.7	0.6	2.29
AP-6	0.53	1.9	1.5	4.2	4.1	0.6	2.44
AP-8	0.82	8.1	5.7	7.7	8.5	1.2	1.17
AP-9	>0.95	9.8	5.4	8.8	9.9	1.2	1.23
AP-10	>0.95	13.7	10.1	28.9	21.1	1.2	2.10
AP-11	0.78	2.08	2.86	2.91	4.28	0.6	1.46
AP-13	0.71	2.08	2.10	4.01	3.83	1.2	1.88
AP-14	0.71	2.9	3.0	4.61	4.53	1.2	1.52
AP-16	0.83	2.6	2.5	3.8	43.9	1.2	1.51
HP-7	>0.90	3.7	3.5	2.1	2.3	0.6	0.8
HP-2	>0.95	8.8	6.9	11.0	10.9	1.2	1.39
HP-3	>0.95	7.6	8.6	10.8	10.6	1.2	1.32
HP-6	0.88	12.4	8.4	21.7	18.6	1.2	1.94

¹L.L.D.=Lower Limit of Detectability=1.5a, where a is defined by Equation 3-25

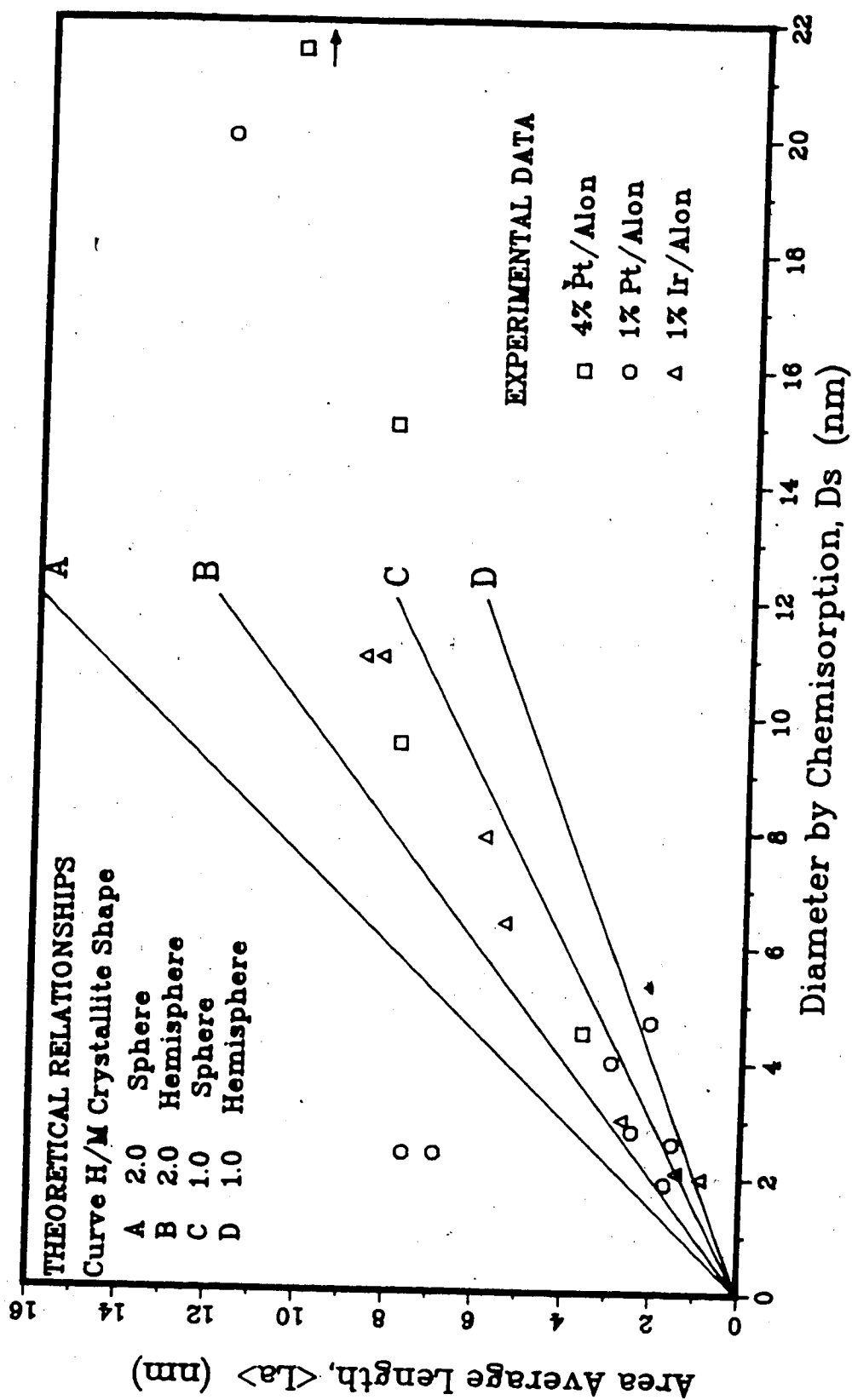


FIGURE 7.5 Comparison of X-ray and Chemisorption Sizes

these deviations. However, this can be disputed by the fact that deviations lie on both sides of the curve. It is important to note that the catalysts with significantly higher $\langle La \rangle$ than the curve also show a larger $\langle Lv \rangle / \langle La \rangle$ ratio and the problems may be due only to the broad particle size distribution.

7.5 The Length Distribution Function

As has been previously mentioned, the ratio $\langle Lv \rangle / \langle La \rangle$ can be used as a simple indicator of the breadth of the PSDF. The broader the LDF, for a constant particle shape, the larger the ratio. However, even for a Dirac delta type PSDF, the ratio changes as a result of particle shape. The ratio is 1.0 (the theoretical minimum) for correctly oriented unisized cubes, 1.12 for spheres, and 1.4 for correctly oriented tetrahedra. One can imagine shapes having even large $\langle Lv \rangle / \langle La \rangle$ but since the metals seek to minimize their surface area, these are not very likely. The calculated ratios are also questionable at low average lengths. Figure 7.5 shows that the error in $\langle La \rangle$ can easily be 50% for small particle sizes. One should be skeptical about $\langle Lv \rangle / \langle La \rangle$ in such cases, although it was shown in the numerical analysis that $\langle Lv \rangle / \langle La \rangle$ is more accurate in these cases than either $\langle Lv \rangle$ or $\langle La \rangle$ alone.

In general, for Ir catalysts, it appears that the PSDF becomes broader after oxygen treatment and does not change much for H_2 treatments. The fresh and lightly sintered Pt

catalysts show much higher $\langle L_v \rangle / \langle L_a \rangle$. This may be due to strong metal-support interactions causing some raft-like structures. Oxygen treatment at 600 °C seems to cause narrowing of the PSDF while at higher temperatures, broader PSDF's are observed. Hydrogen treatment has less effect on the LDF with $\langle L_v \rangle / \langle L_a \rangle$ being about 1.5, for most cases.

Figure 7.6 shows the area and volume weighted length distribution function for the (111) profile of catalyst HP-3. The shapes are typical of the (111) profile of all the catalysts studied. For the area weighted LDF, an initial maximum occurs at about 2.0 nm (corresponding to about the fourth Fourier coefficient), and is followed by a more-or-less steady decline (or in some cases, a much lower local maximum) to zero at large (here about 25 nm) lengths. This initial maximum was first believed to be caused by particle size distribution, but is now believed to be due to particle shape. The volume weighted LDF shows more emphasis on the larger lengths, and so is more frequently unimodal.

One possible explanation for the initial maximum in the area weighted length distribution function is that it is entirely spurious, i.e. the shape of the LDF is due to the fitting function far from the centroid of the peak where the error of the curve fit can be relatively large. This objection has been dealt with in some detail in Section 6.3 as part of the discussion of the lower limit of detectability.

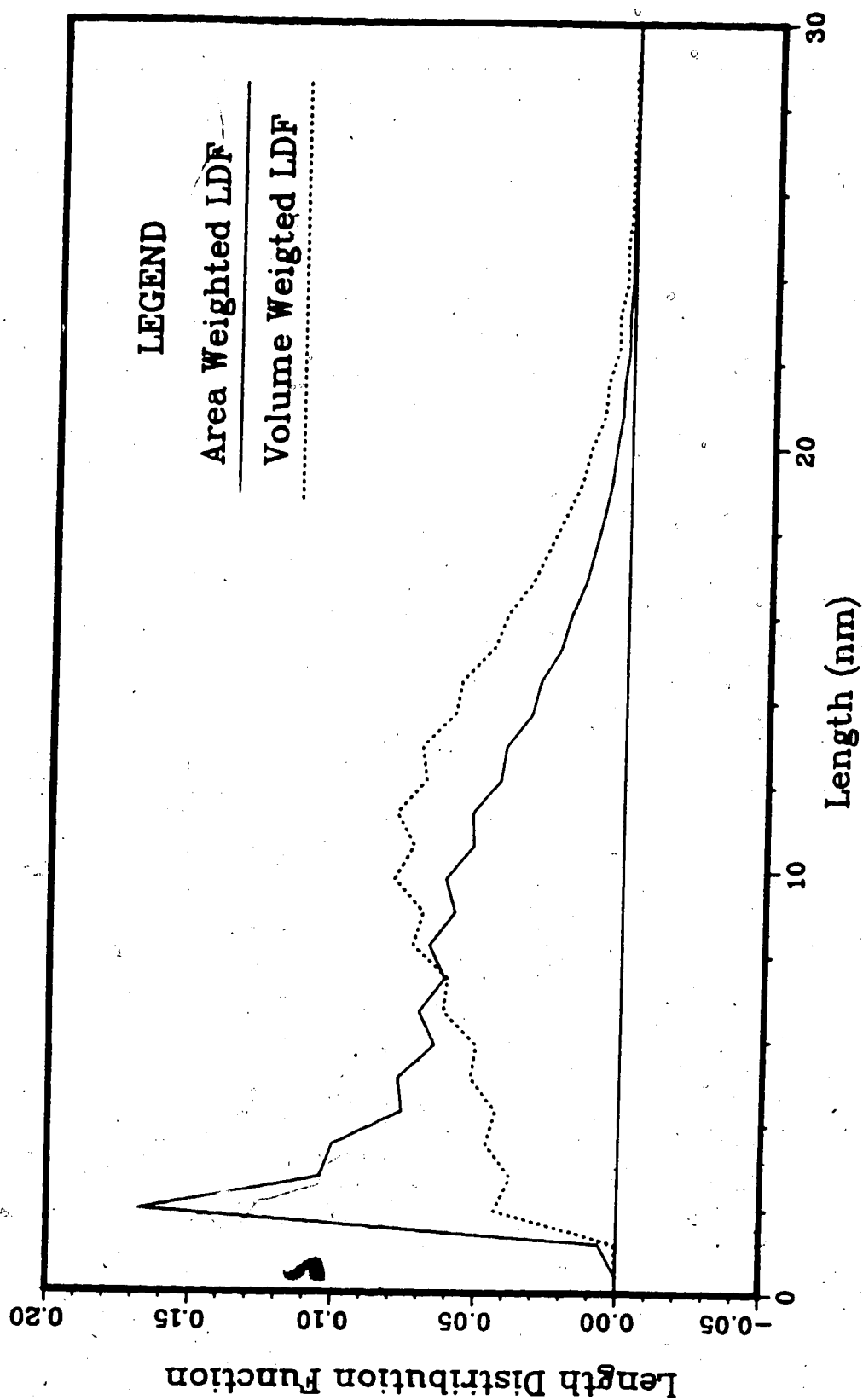


FIGURE 7.6 Area and Volume Weighted LDF's for Catalyst HP-3

The shape of the LDF is apparent even up to lengths of as high as 5 or 6 nm which corresponds to an integral breadth of about 2° of 2θ (solving for B in Equation 3-10) and to a range of about 1.6° of 2θ (solving for θ_{mx} and θ_{mn} using Equation 3-21). This behaviour is clearly not an artifact of the fitting function.

The same fit procedure was applied to several artificially generated 'noisy' profiles as part of the numerical check. Since several different LDF's were successfully regenerated, this shape is not solely a result of the curve fitting.

A second possible explanation for the repeated shape is that the particle size distributions actually do maintain a large number of small particles for all cases. Since the ratio of $\langle La \rangle$ to D, remains fairly constant over a wide range of particle sizes, it can at least be inferred that the particle shape does not change greatly as the particle size changes. However, there could be sharp edges on the crystals to a fairly large length which would give rise to this kind of LDF. It is probably not possible to infer which possible cause (shape, or a large number of small particles) actually caused this shape of the LDF.

7.6 Summary of Results

For bimetallic catalysts, X-ray diffraction is unique among the common experimental techniques in that it can show the nature of the phases present. This ability allowed

demonstration that oxygen treatments at elevated temperatures cause separation of the Pt/Ir phases while hydrogen treatments do not. It was also possible to show that the mechanism of this change is the formation of large IrO_2 crystallites.

X-ray diffraction can also be used to determine particle size and shape information. Although results of shape studies are inconclusive, the size information correlates very well with that obtained by chemisorption for $\langle L_v \rangle > 2$ nm. It is not possible to determine the exact stoichiometry or particle shape from these results due to the overlapping of the two effects. The shape-strain study of one catalyst demonstrated negligible strain but the variations in $\langle L_v \rangle$ for different (hkl) peaks were small but measurable. This tends to point to approximately spherical (or hemispherical) particles.

The particle size distribution function is so closely tied to the particle shape that it is difficult to separate one from the other. Some generalities can however be drawn about the breadth of the PSDF. For both Pt and Ir, hydrogen treatment has less effect on both the average size and on the PSDF than oxygen treatment. For platinum, treatment at about 500°C seems to broaden the LDF while the LDF is narrowed by treatment at 600° and above. By implication, assuming constant particle shape, the PSDF exhibits the same characteristics.

8. CONCLUSIONS

The most important development in this work is the technique used to eliminate the patterns caused by slightly crystalline supports from the peaks due to the metal in observed catalyst patterns. This technique involves the weighted point-by-point subtraction of the support profile from the catalyst profile followed by a linear baseline correction. Without this technique, analysis of the metal profile would be impossible.

The most valuable new data which can be extracted from these X-ray patterns is the phases which are present in bimetallic catalysts. It was shown that oxygen treatment tends to cause growth of large Pt and Ir crystallites while hydrogen treatment at similar elevated temperatures does not have this effect.

Quantitative information about particle sizes can also be extracted from these metal profiles. While the different weightings produced by electron microscopy, chemisorption and X-ray diffraction are well documented, it is not common knowledge that number, area, and volume weighted average crystallite lengths can be extracted from X-ray diffraction data alone. By making reasonable assumptions about the crystallite shape, (as is necessary in chemisorption) these average crystallite lengths are easily converted to average crystallite sizes. References to the large effect that particle shape can have on this conversion are also uncommon in the catalyst literature.

Numerical techniques were used to identify the preferred techniques for the analysis of XRD profiles. These include the use of integral breadth rather than width at 1/2 of peak height, and instrument broadening correction assuming Gaussian profile shape for the Scherrer equation. A curve fitting technique combined with Fourier analysis was found to give accurate information about crystallite size down to about $\langle La \rangle = 2$ nm. The Fourier method does not fail to resolve sizes smaller than 2.0 nm, but accuracy decreases significantly for sizes below 2.0 nm.

It was shown that $\langle La \rangle$ measured by Fourier analysis of the fitted metal profiles correlates well with the diameter derived from chemisorption for $\langle La \rangle \geq 2$ nm. However, owing to complexities in the relationship between $\langle La \rangle$, particle shape, and stoichiometry of adsorption, neither adsorption stoichiometry nor particle shape can be uniquely determined. One reasonable hypothesis is that particles are hemispheres with adsorption stoichiometries of $H/M=1.6$.

8.1 Future Work

In addition to covering the details outlined in this work, future investigators should consider the following:

1. Use of supports with the same heat treatment as the catalyst sample to correct for support effects.

Alternatively, a bank of support profiles could be collected and a weighted average based on both time and temperature treatment could be used to simulate the

catalyst support.

2. Much more detailed attention should be paid to water vapour adsorbed on the sample. Dehydration at elevated temperatures before each XRD run might be necessary.
3. Evaluate the the effect of air pressure on peak intensity to determine whether measurement of and correction for air pressure variations is valuable.
4. Especially for runs with low metal intensities, at least two runs with repacked samples should be averaged before analysis of X-ray data.
5. Use of a fast Fourier transform algorithm to allow use of longer series and produce less numerical error.
6. Correction of the angle dependent factors in the X-ray diffraction profile should be considered. This is especially true if more detailed study of different peaks is performed in order to get improved LDF information.
7. X-ray diffraction results should be compared to those obtained by electron microscopy to further verify these methods.

If the other experimental errors can be reduced by the methods described above, less curve fitting should be necessary. Curve fitting of only the peak tails should allow more accurate determination of the length distribution functions.

9. NOMENCLATURE

In this section, the first use of the variable with the same meaning as the definition is given in parentheses. Brackets indicate units, while unitless expressions are indicated by [-].

Latin

a	=	dummy variable of integration (Equation 3-15) [-]
a	=	Fourier length (Equation 3-25) [nm]
a	=	factor to define changes in monochromator intensity (Equation 6-3)[-]
A	=	irradiated area (Equation 3-3) [m ²]
b_i	=	fit parameters, $i = 1, 2, 3, 4, 5$ (Equation 3-44)[-]
B	=	breadth of X-ray profile (Equation 3-6) [radian 2θ]
B_z	=	peak broadening due to crystallite size (Equation 3-13) [radian 2θ]
B_n	=	peak broadening due to crystallite strain (Equation 3-13) [radian 2θ]
C_i	=	concentration of component 'i' in a mixture (Equation 3-4) [-]
C_a	=	constant (Equation 3-26) [-]
C_n	=	constant (Equation 3-33) [-]
C_v	=	constant (Equation 3-30) [-]

- d = distance between interatomic planes (Equation 3-1) [nm]
- D = characteristic crystallite size (diameter for spherical crystallites) (Equation 3-35) [nm]
- e = charge of an electron (Equation 3-3) [C]
- $\langle e^2 \rangle^{1/2}$ = root mean square crystallite strain (Equation 3-12) [-]
- f = fitting function (Equation 3-41) [-]
- F = structure factor (Equation 3-4) [-]
- F_i = functions, $i=1,2$ (Equation 3-44) [-]
- $f(L,D)$ = shape distribution function corresponding to length L , particle size, D (Equation 3-37) [-]
- $f(s)$ = functional form of the pure peak (Equation 3-15) [c/s]
- $F(j)$ = Fourier transform of $f(s)$ (Equation 3-16) [c/s]
- $g(s)$ = functional form of a peak broadened only instrument effects (Equation 3-15) [c/s]
- $G(j)$ = Fourier transform of $g(s)$ (Equation 3-16) [c/s]
- $h(s)$ = functional form of a peak broadened by both instrumental and particle effects (Equation 3-15) [c/s]
- $H(j)$ = Fourier transform of $h(s)$ (Equation 3-16) [c/s]
- $h(k)$ = hanned intensity at point k (Equation 3-45) [c/s]
- $hm(k)$ = measured intensity at point k (Equation 3-45)

[c/s]

$I =$ intensity of X-ray beam in a sample (Equation 3-2)
[J/m² s]

$I_d =$ integrated intensity of an X-ray line (Equation 3-3) [J/m s]

$I(s) =$ intensity of X-ray line profile at dimensionless distance, s (Equation 3-8) [c/s]

$I_{xyz i} =$ integrated intensity of X-ray line profile, [radian $2\theta \cdot c/s$]

$j =$ Fourier number, $j=0,1,2 \dots J$ (Equation 3-16) [-]

$j_i =$ intercept of the initial Fourier coefficients used to determine $\langle La_i \rangle$ (Equation 3-23) [-]

$J =$ maximum Fourier number (there are $J+1$ Fourier coefficients) (Equation 3-19) [-]

$k =$ various constants (Equations 3-11, 38, 39, 41)

$k =$ data point counter, $-J < k < J$ (Equation 3-45) [-]

$K =$ constant defining the magnitude of the X-ray peak (Equation 3-8) [count/second]

$K_i =$ various constants (Equations 3-41, 3-42, 3-43)

$K_s =$ Scherrer constant (Equation 3-10) [nm]

$K_{xyz i} =$ constant defining the peak height of the X-ray peak for Miller index (xyz) corresponding to the i -th component in a mixture (Equation 3-4) [radian $2\theta \cdot \text{count} \cdot \text{cm}$]

$L =$ Length in length distribution function (Equation 3-26) [nm]

- L_i = i th length (of volume fraction, V_i) (Equation 3-11) [nm]
- $\langle La_1 \rangle$ = area weighted average crystallite length (Equation 3-23) [nm]
- $\langle La_2 \rangle$ = area weighted average crystallite length (Equation 3-29) [nm]
- $\langle Lv_1 \rangle$ = volume weighted average crystallite length determined by Scherrer equation (Equation 3-10) [nm]
- $\langle Lv_2 \rangle$ = volume weighted average crystallite length (Equation 3-31) [nm]
- m = mass of an electron (Equation 3-3) [kg]
- M = term in temperature factor for the intensity of an X-ray peak (Equation 3-3) [-]
- M = number of hanned points at the end of each hanning window (Equation 3-46) [-]
- n = order of reflection (Equation 3-1) [-]
- N = number of reflecting planes in the (hkl) direction (Equation 3-8) [-]
- N_i = number of reflecting planes of the i -th length, L_i (Equation 3-11) [-]
- N_p = total number of discrete lengths in the (discrete) Length Distribution Function (Equation 3-11) [-]
- P = multiplicity factor, the number of different planes with the same m Miller index (Equation 3-3) [-]
- $Pa(L)$ = area weighted length distribution function evaluated at length, L (Equation 3-26) [-]

- $P_n(L)$ = length distribution function weighted by number of particles (Equation 3-33) [-]
- $P_s(L)$ = Area weighted particle size distribution function evaluated at length, L (Equation 3-37) [-]
- $P_v(L)$ = Volume weighted length distribution function evaluated at length, L (Equation 3-30) [-]
- r = diffractometer radius (Equation 3-3) [m]
- R_i = radius of particles of component i (Equation 3-4) [cm]
- s = dimensionless Bragg distance, Equation 3-9 [-]
- s = constant (Equation 4-1) [-]
- Δs = step size in constant dimensionless Bragg distance (Equation 3-17) [-]
- t = constant (Equation 4-1) [-]
- T_1 = term used to determine the integrated intensity of an X-ray peak, (Equation 3-3) [$J\ m^2/s$]
- T_2 = term used to calculate the integrated intensity of an X-ray peak (Equation 3-3) [m^{-3}]
- T_3 = term used to determine the integrated intensity of an X-ray diffraction peak (Equation 3-3) [-]
- u = constant (Equation 4-1) [-]
- V = volume of a unit cell (Equation 3-3) [m^3]
- v_i = average volume of particles of component i (Equation 3-4) [m^3]

V_i = the i -th volume fraction of a collection of particles represented by N_p discrete lengths (Equation 3-11) [-]

x = distance into X-ray sample (Equation 3-2) [cm or m]

Y' = intensity factor (Equation 6-1) [c/s·cm]

Y = intensity factor (Equation 6-3) [radian·c·cm²/(s·g)]

Greek

a = ratio of peak intensity studied to peak intensity of the internal standard, internal standard method (Equation 2-1) [-]

θ = goniometer angle (Equation 3-9) [radian or ° arc]

θ_{mn} = goniometer angle corresponding to the minimum angle in the Fourier analysis (Equation 3-25) [radian or ° arc]

θ_{mx} = goniometer angle corresponding to the maximum angle of the Fourier analysis (Equation 3-25) [radian or ° arc]

θ_x = Bragg angle (Equation 3-1) [radian or ° arc]

$2\theta_0$ = fit Bragg angle (Equation 3-43) [radian or ° arc]

λ = X-ray wavelength (Equation 3-1) [nm]

μ = X-ray linear absorption coefficient (Equation 3-2) [cm⁻¹]

μ_0 = conversion factor (Equation 3-3) $4\pi(10^{-7})$ kg·m·C⁻²

- ρ = density (Equation 3-4) [kg/m³]
- τ_i = particle absorption factor (Equation 3-4) [-]
- ω_j = Fourier frequency (Equation 3-18) [-]

Subscripts

- i = referring to component i in a mixture of diffracting phases (Equation 3-4)
- i = referring to the integrated intensity method of measuring peak broadening (Equation 3-5)
- i = referring to the i -th length fraction (Equation 3-11)
- i = imaginary part of the Fourier coefficient, (for example, F_i in Equation 3-21)
- m = measured value (Equation 2-1)
- m = value for the mixture (Equation 3-4)
- mn = evaluated at the minimum goniometer angle (Equation 3-18)
- mx = evaluated at the maximum goniometer angle (Equation 3-18)
- o = incident value (Equation 3-3)
- r = real part of Fourier coefficient (eg. F_r , Equation 3-21)
- t = theoretical value (Equation 2-1)

xyzi = referring to the peak due to planes of Miller index (xyz), for the i-th component of a mixture (Equation 3-4)

$1/2$ = determined by width at $1/2$ of the peak height

Superscripts

m = measured breadth of the profile (Equation 3-6)

s = standard for a profile with broadening only due to instrumental factors (Equation 3-6)

Abbreviations

$\langle x \rangle$ = average value of 'x'

ALDF = Area weighted length distribution function

LDF = Length distribution function

PSDF = Particle size distribution function

SMC = Supported metal catalysts

VLDF = Volume weighted length distribution function

10. REFERENCES

1. Satterfield, C.N., "Heterogeneous Catalysis in Practice", McGraw-Hill Book Co., New York (1980).
2. Sinfelt, J.H., Via, G.H., Lytle, F.W., J. Chem. Phys., 76, 2779 (1982).
3. Krishnamurthy, S., Landolt, G.R., Schoennagel, H.O., J. Cat., 78, 319 (1982).
4. Flynn, P., Wanke, S.E., Turner, J. Cat., 33, 233 (1974).
5. Adams, C.R., Benesi, H.A., Curtis, R.M., Meisenheimer, R.G., J. Cat., 1, 336 (1962).
6. Pope, D., Smith, W.L., Eastlake, M.J., Moss, R.L., J. Cat., 22, 72 (1971).
7. Smith, W.L., J. Appl. Cryst., 1, 127 (1962).
8. Pausescu, P., Manaila, R., Popescu, M. Jijovici, E., J. Appl. Cryst. 7, 281 (1974).
9. van Nordstrand, R.A., Lincoln, A.J., Carnevale, A., Anal. Chem., 36, 819 (1964).
10. Sashital, S.R., Cohen, J.B., Burwell Jr., R.L., Butt, J.B., J. Cat., 50, 479 (1977).
11. Ganesan, P., Kuo, H.K., Saavedra, A., De Angelis, R.J., J. Cat., 52, 310 (1978).
12. Nandi, R.K., Pitchai, R., Wong, S.S., Cohen, J.B., Burwell Jr., R.L., Butt, J.B., J. Cat., 70, 298 (1981).
13. Nandi, R.K., Molinaro, F., Tang, C., Cohen, J.B., Butt, J.B., Burwell Jr., R.L., J. Cat., 78, 289 (1982).

14. Dorling, T.A., Lynch, W.J., Moss, R.L., J. Cat., 20, 190 (1971).
15. Gangulee, A., J. Appl. Cryst., 7, 434 (1974).
16. Sinfelt, J.H., Via, G.H., J. Cat., 56, 1 (1979).
17. Smith, W.L., J. Appl. Cryst. 9, 187 (1976).
18. Taylor, A., "X-ray Metallography", John Wiley and Sons, New York (1961).
19. Cullity, B.D., "Elements of X-ray Diffraction", Addison-Wesley Publishing Co., Reading, Mass. (1978).
20. Klug, H.P., Alexander, L.E., "X-ray Diffraction Procedures for Polycrystalline and Amorphous Materials", John Wiley and Sons, New York (1974).
21. Zachariassen, W.H., "Theory of X-ray Diffraction in Crystals", Dover Publications, New York (1945).
22. Langford, J.I., in "National Bureau of Standards Special Publication Number 567", 225 (1980).
23. Delhez, R., de Keijser, T.H., Mittemeijer, E.J., Fresenius Z. Anal. Chem., 312, 1 (1982).
24. Delhez, R., de Keijser, T.H., Mittemeijer, E.J., in "National Bureau of Standards Special Publication Number 567", 213 (1980).
25. Warren, B.E., Prog. in Metal Phys., 8, 147 (1959).
26. Stokes, A.R., Wilson, A.J.C., Proc. Phys. Soc. Lond., 56, 174 (1944).
27. Vogel, W., Hosemann, R., Z. Phys. Chem. Neue Folge, 121, 193 (1980).

28. Bloomfield, P., "Fourier Analysis of Time Series: An Introduction", John Wiley and Sons, New York, 1976.
29. Graham, A.G., Wanke, S.E., J. Cat., 68, 1 (1981)
30. Kuester, J. L., Mize, J.H., "Optimization Techniques with Fortran", pp. 240-250 McGraw-Hill Book Co., New York (1973)
31. Schaefer, H., and Heitland, H.J., Z. Anorg. Allg. Chem., 304, 317 (1960).
32. Fiederow, R.M.J., unpublished results (1975)

11. APPENDIX A: Plots of Raw Data

This Appendix contains plots of the X-ray patterns for the catalysts, supports and standards used in this study. The plots were made directly from the data stored on magnetic tapes using the HP-1000 plotting packages available in the Department of Chemical Engineering DACS centre.

Several related patterns are included on each plot for economy and to emphasize the subtle differences in peak shape between patterns. These are offset by the indicated amount for clarity.

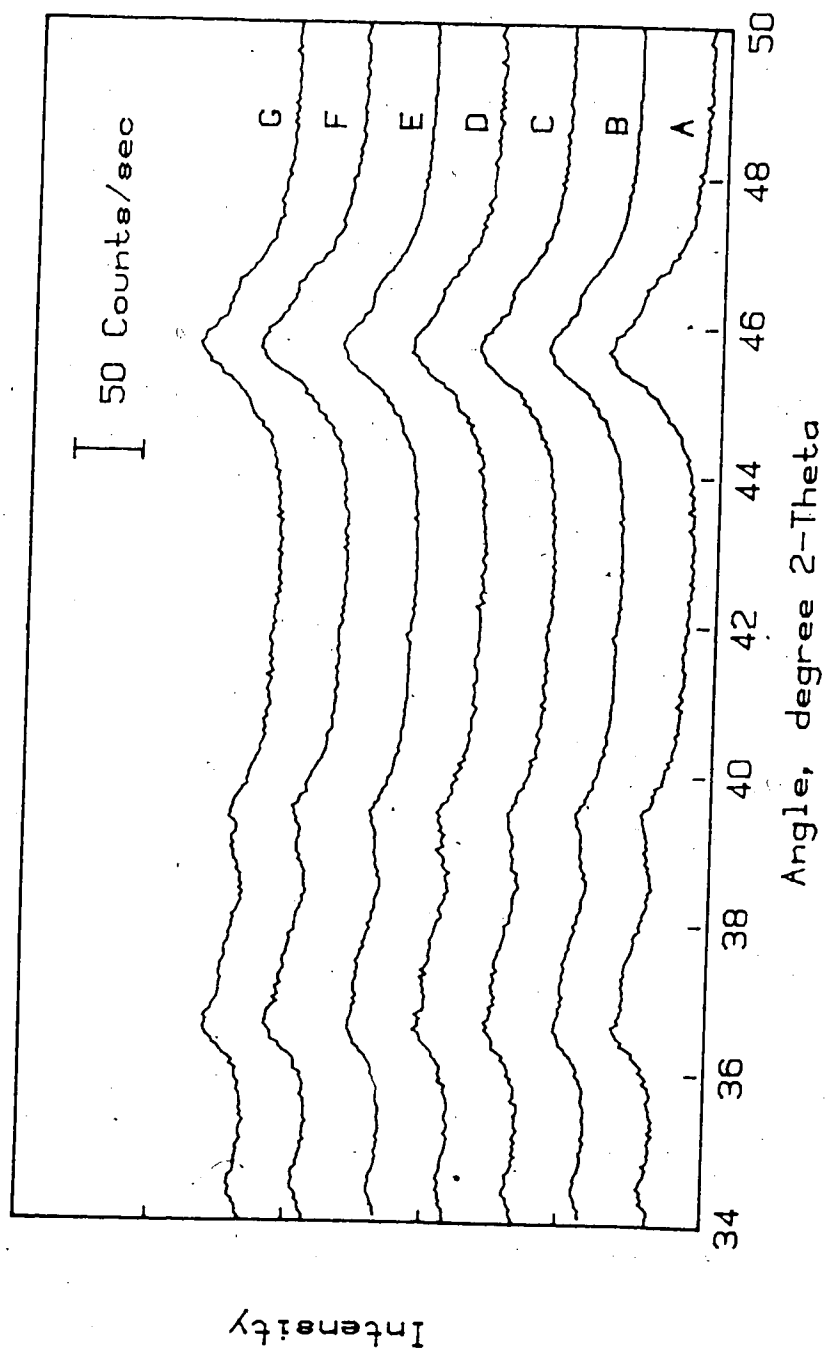


FIGURE A-1: Support Profiles

-Each profile is offset by 50 counts/sec

A=A1, B=A3-1, C=A3-2, D=A3-3,

E=A9, F=A11, G=A12

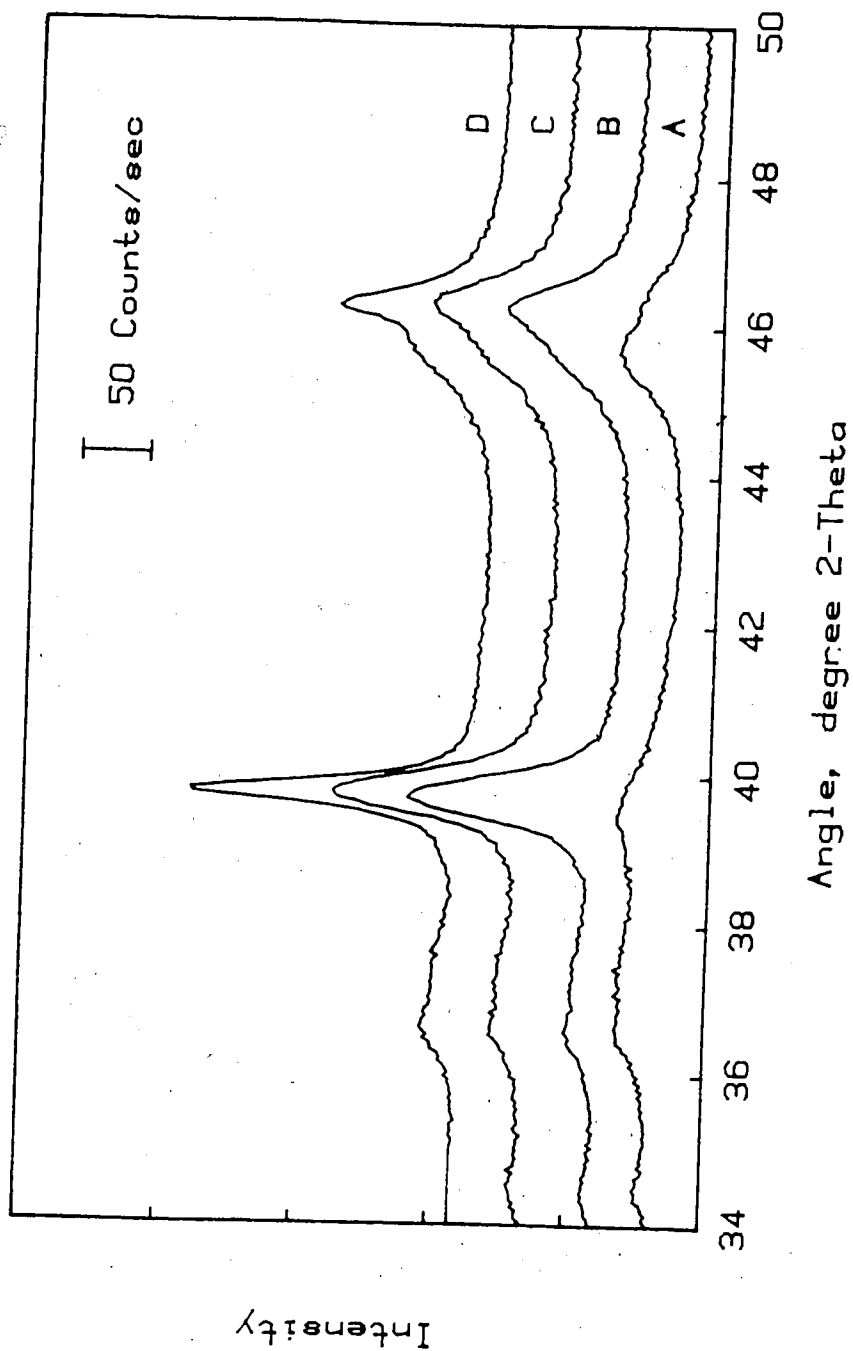


FIGURE A-2: Profiles of 4% Pt/Alon Catalysts
-Each profile is offset by 50 counts/sec
A=HP-6, B=HP-2, C=HP-3, D=HP-7

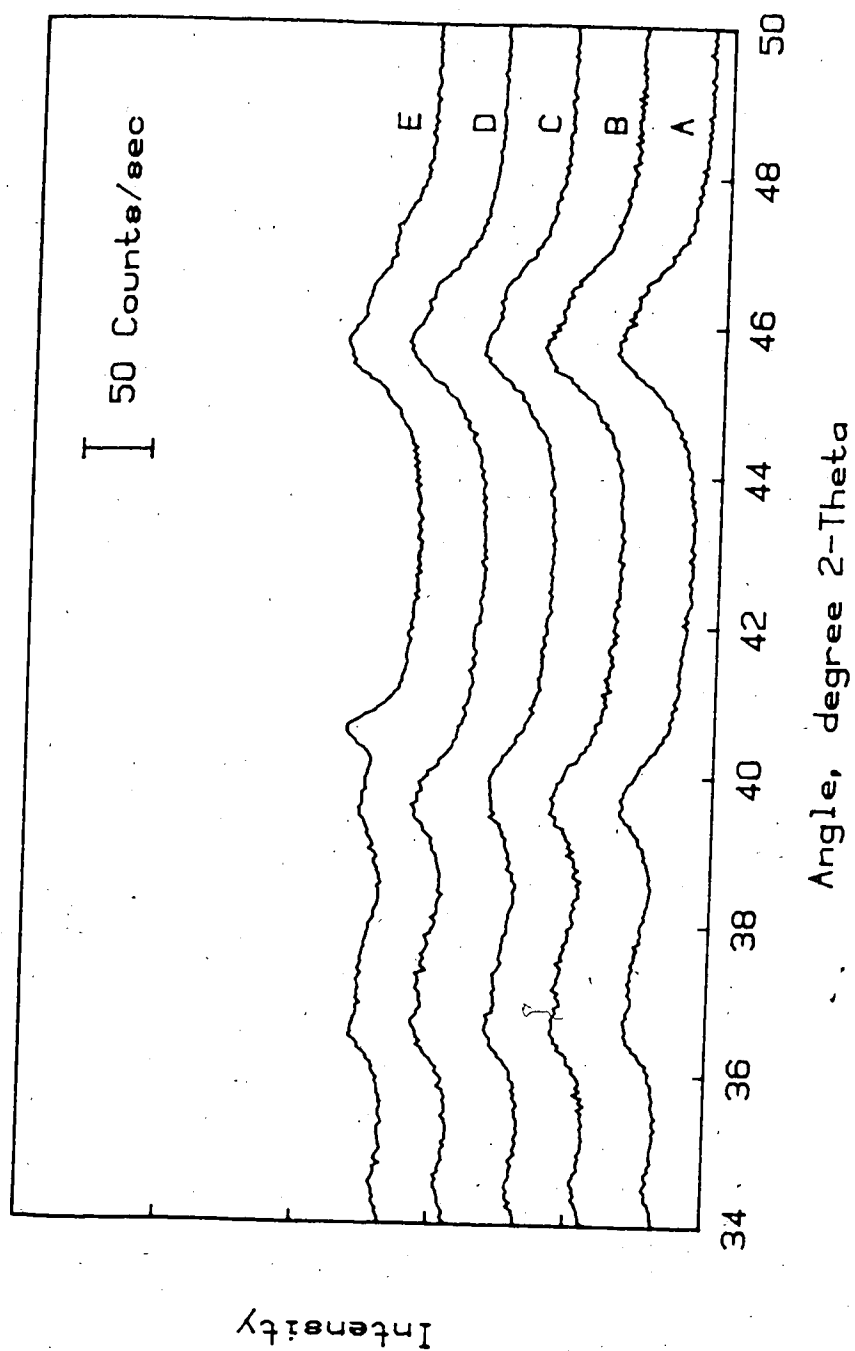


FIGURE A-3: Profiles of 1% Pt + 1% Ir Catalysts
 -Each profile is offset by 50 counts/sec
 A=PI-14, B=PI-16, C=PI-17, D=PI-2
 E=PI-8

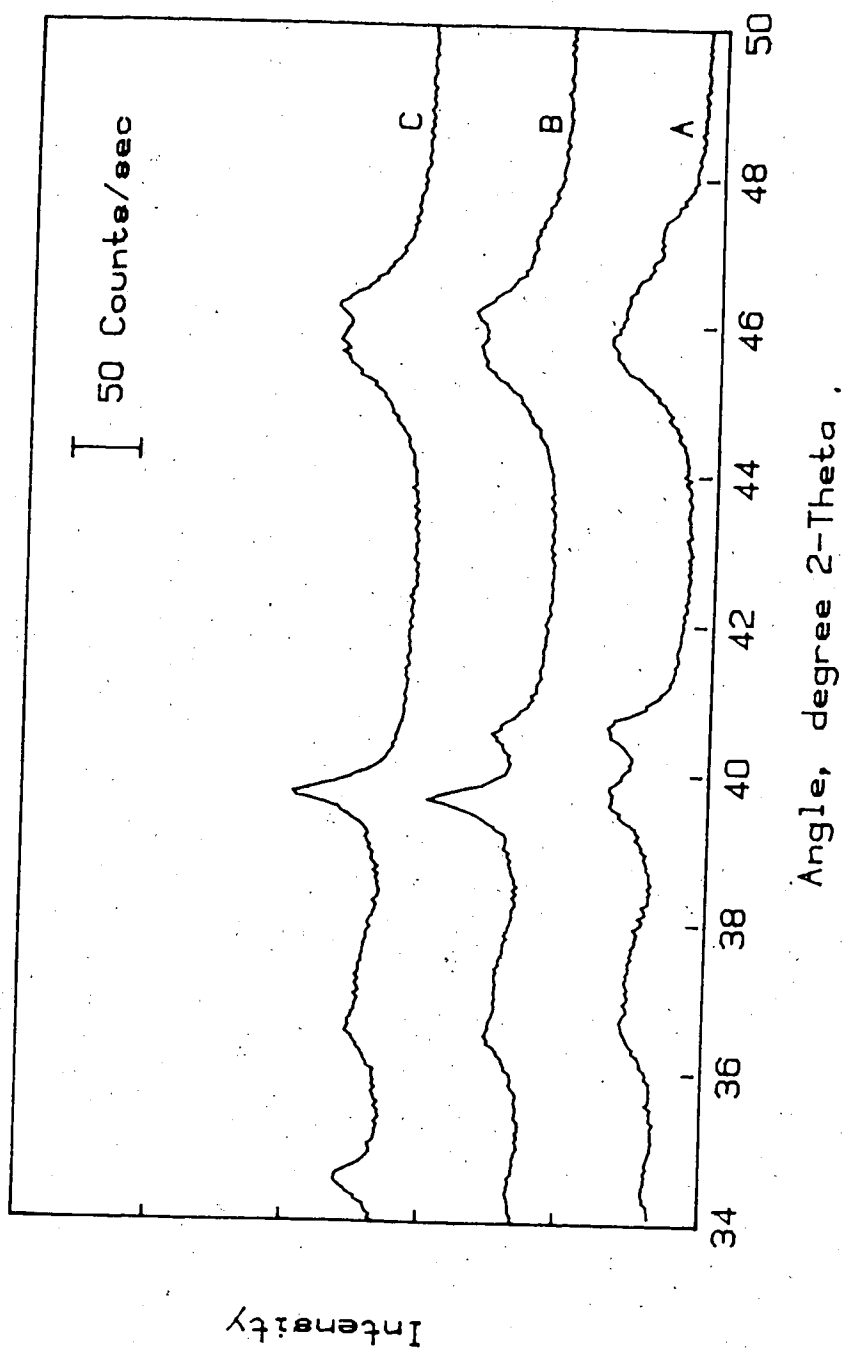


FIGURE A-4: Profiles of 1%Pt + 1%Ir/Alon Catalysts
 -Each profile is offset by 100 counts/sec
 A=PI-12, B=PI-19, C=PI-18

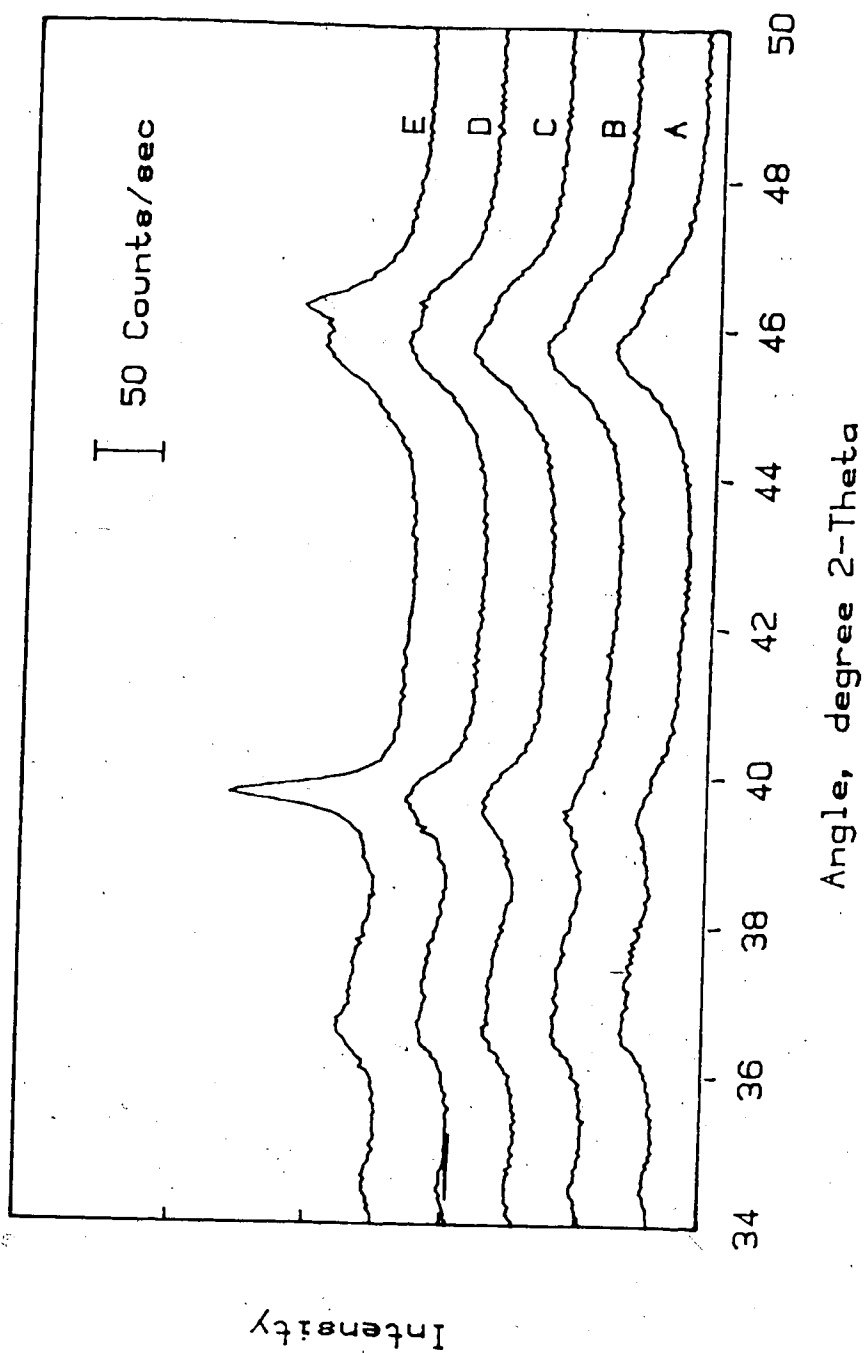


FIGURE A-5: Profiles of 1% Pt/Alon Catalysts
 -Each profile is offset by 50 counts/sec
 A=AP-1, B=AP-6, C=AP-8, D=AP-9
 E=AP-10

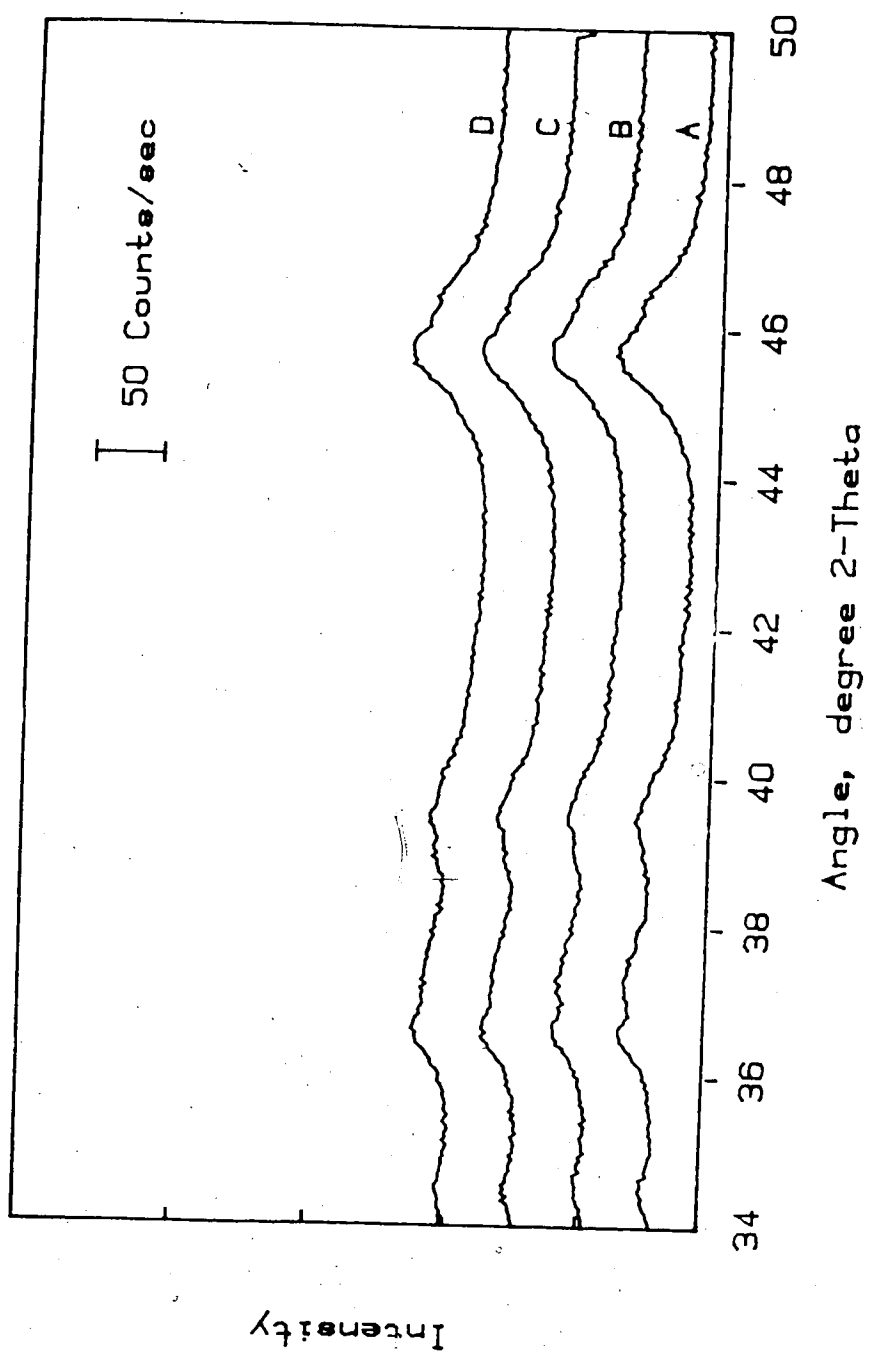


FIGURE A-6: Profiles of 1% Pt/Alon Catalysts
 -Each profile is offset by 50 counts/sec
 A=AP-11, B=AP-13, C=AP-14, D=AP-16

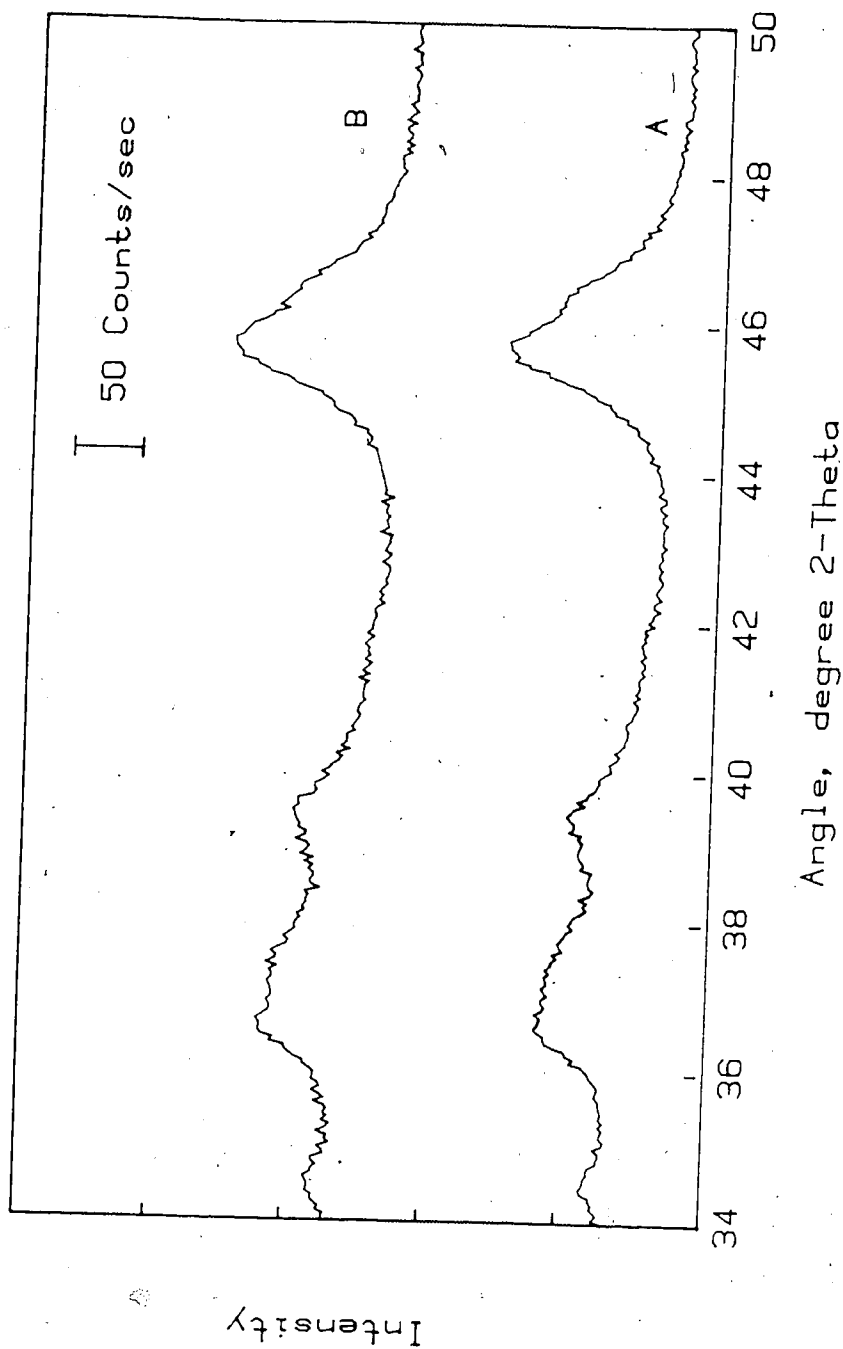


FIGURE A-7: Profiles of 1% Ir Catalysts
-Each profile is offset by 100 counts/sec
A=AI-13, B=AI-2

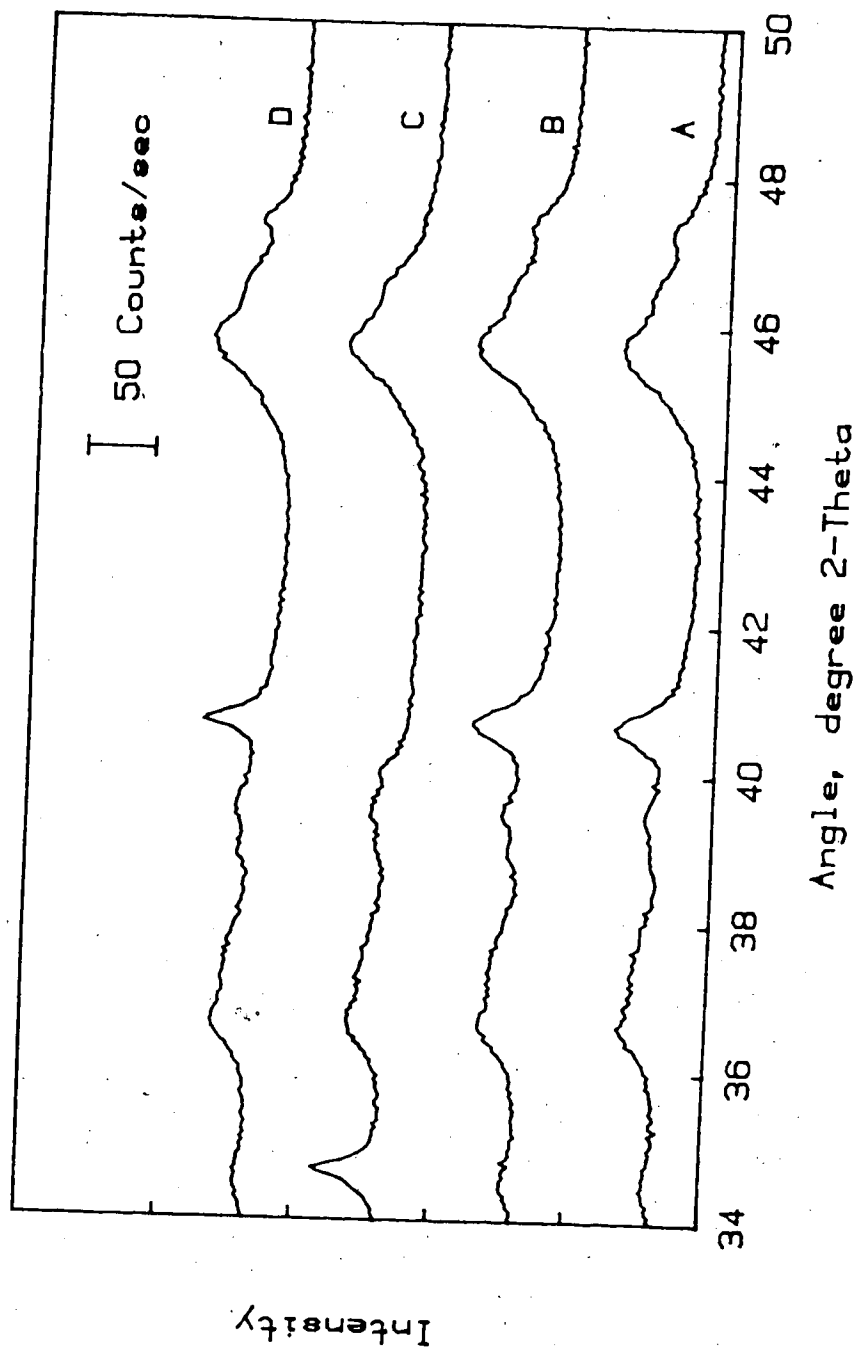


FIGURE A-8: Profiles of 1% Ir/Alon Catalysts
 -Each profile is offset by 100 counts/sec
 A=AI-8 (run before re-alignment)
 B=AI-8 (run after re-alignment)
 C=AI-15, D=AI-16

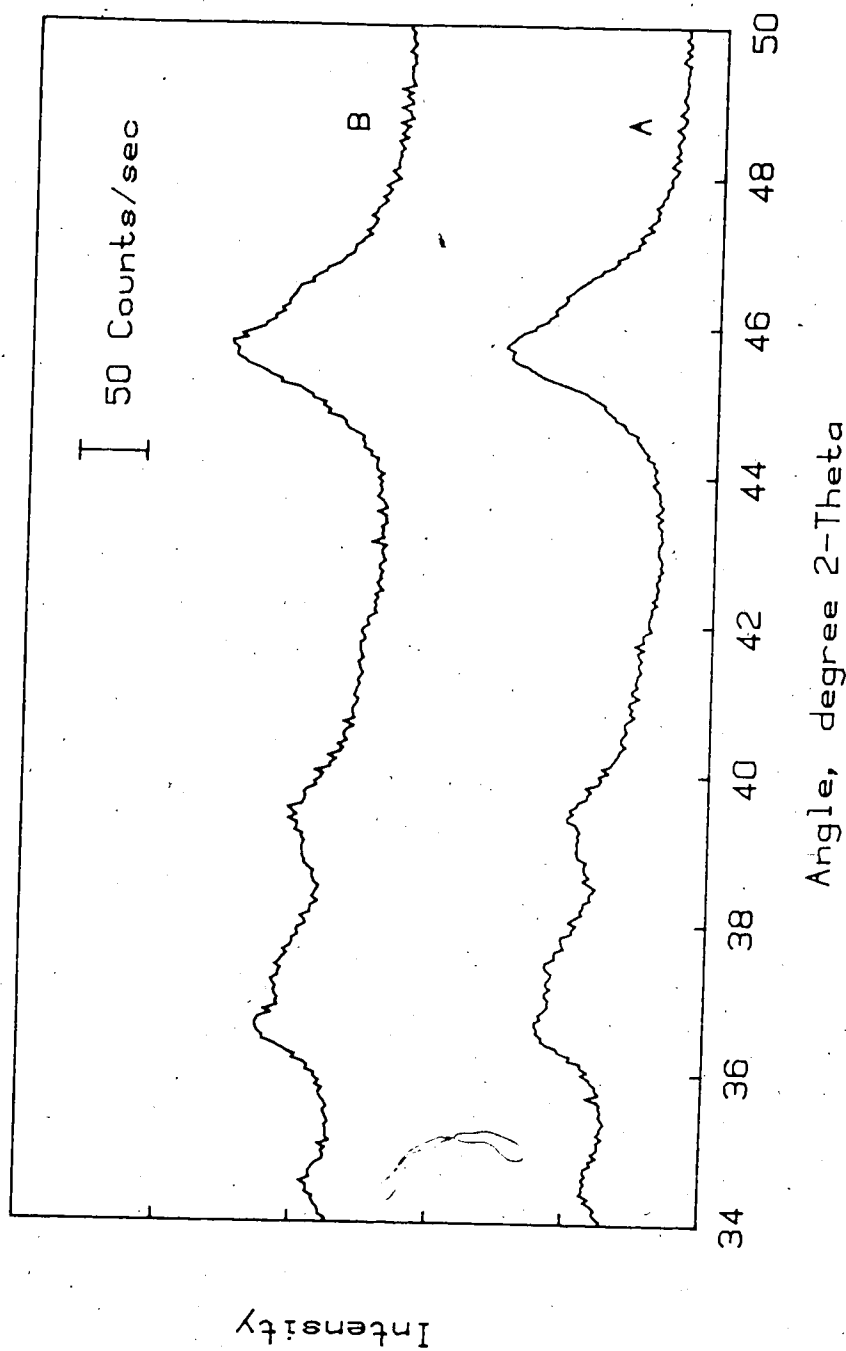


FIGURE A-9: Profiles of 1% Ir Catalysts
-Each profile is offset by 100 counts/sec
A=AI-12, B=AI-14

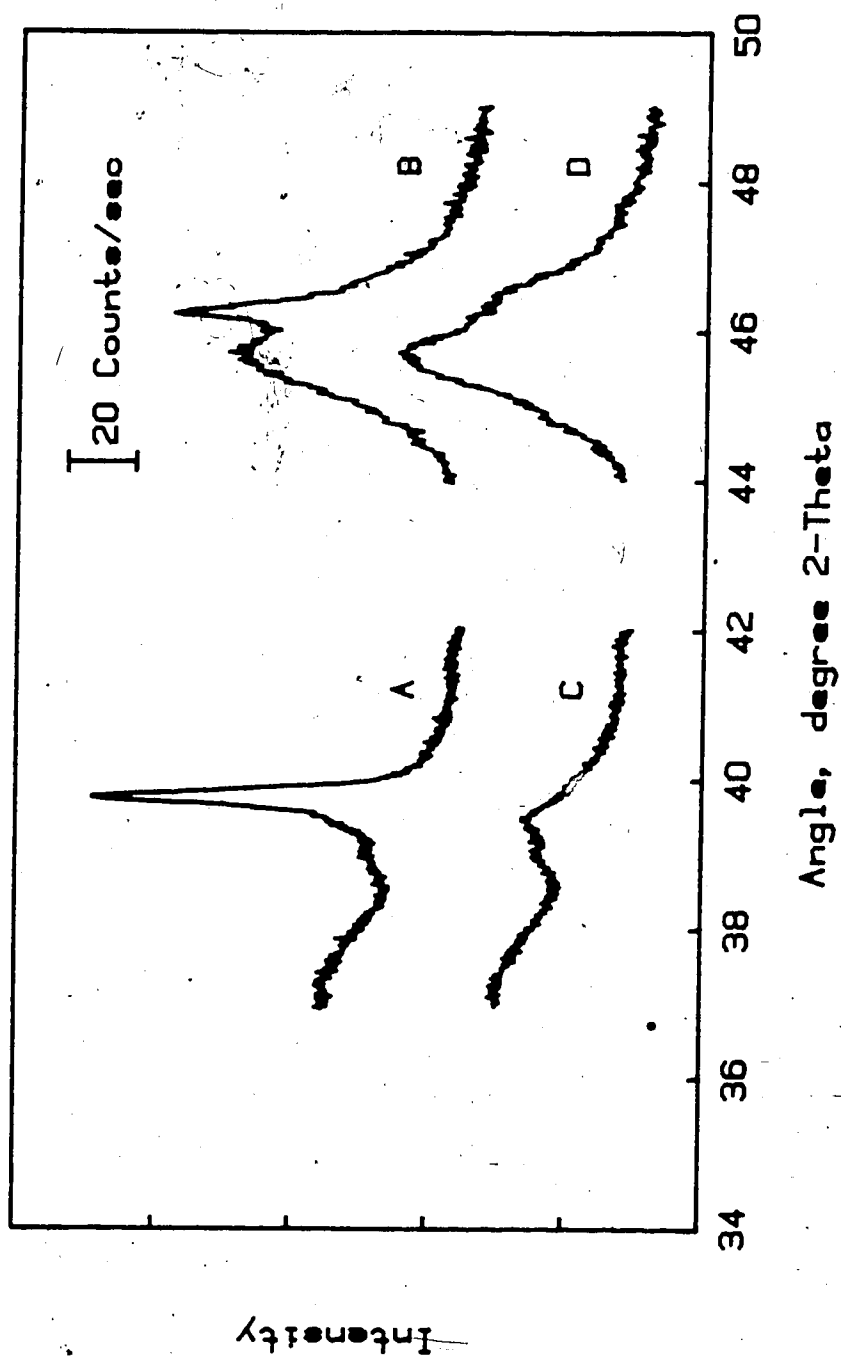


FIGURE A-10: Standard and Support Profiles used

-Each profile is offset by 50 counts/sec

A-MP-11 Pt(111), B-MP-11 Pt(200), C-A9, D-A10

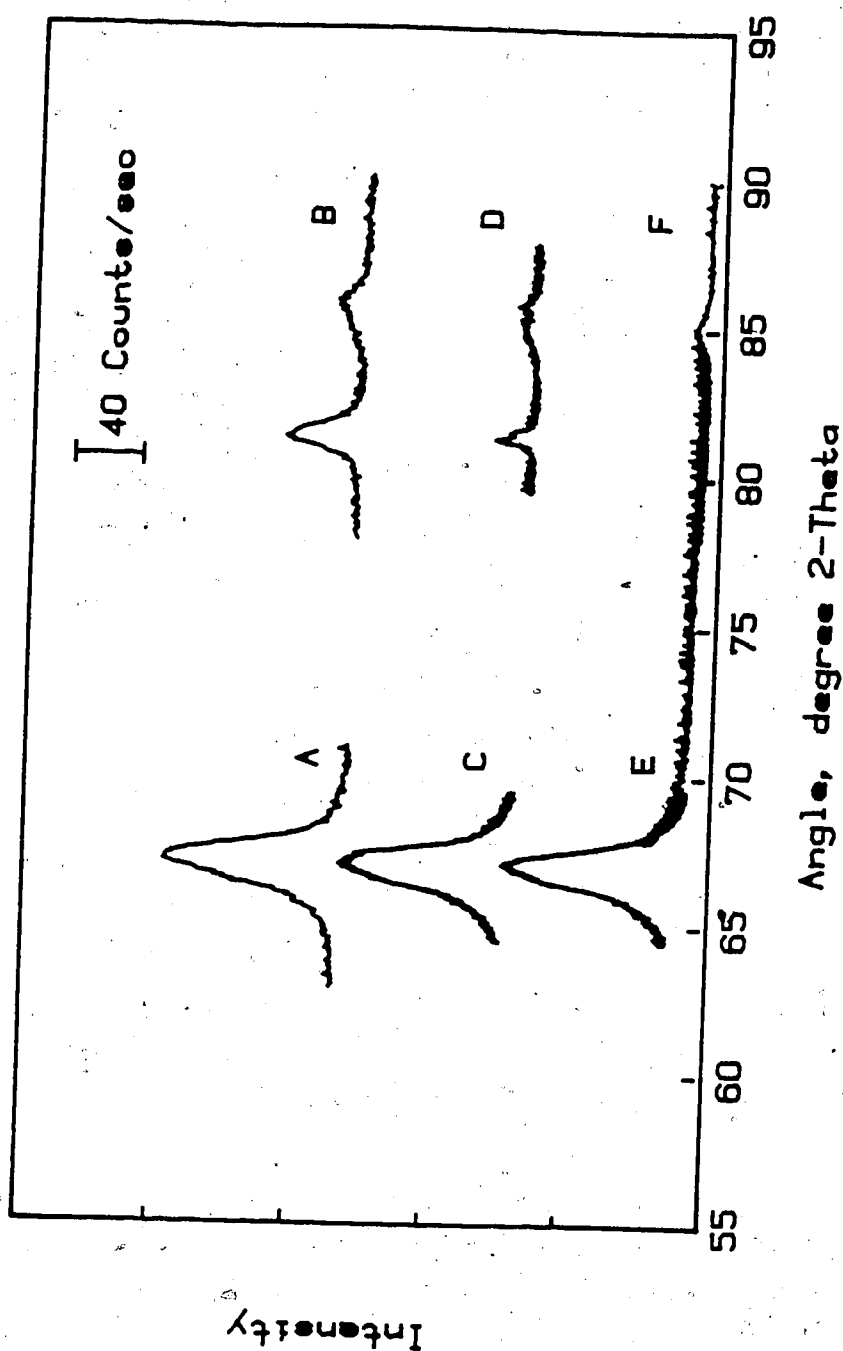


FIGURE A-11: Profiles for Size-Strain Analysis of catalyst HP-3

-Each profile is offset by 100 counts/100

A=HP-3, B=HP-3, C=MP-11, D=MP-11, E=A10, F=A10

12. APPENDIX B: Catalyst Analyses

This Appendix presents the results of XRD analysis of the catalysts used in this work. Unavailable or unreasonable results are indicated using asterices.

CATALYST AND SUPPORT IDENTIFICATION

***** **

Analysis of Catalyst: HP-2

For Miller Index: (111)

Support treatment: A-3

Catalyst Data File: XRAY59

Support Data File: XRAY69

SUPPORT CORRECTION

Support Scaling Factor: 0.80

Linear Baseline ($(2\theta_{mn}, I_{mn})$ to $(2\theta_{mx}, I_{mx})$)
(34.° 2 θ , 4.0 c/s) (50.° 2 θ , 2.0 c/s)

MAGNITUDE AND LOCATION OF "SPURIOUS" PEAKS

(Due to Heat Treatment Support Changes)

Angle (° 2 θ)	Magnitude (c/s)
37.25	3.5

MARQUARDT FIT OF THE DATA

Centre of Fit Range: 39.80

Range Studied: 9.00 ° 2 θ

No. Iterations: 9 Converged: YES

 Σ (error)²/Angle: 66.56(C/S)**2/° 2 θ

FIT PARAMETERS (see Equation 3-44):

B1=	71.8	B2=	10.19	X0=	39.759	T=	0.87750
B3=	71.964	B4=	8.7550	B5=	0.9627		

RESULTS CALCULATED DIRECTLY FROM FIT:

Peak height: 143.80 c/s $B_{1/2}$: 0.01075 rad

Area: 2.2136 rad*c/s Integral Breadth: 0.015390 rad

CALCULATED WITH OTHER RESULTS,

From File: XRAY27 Standard Integral Breadth= 0.004008

<La1> (Geometric, Fc) = 8.80 nm

<La2> (Numerical, Fc) = 6.92 nm

<Lv1> (Scherrer) = 11.04 nm

<Lv2> (Numerical, Foc) = 10.98 nm

Fraction Detected > 0.950 <Lv>/<La> = 1.40

CATALYST AND SUPPORT IDENTIFICATION

***** **

Analysis of Catalyst: HP-3

For Miller Index: (111)

Support treatment: A-3

Catalyst Data File: XRAY71

Support Data File: XRAV69

SUPPORT CORRECTION

Support Scaling Factor: 0.80

Linear Baseline ($(2\theta_{mn}, I_{mn})$ to $(2\theta_{mx}, I_{mx})$)
(34.° 2θ , 0.0 c/s) (50.° 2θ , 0.0 c/s)

MAGNITUDE AND LOCATION OF "SPURIOUS" PEAKS

(Due to Heat Treatment Support Changes)

Angle (° 2θ)	Magnitude (c/s)
36.50	2.0
37.50	2.0

MARQUARDT FIT OF THE DATA

Centre of Fit Range: 39.80

Range Studied: 4.00 ° 2θ

No. Iterations: 12 Converged: YES

 $\Sigma (\text{error})^2 / \text{Angle} : 26.65 (\text{C/S}) ** 2 / ^\circ 2\theta$

FIT PARAMETERS (see Equation 3-44):

B1= 65.8 B2= 6.68 X0= 39.706 T= 0.99898

B3= 73.807 B4= 8.4610 B5= 0.9318

RESULTS CALCULATED DIRECTLY FROM FIT:

Peak height: 139.60 c/s $B_{1/2}$: 0.01141 rad

Area: 2.1928 rad*c/s, Integral Breadth: 0.015700 rad

CALCULATED WITH OTHER RESULTS,

From File: XRAY27 Standard Integral Breadth= 0.004008

<La1> (Geometric, Fourier) = 8.52 nm

<La2> (Numerical, Fourier) = 8.05 nm

<Lv1> (Scherrer) = 10.80 nm

<Lv2> (Numerical, Fourier) = 10.70 nm

Fraction Detected > 0.950 <Lv>/<La> = 1.30

CATALYST AND SUPPORT IDENTIFICATION

***** **

Analysis of Catalyst: HP-3

For Miller Index: (200)

Support treatment: A-3

Catalyst Data File: XRAY71

Support Data File: XRAV69

SUPPORT CORRECTION

Support Scaling Factor: 0.80

Linear Baseline ($(2\theta_{mn}, I_{mn})$ to $(2\theta_{mx}, I_{mx})$)
(34.° 2 θ , 0.5 c/s) (50.° 2 θ , 0.5 c/s)

MAGNITUDE AND LOCATION OF "SPURIOUS" PEAKS

(Due to Heat Treatment Support Changes)

Angle (° 2 θ)	Magnitude (c/s)
36.50	0.0

MARQUARDT FIT OF THE DATA

Centre of Fit Range: 46.30

Range Studied: 6.00 ° 2 θ

No. Iterations: 16 Converged: YES

 $\Sigma (\text{error})^2 / \text{Angle} : 28.45 (\text{C/S})^{**2} / ^\circ 2\theta$

FIT PARAMETERS (see Equation 3-44):

B1=	56.6	B2=	3.91	X0=	46.221	T=	2.77800
B3=	5.575	B4=	0.6207	B5=	0.6181		

RESULTS CALCULATED DIRECTLY FROM FIT:

Peak height: 62.12 c/s $B_{1/2}$: 0.01146 rad

Area: 0.9518 rad*c/s Integral Breadth: 0.015320 rad

CALCULATED WITH OTHER RESULTS,

From File: XRAYE3 Standard Integral Breadth= 0.003950

<La1> (Geometric, Fourier) = 0.00 nm

<La2> (Numerical, Fourier) = 0.0 nm

<Lv1> (Scherrer) = 11.32 nm

<Lv2> (Numerical, Fourier) = 0.0 nm

Fraction Detected = 0.0 <Lv>/<La> = ****

CATALYST AND SUPPORT IDENTIFICATION

***** **

Analysis of Catalyst: HP-3

For Miller Index: (220)

Support treatment: A-3

Catalyst Data File: XRAYD9

Support Data File: XRAYD4

SUPPORT CORRECTION

Support Scaling Factor: 0.80

Linear Baseline ($(2\theta_{mn}, I_{mn})$ to $(2\theta_{mx}, I_{mx})$)
(63.° 2 θ , 0.0 c/s) (71.° 2 θ , 0.0 c/s)

MAGNITUDE AND LOCATION OF "SPURIOUS" PEAKS

(Due to Heat Treatment Support Changes)

Angle (° 2 θ)	Magnitude (c/s)
70.00	0.0

MARQUARDT FIT OF THE DATA

Centre of Fit Range: 67.50

Range Studied: 6.00 ° 2 θ

No. Iterations: 50 Converged: NO

 $\Sigma (\text{error})^2 / \text{Angle} = 0.50 (\text{C/S})^{**2} / ^\circ 2\theta$

FIT PARAMETERS (see Equation 3-44):

B1= 4.4	B2= 0.37	X0= 67.485	T= 1.34260
B3= 34.590	B4= 5.6850	B5= 0.7523	

RESULTS CALCULATED DIRECTLY FROM FIT:

Peak height: 39.01 c/s $B_{1/2}$: 0.01419 rad

Area: 0.7793 rad*c/s Integral Breadth: 0.019980 rad

CALCULATED WITH OTHER RESULTS,

From File: XRAYE1 Standard Integral Breadth= 0.004220

<La1> (Geometric, Fourier)	= 0.00 nm
<La2> (Numerical, Fourier)	= 0.0 nm
<Lv1> (Scherrer)	= 9.46 nm
<Lv2> (Numerical, Fourier)	= 0.0 nm

Fraction Detected = 0.0 <Lv>/<La> = ****

CATALYST AND SUPPORT IDENTIFICATION

***** **

Analysis of Catalyst: HP-3

For Miller Index: (311)

Support treatment: A-3

Catalyst Data File: XRAYE0

Support Data File: XRAYD7

SUPPORT CORRECTION

Support Scaling Factor: 0.80

Linear Baseline ($(2\theta_{mn}, I_{mn})$ to $(2\theta_{mx}, I_{mx})$)
(78.° 2 θ , 2.0 c/s) (90.° 2 θ , 2.0 c/s)

MAGNITUDE AND LOCATION OF "SPURIOUS" PEAKS

(Due to Heat Treatment Support Changes)

Angle (° 2 θ)	Magnitude (c/s)
30.00	0.0

MARQUARDT FIT OF THE DATA

Centre of Fit Range: 81.10

Range Studied: 5.00 ° 2 θ

No. Iterations: 23 Converged: YES

 Σ (error)²/Angle: 0.10(C/S)**2/° 2 θ

FIT PARAMETERS (see Equation 3-44):

B1= 10.4	B2= 0.56	X0= 81.260	T= 1.63550
B3= 33.410	B4= 4.9680	B5= 0.9305	

RESULTS CALCULATED DIRECTLY FROM FIT:

Peak height: 43.80 c/s $B_{1/2}$: 0.01545 rad

Area: 0.9893 rad*c/s Integral Breadth: 0.022590 rad

CALCULATED WITH OTHER RESULTS,

From File: XRAYE2 Standard Integral Breadth= 0.006720

<La1> (Geometric, Fourier)	= 0.00 nm
<La2> (Numerical, Fourier)	= 0.0 nm
<Lv1> (Scherrer)	= 9.42 nm
<Lv2> (Numerical, Fourier)	= 0.0 nm

Fraction Detected = 0.0 <Lv>/<La> = ****

CATALYST AND SUPPORT IDENTIFICATION

***** **

Analysis of Catalyst: HP-3

For Miller Index: (222)

Support treatment: A-3

Catalyst Data File: XRAYE0

Support Data File: XRAYD6

SUPPORT CORRECTION

Support Scaling Factor: 1.00

Linear Baseline ($(2\theta_{mn}, I_{mn})$ to $(2\theta_{mx}, I_{mx})$)
(80.° 2 θ , 0.0 c/s) (88.° 2 θ , 0.0 c/s)

MAGNITUDE AND LOCATION OF "SPURIOUS" PEAKS

(Due to Heat Treatment Support Changes)

Angle (° 2 θ)	Magnitude (c/s)
30.00	0.0

MARQUARDT FIT OF THE DATA

Centre of Fit Range: 85.80

Range Studied: 2.00 ° 2 θ

No. Iterations: 40

Converged: YES

 $\Sigma (\text{error})^2 / \text{Angle} : 51.65 (\text{C/S}) ** 2 / ^\circ 2\theta$

FIT PARAMETERS (see Equation 3-44):

B1= 4.4 B2= 0.80 X0= 85.722 T= 19.61501

B3= 9.719 B4= 1.9650 B5= 0.8317

RESULTS CALCULATED DIRECTLY FROM FIT:

Peak height: 14.08 c/s B_{1/2}: 0.01574 rad

Area: 0.2608 rad*c/s Integral Breadth: 0.018520 rad

CALCULATED WITH OTHER RESULTS,

From File: XRAY00 Standard Integral Breadth= 0.006000

<La1> (Geometric, Fourier) = 0.00 nm

<La2> (Numerical, Fourier) = 0.0 nm

<Lv1> (Scherrer) = 12.10 nm

<Lv2> (Numerical, Fourier) = 0.0 nm

Fraction Detected = 0.0

<Lv>/<La> = ****

CATALYST AND SUPPORT IDENTIFICATION

***** **

Analysis of Catalyst: HP-6

For Miller Index: (111)

Support treatment: A-3

Catalyst Data File: XRAY63

Support Data File: XRAY69

SUPPORT CORRECTION

Support Scaling Factor: 0.80

Linear Baseline ($(2\theta_{mn}, I_{mn})$ to $(2\theta_{mx}, I_{mx})$)
(34.° 2 θ , 2.0 c/s) (50.° 2 θ , 0.5 c/s)

MAGNITUDE AND LOCATION OF "SPURIOUS" PEAKS

(Due to Heat Treatment Support Changes)

Angle (° 2 θ) Magnitude (c/s)

36.75 5.0

37.50 3.0

MARQUARDT FIT OF THE DATA

Centre of Fit Range: 39.80

Range Studied: 6.00 ° 2 θ

No. Iterations: 12 Converged: YES

 $\Sigma (\text{error})^2 / \text{Angle}$: 21.57(C/S)**2/° 2 θ

FIT PARAMETERS (see Equation 3-44):

B1= 183.2 B2= 94.16 X0= 39.757 T= 0.78738

B3= 38.332 B4= 11.3790 B5= 0.7906

RESULTS CALCULATED DIRECTLY FROM FIT:

Peak height: 221.53 c/s $B_{1/2}$: 0.00521 rad

Area: 1.8954 rad*c/s Integral Breadth: 0.008554 rad

CALCULATED WITH OTHER RESULTS,

From File: XRAY27 Standard Integral Breadth= 0.004008

<La1> (Geometric, Fourier) = 12.39 nm

<La2> (Numerical, Fourier) = 8.42 nm

<Lv1> (Scherrer) = 21.70 nm

<Lv2> (Numerical, Fourier) = 18.60 nm

Fraction Detected = 0.876 <Lv>/<La> = 1.94

CATALYST AND SUPPORT IDENTIFICATION

***** *** ***** *****

Analysis of Catalyst: HP-7

For Miller Index: (111)

Support treatment: A-3

Catalyst Data File: XRAYE5

Support Data File: XRAV11

SUPPORT CORRECTION

Support Scaling Factor: 0.80

Linear Baseline ($(2\theta_{mn}, I_{mn})$ to $(2\theta_{mx}, I_{mx})$)
(34.° 2 θ , 8.0 c/s) (50.° 2 θ , 6.0 c/s)

MAGNITUDE AND LOCATION OF "SPURIOUS" PEAKS

(Due to Heat Treatment Support Changes)

Angle (° 2 θ)	Magnitude (c/s)
36.50	0.0

MARQUARDT FIT OF THE DATA

Centre of Fit Range: 39.80

Range Studied: 8.00 ° 2 θ

No. Iterations: 20 Converged: NO

 $\Sigma (\text{error})^2 / \text{Angle} : 38.73(\text{C/S})^{**2} / ^\circ 2\theta$

FIT PARAMETERS (see Equation 3-44):

B1= 17.1 B2= 1.74 X0= 39.819 T= 0.50000

B3= 3.381 B4= 0.2987 B5= 0.5082

RESULTS CALCULATED DIRECTLY FROM FIT:

Peak height: 20.48 c/s $B_{1/2}$: 0.05727 rad

Area: 2.2724 rad*c/s Integral Breadth: 0.110900 rad

CALCULATED WITH OTHER RESULTS,

From File: XRAY27 Standard Integral Breadth= 0.004008

<La1> (Geometric, Fourier) = 3.66 nm

<La2> (Numerical, Fourier) = 1.77 nm

<Lv1> (Scherrer) = 2.30 nm

<Lv2> (Numerical, Fourier) = 1.48 nm

Fraction Detected = 0.900 <Lv>/<La> = 0.70

CATALYST AND SUPPORT IDENTIFICATION

***** **

Analysis of Catalyst: AI-13

For Miller Index: (111)

Support treatment: A-3

Catalyst Data File: XRAY83

Support Data File: XRAV69

SUPPORT CORRECTION

Support Scaling Factor: 0.95

Linear Baseline ($(2\theta_{mn}, I_{mn})$ to $(2\theta_{mx}, I_{mx})$)
(34.° 2θ , 1.0 c/s) (50.° 2θ , 1.0 c/s)

MAGNITUDE AND LOCATION OF "SPURIOUS" PEAKS

(Due to Heat Treatment Support Changes)

Angle (° 2θ)	Magnitude (c/s)
38.00	4.0

MARQUARDT FIT OF THE DATA

Centre of Fit Range: 41.00

Range Studied: 6.00 ° 2θ

No. iterations: 0 Converged: UNK

 $\Sigma (\text{error})^2 / \text{Angle}: 34.50(\text{C/S})^{**2} / \text{° } 2\theta$

FIT PARAMETERS (see Equation 3-44):

B1= 1.7 B2= 0.05 X0= 39.819 T= 40.53000

B3= 6.162 B4= 2.9830 B5= 0.2325

RESULTS CALCULATED DIRECTLY FROM FIT:

Peak height: 4.66 c/s $B_{1/2}$: 0.08604 rad

Area: 0.4360 rad*c/s Integral Breadth: 0.093450 rad

CALCULATED WITH OTHER RESULTS,

From File: XRAY27 Standard Integral Breadth= 0.004008

<La1> (Geometric, Fourier) = 1.50 nm

<La2> (Numerical, Fourier) = 1.49 nm

<Lv1> (Scherrer) = 1.76 nm

<Lv2> (Numerical, Fourier) = 1.70 nm

Fraction Detected = 0.700 <Lv>/<La> = 1.16

CATALYST AND SUPPORT IDENTIFICATION

Analysis of Catalyst: AI-2

For Miller Index: (111)

Support treatment: A-3

Catalyst Data File: XRAY92

Support Data File: XRAY69

SUPPORT CORRECTION

Support Scaling Factor: 1.0

Linear Baseline - ((2 θ_{min} , I $_{min}$) to (2 θ_{max} , I $_{max}$))
(34.° 2 θ , 0.0 c/s) (50.° 2 θ , 0.0 c/s)

MAGNITUDE AND LOCATION OF "SPURIOUS" PEAKS

(Due to Heat Treatment Support Changes)

Angle (° 2 θ)	Magnitude (c/s)
30.00	0.0

MARQUARDT FIT OF THE DATA

Centre of Fit Range: 40.70

Range Studied: 8.00 ° 2 θ

No. Iterations: 20 Converged: NO

 Σ (error)²/Angle: 47.23(C/S)**2/° 2 θ

FIT PARAMETERS (see Equation 3-44):

B1= 3.0 B2= 0.37 X0= 40.434 T= 0.50000

B3= 2.004 B4= 4.7900 B5= 0.1173

RESULTS CALCULATED DIRECTLY FROM FIT:

Peak height: 4.98 c/s B_{1/2}: 0.12025 rad

Area: 0.8159 rad*c/s Integral Breadth: 0.163800 rad

CALCULATED WITH OTHER RESULTS,

From File: XRAY27 Standard Integral Breadth= 0.004008

<La1> (Geometric, Fourier) = 1.00 nm

<La2> (Numerical, Fourier) = 0.82 nm

<Lv1> (Scherrer) = 1.00 nm

<Lv2> (Numerical, Fourier) = 1.17 nm

Fraction Detected = 0.850 <Lv>/<La> = 1.19

CATALYST AND SUPPORT IDENTIFICATION

Analysis of Catalyst: AI-4

For Miller Index: (111)

Support treatment: A-3

Catalyst Data File: XRAY17

Support Data File: XRAY11

SUPPORT CORRECTION

Support Scaling Factor: 0.95

Linear Baseline ($(2\theta_{mn}, I_{mn})$ to $(2\theta_{mx}, I_{mx})$)
(34.° 2 θ , 0.0 c/s) (50.° 2 θ , 0.0 c/s)

MAGNITUDE AND LOCATION OF "SPURIOUS" PEAKS

(Due to Heat Treatment Support Changes)

Angle (° 2 θ)	Magnitude (c/s)
39.00	2.0

MARQUARDT FIT OF THE DATA

Centre of Fit Range: 41.60

Range Studied: 4.00 ° 2 θ

No. Iterations: 4 Converged: YES

 $\Sigma (\text{error})^2 / \text{Angle} = 21.95 (\text{C/S})^{**2} / ^\circ 2\theta$

FIT PARAMETERS (see Equation 3-44):

B1= 45.6 B2= 20.85 X0= 40.634 T= 0.84830

B3= 4.723 B4= 8.9980 B5= 0.7380

RESULTS CALCULATED DIRECTLY FROM FIT:

Peak height: 50.27 c/s $B_{1/2}$: 0.00944 rad

Area: 0.7805 rad*c/s Integral Breadth: 0.015420 rad

CALCULATED WITH OTHER RESULTS,

From File: XRAY27 Standard Integral Breadth= 0.004009

<La1> (Geometric, Fourier) = 1.00 nm

<La2> (Numerical, Fourier) = 7.70 nm

<Lv1> (Scherrer) = 5.82 nm

<Lv2> (Numerical, Fourier) = 10.91 nm

Fraction Detected > 0.950 <Lv>/<La> = 1.92

CATALYST AND SUPPORT IDENTIFICATION

***** **

Analysis of Catalyst: AI-5

For Miller Index: (111)

Support treatment: A-3

Catalyst Data File: XRAY19

Support Data File: XRAY11

SUPPORT CORRECTION

Support Scaling Factor: 0.95

Linear Baseline ($(2\theta_{mn}, I_{mn})$ to $(2\theta_{mx}, I_{mx})$)
(34.° 2 θ , 0.0 c/s) (50.° 2 θ , 0.0 c/s)

MAGNITUDE AND LOCATION OF "SPURIOUS" PEAKS

(Due to Heat Treatment Support Changes)

Angle (° 2 θ)	Magnitude (c/s)
39.00	2.0

MARQUARDT FIT OF THE DATA

Centre of Fit Range: 41.50

Range Studied: 4.00 ° 2 θ

No. Iterations: 31 Converged: YES

 $\Sigma (\text{error})^2 / \text{Angle} : 29.50 (\text{C/S}) ** 2 / ^\circ 2\theta$

FIT PARAMETERS (see Equation 3-44):

B1= 14.6 B2= 1.23 X0= 40.662 T= 1.80320

B3= 20.316 B4= 13.5300 B5= 0.6696

RESULTS CALCULATED DIRECTLY FROM FIT:

Peak height: 34.98 c/s $B_{1/2}$: 0.01179 rad

Area: 0.6445 rad*c/s Integral Breadth: 0.018440 rad

CALCULATED WITH OTHER RESULTS,

From File: XRAY27 Standard Integral Breadth= 0.004008

<La1> (Geometric, Fourier) = 5.24 nm

<La2> (Numerical, Fourier) = 5.57 nm

<Lv1> (Scherrer) = 9.10 nm

<Lv2> (Numerical, Fourier) = 9.50 nm

Fraction Detected > 0.950 <Lv>/<La> = 1.72

CATALYST AND SUPPORT IDENTIFICATION

***** **

Analysis of Catalyst: AI-16

For Miller Index: (111)

Support treatment: A-3

Catalyst Data File: XRAY98

Support Data File: XRAY69

SUPPORT CORRECTION

Support Scaling Factor: 0.95

Linear Baseline ($(2\theta_{mn}, I_{mn})$ to $(2\theta_{mx}, I_{mx})$)
(34.° 2 θ , 0.0 c/s) (50.° 2 θ , 0.0 c/s)

MAGNITUDE AND LOCATION OF "SPURIOUS" PEAKS

(Due to Heat Treatment Support Changes)

Angle (° 2 θ)	Magnitude (c/s)
38.00	0.0

MARQUARDT FIT OF THE DATA

Centre of Fit Range: 40.60

Range Studied: 4.00 ° 2 θ

No. Iterations: 15 Converged: YES

 $\Sigma (\text{error})^2 / \text{Angle} : 42.92 (\text{C/S}) ** 2 / ^\circ 2\theta$

FIT PARAMETERS (see Equation 3-44):

B1= 33.7 B2= 41.85 X0= 40.660 T= 0.77350

B3= 24.450 B4= 72.9890 B5= 2.0640

RESULTS CALCULATED DIRECTLY FROM FIT:

Peak height: 58.15 c/s $B_{1/2}$: 0.00377 rad

Area: 0.5273 rad*c/s Integral Breadth: 0.009070 rad

CALCULATED WITH OTHER RESULTS,

From File: XRAY27 Standard Integral Breadth= 0.004008

<La1> (Geometric, Fourier) = 5.90 nm

<La2> (Numerical, Fourier) = 5.12 nm

<Lv1> (Scherrer) = 20.27 nm

<Lv2> (Numerical, Fourier) = 17.12 nm

Fraction Detected = 0.850 <Lv>/<La> = 3.39

CATALYST AND SUPPORT IDENTIFICATION

***** **

Analysis of Catalyst: AI-8

For Miller Index: (111)

Support treatment: A-3

Catalyst Data File: XRAY58

Support Data File: XRAY69

SUPPORT CORRECTION

Support Scaling Factor: 0.95

Linear Baseline: $(2\theta_{mn}, I_{mn})$ to $(2\theta_{mx}, I_{mx})$
(34.° 2 θ , 0.0 c/s) (50.° 2 θ , 0.0 c/s)

MAGNITUDE AND LOCATION OF "SPURIOUS" PEAKS

(Due to Heat Treatment Support Changes)

Angle (° 2 θ)	Magnitude (c/s)
30.00	0.0

MARQUARDT FIT OF THE DATA

Centre of Fit Range: 41.00

Range Studied: 3.00 ° 2 θ

No. Iterations: 24 Converged: YES

 $\Sigma (\text{error})^2 / \text{Angle} = 27.87 (\text{C/S})^{**2} / ^\circ 2\theta$

FIT PARAMETERS (see Equation 3-44):

B1= 14.0 B2= 0.83 X0= 40.610 T= 2.57600

B3= 34.393 B4= 11.8160 B5= 1.0570

RESULTS CALCULATED DIRECTLY FROM FIT:

Peak height: 48.43 c/s $B_{1/2}$: 0.00977 rad

Area: 0.6535 rad*c/s Integral Breadth: 0.013500 rad

CALCULATED WITH OTHER RESULTS,

From File: XRAY27 Standard Integral Breadth= 0.004040

<La1> (Geometric, Fourier) = 8.20 nm

<La2> (Numerical, Fourier) = 8.40 nm

<Lv1> (Scherrer) = 11.40 nm

<Lv2> (Numerical, Fourier) = 13.30 nm

Fraction Detected > 0.950 <Lv>/<La> = 1.49

CATALYST AND SUPPORT IDENTIFICATION

***** **

Analysis of Catalyst: AI-8

For Miller Index: (111)

Support treatment: A-3

Catalyst Data File: XRAY25

Support Data File: XRAY06

SUPPORT CORRECTION

Support Scaling Factor: 0.95

Linear Baseline ($(2\theta_{mn}, I_{mn})$ to $(2\theta_{mx}, I_{mx})$)
(34.° 2 θ , 0.0 c/s) (50.° 2 θ , 0.0 c/s)

MAGNITUDE AND LOCATION OF "SPURIOUS" PEAKS

(Due to Heat Treatment Support Changes)

Angle (° 2 θ)	Magnitude (c/s)
30.00	0.0

MARQUARDT FIT OF THE DATA

Centre of Fit Range: 40.60

Range Studied: 2.00 ° 2 θ

No. Iterations: 12 Converged: YES

 Σ (error)²/Angle: 34.55(C/s) *2/° 2 θ

FIT PARAMETERS (see Equation 3-44):

B1= 39.4 B2= 16.88 X0= 40.620 T= 0.92816

B3= 13.550 B4= 5.2990 B5= 1.1130

RESULTS CALCULATED DIRECTLY FROM FIT:

Peak height: 52.99 c/s $B_{1/2}$: 0.00969 rad

Area: 0.7336 rad*c/s Integral Breadth: 0.013840 rad

CALCULATED WITH OTHER RESULTS:

From File: XRAY27 Standard Integral Breadth= 0.004000

<La1> (Geometric, Fourier) = 9.20 nm

<La2> (Numerical, Fourier) = 8.20 nm

<Lv1> (Scherrer) = 14.90 nm

<Lv2> (Numerical, Fourier) = 12.90 nm

Fraction Detected > 0.950 <Lv>/<La> = 1.60

CATALYST AND SUPPORT IDENTIFICATION

***** **

Analysis of Catalyst: AI-12

For Mill Index: (111)

Support treatment: A-3

Catalyst Data File: XRAY85

Support Data File: XRAY69

SUPPORT CORRECTION

Support Scaling Factor: 0.95

Linear Baseline ($(2\theta_{mn}, I_{mn})$ to $(2\theta_{mx}, I_{mx})$)
(34.° 2 θ , 1.0 c/s) (50.° 2 θ , 1.0 c/s)

MAGNITUDE AND LOCATION OF "SPURIOUS" PEAKS

(Due to Heat Treatment Support Changes)

Angle (° 2 θ)	Magnitude (c/s)
37.50	3.5

MARQUARDT FIT OF THE DATA

Centre of Fit Range: 41.50

Range Studied: 5.00 ° 2 θ

No. Iterations: 19 Converged: YES

 Σ (error)² angle: 27.28 (C/S)**2/° 2 θ

FIT PARAMETERS (see Equation 3-44):

B1= 0.5 B2= 0.06 X0= 40.522 T= 19.79601

B3= 4.480 B4= 0.3310 B5= 0.7505

RESULTS CALCULATED DIRECTLY FROM FIT:

Peak height: 4.94 c/s $B_{1/2}$: 0.05653 rad

Area: 0.3056 rad*c/s Integral Breadth: 0.061910 rad

CALCULATED WITH OTHER RESULTS,

From File: XRAY27 Standard Integral Breadth= 0.004008

<La1> (Geometric, Fourier) = 2.39 nm

<La2> (Numerical, Fourier) = 2.79 nm

<Lv1> (Scherrer) = 2.65 nm

<Lv2> (Numerical, Fourier) = 3.15 nm

Fraction Detected = 0.500 <Lv>/<La> = 1.12

CATALYST AND SUPPORT IDENTIFICATION

***** **

Analysis of Catalyst: AI-14

For Miller Index: (111)

Support treatment: A-3

Catalyst Data File: XRAY89

Support Data File: XRAV69

SUPPORT CORRECTION

Support Scaling Factor: 0.95

Linear Baseline ($(2\theta_{mn}, I_{mn})$ to $(2\theta_{mx}, I_{mx})$)
(34.° 2 θ , 1.0 c/s) (50.° 2 θ , 1.0 c/s)

MAGNITUDE AND LOCATION OF "SPURIOUS" PEAKS

(Due to Heat Treatment Support Changes)

Angle (° 2 θ)	Magnitude (c/s)
36.80	3.0

MARQUARDT FIT OF THE DATA

Centre of Fit Range: 41.00

Range Studied: 6.00 ° 2 θ

No. Iterations: 30 Converged: NO

 $\Sigma (\text{error})^2 / \text{Angle} : 44.00 (\text{C/S}) ** 2 / ^\circ 2\theta$

FIT PARAMETERS (see Equation 3-44):

B1= 2.9 B2= 0.07 X0= 40.522 T= 40.33900

B3= 3.160 B4= 3.7550 B5= 0.1826

RESULTS CALCULATED DIRECTLY FROM FIT:

Peak height: 6.61 c/s $B_{1/2}$: 0.06084 rad

Area: 0.4445 rad*c/s Integral Breadth: 0.067200 rad

CALCULATED WITH OTHER RESULTS,

From File: XRAY27 Standard Integral Breadth= 0.004008

<La1> (Geometric, Fourier) = 2.04 nm

<La2> (Numerical, Fourier) = 2.23 nm

<Lv1> (Scherrer) = 2.44 nm

<Lv2> (Numerical, Fourier) = 2.49 nm

Fraction Detected = 0.718 <Lv>/<La> = 1.15

CATALYST AND SUPPORT IDENTIFICATION

***** **

Analysis of Catalyst: AP-1

For Miller Index: (111)

Support treatment: A-3

Catalyst Data File: XRAY34

Support Data File: XRAV69

SUPPORT CORRECTION

Support Scaling Factor: 0.95

Linear Baseline ($(2\theta_{mn}, I_{mn})$ to $(2\theta_{mx}, I_{mx})$)
(34.° 2 θ , 0.0 c/s) (50.° 2 θ , 0.0 c/s)

MAGNITUDE AND LOCATION OF "SPURIOUS" PEAKS

(Due to Heat Treatment Support Changes)

Angle (° 2 θ)	Magnitude (c/s)
38.00	2.0

MARQUARDT FIT OF THE DATA

Centre of Fit Range: 40.50

Range Studied: 3.00 ° 2 θ

No. Iterations: 30 Converged: NO

 $\Sigma (\text{error})^2 / \text{Angle} : 27.83 (\text{C/S})^{**2} / ^\circ 2\theta$

FIT PARAMETERS (see Equation 3-44):

B1= 2.7 B2= 1.80 X0= 39.900 T= 0.50000

B3= 4.283 B4= 3.4750 B5= 0.6956

RESULTS CALCULATED DIRECTLY FROM FIT:

Peak height: 6.96 c/s $B_{1/2}$: 0.02204 rad

Area: 0.3364 rad*c/s Integral Breadth: 0.048360 rad

CALCULATED WITH OTHER RESULTS

From File: XRAY27 Standard Integral Breadth= 0.004000

<La1> (Geometric, Fourier) = 1.71 nm

<La2> (Numerical, Fourier) = 1.39 nm

<Lv1> (Scherrer) = 3.40 nm

<Lv2> (Numerical, Fourier) = 3.70 nm

Fraction Detected = 0.544 <Lv>/<La> = 2.29

CATALYST AND SUPPORT IDENTIFICATION

***** **

Analysis of Catalyst: AP-6

For Miller Index: (111)

Support treatment: A-3

Catalyst Data File: XRAY35

Support Data File: XRAV69

SUPPORT CORRECTION

Support Scaling Factor: 0.95

Linear Baseline ($(2\theta_{mn}, I_{mn})$ to $(2\theta_{mx}, I_{mx})$)
(34.° 2 θ , 0.0 c/s) (50.° 2 θ , 0.0 c/s)

MAGNITUDE AND LOCATION OF "SPURIOUS" PEAKS

(Due to Heat Treatment Support Changes)

Angle (° 2 θ)	Magnitude (c/s)
38.00	3.0

MARQUARDT FIT OF THE DATA

Centre of Fit Range: 40.50

Range Studied: 3.00 ° 2 θ

No. Iterations: 30 Converged: NO

 $\Sigma (\text{error})^2 / \text{Angle}$: 27.73(C/S)**2/° 2 θ

FIT PARAMETERS (see Equation 3-44):

B1= 6.1 B2= 8.75 X0= 39.760 T= 0.50000

B3= 2.267 B4= 2.2150 B5= 1.5000

RESULTS CALCULATED DIRECTLY FROM FIT:

Peak height: 8.40 c/s B_{1/2}: 0.0 rad

Area: 0.3622 rad*c/s Integral Breadth: 0.039170 rad

CALCULATED WITH OTHER RESULTS,

From File: XRAY27 Standard Integral Breadth= 0.004000

<La1> (Geometric, Fourier) = 1.88 nm

<La2> (Numerical, Fourier) = 1.51 nm

<Lv1> (Scherrer) = 4.21 nm

<Lv2> (Numerical, Fourier) = 4.14 nm

Fraction Detected = 0.532 <Lv>/<La> = 2.46

CATALYST AND SUPPORT IDENTIFICATION

***** **

Analysis of Catalyst: AP-8

For Miller Index: (111)

Support treatment: A-3

Catalyst Data File: XRAY74

Support Data File: XRAY69

SUPPORT CORRECTION

Support Scaling Factor: 0.95

Linear Baseline ($(2\theta_{mn}, I_{mn})$ to $(2\theta_{mx}, I_{mx})$)
(34.° 2 θ , 0.0 c/s) (50.° 2 θ , 0.0 c/s)

MAGNITUDE AND LOCATION OF "SPURIOUS" PEAKS

(Due to Heat Treatment Support Changes)

Angle (° 2 θ)	Magnitude (c/s)
37.20	2.0

MARQUARDT FIT OF THE DATA

Centre of Fit Range: 40.50

Range Studied: 3.00 ° 2 θ

No. Iterations: 30 Converged: NO

 Σ (error)²/Angle: 32.67(C/S)**2/° 2 θ

FIT PARAMETERS (see Equation 3-44):

B1= 5.5 B2= 19.81 X0= 39.726 T= 0.50000

B3= 17.853 B4= 3.3030 B5= 1.0004

RESULTS CALCULATED DIRECTLY FROM FIT:

Peak height: 23.38 c/s B_{1/2}: 0.01562 rad

Area: 0.5064 rad*c/s Integral Breadth: 0.021660 rad

CALCULATED WITH OTHER RESULTS,

From File: XRAY27 Standard Integral Breadth= 0.004000

<La1> (Geometric, Fourier) = 8.13 nm

<La2> (Numerical, Fourier) = 5.77 nm

<Lv1> (Scherrer) = 7.70 nm

<Lv2> (Numerical, Fourier) = 8.61 nm

Fraction Detected = 0.820 <Lv>/<La> = 1.17

CATALYST AND SUPPORT IDENTIFICATION

***** **

Analysis of Catalyst: AP-9

For Miller Index: (111)

Support treatment: A-3

Catalyst Data File: XRAY36

Support Data File: XRAY69

SUPPORT CORRECTION

Support Scaling Factor: 0.95

Linear Baseline ($(2\theta_{mn}, I_{mn})$ to $(2\theta_{mx}, I_{mx})$)
($1.^\circ 2\theta, *** \text{ c/s}$) ($-1.^\circ 2\theta, 0.0 \text{ c/s}$)

MAGNITUDE AND LOCATION OF "SPURIOUS" PEAKS

(Due to Heat Treatment Support Changes)

Angle ($^\circ 2\theta$)	Magnitude (c/s)
38.00	0.0

MARQUARDT FIT OF THE DATA

Centre of Fit Range: 39.80

Range Studied: $4.00^\circ 2\theta$

No. Iterations: 28 Converged: YES

 $\Sigma (\text{error})^2 / \text{Angle} : 46.90 (\text{C/S})^2 / ^\circ 2\theta$

FIT PARAMETERS (see Equation 3-44):

B1= 11.6 B2= 49.80 X0= 39.730 T= 0.50000

B3= 20.310 B4= 4.9370 B5= 0.8079

RESULTS CALCULATED DIRECTLY FROM FIT:

Peak height: 31.94 c/s $B_{1/2}$: 0.01252 rad

Area: 0.6072 rad*c/s Integral Breadth: 0.019010 rad

CALCULATED WITH OTHER RESULTS,

From File: XRAY27 Standard Integral Breadth= 0.004000

<La1> (Geometric, Fourier) = 9.85 nm

<La2> (Numerical, Fourier) = 5.36 nm

<Lv1> (Scherrer) = 3.63 nm

<Lv2> (Numerical, Fourier) = 9.92 nm

Fraction Detected > 0.950 <Lv>/<La> = 0.89

CATALYST AND SUPPORT IDENTIFICATION

***** **

Analysis of Catalyst: AP-10
 For Miller Index: (111)
 Support treatment: A-3

Catalyst Data File: XRAY14

Support Data File: XRAY11

SUPPORT CORRECTION

Support Scaling Factor: 0.95

Linear Baseline ($(2\theta_{mn}, I_{mn})$ to $(2\theta_{mx}, I_{mx})$)
 ($1.^\circ 2\theta, *** \text{ c/s}$) ($0.^\circ 2\theta, *** \text{ c/s}$)

MAGNITUDE AND LOCATION OF "SPURIOUS" PEAKS

(Due to Heat Treatment Support Changes)

Angle ($^\circ 2\theta$)	Magnitude (c/s)
36.50	2.5

MARQUARDT FIT OF THE DATA

Centre of Fit Range: 40.10

Range Studied: $3.00^\circ 2\theta$

No. Iterations: 14 Converged: YES

 $\Sigma (\text{error})^2 / \text{Angle}: 26.20 (\text{C/S})^{**2} / ^\circ 2\theta$

FIT PARAMETERS (see Equation 3-44):

B1= 116.0 B2= 104.64 X0= 39.750 T= 0.89370

B3= 8.558 B4= 14.6640 B5= 0.6694

RESULTS CALCULATED DIRECTLY FROM FIT:

Peak height: 124.58 c/s $B_{1/2}$: 0.00432 rad

Area: 0.8664 rad*c/s Integral Breadth: 0.006950 rad

CALCULATED WITH OTHER RESULTS,

From File: XRAY27 Standard Integral Breadth= 0.004010

<La1> (Geometric, Fourier) = 13.70 nm

<La2> (Numerical, Fourier) = 10.10 nm

<Lv1> (Scherrer) = 28.87 nm

<Lv2> (Numerical, Fourier) = 21.11 nm

Fraction Detected > 0.950 $\langle Lv \rangle / \langle La \rangle = 2.10$

CATALYST AND SUPPORT IDENTIFICATION

***** **

Analysis of Catalyst: AP-11

For Miller Index: (111)

Support treatment: A-3

Catalyst Data File: XRAY72

Support Data File: XRAY69

SUPPORT CORRECTION

Support Scaling Factor: 0.95

Linear Baseline ($(2\theta_{mn}, I_{mn})$ to $(2\theta_{mx}, I_{mx})$)
(34.° 2 θ , 1.0 c/s) (50.° 2 θ , 0.0 c/s)

MAGNITUDE AND LOCATION OF "SPURIOUS" PEAKS

(Due to Heat Treatment Support Changes)

Angle (° 2 θ)	Magnitude (c/s)
38.00	0.0

MARQUARDT FIT OF THE DATA

Centre of Fit Range: 39.80

Range Studied: 6.00 ° 2 θ

No. Iterations: 19 Converged: YES

 $\Sigma (\text{error})^2 / \text{Angle}: 42.33(\text{C/S})^{**2} / ^\circ 2\theta$

FIT PARAMETERS (see Equation 3-44):

B1= 4.0 B2= 0.44 X0= 39.935 T= 1.06250 °

B3= 4.571 B4= 9.1160 B5= 2.4960

RESULTS CALCULATED DIRECTLY FROM FIT:

Peak height: 8.52 c/s B_{1/2}: 0.0 rad

Area: 0.4808 rad*c/s Integral Breadth: 0.056440 rad

CALCULATED WITH OTHER RESULTS,

From File: XRAY27 Standard Integral Breadth= 0.004010

<La1> (Geometric, Fourier) = 2.86 nm

<La2> (Numerical, Fourier) = 2.08 nm

<Lv1> (Scherrer) = 2.91 nm

<Lv2> (Numerical, Fourier) = 4.28 nm

Fraction Detected = 0.780 <Lv>/<La> = 1.46

CATALYST AND SUPPORT IDENTIFICATION

***** **

Analysis of Catalyst: AP-13

For Miller Index: (111)

Support treatment: A-3

Catalyst Data File: XRAY37

Support Data File: XRAV69

SUPPORT CORRECTION

Support Scaling Factor: 0.95

Linear Baseline ($(2\theta_{mn}, I_{mn})$ to $(2\theta_{mx}, I_{mx})$)
(34.° 2θ , 0.0 c/s) (50.° 2θ , 0.0 c/s)

MAGNITUDE AND LOCATION OF "SPURIOUS" PEAKS

(Due to Heat Treatment Support Changes)

Angle (° 2θ)	Magnitude (c/s)
38.00	0.3

MARQUARDT FIT OF THE DATA.

Centre of Fit Range: 40.50

Range Studied: 5.00 ° 2θ

No. Iterations: 20 Converged: NO

 $\Sigma (\text{error})^2 / \text{Angle}$: 8.47(C/S)**2/° 2θ

FIT PARAMETERS (see Equation 3-44):

B1= 4.8 B2= 0.02 X0= 39.935 T= 16.41000

B3= 5.938 B4= 8.4180 B5= 0.5108

RESULTS CALCULATED DIRECTLY FROM FIT:

Peak height: 10.75 c/s $B_{1/2}$: 0.02019 rad

Area: 0.4410 rad*c/s Integral Breadth: 0.041000 rad

CALCULATED WITH OTHER RESULTS,

From File: XRAY27 Standard Integral Breadth= 0.004010

<La1> (Geometric, Fourier) = 2.08 nm

<La2> (Numerical, Fourier) = 2.10 nm

<Lv1> (Scherrer) = 4.01 nm

<Lv2> (Numerical, Fourier) = 3.92 nm

Fraction Detected = 0.720 <Lv>/<La> = 1.90

CATALYST AND SUPPORT IDENTIFICATION

***** **

Analysis of Catalyst: AP-14

For Miller Index: (111)

Support treatment: A-3

Catalyst Data File: XRAY73

Support Data File: XRAY69

SUPPORT CORRECTION

Support Scaling Factor: 0.95

Linear Baseline ($(2\theta_{mn}, I_{mn})$ to $(2\theta_{mx}, I_{mx})$)
(34.° 2 θ , 0.5 c/s) (50.° 2 θ , 0.0 c/s)

MAGNITUDE AND LOCATION OF "SPURIOUS" PEAKS

(Due to Heat Treatment Support Changes)

Angle (° 2 θ)	Magnitude (c/s)
36.70	2.0
45.00	1.0

MARQUARDT FIT OF THE DATA

Centre of Fit Range: 39.80

Range Studied: 4.00 ° 2 θ

No. Iterations: 20 Converged: NO

 $\Sigma (\text{error})^2 / \text{Angle} : 33.50 (\text{C/S}) ** 2 / ^\circ 2\theta$

FIT PARAMETERS (see Equation 3-44):

B1= 4.8 B2= 2.98 X0= 39.820 T= 2.59300

B3= 5.684 B4= 0.2900 B5= 1.1654

RESULTS CALCULATED DIRECTLY FROM FIT:

Peak height: 10.53 c/s $B_{1/2}$: 0.02467 rad

Area: 0.3757 rad*c/s Integral Breadth: 0.035670 rad

CALCULATED WITH OTHER RESULTS,

From File: XRAY27 Standard Integral Breadth= 0.004010

<La1> (Geometric, Fourier) = 2.91 nm

<La2> (Numerical, Fourier) = 3.00 nm

<Lv1> (Scherrer) = 4.63 nm

<Lv2> (Numerical, Fourier) = 4.47 nm

Fraction Detected = 0.607 <Lv>/<La> = 1.54

CATALYST AND SUPPORT IDENTIFICATION

***** *** ***** *****

Analysis of Catalyst: AP-16

For Miller Index: (111)

Support treatment: A-3

Catalyst Data File: XRAY87

Support Data File: XRAV69

SUPPORT CORRECTION

Support Scaling Factor: 0.95

Linear Baseline ($(2\theta_{mn}, I_{mn})$ to $(2\theta_{mx}, I_{mx})$)
(34.° 2 θ , 0.0 c/s) (50.° 2 θ , 0.0 c/s)MAGNITUDE AND LOCATION OF "SPURIOUS" PEAKS
(Due to Heat Treatment Support Changes)Angle (° 2 θ) Magnitude (c/s)
32.00 0.1

MARQUARDT FIT OF THE DATA

Centre of Fit Range: 40.00

Range Studied: 6.00 ° 2 θ

No. Iterations: 20 Converged: NO

 $\Sigma (\text{error})^2 / \text{Angle} : 32.67(\text{C/S})^{**2} / ^\circ 2\theta$

FIT PARAMETERS (see Equation 3-44):

B1= 6.7 B2= 9.62 X0= 40.050 T= 0.77870

B3= 5.153 B4= 0.1773 B5= 1.1834

RESULTS CALCULATED DIRECTLY FROM FIT:

Peak height: 11.83 c/s $B_{1/2}$: 0.02796 rad

Area: 0.5121 rad*c/s Integral Breadth: 0.043270 rad

CALCULATED WITH OTHER RESULTS,

From File: XRAY27 Standard Integral Breadth= 0.004010

<La1> (Geometric, Fourier) = 2.62 nm

<La2> (Numerical, Fourier) = 2.46 nm

<Lv1> (Scherrer) = 3.81 nm

<Lv2> (Numerical, Fourier) = 3.90 nm

Fraction Detected = 0.830 <Lv>/<La> = 1.52

12.1 Program RXRAY

12.1.1 User Documentation

THE UNIVERSITY OF ALBERTA

DEPT. OF CHEMICAL ENGINEERING

DACS CENTRE

PROGRAM DOCUMENTATION

THE UNIVERSITY OF ALBERTA

DEPT. OF CHEMICAL ENGINEERING

DACS CENTRE

PROGRAM DOCUMENTATION

NAME: RXRAY

DATE: 83-07-15

ABSTRACT: This program is used to collect data from the x-ray diffraction machine and store them on disc file. The name of the file is:

XRAYnn

where 'nn' is to be designated by the user. The data is stored as pairs (angle-intensity) with,

Angle = $2 * \text{THETA} * 100 \text{ Degrees}$ (Integer)
Intensity = Counts per second (Real)

AUTHOR: Bill Pick

SOURCE LANGUAGE: FORTRAN

TYPE: Program (Real-time)

LOCATION: &RXRAY::135

USAGE:

In running the program, the user is required to input the necessary information through the terminal. The program will prompt the user for the following:

- (1) Run number for the experiment in 2 alpha-numerical characters. These two characters will become the second part (the 'nn') of the output filename, XRAYnn
- (2) Maximum angle for measurement in $2 * \text{THETA} * 100 \text{ Degrees}$
- (3) Time per step in seconds.

After the time per step is input by the user, the operation of the program will be detached from the terminal. To recover the operation of the terminal, press the key 'RETURN' and answer the 'S=21 COMMAND ?' with 'RS'. The program is now ready to collect data from the X-ray machine and store them in the designated file. When the maximum angle for measurement has been reached, the program will stop automatically. The resulting data file can be listed on a terminal by typing in the following command:

```
:LI,XRAYnn:JU:135
```

where 'JU' is the security code and '135' is the cartridge number of the file 'XRAYnn'.

ADDITIONAL INFORMATION:

Any data file can be represented graphically and plotted by using the Auto Plot feature of the HP 2648A terminal. For the plotting instructions, please see the user's manual for the HP 2648A terminal in the DACS centre.

EXAMPLE:

Given the following information of a x-ray diffraction run,

```
Minimum Angle = 34.0 (2*THETA) Degrees
Maximum Angle = 84.0 (2*THETA) Degrees
Scanning Rate = 100 Seconds Per 0.05 (2*THETA) Degrees
Data to be stored in file: XRAYL1
```

a typical printout of the terminal session in running the program RXRAY is as followed:

```
*****
:RUN,RXRAY
      ENTER THE RUN # FOR THIS RUN
L1
      ENTER THE MAX. ANGLE AT WHICH READING WILL STOP
8400
      ENTER THE TIME PER STEP
100.0
S=21 COMMAND ?RS
FMG32 ABORTED
:
*****
```

12.1.2 FORTRAN Program RXRAY FTN4

```

PROGRAM RXRAY(3,70), PROGRAM TO COLLECT REAL DATA <840707.2129>
DIMENSION IDCB(144),NAME(5),IBUF(10),ISIZE(2),INBUF(40)
DATA NAME/2HXR,2H ,2H /,40,10/
DATA LAST1,LAST2/0,0/

C
LU=1
LUT=22

C
C
10 WRITE(LU,100)
100 FORMAT(/5X,'ENTER THE RUN # (FOUR DIGITS) FOR THIS RUN')
READ(LU,110) NAME(2),NAME(3)
110 FORMAT(2A2)
DO 1000 I=1,10
1000 IBUF(I)=2H
WRITE(LU,1100)
1100 FORMAT(5X,'ENTER SECURITY CODE FOR YOUR DATA FILE')
READ(LU,210) (IBUF(I),I=1,10)
CALL PARSE(IBUF,20,INBUF)
NAME(4)=INBUF(2)
WRITE(LU,1200)
1200 FORMAT(5X,'ENTER CART. NO. WHERE YOUR FILE IS TO BE CREATED')
READ(LU,*) NAME(5)
IF(NAME(5).EQ.0) NAME(5)=135
IF(INBUF(1).EQ.0.OR.INBUF(1).EQ.2) WRITE(LU,1300) (NAME(I),I=1,5)
1300 FORMAT(//,2X,'YOUR FILE IS: ',3A2,' ',A2,' ',I3)
IF(INBUF(1).EQ.1) WRITE(LU,1400) (NAME(I),I=1,5)
1400 FORMAT(//,2X,'YOUR FILE IS: ',3A2,' ',I5,' ',I3)
WRITE(LU,1500)
1500 FORMAT(2X,'IS THE INFORMATION CORRECT? (Y/N)')
READ(LU,1600) IANS
1600 FORMAT(A1)
IF(IANS.NE.1HY) GO TO 10

C
115 WRITE(LU,120)
120 FORMAT(/5X,'ENTER THE MAX. ANGLE AT WHICH READING WILL STOP')
READ(LU,*) MAXANG
IF(MAXANG.GT.10700) GO TO,115
WRITE(LU,130)
130 FORMAT(/,5X,'ENTER THE TIME PER STEP')
READ(LU,*) TIME

C
CALL DTACH

C
CALL CREAT(IDCB,IERR,NAME,ISIZE,3,NAME(4),NAME(5))
IF(IERR.LT.0) GO TO 888

C
CALL OPEN(IDCB,IERR,NAME,0,NAME(4),NAME(5))
IF(IERR.LT.0) GO TO 888

C
200 CONTINUE
READ(LUT,210) INBUF

```

```
210 FORMAT(40A2)
    CALL CODE
    READ(IBUF,*) IANGLE,RINTEN
    IF(IAngle.GT.MAXANG) GO TO 800
    IF(IAngle.NE.LAST1.OR.RINTEN.NE.RLAST2) GO TO 300
    GO TO 200
C
300 RINTT=RINTEN/TIME
    DO 305 I=1,10
305  IBUF(I)=2H
    CALL CODE
    WRITE(IBUF,310) IANGLE,RINTT
310  FORMAT(X,I5,2X,F8.2)
    CALL WRITF(IDCBIERR,IBUF,10)
    IF(IERR.LT.0) GO TO 888
    LAST1=IAngle
    RLAST2=RINTEN
    GO TO 200
C
800 CALL CLOSE IDCBIERR)
    IF(IERR.LT.0) GO TO 888
    GO TO 999
C
888 WRITE(LU,890) IERR
890 FORMAT(/5X,'TROUBLE IN FMP CALL CIERR ='I5)
C
999 STOP
    END
```

12.2 Program XRMD

12.2.1. User Documentation

THE UNIVERSITY OF ALBERTA DEPT. OF CHEMICAL ENGINEERING

DAQS CENTRE PROGRAM DOCUMENTATION

NAME: XRMD

DATE: 83-07-18

ABSTRACT: This program is used to perform point-by-point subtraction between two data files or diffraction profiles and store the results on disc file. The name of the resulting file is:

XPTDnn

where 'nn' is to be designated by the user. The data is stored as pairs (angle-intensity) with,

Angle = $2 * \text{THETA} * 100$ Degrees (Integer)
Intensity = Counts per second (Real)

AUTHOR: Bill Pick

SOURCE LANGUAGE: FORTRAN

TYPE: Program

LOCATION: &XRMD:135

USAGE:

In running the program, the user is required to input the necessary information through the terminal. The program will prompt the user for the following:

- (1) Filename for input file #1. For example, this can be the filename of a diffraction profile of a catalyst.
- (2) Filename for input file #2. For example, this can be the filename of a diffraction profile of a catalyst support. (Same catalyst support as in file #1.)
- (3) Angle shift for file #1. The angle is a integer in degrees of $2 * \text{THETA} * 100$.

- (4) Angle shift for file #2. The angle is a integer in degrees of $2 * \text{THETA} * 100$.
- (5) Scaling factor for file #1. Enter 1.0 to retain the original data.
- (6) Scaling factor for file #2. Enter 1.0 to retain the original data.
- (7) Name of the resulting file in 2 alpha-numerical characters. These two characters will become the second part (the 'nn') of the output filename, XPTDnn.
- (8) Location of the baseline. The baseline is specified by giving its two endpoints in the following order,

IANGL, BASE1, IANG2, BASE2

where IANG1 and IANG2 are the angles in degrees $2 * \text{THETA} * 100$
 BASE1 and BASE2 are the intensities in counts per second

- (9) Enter '0' to zero all negative results if desired.

ADDITIONAL INFORMATION:

Any data file can be represented graphically and plotted by using the Auto Plot feature of the HP 2648A terminal. For the plotting instructions, please see the user's manual for the HP 2648A terminal in the DACS centre.

EXAMPLE: Given the following information,

Name of file #1 = XRAYL9 (Catalyst support)
 Name of file #2 = XRAYL8 (Catalyst)
 Angle shift for file #1 = 0
 Angle shift for file #2 = 0
 Scaling factor for file #1 = 1.0
 Scaling factor for file #2 = 1.0
 Endpoints of the baseline = (4200,0.0), (5000,0.0)
 Subtracted profile to be in file: XPTDL1

a typical printout of the terminal session in running the program XCMD is as follows:

:RUN,XCMD

ENTER THE FILENM FOR INPUT FILE 1
 XRAYL9

ENTER THE SCALING FACTOR FOR FILE 1
 1.0

ENTER THE INTEGER ANGLE SHIFT FOR FILE 1

DEGREES 2*THETA * 100

0

ENTER THE FILENM FOR FILE 2
XRAYL8

ENTER THE SCALING FACTOR FOR FILE 2

1.0

ENTER THE ANGLE SHIFT FOR FILE 2

0

ENTER THE # FOR THE XPTD FILE

L1

ENTER THE TWO POINTS FOR LINEAR BASELINE AS...

IANG1, BASE1, IANG2, BASE2

4200, 0.00, 5000, 0.00

ENTER '0' TO ZERO ALL NEGATIVE RESULTS

1

XRM21 : STOP 0000

12.2.2 FORTRAN Program XRMD

FTN4

```

PROGRAM XRMD(), PROGRAM FOR CALCULATE THE X-RAY METAL DIFFRACTION
INTEGER A,C,X
DIMENSION IDCB1(144),IDCB2(144),IDCB3(144),NAME1(5),NAME2(5),
DIMENSION NAME3(5),IBUF(10),ISIZE(2)
DATA ISIZE/40,10/,C/O/,D/O./,NAME1/2HXR,2HAV,2H00,2HJU/
DATA NAME2/2HXR,2HAV,2H00,2HJU/
DATA NAME3/2HXP,2HTD,2H00,0,135/

```

Key Variables:

```

C      A - Integer Angle in first file (DEG 2*THETA*100)
C      I - Real Intensity from file #1 (C/S)
C      J - Integer Angle, file #2
C      K - Real Intensity, file #2 (C/S)
C      L - Integer Angle for Output
C      Y - Output Intensity
C

```

```

C      WRITE (1,10)
10  FORMAT(/,'ENTER THE FILENM FOR INPUT FILE 1')
    READ(1,20) (NAME1(J),J=1,3)
20  FORMAT(3A2)
    IF(OPEN(IDCB1,IERR,NAME1,0,NAME1(4),NAME1(5)).LT.0) GO TO 888
    WRITE(1,23)
23  FORMAT(/,'ENTER THE SCALING FACTOR FOR FILE 1')
    READ(1,*) SCAL1
    WRITE(1,27)
27  FORMAT('ENTER THE INTEGER ANGLE SHIFT FOR FILE 1',
    & /,5X,'DEGREES 2*THETA * 100')
    READ(1,*) IMV1
    WRITE(1,30)
30  FORMAT(/,'ENTER THE FILENM FOR INPUT FILE 2')
    READ(1,20) (NAME2(J),J=1,3)
    WRITE(1,33)
33  FORMAT(/,'ENTER THE SCALING FACTOR FOR FILE 2')
    READ(1,*) SCAL2
    WRITE(1,37)
37  FORMAT('ENTER THE ANGLE SHIFT FOR FILE 2')
    READ(1,*) IMV2
    IF(OPEN(IDCB2,IERR,NAME2,0,NAME2(4),NAME2(5)).LT.0) GO TO 888
C
    WRITE(1,40)
40  FORMAT(/,'ENTER THE # FOR THE XPTD FILE')
    READ(1,20) NAME3(3)
    WRITE(1,45)
45  FORMAT('ENTER TWO POINTS FOR A LINEAR BASELINE AS...',
    & /,5X,'IANG1,BASE1,IANG2,BASE2,')
    READ(1,*) IANG1,BASE1,IANG2,BASE2
C
C      BASE1=RK1*IANG +RK2

```

```

C
RK1=(BASE2-BASE1)/FLOAT(IAN2-IAN1)
RK2=BASE1-RK1*FLOAT(IAN1)
WRITE(1,50)
50  FORMAT('ENTER "0" TO ZERO ALL NEGATIVE RESULTS')
READ(1,*) IZERO
CALL CREAT(IDCB3,IERR,NAME3,ISIZE,3,NAME3(4),NAME3(5))
IF(IERR.LT.0) GO TO 888
IF(OPEN(IDCB3,IERR,NAME3,0,NAME3(4),NAME3(5)).LT.0) GO TO 888
C
C
100  DO 110 I=1,10
110  IBUF(I)=2H
C
CALL READF(IDCB1,IERR,IBUF,10,LEN)
IF(IERR.LT.0) GO TO 888
IF(LEN.EQ.-1) GO TO 500
CALL CODE
READ(IBUF,*) A,B
A=A+IMV1
IF(A.EQ.C) GO TO 600
IF(A.LT.C) GO TO 100
C
200  DO 210 I=1,10
210  IBUF(I)=2H
C
CALL READF(IDCB2,IERR,IBUF,10,LEN)
IF(IERR.LT.0) GO TO 888
IF(LEN.EQ.-1) GO TO 500
CALL CODE
READ(IBUF,*) C,D
C=C+IMV2
IF(C.EQ.A) GO TO 600
IF(C.LT.A) GO TO 200
GO TO 100
C
500  IEND=1
C
600  X=A
BASEL=RK1*X + RK2
Y=B*SCAL1-D*SCAL2 - BASEL
IF(IZERO.EQ.0.AND.Y.LT.0.0) Y=0.0
DO 610 I=1,10
610  IBUF(I)=2H
CALL CODE
WRITE(IBUF,620) X,Y
620  FORMAT(I5,2X,F8.2)
CALL WRITEF(IDCB3,IERR,IBUF,10,LEN)
IF(IERR.LT.0) GO TO 888
IF(IEND.EQ.1) GO TO 777
GO TO 100
C
777  IF(CLOSE(IDCB1,IERR).LT.0) GO TO 888
IF(CLOSE(IDCB2,IERR).LT.0) GO TO 888

```


IF(CLOSE(IDC3,IERR).LT.0) GO TO 888
GO TO 999

C

888 WRITE(1,890) IERR

890 FORMAT(/5X, 'TROUBLE IN FMP CALL. IERR= 'I5)

C

999 STOP

END

12.3 Program XRDAV

12.3.1 User Documentation
THE UNIVERSITY OF ALBERTA

DEPT. OF CHEMICAL ENGINEERING

DACS CENTRE

PROGRAM DOCUMENTATION

NAME: XRDAV

DATE: 83-07-18

ABSTRACT: This program is used to perform point-by-point averaging between two data files or diffraction profiles and store the results on disc file. The name of the resulting file is:

XRAVnn

where 'nn' is to be designated by the user. The data is stored as pairs (angle-intensity) with,

Angle = 2 * THETA * 100 Degrees (Integer)
Intensity = Counts per second (Real)

AUTHOR: Bill Pick

SOURCE LANGUAGE: FORTRAN

TYPE: Program

LOCATION: &XRDAV::135

USAGE:

In running the program, the user is required to input the necessary information through the terminal. The program will prompt the user for the following:

- (1) Filename for input file #1.
- (2) Filename for input file #2.
- (3) Name of the resulting file in 2 alpha-numerical characters. These two characters will become the second part (the 'nn') of the output filename, XRAVnn.

ADDITIONAL INFORMATION:

Any data file can be represented graphically and plotted by using the Auto Plot feature of the HP 2648A terminal. For the plotting instructions, please see the user's manual for the HP 2648A terminal in the DACS centre.

EXAMPLE:

The average diffraction profile between XPTDL1 and XPTDL2 is to be calculated. The results are to be stored in file XRAYL1. A typical printout of the terminal session in running the program XRDAVL1 is as follows:

:RUN,XRDAV

ENTER INPUT FILE 1
XPTDL1

ENTER INPUT FILE 2
XPTDL2

ENTER THE # FOR THE XRAV FILE
L1

XRDAV : STOP 0000

12.3.2 FORTRAN Program XRDAV

FTN4

```

PROGRAM XRDAV(), PROGRAM FOR CALCULATE THE X-RAY DIFF.AVERAGE
INTEGER A,C,X
DIMENSION IDCB1(144),IDCB2(144),IDCB3(144),NAME1(5),NAME2(5)
DIMENSION NAME3(5),IBUF(10),ISIZE(2)
DATA ISIZE/40,10/,C/0/,D/0./,NAME1/2HXR,2HAY,2H00,2HJU,135/
DATA NAME2/2HXR,2HAY,2H00,2HJU,135/
DATA NAME3/2HXR,2HAV,2H00,2HJU,135/

```

Key Variables:

```

A - Integer Angle in first file (DEG 2*THETA*100)
B - Real Intensity from file #1 (C/S)
C - Integer Angle, file #2
D - Real Intensity, file #2 (c/s)
X - Integer Angle for Output
Y - Output Intensity

```

```

C
C
C
C
C
C
C
C
C
C
WRITE (1,10)
10  FORMAT(/,'ENTER INPUT FILE 1')
    READ(1,20) (NAME1(I),I=1,3)
20  FORMAT(3A2)
    IF(OPEN(IDCB1,IERR,NAME1,0,NAME1(4),NAME1(5)).LT.0) GO TO 888
    WRITE(1,30)
30  FORMAT(/,'ENTER INPUT FILE 2')
    READ(1,20) (NAME2(I),I=1,3)
    IF(OPEN(IDCB2,IERR,NAME2,0,NAME2(4),NAME2(5)).LT.0) GO TO 888
C
    WRITE(1,40)
40  FORMAT(/,'ENTER THE # FOR THE XRAV FILE')
    READ(1,20) NAME3(3)
    CALL CREAT(IDCB3,IERR,NAME3,ISIZE,3,NAME3(4),NAME3(5))
    IF(IERR.LT.0) GO TO 888
    IF(OPEN(IDCB3,IERR,NAME3,0,NAME3(4),NAME3(5)).LT.0) GO TO 888
C
C
100 DO 110 I=1,10
110 * IBUF(I)=2H
C
    CALL READF(IDCB1,IERR,IBUF,10,LEN)
    IF(IERR.LT.0) GO TO 888
    IF(LEN.EQ.-1) GO TO 500
    CALL CODE
    READ(IBUF,*) A,B
    IF(A.EQ.C) GO TO 600
    IF(A.LT.C) GO TO 100
C
200 DO 210 I=1,10
210  IBUF(I)=2H
C
    CALL READF(IDCB2,IERR,IBUF,10,LEN)
    IF(IERR.LT.0) GO TO 888
    IF(LEN.EQ.-1) GO TO 500
    CALL CODE

```

```

      READ(IBUF,*) C,D
      IF(C.EQ.A) GO TO 600
      IF(C.LT.A) GO TO 200
      GO TO 100
C
500   IEND=1
C
600   X=A
      Y=(B+D)/2.
      DO 610 I=1,10
610   IBUF(I)=2H
      CALL CODE
      WRITE(1,620) X,Y
620   FORMAT(15,2X,F8.2)
      CALL WRITE(IDCB3,IERR,IBUF,10,LEN)
      IF(IERR.LT.0) GO TO 888
      IF(IEND.EQ.1) GO TO 777
      GO TO 100
C
777   IF(CLOSE(IDCB1,IERR).LT.0) GO TO 888
      IF(CLOSE(IDCB2,IERR).LT.0) GO TO 888
      IF(CLOSE(IDCB3,IERR).LT.0) GO TO 888
      GO TO 999
C
888   WRITE(1,890) IERR
890   FORMAT(/5X,'TROUBLE IN EMP CALL. IERR= '15)
C
999   STOP
      END

```

12.4 Program XINTG

12.4.1 User Documentation
THE UNIVERSITY OF ALBERTA

DEPT. OF CHEMICAL ENGINEERING

DACS CENTRE

PROGRAM DOCUMENTATION

NAME: XINTG

DATE: 83-07-18

ABSTRACT: This program is used to calculate the area under a x-ray diffraction profile with,

$$\text{Integrated Area} = (\text{Delta Angle}) * \text{Rint}$$

where

Delta Angle is typically 0.05 Degrees (2*THETA)
this can be any value, but must be the same
throughout input file

Rint = Intensity in counts per second

The results are output either to the terminal or line printer specified by the user. Five columns of numerical results are presented in the results,

- (1) 1st Columns. The angle in degrees 2*THETA.
- (2) 2nd and 3rd Columns. The cumulative integrated areas and the standard deviations.
- (3) 4th and 5th Columns. The integrated areas for each interval and their standard deviations.

In addition, an option for printing out the autocorrelation coefficients is provided.

AUTHOR: Bill Pick

SOURCE LANGUAGE: FORTRAN

TYPE: Program

LOCATION: &XINTG::135

USAGE:

In running the program, the user is required to input the necessary information through the terminal. The program will prompt the user for the following:

- (1) Input filename with the diffraction profile of interest.
- (2) Catalyst identification code in 4 alpha-numerical characters. This will be printed out along with the results.
- (3) Minimum and maximum angles in degrees (2θ) for the integration to take place.
- (4) Data output device. Enter '1' for terminal or '6' for line printer as output device.
Output can also be to a disc file - see DACS centre for details
- (5) Scaling factor for the input file. Enter 1.0 to retain the original data.
- (6) Enter '1' to list the autocorrelation coefficients if desired.
- (7) Enter '1' to perform a new integration or '0' to stop.

EXAMPLE:

Given the following information,

Name of input file = XPTDL1 (Subtracted Profile)
 Catalyst ID code = CAT1
 Minimum angle (start integration) = 42.5 Degrees (2θ)
 Maximum angle (stop integration) = 49.5 Degrees (2θ)
 Output device = Line printer

A typical printout of the terminal session in running the program XINTG is as followed:

:RUN,XINTG

ENTER THE FILE LOCATION OF THE SUBTRACTED DATA
 XPTDL1

ENTER THE CATALYST IDENTIFICATION CODE (EG PI16)
 CAT1

ENTER THE MIN AND MAXIMUM ANGLES OF INTEREST
 42.5 49.5

ENTER DATA OUTPUT DEVICE (1=TERMINAL,6=LINE PRINTER)
 6

ENTER THE SCALING FACTOR FOR FILE XPTDL1

1.0
 ENTER '1' TO LIST THE AUTOCORRELATION COEFFICIENTS
 1

ENTER '1' TO CONTINUE, '0' TO STOP

0

XIN21 : STOP 0000

:

SAMPLE OUTPUT:

CUMULATIVE INTEGRATED PEAK AREAS

FOR CATALYST:CAL2

IN FILE:XPTDL2

ANGLE	CUMULATIVE		LAST	
	INT	STD. DEV.	INT	STD. DEV.
42.50	0.000	0.000	0.000	0.000
43.00	.192	.794	.384	.738
43.50	.299	.710	.214	.614
44.00	.091	.806	-.416	.923
44.50	.132	.815	.081	.882
45.00	.191	.971	.118	1.509
45.50	.059	1.001	-.264	1.163
46.00	.682	1.073	1.246	.764
46.50	2.023	1.445	2.702	1.289
47.00	2.657	1.437	1.249	.664
47.50	2.737	1.389	.160	.874
48.00	-3.680	7.510	-12.835	22.041
48.50	2.110	9.356	11.581	18.144
H 49.00	2.259	8.994	.298	1.091

AUTO CORRELATION COEFFICIENTS, AVG= .296

K	C(K)
0	74.631
1	23.629
2	-.492
3	5.370
4	-16.999
5	-19.442
6	-12.437
7	-6.782
8	-2.282

9	.105
10	-.593
11	-.597
12	-.981
13	-.335
14	1.253
15	-.458
16	-1.559
17	-.405
18	1.219
19	-1.145
20	-2.456

12.4.2 FORTRAN Program XINTG

FTN4

PROGRAM XINTG

C
C
C
C
C
C
C
C
C
C
C
C
C
C
C

INTEGRATED AREA=(DELTA ANGLE)*RINT

Key Variables:

DELTA = Calculated Angle Step, Degree 2Theta

ANG = Angle, Degree 2Theta

SUM = Cumulative Intensity, C/S

SDT = Cumulative Standard Deviation, C/S

AVINT = Average Intensity for Previous 10 points

SD = Std. Dev. for Previous 10 points

C(KK) = KKth Auto-correlation coefficient
of the Data

DIMENSION IANG(1000),RINT(1000),IDCB(144)

DIMENSION ICAT(2),NAME(5)

DATA NAME/2H ,2H ,2H ,2H ,135/

10 CONTINUE

CALL INIT(NAME,IOUT,ICAT,MINAN,MAXAN)

CALL RREAD(IDCB,NAME,MINAN,MAXAN,IANG,RINT,IDIM)

WRITE(IOUT,20) (ICAT(I),I=1,2),(NAME(I),I=1,3)

20 FORMAT(//,5X,'*CUMULATIVE INTEGRATED PEAK AREAS*',
& //,10X,'FOR CATALYST:',2A2,/,10X,'IN FILE:',3A2)

CALL INTG(MINAN,MAXAN,IANG,RINT,IDIM,IOUT)

WRITE(1,30)

30 FORMAT(//,5X,'ENTER "1" TO CONTINUE,"0" TO STOP')

READ(1,*) ICONT

IF(ICONT.GT.0) GO TO 10

C

STOP

END

C

C*****

C

SUBROUTINE INIT(NAME,IOUT,ICAT,MINAN,MAXAN)

DIMENSION NAME(5),ICAT(2)

C

WRITE(1,10)

10 FORMAT(//,'ENTER THE FILE LOCATION OF THE SUBTRACTED DATA')

READ(1,15) (NAME(I),I=1,3)

15 FORMAT(3A2)

C

WRITE(1,20)

20 FORMAT(//,'ENTER THE CATALYST IDENTIFICATION CODE (EG PI16)')

READ(1,25) (ICAT(I),I=1,2)

25 FORMAT(2A2)

WRITE(1,40)

40 FORMAT(//,'ENTER THE MIN AND MAXIMUM ANGLES OF INTEREST')

READ(1,*)ANGMN,ANGMX

MINAN=IFIX(ANGMN*100)

MAXAN=IFIX(ANGMX*100)

```

        WRITE(1,60)
60  FORMAT(/,'ENTER DATA OUTPUT DEVICE (1=TERMINAL,6=LINE PRINTER)')
        READ(1,*) IOUT
        RETURN
END
C
C *****
C
        SUBROUTINE RREAD(IDC, NAME, MINAN, MAXAN, IANG, RINT, IDIM)
        DIMENSION NAME(5), IDC(144), IBUF(20), IANG(1000), RINT(1000)
        DATA IOPTN/0/, IL/10/
        CALL OPEN (IDCB, IERR, NAME, IOPTN, NAME(4), NAME(5))
        IF(IERR.LT.0) GO TO 100
        KK=0
        WRITE(1,5) (NAME(I), I=1,3)
5  FORMAT(/,'ENTER THE SCALING FACTOR FOR FILE ',3A2)
        READ(1,*) SCAL1
        DO 50 K=1,10000
            DO 10 I=1,20
                IBUF(I)=2H
10         CONTINUE
            KK=KK+1
            CALL READF(IDC, IERR, IBUF, IL, LEN)
            IF(IERR.LT.0) GO TO 80
            IF(LEN.EQ.-1) GO TO 100
            CALL CODE
            READ(IBUF,*) IANG(KK), RINT(KK)
            RINT(KK)=RINT(KK)*SCAL1
            IF(IANG(KK).GT.MAXAN) GO TO 55
            IF(IANG(KK).LT.MINAN) KK=0
50         CONTINUE
55         CONTINUE
            IDEL=IANG(3)-IANG(2)
            IDIM=KK
            GO TO 100
80         WRITE(1,90) IERR
90         FORMAT(/,5X,'TROUBLE IN FMP CALL, ROUTINE RREAD. IERR= ',I5)
100        RETURN
END
C
C *****
C
        SUBROUTINE INTG(MINAN, MAXAN, IANG, RINT, IDIM, IOUT)
        DIMENSION IANG(1000), RINT(1000)
        DIMENSION C(21)
        DELAN=FLOAT(IANG(3)-IANG(2))/100.
        SUM=0.
        SUM2=0.
        AVINT=0.
        J=1
        JJ=1
        WRITE(IOUT,10)
10  FORMAT(8X,'ANGLE',16X,'CUMULATIVE',25X,'LAST',
& /,25X,'INT',11X,'STD. DEV.',9X,'INT',9X,'STD. DEV.',/)

```

```

DO 90 I=1, IDIM
  ANG=FLOAT(IANG(J))/100.
  WRITE(IOUT,20) ANG,SUM,SDT,AVINT,SD
20  FORMAT(5X,F8.2,4(7X,F9.3))
  AVINT=0.
  SD=0.
  DO 50 I=1,10
    J=J+1
    IF(IANG(J).GE.MAXAN) GO TO 60
    AVINT=AVINT+RINT(J)/10.
    SUM=SUM+DELAN*RINT(J)
50  CONTINUE
60  DO 70 I=1,10
    JJ=JJ+1
    IF(IANG(JJ).GE.MAXAN) GO TO 80
    SD=SD + (RINT(JJ) - AVINT)**2
    SUM2=SUM2+(RINT(JJ) - SUM/(FLOAT(JJ)))**2
70  CONTINUE
80  SD=SQRT(SD/9.)
    SDT=SQRT(SUM2/FLOAT(JJ-1))
    IF(IANG(JJ).GE.MAXAN) GO TO 91
90  CONTINUE
C
91  WRITE(1,95)
95  FORMAT('ENTER "1" TO LIST THE AUTOCORRELATION COEFFICIENTS')
    READ(1,*)IAUTO
    IF(IAUTO.NE.1) GO TO 200
101  DO 105 K=1,21
105  C(K)=0.
    AVG=SUM/(FLOAT(JJ)*DELAN)
110  WRITE(IOUT,115) AVG
115  FORMAT(//,5X,'AUTO CORRELATION COEFFICIENTS, AVG=',F8.3,
    & /,5X,'K',5X,'C(K)')
    DO 130 KK=1,21
      K=KK-1
      IMAX=JJ-K
      DO 120 I=1,IMAX
        C(KK)=C(KK) + (RINT(I)-AVG)*(RINT(I+K)-AVG)
120  CONTINUE
      C(KK)=C(KK)/FLOAT(JJ-K)
      WRITE(IOUT,125) K,C(KK)
125  FORMAT(2X,15,4X,F8.3)
130  CONTINUE
    WRITE(IOUT,190)
190  FORMAT('1')
200  RETURN
    END

```

12.5 Program XFIT

12.5.1 User Documentation
THE UNIVERSITY OF ALBERTA

DEPT. OF CHEMICAL ENGINEERING

DACS CENTRE

PROGRAM DOCUMENTATION

NAME: XFIT

DATE: 83-08-20

ABSTRACT: This program is used to fit observed X-ray diffraction profiles (generated by subtracting the measured profiles from the support profiles using program XRMD) to a modified Voigt profile with 8 adjustable parameters (B(I)).
The profile has the form:

$$\begin{aligned}
 F &= F1 + F2 & (1) \\
 F1 &= B(1)/(1+U*B(2)*(X-B(3))^{**2})^{**B(4)} \\
 F2 &= B(5)*(EXP(-U*B(6)*(X-B(3))^{**2}))^{**B(7)}
 \end{aligned}$$

Where:

X=the angle in degrees 2*theta
U=1.0 if x<b(3)
u=b(8) if x>b(3)

Since B(6) and B(7) are not independent, B(7) should be set:
B(7)=1.0

by the user.

The actual curve fitting is performed using the routine, BSOLVE, by W. Ball (See Keuster and Mize, "Optimization Techniques with FORTRAN").

The program assumes that the profile is generated by the CuK-alpha doublet X-radiation. Thus two peaks are actually fit, with identical shape but with locations corresponding to Cu-Kalphal (peak ht=2/3*(b(1)+b(5)) and lambda1=0.1540562 nm) and Cu-Kalpha2 (peak ht=1/3*(B(1)+B(5)), lambda2=0.1544390 nm). B(3) corresponds to the Bragg angle for Cu-Kalphal, ie,

$$\begin{aligned}
 \lambda_{1} &= 2*d*\sin(\theta_{1}) \\
 B(3) &= 2*\theta_{1}
 \end{aligned}$$

Both the observed peak, (with the K-alpha broadening), and the K-alpha corrected peak can be generated. On regeneration of the latter the peak is exactly the form given by Equation 1, the former is broadened as suggested in the previous paragraph. The program can also be run to determine the parameters for 2 overlapping peaks. To achieve this, the asymmetrical term, B(8), should be set: B(8)=1.0. It may also be desirable to fix other parameters to reduce run time to a reasonable period.

The program is best operated interactively using The HP-2648A

graphics terminal to plot the fit curve over top of the raw data for comparison.

AUTHOR: Bill Pick

SOURCE LANGUAGE: FORTRAN

TYPE: Program

LOCATION: &XFIT::135

USAGE: See the example run below.

EXAMPLE: A typical printout of the terminal session in running the program XFIT is as follows:

:RUN,XFIT

ENTER THE FILE LOCATION OF THE RAW DATA
OR 'PREFIT' FOR USER ENTERED MOD. VOIGT PARAS.

XPTD17

ENTER THE REGENERATION WIDTH, AND THE (ODD) NUMBER OF DATA POINTS
20.0,201

ENTER THE NUMBER OF PEAKS, NPEAK

1

ENTER DATA OUTPUT DEVICE (1=TERMINAL,6=LINE PRINTER)

1

ENTER THE CATALYST IDENTIFICATION CODE
AND THE PEAK MILLER INDEX, (EG P116 111)

AI-4 111

ENTER THE APPROXIMATE PEAK LOCATION AND THE FIT RANGE
41.6,4.0

ENTER THE SCALING FACTOR FOR FILE XPTD17

1.0

ENTER '1' TO APPLY ANGLE CORRECTION

0

THE PROGRAM WILL ATTEMPT TO FIND 1 PEAKS

ENTER THE INITIAL GUESSES FOR PEAK LOCATION

- 1 - The (111) peaks of Pt and Ir (& of 50% alloy?)
- 2 - The (200) Peaks of Pt and Ir (+50% alloy?)
- 3 - Enter the initial guesses, deg 2*theta

3

40.6

INITIAL GUESSES ARE:

	GUESS	MIN	MAX
1	2.39E+01	1.19E+00	5.97E+01
2	1.00E+00	1.00E-03	1.00E+03
3	4.06E+01	3.25E+01	4.87E+01
4	1.00E+00	5.00E-01	2.00E+01
5	2.39E+01	1.19E+00	5.97E+01
6	1.00E+00	1.00E-01	1.00E+02
7	1.00E+00	1.00E-03	1.00E+03
8	1.00E+00	1.00E-01	1.50E+00

ENTER THE PARAMETER TO BE CHANGED

2

ENTER THE NEW PARAMETER, MIN, AND MAX FOR NO. 2

10.,0.01,1000.,

INITIAL GUESSES ARE:

	GUESS	MIN	MAX
1	2.39E+01	1.19E+00	5.97E+01
2	1.00E+01	1.00E-02	1.00E+03
3	4.06E+01	3.25E+01	4.87E+01
4	1.00E+00	5.00E-01	2.00E+01
5	2.39E+01	1.19E+00	5.97E+01
6	1.00E+00	1.00E-01	1.00E+02
7	1.00E+00	1.00E-03	1.00E+03
8	1.00E+00	1.00E-01	1.50E+00

ENTER THE PARAMETER TO BE CHANGED

0

1 BSOLVE REGRESSION ALGORITHM

INITIAL GUESSES	UPPER LIMITS	LOWER LIMITS
.239E+02	.597E+02	.119E+01
.100E+02	.100E+04	.100E-01
.406E+02	.487E+02	.325E+02
.100E+01	.200E+02	.500E+00
.239E+02	.597E+02	.119E+01
.100E+01	.100E+03+00	
.100E+01	.100E+04	.100E-02
.100E+01	.150E+01	.100E+00

ICON = 8	PH = .47374883E+04	ITERATION NO. = 1
ICON = 8	PH = .31143024E+03	ITERATION NO. = 2
ICON = 7	PH = .30339307E+03	ITERATION NO. = 3
ICON = 6	PH = .17507327E+03	ITERATION NO. = 4
ICON = 6	PH = .16583469E+03	ITERATION NO. = 5
ICON = 6	PH = .16153442E+03	ITERATION NO. = 6
ICON = 6	PH = .15390805E+03	ITERATION NO. = 7

ICON = 6 PH = .13489401E+03 ITERATION NO. = 8

ICON = 6 PH = .11774667E+03 ITERATION NO. = 9

ICON = 6 PH = .11183485E+03 ITERATION NO. = 10

1 5.02681660E+01

2 1.35385970E+01

3 4.06342540E+01

4 9.10909530E-01

5 1.19450000E+00

6 6.99371100E-01

7 3.85308600E+00

8 7.40073440E-01

ENTER '1' TO STOP ITERATIONS.

0

ICON = 6 PH = .10550647E+03 ITERATION NO. = 11

ICON = 6 PH = .93070511E+02 ITERATION NO. = 12

ICON = 7 PH = .92185089E+02 ITERATION NO. = 13

ICON = 7 PH = .89616318E+02 ITERATION NO. = 14

ICON = 7 PH = .88625244E+02 ITERATION NO. = 15

ICON = 7 PH = .88315613E+02 ITERATION NO. = 16

ICON = 7 PH = .88245300E+02 ITERATION NO. = 17

ICON = 7 PH = .88150681E+02 ITERATION NO. = 18

ICON = 7 PH = .88076569E+02 ITERATION NO. = 19

ICON = 7 PH = .87999039E+02 ITERATION NO. = 20

1 4.75993650E+01

2 1.91028790E+01

3 4.06340790E+01

4 8.87496110E-01

5 2.65672400E+00

6 2.01073840E+00

7 5.05129150E+00

8 7.42260460E-01

ENTER '1' TO STOP ITERATIONS

ICON = 7 PH = .87953918E+02 ITERATION NO. = 21

ICON = 7 PH = .87830215E+02 ITERATION NO. = 22

ICON = 7 PH = .87815933E+02 ITERATION NO. = 23

ICON = 7 PH = .87809830E+02 ITERATION NO. = 24

ICON = 5 PH = .87809769E+02 ITERATION NO. = 25
 ICON = 2 PH = .87809662E+02 ITERATION NO. = 26
 ICON = 3 PH = .87809616E+02 ITERATION NO. = 27
 ICON = -1 PH = .87809616E+02 ITERATION NO. = 28

NO FUNCTION IMPROVEMENT POSSIBLE

SOLUTIONS OF EQUATIONS

B(1) = .45558617E+02
 B(2) = .20868511E+02
 B(3) = .40634384E+02
 B(4) = .84808612E+00
 B(5) = .47186470E+01
 B(6) = .20422163E+01
 B(7) = .43941460E+01
 B(8) = .73800778E+00

THE LEAST SQUARES OBJECTIVE FUNCTION = .878096E+02

OBSERVED PEAK:

ENTER '1' TO LIST THE CAUCHY FIT PEAK
 0

K-ALPHA BROADENING CORRECTED

ENTER '1' TO LIST THE CAUCHY FIT PEAK
 0

THE PEAK IS AT: \$\$\$\$\$\$\$% OF ITS MAXIMUM AT THE BOUNDARY
 THE AREA OF THE PEAK IS ABOUT 44.7220C*DEG/S
 THE AREA STUDIED IF:100.0000% OF THIS TOTAL
 /XFI21 : 03 UN 23540B

1

REPORT FOR CATALYST: AI-4 PEAK: (111)

LOCATED IN FILE: XPTD17

MODIFIED VOIGT PARAMETERS

I	B(I)
1	45.55862
2	20.86851
3	40.63438
4	.84809
5	4.71865
6	2.04222
7	4.39415
8	.73801

MEASURED RESULTS:

PEAK HEIGHT= 50.27727

HALF WIDTH= .54099

AREA= 44.72196

CALCULATED PARAMETERS

BETA= 1.522E-02 RADIANS

PHI=(HALF WIDTH)/(INT BREDTH)= 6.082E-01

OBSERVED CAUCHY BREDTH: 1.664E-02

OBSERVED GAUSSIAN BREDTH: -1.041E-04

XFI21 : STOP 0000

12.5.2 FORTRAN Program XFIT

FTN4

PROGRAM XFIT(4,200)

```

C
C      PROGRAM TO FIT DATA TO THE MODIFIED CAUCHY PROFILE
C
C      SUBSCRIPT(K)-REFERS TO THE ANGLE OR TIME DOMAIN
C      LOCATION
C      X(K)=ANGLE, DEG 2*THETA
C      X(500) = 0 => OUTPUT FOR NEW PEAK INCLUDES
C      K-ALPHA BROADENING
C      =-1 => OUTPUT FOR NEW PEAK IS K-ALPHA
C      BROADENING CORRECTED
C      IANG(K)=ANGLE, DEG 2*THETA*100
C      RINT(K)= INPUT INTENSITY CORRESPONDING TO IANG(K)
C
C      X(K)  = NEW ANGLE
C      RINTN(K) = NEW (FIT) INTENSITY CORRESPONDING TO X(K)
C      PARA(I)=PARAMETERS FOR MODIFIED VOIGT PROFILE,
C      8 REQUIRED PER PEAK, UP TO 2 PEAKS
C      NPAR = NO. OF PARAMETERS, INTERNALLY CALCULATED
C      (SEE ALSO ROUTINE FUNC)
C
C      DIMENSION IANG(500),RINT(500),RINTN(500)
C      DIMENSION PARA(16),PARMN(16),PARMX(16)
C      DIMENSION NAME1(9),IDCB1(144),IBUF(32)
C      COMMON X(500)
C      DATA NAME1/2H ,2H ,2H ,2HJU,135/
C      IDIM=500
C      IAGAN=0
C      IOUT1=1
C
C      WRITE(1,10)
10  FORMAT(/,'ENTER THE FILE LOCATION OF THE RAW DATA ',
& /,'OR "PREFIT" FOR USER ENTERED MOD. VOIGT PARAS.')
      READ(1,15) (NAME1(I),I=1,3)
15  FORMAT(4A2)
      WRITE(1,45)
45  FORMAT('ENTER THE REGENERATION WIDTH, AND THE (ODD) NUMBER',
& ' OF DATA POINTS')
      READ(1,*) WIDTH,IDIMR
      NFOR=(IDIMR-1)/2
      KCNTR=NFOR+1
      WRITE(1,50)
50  FORMAT(/,' ENTER THE NUMBER OF PEAKS, NPEAK')
      READ(1,*) NPEAK
      NPAR=NPEAK*8
      WRITE(1,60)
60  FORMAT(/,'ENTER DATA OUTPUT DEVICE (1=TERMINAL,6=LINE PRINTER)')

```

```

      READ(1,*) IOUT
      WRITE(1,70)
70  FORMAT('ENTER THE CATALYST IDENTIFICATION CODE ',
    & /, 'AND THE PEAK MILLER INDEX, (EG PI16 111)')
      READ(1,15) (NAME1(I), I=6,9)
      IF(NAME1(1).EQ.2HPR) GO TO 80
C
      WRITE(1,75)
75  FORMAT(/, 'ENTER THE APPROXIMATE PEAK LOCATION AND THE FIT',
    & ' RANGE')
      READ(1,*) PMAX, PRANG
      MINAN=IFIX((PMAX-PRANG/2.)*100.)
      MAXAN=IFIX((PMAX+PRANG/2.)*100.)
      CALL RREAD(IDCBL, NAME1, MINAN, MAXAN, IDEL, IDIM, IANG, RINT)
      CALL DIST(IANG, RINT, IDIM)
      CALL ESTB(RINT, IANG, IDIM, NPAR, PARA, PARMN, PARMX)
      CALL FIT(IDIM, NPAR, PARA, PARMN, PARMX, RINT, IOUT1)
      GO TO 90
80  WRITE(1,85)
85  FORMAT(' ENTER THE 8 PARAMETERS FOR THE PEAK')
      READ(1,*) (PARA(I), I=1,8)
      IF(NPEAK.LE.1) GO TO 90
      WRITE(1,87)
87  FORMAT('ENTER THE 8 PARAMETERS FOR THE SECOND PEAK')
      READ(1,*) (PARA(I), I=9,16)
90  CALL NEWX(PARA, IDIMR, WIDTH)
      WRITE(1,95)
95  FORMAT(10X, 'OBSERVED PROFILE:')
      CALL NEWPK(PARA, NPAR, IDIMR, RINTN, IANG, RINT, IOUT1)
      X(500)=-1.
      WRITE(1,98)
98  FORMAT(/, 5X, 'K-ALPHA BROADENING CORRECTED')
      CALL NEWPK(PARA, NPAR, IDIM, RINTN, IANG, RINT, IOUT)
C
      IF(NPEAK.GT.1) GO TO 100
      CALL RPORT(PARA, IDIMR, WIDTH, KCNTR, NFOR, RINTN, NAME1, IOUT)
      GO TO 999.
100 NPAR=8
      WRITE(IOUT,110)
110  FORMAT(10X, 'HIGHER SPACING PEAK-USUALLY PT')
      CALL NEWPK(PARA, NPAR, IDIM, RINTN, IANG, RINT, IOUT)
      CALL RPORT(PARA, IDIMR, WIDTH, KCNTR, NFOR, RINTN, NAME1, IOUT)
      DO 120 I=1,8
        PARA(I)=PARA(I+8)
120  CONTINUE
      WRITE(IOUT,130)
130  FORMAT( , 10X, 'LOWER SPACING PEAK-USUALLY IR')
      CALL NEWPK(PARA, NPAR, IDIM, RINTN, IANG, RINT, IOUT)
      CALL RPORT(PARA, IDIMR, WIDTH, KCNTR, NFOR, RINTN, NAME1, IOUT)
C
      999 STOP
END
C
C*****

```

```

C
  FUNCTION FPRIM(B,X1)
  DIMENSION B(8)
  U=B(8)
  IF(X1.GT.B(3)) U=1.
  DELX=X1-B(3)
  P1=B(1)*B(2)*B(4)/(1.+U*B(2)*DELX**2)**(B(4)+1.)
  P2=B(5)*B(6)*B(7)*(EXP(-U*B(6)*DELX**2))**B(7)
  FPRIM=-2.*U*DELX*(P1+P2)
  RETURN
END
C
C*****
C
  SUBROUTINE RPORT(B, IDIM, WIDTH, KCNTR, NFOR, RINTN, NAME1, IOUT)
  COMMON X(500)
  DIMENSION RINTN(IDIM), NAME1(9), B(8)
  RAD=0.01745329
  HT=B(1)+B(5)
  HO2=HT/2.
C
C      NEWTON'S METHOD TO DETERMIN XHLO AND XHHI
C
  XHLO=B(3)-(B(1)*SQRT((2.**((1./B(4))-1.)/(B(8)*B(2)))+
& B(5)*SQRT(-ALOG(0.5**((1./B(7)))/(B(8)*B(6))))/HT
  XHHI=B(3)+(B(1)*SQRT((2.**((1./B(4))-1.)/B(2))+
& B(5)*SQRT(-ALOG(0.5**((1./B(7)))/B(6))))/HT
  DO 30 I=1,5
  XHLO=XHLO-(PK(B,XHLO)-HO2)/FPRIM(B,XHLO)
  XHHI=XHHI-(PK(B,XHHI)-HO2)/FPRIM(B,XHHI)
30 CONTINUE
  WHAF=XHHI-XHLO
C
C
  CALL ALINE(PARA, IDIM, WIDTH, KCNTR, NFOR, RINTN, AREA1)
  BETA=RAD*AREA1/HT
  PHI=WHAF/(AREA1/HT)
  BCAUCH=BETA*(2.0207-0.4803*PHI-1.7756*PHI*PHI)
  BGAUS=0.6420+1.4187*SQRT(PHI-0.63662)-2.2043*PHI+
& 1.8706*PHI*PHI
  BGAUS=BGAUS*BETA
  WRITE(IOUT,60) (NAME1(I), I=6,9)
60  FORMAT(/,10X,'REPORT FOR CATALYST: ',2A2,' PEAK: (',2A2,')')
  WRITE(IOUT,65) (NAME1(I), I=1,3)
65  FORMAT(/,10X,'LOCATED IN FILE: ',3A2)
  WRITE(IOUT,70) (I,B(I), I=1,8)
70  FORMAT(/,10X,'MODIFIED VOIGT PARAMETERS',/,14X,'I',7X,'B(I)',
& /,8(/,10X,I5,5X,F10.5))
  WRITE(IOUT,80) HT,WHAF,AREA1
80  FORMAT(/,10X,'MEASURED RESULTS:',/,10X,'PEAK HEIGHT= ',F10.5,
& /,10X,'HALF WIDTH= ',F10.5,/,10X,'AREA= ',F10.5)
  WRITE(IOUT,90) BETA,PHI,BCAUCH,BGAUS
90  FORMAT(/,10X,'CALCULATED PARAMETERS',/,10X,'BETA=',1PE12.3,
& ' RADIANS',/,10X,'PHI=(HALF WIDTH)/(INT BREDTH)=' ,1PE12.3,

```

```
& /,10X,'OBSERVED CAUCHY BREDTH: ',1PE12.3,/,10X,  
& 'OBSERVED GAUSSIAN BREDTH: ',1PE12.3,/, '1')  
RETURN  
END
```

12.6 Program XPROF

FTN4

PROGRAM XPROF(4, 200), <;80307.1315>

Program uses 6 parameter modified Cauchy profiles to
determine the Fourier coefficients

PROGRAM TO CALCULATE THE PURE XRAY DIFFRACTION PROFILE (F)
FROM THE FOURIER SERIES OF AN ACTUAL PROFILE (H) AND A
PROFILE FOR 'INFINITELY' LARGE CRYSTALITES (G)

F=H/G

FR=(Hr*Gr + Hi*Gi)/(Gr**2+Gi**2)

Fi=(Hi*Gr + Hr*Gi)/(Gr**2 + Gi**2)

File 1=RAW DATA FOR THE PEAK

File 2=DATA FROM REFERENCE PEAK

File 3=RESULTS

SUBSCRIPT(J)-REFERS TO THE FOURIER FREQUENCY
-FOURIER COEFFICIENTS ARE STORED IN THE
(J+1)TH ELEMENT OF THE ARRAY
-Fr(0) IS STORED IN FR(1) ETC.

SUBSCRIPT(K)-REFERS TO THE ANGLE OR TIME DOMAIN
LOCATION

MAIN CONTROL VARIABLES:

NANAL- Peak to be analyzed (1,2, or 3)

IFIT=0=fit a profile from a given data file

1=use coefficients from XPTD68 (Pt(111))

2=use coefficients from XPTD68 (Pt(200))

(NOT AVAILABLE:83:04:05)

DOUBLE PRECISION FR(250),FI(250),HR(250),HI(250),GR(250),GI(250)

DIMENSION IANG(500),RINT(500),RINTN(500)

DIMENSION PARA(16),PARMN(16),PARMX(16)

DIMENSION NAME1(5),IDCB1(144),IBUF(32)

DIMENSION NAME2(5),IDCB2(144),NAME3(5),IDCB3(144)

DIMENSION VDF(250),PS(250),ADF(250)

COMMON X(500)

DATA NAME1/2H ,2H ,2H ,2HJU,135/

DATA NAME2/2H ,2H ,2H ,2HJU,135/

DATA NAME3/2HXF,2HOR,2H ,2HJU,135/

IDIM=500

NPAR=8

CALL INIT(NAME1,NAME2,NAME3,MINAN,MAXAN,NPAR,IOUT)

WRITE(1,20)

```

20  FORMAT(2X,'ENTER THE REGENERATION WIDTH, DEG*2*THETA',
      & /, 'AND THE NUMBER OF FOURIER COEFFICIENTS, NFOR')
      READ(1,*) WIDTH,NFOR
      IF(NAME1(1).NE.2HPR) GO TO 100
      WRITE(1,21)
21  FORMAT(2X,'ENTER THE 8 PARAMETERS FOR FIRST PEAK')
      READ(1,*) (PARA(I),I=1,8)
C
      NPAR=8
C
29  IDIM=NFOR*2+1
      KCNTR=NFOR+1
C
      PERFORM FOURIER ANALYSIS ON THE OBSERVED PEAK].
      GET THE FOURIER COEFFS: HR AND HI
C
40  CALL NEWX(PARA,IDIM,WIDTH)
      CALL NEWPK(PARA,NPAR,IDIM,RINTN,IANG,RINT,IOUT)
      CALL WIND1(RINTN,KCNTR,NFOR,IDIM)
      CALL ALINE(PARA,IDIM,WIDTH,KCNTR,NFOR,RINTN,AREA1)
      CALL FOR(RINTN,IDIM,KCNTR,NFOR,HR,HI,IOUT)
      CALL PEAK(IDIM,KCNTR,NFOR,IANG,HR,HI,IOUT)
      ANCNT=PARA(3)
C
C
C      IF(NAME2(1).NE.2HPR) GO TO 100
C      WRITE(1,41)
C 41  FORMAT('ENTER THE 8 PARAMETERS FOR THE SECOND PEAK')
C      READ(1,*) (PARA(I),I=1,8)
C      GO TO 70
C 60 DO 65 K=1,500
C      IANG(K)=0
C      RINT(K)=0.
C      X(K)=0.
C 65 CONTINUE
C      IDIM=NFOR*2+1
C      KCNTR=NFOR+1
C 70 PARA(3)=ANCNT
      CALL NEWX(PARA,IDIM,WIDTH)
C      CALL NEWPK(PARA,NPAR,IDIM,RINTN,IANG,RINT,IOUT)
C      CALL WIND1(RINTN,KCNTR,NFOR,IDIM)
C 75 CALL ALINE(PARA,IDIM,WIDTH,KCNTR,NFOR,RINTN,AREA2)
C      DO 79 K=1,IDIM
C          RINTN(K)=RINTN(K)*AREA1/AREA2
C 79 CONTINUE
C
C      COLLECT AND NORMALIZE THE FOURIER COEFFS FOR THE
C      STD. PEAK, GR AND GI
C
      CALL READP(IDC2,NAME2,GR,GI,NFOR)
      DO 75 JP1=1,NFOR
          GR(JP1)=GR(JP1)*HR(1)
          GI(JP1)=GI(JP1)*HR(1)
75 CONTINUE

```



```
C      CALL FOR(RINTN, IDIM, KCNTR, NFOR, GR, GI, IOUT)
C      CALL PEAK(IDIM, KCNTR, NFOR, IANG, GR, GI, IOUT)
C
C      DETERMINE THE TRUE PEAK PARAMETERS AND SAVE THEM
C      IF DESIRED
C
C      80 CALL PROF(HR, HI, GR, GI, FR, FI, NFOR, IOUT)
C         CALL SAVE1(NFOR, FR, FI, NAME1, MINAN, MAXAN, PARA)
C
C      DETERMINE VLDF AND ALDF FOR THE FOURIER COEFFICIENTS
C
C      MINAN=IFIX((ANCNT-WIDTH/2.)*100.)
C      MAXAN=IFIX((ANCNT+WIDTH/2.)*100.)
C      CALL DETLO(MINAN, MAXAN, IOUT, PARA, A, JP1LO)
C      CALL ARADF(FR, NFOR, ADF, PS, NADF, AREA1, IOUT, A, JP1LO)
C      CALL VOLDF(FR, NFOR, VDF, PS, NVDF, AREA1, IOUT, A, JP1LO)
C
C      100 CALL LURQ(100000B, 6, 1)
C
C      STOP
C      END
```

12.7 Program XPURE

```

FTN4
PROGRAM XPURE(4,200), <840521.1326>

C
C      PROGRAM TO GENERATE THE PURE SIZE BROADENED
C      XRD PROFILE FOR DIFFERENT ASSUMED LENGTH
C      DISTRIBUTION FUNCTIONS
C
      DIMENSION IDCB(144),NAME(5),IBUF(10),ISIZE(2)
      DIMENSION DP(50),VFRAC(50)
      DATA NAME/2HXP,2HUR,2H ,2HJU,135/,ISIZE/40,10/
C      DP(I)=LENGTH OF PARTICLE SIDE
C      VFRAC(I)=VOLUME FRACTION OF PARTICLES SIZE DP(I)
C
C      EPSILON IN RADIANS OF THETA
C
C      ASSUME RLAM=0.1542 NM
      WRITE(1,3)
3  FORMAT('ENTER THE NUMBER OF PARTICLE SIZES IN THE PSDF')
      READ(1,*) NPS
      WRITE(1,4)
4  FORMAT('ENTER PROFILE STEP SIZE, DEG 2*THETA')
      READ(1,*) DELTH
      WRITE(1,7)
7  FORMAT('ENTER CONTROL DIGIT, ICON:',/,
& 5X,'1=USE GAUSSIAN (NORMAL) LENGTH DISTRIBUTION',/,
& 5X,'2=USE ONE SIZE SPHERICAL PARTICLES',/,
& 5X,'3=LOG-NORMAL LENGTH DISTRIBUTION',/,
& 5X,'4=USER ENTERED LENGTH DISTRIBUTION FUNCTION')
      READ(1,*) ICON
      IF(ICON.GT.3) GO TO 14
      IF(ICON.GT.2) GO TO 12
      IF(ICON.GT.1) GO TO 10
      CALL NLDF(DP,VFRAC,NPS)
      GO TO 19
10 CALL SLDF(DP,VFRAC,NPS)
      GO TO 19
12 CALL LNLDF(DP,VFRAC,NPS)
      GO TO 19
14 CALL ULDF(DP,VFRAC,NPS)
19 CALL LAVG(DP,VFRAC,NPS)
      WRITE(1,20)
20  FORMAT('ENTER THE "XPURnn" FILE NUMBER')
      READ(1,25) NAME(3)
25  FORMAT(3A2)
      WRITE(1,27)
27  FORMAT('ENTER "1" TO LIST THE VOL WEIGHTED LENGTH DISTRIBUTION')
      READ(1,*) ILDF
      IF(ILDF.NE.1) GO TO 29
      CALL LDF(DP,VFRAC,NPS)

```

```

29 WRITE(1,30)
30 FORMAT('ENTER THE BRAGG ANGLE AND RANGE OF INTEREST, ',
  & 'DEG 2*THETA')
  READ(1,*) ANG,WIDTH
C
  PI=3.1415926
  RAD=0.017453
  RLAM=0.1542
  THETB=RAD*ANG/2.
  DS=RLAM/(2.*SIN(THETB))
  ILAST=IFIX(WIDTH/DELTH)+1
  IANMN=IFIX((ANG-WIDTH/2.)*100.)
C
C
  CALL CREAT(IDCB,IERR,NAME,ISIZE,3,NAME(4),NAME(5))
  IF(IERR.LT.0) GO TO 90
  CALL OPEN(IDCB,IERR,NAME,0,NAME(4),NAME(5))
  IF(IERR.LT.0) GO TO 90
C
C
C
C
  DO 70 K=1,ILAST
    IANG=IANMN+IFIX(DELTH*100.)*(K-1)
    SUM=0.
    THETA=RAD*FLOAT(IANG)/200.
    S=2.*DS*SIN(THETA)/RLAM-1.
    IF(ABS(S).LT.1.E-4) GO TO 52
    RINT=1./(SIN(PI*S)**2)
    DO 50 I=1,NPS
      ARG=PI*S*DP(I)/DS
      SUM=SUM+SIN(ARG)*SIN(ARG)*VFRAC(I)/DP(I)
50.    CONTINUE
      RINT=RINT*SUM
      GO TO 55
52.    DO 54 I=1,NPS
54.    SUM=SUM+((DP(I)/DS)**2)*VFRAC(I)/DP(I)
      RINT=SUM
55.    DO 57 J=1,10
57.    IBUF(J)=2H
      CALL CODE
      WRITE(IBUF,60) IANG,RINT
60.    FORMAT(1X,I5,3X,F9.3)
      CALL WRITF(IDCB,IERR,IBUF,10)
      IF(IERR.LT.0) GO TO 90
70.    CONTINUE
      CALL CLOSE(IDCB,IERR)
      IF(IERR.LT.0) GO TO 90
      GO TO 100.
C
C
90.    WRITE(1,91) IERR
91.    FORMAT(/,2X,'ERROR IN FMP CALL. IERR= ',I3)
100.    STOP

```

```

END
C
C*****
C
      SUBROUTINE ULDF(DP,VFRAC,NL)
      DIMENSION DP(NL),VFRAC(NL)
      5 DO 20 J=1,NL
        WRITE(1,10) J
      10  FORMAT(/,5X,'ENTER THE PARTICLE SIZE, NM',/
        & 'AND THE MASS FRACTION FOR SIZE NO. ',I3)
        READ(1,*) DP(J),VFRAC(J)
      20 CONTINUE
        WRITE(1,30)
      30  FORMAT('LENGTH DISTRIBUTION FUNCTION',/,10X,'DP',10X,'VFRAC')
        DO 40 J=1,NL
          WRITE(1,35) DP(J),VFRAC(J)
      35  FORMAT(2(5X,F10.5))
      40 CONTINUE
        WRITE(1,50)
      50  FORMAT('ENTER "1" TO RE-ENTER THE LDF')
        READ(1,*) IREAD
        IF(IREAD.EQ.1) GO TO 5
        RETURN

```

```

END
C
C*****
C
      SUBROUTINE NLDF(DP,VFRAC,NL)
      DIMENSION DP(NL),VFRAC(NL)
      WRITE(1,10)
      10  FORMAT('ENTER THE AVERAGE LENGTH, RLAV (NM)')
      READ(1,*) RLAV
      SIGMAX=RLAV/2.71523
      WRITE(1,20) SIGMAX
      20  FORMAT('ENTER THE STD. DEV. OF LDF, MAX. REALISTIC=',F8.3)
      READ(1,*) SIG
      XLO=RLAV-2.71523*SIG
      DELX=SIG*2.71523*2./FLOAT(NL-1)
      SUM1=0.
      SUM2=0.
      DO 30 J=1,NL
        DP(J)=XLO + FLOAT(J-1)*DELX
        Z=(DP(J)-RLAV)/SIG
        VFRAC(J)=0.3989*EXP(-Z*Z/2.)
        SUM1=SUM1+VFRAC(J)
      30 CONTINUE
        WRITE(1,40)
      40  FORMAT(/,10X,'NORMALIZED PARTICLE SIZE DIST. FUNCTION',/
        & 10X,'DP',10X,'VFRAC')
        DO 50 J=1,NL
          VFRAC(J)=VFRAC(J)/SUM1
          PV=VFRAC(J)/DELX
          WRITE(1,45) DP(J),PV
      45  FORMAT(2(5X,F10.4))

```

```

50 CONTINUE
   RETURN
END
C
C*****
C
      SUBROUTINE SLDF(DP,VFRAC,NPS)
      DIMENSION DP(NPS),VFRAC(NPS)
      5 WRITE(1,10)
      10 FORMAT('ENTER THE PARTICLE DIAMETER')
      READ(1,*)DIA
      RLAVG=0.75*DIA
      WRITE(1,20)RLAVG
      20 FORMAT(/,2X,'WEIGHT AVERAGE LENGTH IS: ',F10.3,' NM',
        & /,'ENTER "1" TO RE-ENTER')
      READ(1,*) ICON
      IF(ICON.EQ.1) GO TO 5
      DELX=DIA/FLOAT(NPS)
      SUM1=0.
      DO 30 J=1,NPS
        DP(J)=DELX/2. + DELX*FLOAT(J-1)
        VFRAC(J)=3.*(DP(J)/DIA)**2
        SUM1=SUM1+VFRAC(J)
      30 CONTINUE
C
      WRITE(1,40)
      40 FORMAT('NORMALIZED VOLUME WEIGHTED LENGTH DISTRIBUTION FUNCTION',
        & 10X,'DP',10X,'VFRAC')
      DO 50 J=1,NPS
        VFRAC(J)=VFRAC(J)/SUM1
        PV=VFRAC(J)/DELX
        WRITE(1,45) DP(J),PV
      45 FORMAT(2(5X,F10.4))
      50 CONTINUE
      RETURN
      END
C
C*****
C
      SUBROUTINE LNLDF(DP,VFRAC,NL)
      DIMENSION DP(NL),VFRAC(NL)
      5 WRITE(1,10)
      10 FORMAT('ENTER THE THREE PARAMETERS R, T, AND U')
      READ(1,*)R,T,U
      RK=R/(T*U)
      PVMAX=RK**(R/T)*EXP(-U*RK)
      XMAX=RK**(1./T)
C
C
      XP=2.*XMAX
      XN=XP
      DO 30 J=1,30
        FUN=(XP**R)*EXP(-U*(XP**T))- PVMAX/50.
        DFUN=EXP(-U*(XP**T))*(R*XP**(R-1.) - T*U*(XP**(R+T-1.)))

```

```

      XN=XP- FUN/DFUN
      IF(ABS(XN-XP).LT.1.E-3) GO TO 40
      XP=XN
30  CONTINUE
40  DELX=XN/FLOAT(NL)
      SUM1=0.
      DO 50 J=1,NL
          DP(J)=DELX*(FLOAT(J)-0.5)
          VFRAC(J)=DP(J)**R*EXP(-U*(DP(J)**T))
          SUM1=SUM1+VFRAC(J)
50  CONTINUE
C
      WRITE(1,60) R,T,U
60  FORMAT(/,10X,'NORMALIZED LENGTH DISTRIBUTION FUNCTION',//
&5X,'FOR LOG-NORMAL DISTRIBUTION: R= ',F8.4,' T= ',F8.4,' U= ',F8.4,
& //,10X,'DP',10X,'VFRAC')
C
      DO 80 J=1,NL
          VFRAC(J)=VFRAC(J)/SUM1
          PV=VFRAC(J)/DELX
          WRITE(1,70) DP(J),PV
70  FORMAT(2(5X,F10.4))
80  CONTINUE
      RETURN
      END
C
C*****
C
      SUBROUTINE LAVG(DP,VFRAC,NPS)
      DIMENSION DP(NPS),VFRAC(NPS)
      REAL NAVG
C
      SUMV=0.
      SUMA=0.
      SUMN1=0.
      SUMN2=0.
C
      DO 20 J=1,NPS
          SUMV=SUMV+VFRAC(J)*DP(J)
          SUMA=SUMA+VFRAC(J)/DP(J)
          SUMN1=SUMN1+VFRAC(J)/(DP(J)*DP(J))
          SUMN2=SUMN2+VFRAC(J)/(DP(J)**3)
20  CONTINUE
C
      VAVG=SUMV
      AAVG=1./SUMA
      NAVG=SUMN1/SUMN2
      VOA=VAVG/AAVG
      WRITE(1,30) VAVG,AAVG,VOA,NAVG
30  FORMAT(/,5X,'THE VOLUME AVERAGE LENGTH IS: ',F6.2,' NM',
& /,5X,'THE AREA AVERAGE LENGTH IS: ',F6.2,' NM',
& /,5X,'THE RATIO <Lv>/<La> IS: ',F6.3,
& /,5X,'THE NUMBER AVERAGE LENGTH IS: ',F6.2,' NM')
      RETURN

```

```
END
C
C*****
C
  SUBROUTINE LDF(DP,VFRAC,NPS)
  DIMENSION DP(NPS),VFRAC(NPS)
C
  DELDP=DP(2)-DP(1)
C
  WRITE(1,10)
10  FORMAT(2X,'ENTER LU FOR OUTPUT (TERMINAL=1):')
  READ (1,*) LUW
C
C
  DO 30 J=1,NPS
    VLDFJ=VFRAC(J)/DELD
    WRITE(LUW,20) DP(J),VLDFJ
20  FORMAT(3X,F10.4,5X,F10.4)
30  CONTINUE
C
  RETURN
  END
```

12.8 Program XNUMT

FTN4

PROGRAM XNUMT(4,200), <;80307.1351>

H=F*G

PROGRAM TO FOLD THE (NUMERICALLY GENERATED) PURE
 PROFILE (F) WITH THE MACHINE PROFILE (G) AND
 GENERATE THE 'NUMERICALLY PRODUCED OBSERVED'
 PROFILE (H)

DOUBLE PRECISION FR(125),FI(125),HR(125),HI(125),GR(125),GI(125)
 DIMENSION IANG(500),RINT(500),RINTN(500)

DIMENSION NAME1(5),NAME2(5),NAME3(5),IDCB(144),IBUF(32)
 DIMENSION B(12)

DIMENSION VDF(125),ADF(125),PS(125)

COMMON X(500)

DATA NAME1/2H ,2H ,2H ,2HJU/

DATA NAME2/2H ,2H ,2H ,2HJU,135/

DATA NAME3/2H ,2H ,2H ,2HJU,135/

RLAM=0.1542

RAD=3.141593/180.

IDIM=500

READ IN THE PURE PROFILE AND CENTRE IT FOR FOURIER
 ANALYSIS

CALL INIT(NAME1,NAME2,NAME3,MINAN,MAXAN,NPAR,IOUT)

CALL RREAD(IDCB,NAME1,MINAN,MAXAN,IDEL,IDIM,IANGL,RINT)

CALL CNTRD(NAME1,IDIM,IANGL,RINT,MINAN,MAXAN,CNTR,IOUT,AREAL)

CALL ALIGN(IANGL,IDEL,CNTR,IDIM,KCNTR,NFOR,IOUT)

APPLY THE HANNING WINDOW (IF DESIRED) AND PERFORME
 THE FOURIER ANALYSIS

CALL WIND1(RINT,KCNTR,NFOR,IDIM)

CALL FOR(RINT,IDIM,KCNTR,NFOR,FR,FI,IOUT)

CALL PEAK(IDIM,KCNTR,NFOR,IANGL,FR,FI,IOUT)

ANMIN=RAD*FLOAT(IANGL(KCNTR-NFOR))/(100.*2.)

ANMAX=RAD*FLOAT(IANGL(KCNTR+NFOR))/(100.*2.)

A=(RLAM/2.)/(SIN(ANMAX)-SIN(ANMIN))

JP1LO=3

CALL ARADF(FR,NFOR,ADF,PS,NADF,AREAL,IOUT,A,JP1LO)

CALL VOLDF(FR,NFOR,VDF,PS,NVDF,AREAL,IOUT,A,JP1LO)

WRITE(1,10)

10 FORMAT('ENTER "1" TO CONTINUE')

READ(1,*) ICON

IF(ICON.NE.1) GO TO 100


```

IDIM=NFOR*2+1
WIDTH=FLOAT(NFOR*IDEL)/50.
B(3)=FLOAT(IANG(KCNTR))/100.
CALL NEWX(B, IDIM, WIDTH)
C CALL NEWPK(B, NPAR, IDIM, RINTN, IANG, RINT, IOUT)
C CALL ALINE(B, IDIM, WIDTH, KCNTR, NFOR, RINTN, AREA2)
C DO 20 K=1, IDIM
C   RINTN(K)=RINTN(K)*AREAL/AREA2
C 20 CONTINUE
C CALL WIND1(RINTN, KCNTR, NFOR, IDIM)
C CALL FOR(RINTN, IDIM, KCNTR, NFOR, GR, GI, IOUT)
C CALL PEAK(IDIM, KCNTR, NFOR, IANG, GR, GI, IOUT)
C IDEL1=3
C IDEL2=1
C CALL NURNG(GR, GI, IDEL1, IDEL2, NFOR, IOUT)
C WIDTH=WIDTH*FLOAT(IDEL1)/FLOAT(IDEL2)
C CALL NEWX(B, IDIM, WIDTH)
C CALL PEAK(IDIM, KCNTR, NFOR, IANG, GR, GI, IOUT)
C
C   GET THE FOURIER COEFFICIENTS OF THE PURE PROFILE
C   AND NORMALIZE THEM
C
CALL READP(IDC, NAME2, GR, GI, NFOR)
DO 25 JP1=1, NFOR
  GR(JP1)=GR(JP1)*FR(1)
  GI(JP1)=GI(JP1)*FR(1)
25 CONTINUE
CALL MACHP(FR, FI, GR, GI, NFOR, HR, HI)
WRITE(1, 30)
30 FORMAT('FOURIER COEFFICIENTS OF THE OBSERVED PROFILE, H'
& /, 3X, 'J', 11X, 'HR', 20X, 'HI')
DO 50 JP1=1, NFOR
  J=JP1-1
  FR(JP1)=0.
  FI(JP1)=0.
  WRITE(1, 40) J, HR(JP1), HI(JP1)
40 FORMAT(I4, 2(10X, 1PE10.2))
50 CONTINUE
WRITE(1, 60)
60 FORMAT('CHOOSE "1" NEXT TIME TO SAVE THE PEAK')
CALL PEKES(IDIM, KCNTR, NFOR, IANG, HR, HI, IOUT)
CALL PROF(HR, HI, GR, GI, FR, FI, NFOR, IOUT)
CALL PEAK(IDIM, KCNTR, NFOR, IANG, FR, FI, IOUT)
CALL VOLDF(FR, NFOR, IANG(KCNTR-NFOR), IANG(KCNTR+NFOR), VDF, PS,
& NVDF, AREAL, IOUT)
CALL LURQ(100000B, 6, 1)
100 STOP
END
C
C*****
C
SUBROUTINE PEKES(IDIM, KCNTR, NFOR, IANG, A, B, IOUT)
DIMENSION IANG(IDIM), NAME(5), IDC(144), ISIZE(2), IBUF(40)
DOUBLE PRECISION A(NFOR), B(NFOR)

```

```

DOUBLE PRECISION ARG,SUM,PI
COMMON X(500)
DATA ISIZE/40,10/,NAME/2H ,2H ,2H ,2HJU,135/
RMULT=0.
N=2*NFOR + 1
NM1=N-1
PI=3.14159265359
WRITE(1,5)
5  FORMAT(2X,'ENTER 1 TO REGENERATE THE PEAK FROM THE TRANSFORM')
   READ(1,*) IPEAK
   IF(IPEAK.NE.1) GO TO 100
   WRITE(1,7)
7  FORMAT(2X,'ENTER "1" TO SAVE THE PEAK IN A FILE')
   READ(1,*) ISAVE
   IF(ISAVE.NE.1) GO TO 9
   WRITE(1,110)
110 FORMAT('ENTER THE FILENAME')
   READ(1,120) (NAME(I),I=1,3)
120 FORMAT(3A2)
   CALL CREAT(IDCB,IERR,NAME,ISIZE,3,NAME(4),NAME(5))
   IF(IERR.LT.0) GO TO 555
   CALL OPEN(IDCB,IERR,NAME,0,NAME(4),NAME(5))
   IF(IERR.LT.0) GO TO 555
9  WRITE(1,10)
10 FORMAT(2X,'ENTER 1. TO USE IMAGINARY TERMS (OTHERWISE 0.)')
   READ(1,*) RMULT
   WRITE(1,20)
20  FORMAT(2X,'ENTER NLAST, THE NO. OF FOURIER COEFFS USED')
   READ(1,*) NLAST
   WRITE(1,30)
30  FORMAT(2X,'NEW PROFILE',//,10X,'ANGLE',4X,'INTENSITY')
C
DO 40 KPNT=1,N
  K=KPNT-1-NFOR
  KINDX=KCNTR + K
  M=A(1)/2.
  DO 40 JP1=2,NLAST
    J=JP1-1
    ARG=2.*PI*FLOAT(J)*FLOAT(K)/FLOAT(NM1)
    SUM=SUM + A(JP1)*DCOS(ARG) + RMULT*B(JP1)*DSIN(ARG)
40  CONTINUE
    WRITE(1,45) KPNT,X(KINDX),SUM
45  FORMAT(2X,I3,2(3X,F8.3))
    IF(ISAVE.NE.1) GO TO 50
    DO 210 I=1,10
210  IBUF(I)=2H
        CALL CODE
        WRITE(IBUF,320) IANG(KINDX),SUM
320  FORMAT(1X,I5,2X,F8.2)
        CALL WRITF(IDCB,IERR,IBUF,10)
        IF(IERR.LT.0) GO TO 555
50  CONTINUE
    IF(ISAVE.NE.1) GO TO 90
    CALL CLOSE(IDCB,IERR)

```

```
      IF(IERR.LT.0) GO TO 555
C
  90 WRITE(1,95)
  95  FORMAT(2X,'ENTER 1 TO GENERATE A NEW PROFILE')
     READ(1,*) IOVER
     IF(IOVER.EQ.1) GO TO 9
     GO TO 100
  555 WRITE(1,556) IERR
  556  FORMAT('TROUBLE IN FMP CALL. IERR= 'I5)
  100 RETURN
END
```

12.9 Program XFOR

FTN4

PROGRAM XFOR

C

C

C

C

C

C

Generate the normalized Fourier coefficients for the
machine profile, G and store them in a user given file
240; Fourier coefficients generated about 12. deg 2*theta,
then expand with routine NURNG to 24 deg 2*theta

DOUBLE PRECISION GR(250),GI(250)

DIMENSION IANG(500),RINT(500),RINTN(500)

DIMENSION NAME1(5),NAME2(5),NAME3(5),IDCB(144),IBUF(32)

DIMENSION B(8)

COMMON X(500)

DATA NAME1/2HXP,2HTD,2HE3,2HJU/

DATA B/47.86,248.1,46.249,1.2407,4.5520,42.360,2.475,0.2408/

C

IOUT=1

NPAR=8

NFOR=120

KCNTR=NFOR+1

IDIM=NFOR*2+1

WIDTH=NFOR*2*0.01250

IDEL1=2

IDEL2=1

CALL NEWX(B,IDIM,WIDTH)

DO 20 K=1,IDIM

IANG(K)=IFIX(X(K)*100.)

20 CONTINUE

X(500)=-1.

C

CALL NEWPK(B,NPAR,IDIM,RINTN,IANG,RINT,IOUT)

CALL ALINE(B,IDIM,WIDTH,KCNTR,NFOR,RINTN,AREA2)

CALL WIND1(RINTN,KCNTR,NFOR,IDIM)

CALL FOR(RINTN,IDIM,KCNTR,NFOR,GR,GI,IOUT)

CALL PEAK(IDIM,KCNTR,NFOR,IANG,GR,GI,IOUT)

CALL NURNG(GR,GI,IDEL1,IDEL2,NFOR,IOUT)

RNORM=GR(1)

DO 40 JP1=1,NFOR

GR(JP1)=GR(JP1)/RNORM

GI(JP1)=GI(JP1)/RNORM

40 CONTINUE

C

MINAN=IANG(KCNTR)-FLOAT(IDEL1/IDEL2)*100.*WIDTH/2.

MAXAN=IANG(KCNTR)+FLOAT(IDEL1/IDEL2)*100.*WIDTH/2

CALL SAVE1(NFOR,GR,GI,NAME1,MINAN,MAXAN)

STOP

END

12.10 Program XNOIS

```

FTN4      PROGRAM XNOIS
C
C      PROGRAM TO APPLY NOISE TO XRAY DATA
C
      DIMENSION IDCB1(144),NAME1(5),IDCB2(144),NAME2(5)
      DIMENSION IBUF(32),ISIZE(2)
      DATA NAME1/2H ,2H ,2H ,2HJU,135/
      DATA NAME2/2H ,2H ,2H ,2HJU,135/
      DATA ISIZE/40,10/
      DATA IRAN/333/,RMEAN/0./
      WRITE(1,10)
10  FORMAT(/,'ENTER THE INPUT DATA FILE')
      READ(1,15) (NAME1(I),I=1,3)
15  FORMAT(3A2)
      WRITE(1,20)
20  FORMAT(/,'ENTER THE DATA OUTPUT FILENAME')
      READ(1,15) (NAME2(I),I=1,3)
      WRITE(1,25)
25  FORMAT(/,'ENTER THE STANDARD DEVIATION, C/S')
      READ(1,*) SD
      CALL OPEN(IDCB1,IERR,NAME1,0,NAME1(4),NAME1(5))
      IF(IERR.LT.0) GO TO 90
      CALL CREAT(IDCB2,IERR,NAME2,ISIZE,3,NAME2(4),NAME2(5))
      IF(IERR.LT.0) GO TO 90
C
      DO 60 I=1,10000
C
C      READ FILE 1
C
      DO 30 J=1,10
30  IBUF(J)=2H
      CALL READF(IDCB1,IERR,IBUF,10,LEN)
      IF(IERR.LT.0) GO TO 90
      IF(LEN.EQ.-1) GO TO 70
      CALL CODE
      READ(IBUF,*) IANG,RINT
C
C      APPLY A RANDOM NOISE OF STD DEV SD TO THE DATA
C
      CALL GAUSS(IRAN,SD,RMEAN,V)
      RINT=RINT + V
C
C      WRITE INTO FILE 2
C
      DO 40 J=1,10
40  IBUF(J)=2H
      CALL CODE
      WRITE(IBUF,50) IANG,RINT

```

```

50  FORMAT(2X,I5,5X,F8.2)
    CALL WRITF(IDC2,IERR,IBUF,10,LEN)
    IF(IERR.LT.0) GO TO 90
60  CONTINUE
C
C    CLOSE FILES
C
70  IF(CLOSE(IDC1,IERR).LT.0) GO TO 90
    IF(CLOSE(IDC2,IERR).LT.0) GO TO 90
    GO TO 100
90  WRITE(1,95) IERR
95  FORMAT(/,5X,'TROUBLE IN FMP CALL. IERR=',I5)
100 STOP
END
C
C
C    ROUTINE TO ADD GAUSSIAN NOISE, FROM "SSP" LIBRARY
C
    SUBROUTINE GAUSS(IX,S,AM,V)
    A=0.0
    DO 50 I=1,12
        CALL RANDU(IX,IY,Y)
        IX=IY
        A=A+Y
50  CONTINUE
    V=(A-6.0)*S + AM
    RETURN
    END

```

12.11 Program XLDFD

FTN4

PROGRAM XLDFD(4, 200), <831211.1137>

C

C

Program uses Fourier Coefficients stored in file NAME1
to determine area and length weighted LDF's

C

C

C

C

C

File 1=FOURIER coefficients for the peak

C

C

MAIN CONTROL VARIABLES:

C

DOUBLE PRECISION FR(250),FI(250)

DIMENSION NAME1(5),IDCB1(144),IBUF(32)

DIMENSION NAME2(5),IDCB2(144),NAME3(5),IDCB3(144)

DIMENSION VDF(250),PS(250),ADF(250)

COMMON X(500)

DATA NAME1/2H ,2H ,2H ,2HJU,135/

DATA NAME2/2H ,2H ,2H ,2HJU,135/

DATA NAME3/2HXF,2HOR,2H ,2HJU,135/

IDIM=500

C

CALL INIT(NAME1,NAME2,NAME3,MINAN,MAXAN,NPAR,IOUT)

WRITE(1,20)

20 FORMAT(2X,'ENTER THE NUMBER OF FOURIER COEFFS,NFOR')

READ(1,*) NFOR

C

29 IDIM=NFOR*2+1

KCNTR=NFOR+1

C

RLAM=0.1542

RAD=3.1415926/180.

ANMIN=RAD*FLOAT(MINAN)/(100.*2.)

ANMAX=RAD*FLOAT(MAXAN)/(100.*2.)

A=(RLAM/2.)/(SIN(ANMAX)-SIN(ANMIN))

JP1LO=3

CALL READP(IDCB1,NAME1,FR,FI,NFOR)

CALL ARADF(FR,NFOR,ADF,PS,NADF,AREAL,IOUT,A,JP1LO)

CALL VOLDF(FR,NFOR,VDF,PS,NVDF,AREAL,IOUT,A,JP1LO)

C

100 CALL LURQ(100000B,6,1)

C

STOP

END

12.12 Subroutines Used

These subroutines are used by the previous programs to perform the mathematical manipulations.

12.12.1 Subroutine PEAK

```

FTN4
      SUBROUTINE PEAK(IDIM,KCNTR,NFOR,IANG,A,B,IOUT)
C
C      SUBROUTINE TO INVERT THE FOURIER COEFFICIENTS TO
C      DETERMINE THE REAL DOMAIN PEAK
C
      DIMENSION IANG(IDIM)
      DOUBLE PRECISION A(NFOR),B(NFOR)
      DOUBLE PRECISION ARG,SUM,PI
      COMMON X(500)
      RMULT=0.
      N=2*NFOR + 1
      NM1=N-1
      PI=3.14159265359
      WRITE(1,5)
5    FORMAT(2X,'ENTER 1 TO REGENERATE THE PEAK FROM THE TRANSFORM')
      READ(1,*) IPEAK
      IF(IPEAK.NE.1) GO TO 100
9    WRITE(1,10)
10   FORMAT(2X,'ENTER 1. TO USE IMAGINARY TERMS (OTHERWISE 0.)')
      READ(1,*) RMULT
      WRITE(1,20)
20   FORMAT(2X,'ENTER NLAST, THE NO. OF FOURIER COEFFS USED')
      READ(1,*) NLAST
      WRITE(1,30)
30   FORMAT(2X,'NEW PROFILE',//,10X,'ANGLE',4X,'INTENSITY')
C
      DO 50 KPNT=1,N
        K=KPNT-1-NFOR
        KINDX=KCNTR + K
        SUM=A(1)/2.
        DO 40 JP1=2,NLAST
          J=JP1-1
          ARG=2.*PI*FLOAT(J)*FLOAT(K)/FLOAT(NM1)
          SUM=SUM + A(JP1)*DCOS(ARG) + RMULT*B(JP1)*DSIN(ARG)
40    CONTINUE
        WRITE(1,45) KPNT,X(KINDEX),SUM
45    FORMAT(2X,I3,2(3X,F8.3))
50    CONTINUE
C
90   WRITE(1,95)
95   FORMAT(2X,'ENTER 1 TO GENERATE A NEW PROFILE')
      READ(1,*) IOVER
      IF(IOVER.EQ.1) GO TO 9
100  RETURN
END

```

12.12.2 Subroutine FOR

```

FTN4
      SUBROUTINE FOR(Y, IDIM, KCNTR, NFOR, A, B, IOUT)
C
C      SUBROUTINE TO PERFORM THE FOURIER TRANSFORM ON DATA
C
      DIMENSION Y(IDIM)
      DOUBLE PRECISION A(NFOR), B(NFOR)
      DOUBLE PRECISION ARG, PI, ASUM, BSUM
      PI=3.1415926535898
      N=2*NFOR+1
      NM1=N-1
      DO 50 JP1=1, NFOR
        J=JP1-1
        ASUM=0.
        BSUM=0.
        DO 25 KPNT=1, N
          K=KPNT-1-NFOR
          KINDX=KCNTR+K
          ARG=2.*PI*FLOAT(J*K)/FLOAT(NM1)
          ASUM=ASUM + Y(KINDX)*DCOS(ARG)
          BSUM=BSUM + Y(KINDX)*DSIN(ARG)
25      CONTINUE
        A(JP1)=2.*ASUM/FLOAT(NM1)
        B(JP1)=2.*BSUM/(FLOAT(NM1))
50      CONTINUE
      WRITE(IOUT, 70)
70      FORMAT(/, 12X, 'FOURIER COEFFICIENTS', /, 5X, 'J', 9X, 'A(J)', 9X,
& 'B(J)', 8X, 'AMP(J)', /)
      NFORO=AMINO(41, NFOR)
      DO 90 JP1=1, NFORO
        J=JP1-1
        AMP=(A(JP1)*A(JP1) + B(JP1)*B(JP1))**.5
        WRITE(IOUT, 80) J, A(JP1), B(JP1), AMP
80      FORMAT(3X, I3, 3(5X, 1PE10.3))
90      CONTINUE
      RETURN
      END

```

12.12.3 Subroutine WIND1

```

FTN4
SUBROUTINE WIND1(RINT,KCNTR,NFOR,IDIM)
C
C   SUBROUTINE TO APPLY THE HANNING WINDOW TO THE DATA
C
  DIMENSION RINT(IDIM)
  COMMON X(500)
  N=NFOR*2+1
  PI=3.1415926535
  WRITE(1,10)
10  FORMAT('ENTER "1" TO APPLY THE MODIFIED HANNING WINDOW',
  READ(1,*)IWIN
  IF(IWIN.NE.1) GO TO 100
  WRITE(1,20) N
20  FORMAT('ENTER THE NO. OF TAPERED COEFS. IN THE WINDOW, M2M',
  & /,5X,'(TOTAL NO. OF POINTS=',I4,',')')
  READ(1,*)M2M
  M=M2M/2
  DO 60 K=1,N
    KINDX=KCNTR-NFOR-1+K
    IF(K.GT.M) GO TO 30
    ARG=PI*(FLOAT(K)-1.5)/FLOAT(M)
    WIN=0.5*(1.-COS(ARG))
    GO TO 50
30  IF(K.GT.N-M) GO TO 40
    WIN=1.
    GO TO 50
40  ARG=PI*(FLOAT(N-K)+0.5)/FLOAT(M)
    WIN=0.5*(1.-COS(ARG))
50  RINT(KINDEX)=RINT(KINDEX)*WIN
60  CONTINUE
C
  WRITE(1,70)
70  FORMAT('ENTER "1" TO LIST SPLIT COS BELL WINDOW FITTED SERIES')
  READ(1,*) ILIST
  IF(ILIST.NE.1) GO TO 100
  DO 90 K=1,N
    KINDX=KCNTR-NFOR-1+K
    WRITE(1,80) X(KINDEX),RINT(KINDEX)
80  FORMAT(2(5X,F10.2))
90  CONTINUE
100 RETURN
END

```

12.12.4 Subroutine ALIGN

```

FTN4
SUBROUTINE ALIGN(IANG, IDEL, CNTR, IDIM, KCNTR, NFOR, IOUT)
C
C
C   ROUTINE TO DETERMINE THE CENTRE POINT, KCNTR
C   AND THE MAXIMUM POSSIBLE NUMBER OF COEFFICIENTS
C   WITHIN THE RANGE GIVEN TO INIT AND CONVERTED TO
C   (IDIM*IDEL) BY RREAD
C
C   DIMENSION IANG(IDIM)
C   TEST1=1.E6
C   TEST2=TEST1
C   DO 20 K=1, IDIM
C       TEST1=ABS(FLOAT(IANG(K))/100.-CNTR)
C       IF(TEST1.LT.TEST2) KCNTR=K
C       TEST2=AMIN1(TEST2, TEST1)
20  CONTINUE
C
C   IF(IDIM.GT.20) GO TO 40
C   WRITE(1,30)
30  FORMAT(/,10X,'** ERROR ** RANGE ((MAXAN-MINAN/IDEL) IS TOO',
& 'SMALL')
C   GO TO 99
C
40  NDUM=MINO((KCNTR-1), (IDIM-1-KCNTR))
C   IF(NDUM.GT.10) NFOR=10
C   IF(NDUM.GT.20) NFOR=20
C   IF(NDUM.GT.30) NFOR=30
C   IF(NDUM.GT.40) NFOR=40
C   IF(NDUM.GT.60) NFOR=60
C   IF(NDUM.GT.80) NFOR=80
C   IF(NDUM.GT.100) NFOR=100
C   IF(NDUM.GT.120) NFOR=120
C   CANG=FLOAT(IANG(KCNTR))/100.
C   WRITE(IOUT,50) IDIM, KCNTR, CANG, NFOR
50  FORMAT(/, 'THERE ARE ', I5, ' DATA POINTS',
& /, 'THE CLOSEST TO THE CENTROID IS: ', I5,
& /, 'AT AN ANGLE OF: ', F8.2,
& /, I5, ' FOURIER COEFFICIENTS WILL BE USED')
C   ANGLO=FLOAT(IANG(KCNTR-NFOR))/100.
C   ANGHI=FLOAT(IANG(KCNTR+NFOR))/100.
C   WRITE(IOUT,60) ANGLO, ANGHI
60  FORMAT('THE PEAKS WILL BE STUDIED FROM: ', F8.2, ' TO ', F8.2)
99  RETURN
END

```

12.12.5 Subroutine CNTRD

```

FTN4  SUBROUTINE CNTRD(NAME, IDIM, IANG, RINT, MINAN, MAXAN, CNTR, IOUT, AREA)
C      ROUTINE TO DETERMINE THE CENTROID ANGLE AND AREA OF THE
C      PEAKS
C
      DIMENSION IANG(1000), RINT(1000), NAME(5)
      IDEL=IANG(3)-IANG(2)
      DELAN=FLOAT(IDEL)/100.
      SUM1=0.
      SUM2=0.
C
C      SET NPONT (THE NUMBER OF INTEGRATING POINTS) TO AN ODD NUMBER
C
      NPONT=IDIM
      TEST1=FLOAT(NPONT/2)
      TEST2=FLOAT(NPONT)/2.
      IF((TEST2-TEST1).LT.0.1) NPONT=NPONT-1
C
      DO 20 I=1, NPONT, 2
          XFI=RINT(I)*FLOAT(IANG(I))
          XFIP1=RINT(I+1)*FLOAT(IANG(I+1))
          SUM1=SUM1 + XFI*2. + XFIP1*4.
          SUM2=SUM2 + RINT(I)*2. + RINT(I+1)*4.
20    CONTINUE
      XF1=RINT(1)*FLOAT(IANG(1))
      XFN=RINT(NPONT)*FLOAT(IANG(NPONT))
      SUM1=SUM1-XF1-XFN
      SUM2=SUM2-RINT(1)-RINT(NPONT)
      AREA=DELAN*SUM2/3.
      CNTR=SUM1/(SUM2*100.)
      WRITE(IOUT,25) (NAME(I), I=1,3)
25  FORMAT(/,10X,'** FILE: ',3A2,' **')
      WRITE(IOUT,30) AREA, CNTR
30  FORMAT('THE PEAK AREA IS:',F8.3,' C*DEG/S',
& /, 'THE CENTROID IS AT: ',F8.3,' DEG 2*THETA')
      RETURN
      END

```

12.12.6 Subroutine RREAD

```

FTN4
SUBROUTINE RREAD(IDCB,NAME,MINAN,MAXAN,IDEL,IDIM,IANG,RINT)
C
C   ROUTINE TO READ IN REAL DATA FROM A FILE
C
C   MINAN = MINIMUM ANGLE TO BE EXAMINED, DEG 2THETA*100
C   MAXAN = MAXIMUM ANGLE TO BE EXAMINED
C   IDEL  = STEP SIZE OF RAW DATA
C   IDIM  = NUMBER OF DATA POINTS
C   IANG(K)=ANGLE, DEG 2THETA*100
C   RINT(K)=DATA INTENSITY CORRESPONDING TO IANG(K)
C
  DIMENSION NAME(5),IDCB(144),IBUF(10),IANG(1000),RINT(1000)
  CALL OPEN (IDCB,IERR,NAME,0,NAME(4),NAME(5))
  IF(IERR.LT.0) GO TO 100
  KK=0
  WRITE(1,5) (NAME(I),I=1,3)
5  FORMAT(/,'ENTER THE SCALING FACTOR FOR FILE ',3A2)
  READ(1,*) SCAL1
  DO 50 K=1,10000
    DO 10 I=1,10
      IBUF(I)=2H
10  CONTINUE
      KK=KK+1
      CALL READF(IDCB,IERR,IBUF,10,LEN)
      IF(IERR.LT.0) GO TO 80
      IF(LEN.EQ.-1) GO TO 100
      CALL CODE
      READ(IBUF,*) IANG(KK),RINT(KK)
      RINT(KK)=RINT(KK)*SCAL1
      IF(IANG(KK).GT.MAXAN) GO TO 55
      IF(IANG(KK).LT.MINAN) KK=0
50  CONTINUE
55  CONTINUE
      IDEL=IANG(3)-IANG(2)
      IDIM=KK
      GO TO 100
80  WRITE(1,90) IERR
90  FORMAT(/,5X,'TROUBLE IN FMP CALL, ROUTINE RREAD. IERR= ',I5)
100 RETURN
  END

```

12.12.7 Subroutine INIT

FTN4

SUBROUTINE INIT(NAME1,NAME2,NAME3,MINAN,MAXAN,NPAR,IOUT)

C

ROUTINE TO INITIALIZE SEVERAL PROGRAMS

C

DIMENSION NAME1(5),NAME2(5),NAME3(5),CATID(2)

C

WRITE(1,10)

10 FORMAT(/,'ENTER THE FILE LOCATION OF THE RAW DATA ',
& /,'OR "PREFIT" FOR USER ENTERED MOD. CAUCHY PARAS.')

READ(1,15) (NAME1(I),I=1,3)

15 FORMAT(3A2)

WRITE(1,20)

20 FORMAT(/,'ENTER THE FILE LOCATION OF THE REFERENCE PEAK ',
& /,'OR "PREFIT" FOR THE PT(111) LINE IN XPTD68')

READ(1,15) (NAME2(I),I=1,3)

C

WRITE(1,30)

C

30 FORMAT(/,'ENTER THE FILE NUMBER FOR THE RESULTING DATA')

C

READ(1,35) NAME3(3)

C

35 FORMAT(A2)

C

WRITE(1,40)

40 FORMAT(/,'ENTER THE APPROXIMATE PEAK LOCATION AND THE RANGE',
& ' OF INTEREST')

READ(1,*) PMAX, PRANG

MINAN=IFIX((PMAX-PRANG/2.)*100.)

MAXAN=IFIX((PMAX+PRANG/2.)*100.)

WRITE(1,50)

50 FORMAT(/,' ENTER THE NUMBER OF PEAKS, NPEAK')

READ(1,*) NPEAK

NPAR=NPEAK*4

WRITE(1,60)

60 FORMAT(/,'ENTER DATA OUTPUT DEVICE (1=TERMINAL,6=LINE PRINTER)')

READ(1,*) IOUT

WRITE(1,70)

70 FORMAT('ENTER THE CATALYST IDENTIFICATION CODE (EG P116)')

READ(1,15) (CATID(I),I=1,2)

WRITE(IOUT,80) (CATID(I),I=1,2)

80 FORMAT(/,10X,'FOURIER ANALYSIS OF PEAKS IN CATALYST: ',2A2)

RETURN

END

12.12.8 Subroutine MACHP

FTN4

SUBROUTINE MACHP(FR,FI,GR,GI,NFOR,HR,HI)

C

C

ROUTINE TO FOLD TWO PEAKS TOGETHER

C

 $H = F * G$

C

DOUBLE PRECISION FR(NFOR),FI(NFOR),GR(NFOR),GI(NFOR)

DOUBLE PRECISION HR(NFOR),HI(NFOR)

DO 30 JPl=1,NFOR

HR(JPl)=(FR(JPl)*GR(JPl)-FI(JPl)*GI(JPl))/GR(1)

HI(JPl)=(FR(JPl)*GI(JPl)+FI(JPl)*GR(JPl))/GR(1)

30 CONTINUE

RETURN

END

12.12.9 Subroutine ALINE

FTN4

SUBROUTINE ALINE(B, IDIM, WIDTH, KCNTR, NFOR, RINTN, AREA1)

C

C

C

C

C

C

ROUTINE TO INDICATE FRACTION OF TOTAL AREA WHICH IS
BEING STUDIED IN FOURIER ANALYSIS
(THIS GIVES AN INDICATION OF VALIDITY OF ANALYSIS
AND LIKELY-HOOD OF UNSTABLE OSCILLATIONS IN THE PROFILE)

DIMENSION B(8), RINTN(IDIM)

COMMON X(500)

RAD=0.0174533

W2=WIDTH/2.

WA=0.555556

WB=0.888889

T1=0.774597

IDMM2=IDIM-2

C

C

C

C

C

AREA1= AREA UNDER PEAK THAT IS STUDIED

AREA2 = AREA BETWEEN BOTTOM OF STUDIED PEAK AND S=-0.5

AREA3 = AREA BETWEEN TOP OF STUDIED PEAK AND S=0.5

AREA1=0.

AREA2=0.

C

C

C

SIMPSON'S RULE TO DETERMINE AREA UNDER PEAK, AREA1

DO 20 K=1, IDMM2, 2

AREA1=AREA1 + 2.*RINTN(K) + 4.*RINTN(K+1)

20 CONTINUE

AREA1=(AREA1-RINTN(1)+RINTN(IDIM))*(X(2)-X(1))/3.

C

C

C

GAUSSIAN QUADRATURE TO DETERMINE THE AREA FROM MEASURED TO THE
ENDS OF THE PEAK (AT S=-0.5, S=0.5)

HTFRC=100.*PK(B, X(KCNTR)-W2)/(B(1)+B(5))

A=1./SIN(X(KCNTR)*RAD/2.)

XLO=2.*ATAN(1./SQRT(4*A*A-1.))/RAD

X1=((X(1)-XLO)*(-T1) + X(1) + XLO)/2.

X2=(X(1)+XLO)/2.

X3=((X(1)-XLO)*T1 + X(1) + XLO)/2.

AREA2=(WA*(PK(B, X1)+PK(B, X3)) + WB*PK(B, X2))*(X(1)-XLO)/2.

C

XHI=2.*ATAN(SQRT(4*A*A-1.))/RAD

X1=((X(IDIM)-XHI)*(-T1) + X(IDIM) + XHI)/2.

X2=(X(IDIM) + XHI)/2.

X3=((XHI - X(IDIM))*T1 + X(IDIM) + XHI)/2.

AREA3=(WA*(PK(B, X1)+PK(B, X3)) + WB*PK(B, X2))*(XHI
& -X(IDIM))/2.

C

ARFRC=AREA1/(AREA1+AREA2+AREA3)

```

HITE=B(1)+B(5)
WRITE(1,50) HITE,HTFRC
50 FORMAT(2X,'THE MAX. PEAK HT. IS: ',F8.2,
& /,2X,'THE EDGE IS AT: ',F8.2,' % OF THE PEAK MAX HT')
WRITE(1,60) AREA1, ARFRC
60 FORMAT(2X,'THE AREA STUDIED: ',F8.3,' DEG 2THETA*C/S',
& /,2X,'WHICH IS: ',F8.2,' % OF THE TOTAL AREA')
C
RETURN
END
C
FUNCTION PK(B,ANGL)
DIMENSION B(8)
DELX = ANGLE -B(3)
U=B(8)
IF(ANGL.GT.B(3)) U=1.
F1=B(1)/(1.+U*B(2)*DELX**2)**B(4)
F2=B(5)*EXP(-U*B(6)*DELX**2)**B(7)
PK=F1+F2
RETURN
END

```

12.12.10 Subroutine NEWPK

```

FTN4
      SUBROUTINE NEWPK(B,NPAR,IDIM,RINTN,IANG,RINT,IOUT)
C
C      SUBROUTINE TO GENERATE A PEAK IN REAL SPACE FROM A
C      SET OF PARAMETERS, B, AND PRINT OUT A COMPARISON
C      OF THE NEW PEAK WITH THE INPUT PEAK
C
      DIMENSION B(12),RINTN(IDIM),IANG(IDIM),RINT(IDIM)
      COMMON X(500)
      CALL FUNC(NPAR,B,IDIM,RINTN,FV)
C
      WRITE(1,40)
40  FORMAT('ENTER "1" TO LIST THE CAUCHY FIT PEAK')
      READ(1,*) ILIST
      IF(ILIST.NE.1) GO TO 100
      WRITE(IOUT,50)
50  FORMAT('/', 'PEAK COMPARISON' /, 5X, 'ANGLE', 3X, 'OLD PEAK', 3X,
      & 'NEW ANGLE', 3X, 'NEW PEAK')
      DO 70 K=1, IDIM
      ANG=FLOAT(IANG(K))/100.
      WRITE(IOUT,60) ANG,RINT(K),X(K),RINTN(K)
60  FORMAT(3X,4(5X,F8.2))
70  CONTINUE
100 RETURN
      END

```

12.12.11 Subroutine DETLO

FTN4

```

SUBROUTINE DETLO(MINAN,MAXAN,IOUT,B,A,JPLLO)
DIMENSION B(16)

```

```

C
C   Subroutine to determine the lower limit of detectability of
C   column length of an X-ray diffraction profile
C

```

```

C   KEY VARIABLES

```

```

C   A-The Fourier distance (nm) corresponding to the range
C   MAXAN-MINAN (degree 2*theta*100)
C   ASTUDY= A distance corresponding to the lower limit of
C   detectability for the sample in question
C   This is determined by the point in the profile
C   where the profile height is 1% of the maximum
C   or 0.45 c/s, whichever is greatest

```

```

RLAM=0.1542

```

```

RAD=3.1415926/180.

```

```

ANMIN=RAD*FLOAT(MINAN)/(100.*2.)

```

```

ANMAX=RAD*FLOAT(MAXAN)/(100.*2.)

```

```

A=(RLAM/2.)/(SIN(ANMAX)-SIN(ANMIN))

```

```

YLIM=AMAX1(0.45,0.01*(B(1)+B(5)))

```

```

XHI=B(3)+SQRT(((B(1)/YLIM)**(1./B(4))-1.)/B(2))

```

```

XLO=B(3)-SQRT(((B(1)/YLIM)**(1./B(4))-1.)/(B(2)*B(8)))

```

```

ANXLO=XLO*RAD/2.

```

```

ANXHI=XHI*RAD/2.

```

```

ASTUDY=(RLAM/2.)/(SIN(ANXHI)-SIN(ANXLO))

```

```

JPLLO=MAX0(5,IFIX(ASTUDY/A + 0.5)+2)

```

```

PSMIN=AMAX1(3.5*A,ASTUDY)

```

```

WRITE(IOUT,10) PSMIN

```

```

10 FORMAT(/,2X,'LOWER LIMIT OF DETECTABILITY',/,2X,
& '(INCLUDING BASELINE ERRORS) FOR FIT FUNCTION= ',F8.4,' NM')
RETURN
END

```

12.12.12 Subroutine VOLDF

FTN4

SUBROUTINE VOLDF(FR,NFOR,VDF,PS,NVDF,AREAL,IOUT,A,JP1LO)

SUBROUTINE TO DETERMINE VOLUME WEIGHTED LENGTH DISTRIBUTION
FUNCTION, BY
$$PV(L) = J/CV * d^{**2}(Fr)/dJ^{**2}$$

WHERE $L=A^*J$

$$\text{LAMBDA} = 2 * \text{A} * (\text{SIN}(\text{THETAMAX}) - \text{SIN}(\text{THETAMIN}))$$

```
DOUBLE PRECISION FR(NFOR),SUM1,SUM2
```

DIMENSION VDF(250),PS(250)

```
WRITE(1,10)
```

```
10  FORMAT('ENTER "1" TO LIST THE VOLUME WEIGHTED DIST. FUNCTION')
```

```
READ(1,*) ILIST
```

```
IF(ILIST.NE.1) GO TO 100
```

RLAM=0.1542

RAD=3.1415926/180.

```
WRITE(IOUT,20)
```

```
20  FORMAT(/,5X,'VOLUME WEIGHTED DISTRIBUTION FUNCTION',/,2X,  
    & 'FOURIER FREQUENCY   LENGTH           DISTRIBUTION FUNCTION',/,2X  
    & '                      (NM)           ')
```

SUM1=0.

SUM2=0.

```
NVDF=MINO(NFOR-1, IFIX(50./A)+1)
```

```
DO 30 I=1,NVDF
```

$$PS(I) = 0.$$
$$VDF(I) = 0.$$

30 CONTINUE

DO 35 JP1=2,JP1LO

$$PS(JP1) = (FLOAT(JP1-1) - 0.5) * A$$

35 CONTINUE

DO 40 JP1=JP1LO,NVDF

J=JP1-1

FACT=(FLOAT(J)-0.5)

$$PS(JP1) = (FLOAT(J) - 0.5) * A$$
$$VDF(JP1)=(FR(JP1-2)-FR(JP1-1)-FR(JP1)+FR(JP1+1))*FACT/2.$$

```

SUM1=SUM1+PS(JP1)*VDF(JP1)

```

```
SUM2=SUM2+VDF(JP1)
```

40 CONTINUE

$$PSAV = SUM1 / SUM2$$

DO 60 JP1=1,NVDF

J=JP1-1

$$VDF(JP1)=VDF(JP1)/(SUM2*A)$$

```
      WRITE(IOUT,50) J,PS(JP1),VDF(JP1)
50   FORMAT(5X,I5,10X,F10.3,5X,F10.7)
60 CONTINUE
      WRITE(IOUT,70) PSAV
70   FORMAT(//,2X,'THE AVERAGE PARTICLE SIZE IS: ',F10.2,' NM')
100 RETURN
      END
```

12.12.13 Subroutine ARADF

FTN4

SUBROUTINE ARADF(FR,NFOR,ADF,PS,NADF,AREAL,IOUT,A,JP1LO)

C

C

C

ROUTINE TO DETERMINE THE AREA WEIGHTED LENGTH
DISTRIBUTION FUNCTION BY

C

 $PA(L) = 1/CA * d^{**2}(Fr)/dJ^{**2}$

C

WHERE $L = A * J$

DOUBLE PRECISION FR(NFOR),SUM1,SUM2

DIMENSION ADF(250),PS(250)

C

C

ROUTINE TO DETERMINE THE AREA WEIGHTED LENGTH DISTRIBUTION
FUNCTION FROM THE REAL FOURIER COEFFICIENTS, FR(JP1)

C

C

KEY VARIABLES:

C

A=The Fourier distance, nm

C

PS(JP1)= A length given by: $PS(JP1) = (JP1 - 1.5) * A$

C

ADF(JP1)= The area weighted distribution function
normalized to $\text{sum}(ADF) = 1.0$

C

C

WRITE(1,10)

10 FORMAT('ENTER "1" TO LIST THE AREA WEIGHTED DIST. FUNCTION')

READ(1,*) ILIST

IF(ILIST.NE.1) GO TO 100

C

RLAM=0.1542

RAD=3.1415926/180.

WRITE(IOUT,20)

20 FORMAT(/,5X,'AREA WEIGHTED DISTRIBUTION FUNCTION',/,2X,
& 'FOURIER FREQUENCY LENGTH DISTRIBUTION FUNCTION',/,2X
& ' (NM) ')

C

SUM1=0.

SUM2=0.

NADF=MIN0(NFOR-1,IFIX(50./A)+1)

DO 30 I=1,NADF

PS(I)=0.

ADF(I)=0.

30 CONTINUE

C

DO 35 JP1=2,JP1LO

PS(JP1)=(FLOAT(JP1)-0.5)*A

35 CONTINUE

C

DO 40 JP1=JP1LO,NADF

J=JP1-1

PS(JP1)=(FLOAT(J)-0.5)*A

ADF(JP1)=(FR(JP1-2)-FR(JP1-1)-FR(JP1)+FR(JP1+1))/2.

```
      SUM1=SUM1+PS(JP1)*ADF(JP1)
      SUM2=SUM2+ADF(JP1)
40  CONTINUE
C
      PSAV=SUM1/SUM2
C
      DO 60 JP1=1,NADF
        J=JP1-1
        ADF(JP1)=ADF(JP1)/(SUM2*A)
        WRITE(IOUT,50) J,PS(JP1),ADF(JP1)
50    FORMAT(5X,I5,10X,F10.3,5X,F10.7)
60  CONTINUE
      WRITE(IOUT,70) PSAV
70    FORMAT(//,2X,'THE AREA AVERAGE LENGTH IS: ',F10.2,' NM')
100 RETURN
      END
```


12.12.14 Subroutine SAVE1

FTN4

SUBROUTINE SAVE1(NFOR,A,B,NAME1,MINAN,MAXAN,PARA)

C

C

ROUTINE TO STORE FOURIER COEFFICIENTS, A AND B INTO A FILE

C

DIMENSION NAME2(5),IBUF(90),IDCB1(144),ISIZE(2)

DOUBLE PRECISION A(NFOR),B(NFOR)

DIMENSION NAME1(5),PARA(16)

DATA NAME2/2H00,2H00,2H00,2HJU,135/,ISIZE/40,10/

WRITE(1,10)

10 FORMAT(/,'ENTER "1" TO SAVE THE FOURIER COEFFICIENTS IN A FILE')

READ(1,*) ISAVE

IF(ISAVE.LE.0) GO TO 100

WRITE(1,20)

20 FORMAT(/,'ENTER THE (6 CHAR) FILENAME FOR THE DATA')

READ(1,30) (NAME2(I),I=1,3)

30 FORMAT(3A2)

WRITE(1,40) (NAME2(I),I=1,5)

40 FORMAT(/,'DATA WILL BE STORED IN FILE: ',3A2,':',A2,':',I3)

CALL CREAT(IDCB1,IERR,NAME2,ISIZE,3,NAME2(4),NAME2(5))

IF(IERR.LT.0) GO TO 90

C

C

50 DO 70 JP1=1,NFOR

J=JP1-1

DO 55 I=1,32

55 IBUF(I)=2H

CALL CODE

WRITE(IBUF,60)J,A(JP1),B(JP1)

60 FORMAT(2X,I3,4X,1PE12.5,4X,1PE12.5)

CALL WRITF(IDCB1,IERR,IBUF,32)

IF(IERR.LT.0) GO TO 90

70 CONTINUE

DO 75 I=1,80

75 IBUF(I)=2H

CALL CODE

WRITE(IBUF,80) (PARA(I),I=1,8)

80 FORMAT(1X,8(F10.5,','))

CALL WRITF(IDCB1,IERR,IBUF,90)

IF(IERR.LT.0) GO TO 90

DO 41 I=1,32

41 IBUF(I)=2H

CALL CODE

WRITE(IBUF,42)

42 FORMAT(5X,'FOURIER COEFFICIENTS')

CALL WRITF(IDCB1,IERR,IBUF,32)

C

DO 43 I=1,32

43 IBUF(I)=2H

```
      CALL CODE
      WRITE(IBUF,44) (NAME1(I),I=1,3)
44  FORMAT('FILE: ',3A2)
      CALL WRITF(IDCBI,IERR,IBUF,32)
C
      DO 45 I=1,32
45  IBUF(I)=2H
      CALL CODE
      WRITE(IBUF,46) MINAN,MAXAN
46  FORMAT('ANGLE (2*THETA):',I5,' TO ',I5)
      CALL WRITF(IDCBI,IERR,IBUF,32)
C
C
      CALL CLOSE(IDCBI,IERR)
      IF(IERR.GE.0) GO TO 100
90  WRITE(1,95) IERR
95  FORMAT(/,5X,'TROUBLE IN FMP CALL, ROUTINE SAVE. IERR=',I5)
100 RETURN
      END
```

12.12.15 Subroutine NEWX

```
FTN4
SUBROUTINE NEWX(B, IDIM, WIDTH)
C
C   SUBROUTINE TO DETERMINE NEW VALUES OF X ACROSS
C   A WIDTH
C
  DIMENSION B(6)
  COMMON X(500)
  X(1)=B(3)-WIDTH/2.
  XDEL=WIDTH/FLOAT(IDIM-1)
  DO 20 K=2, IDIM
    X(K)=X(K-1)+XDEL
20 CONTINUE
  RETURN
  END
```

12.12.16 Subroutine FIT

```

FTN4
      SUBROUTINE FIT(IDIM,NPAR,B,BMIN,BMAX,Y,IOUT)
C      MAIN LINE PROGRAM FOR SUBROUTINE BSOLVE
C      WRITTEN BY W.BALL MODIFIED FOR XPROF BY W.C.S. PICK
C
C      DESCRIPTION OF USER PARAMETERS
C
C      NN = NUMBER OF DATA POINTS OR NUMBER OF EQUATIONS
C      KK = NUMBER OF UNKNOWN COEFFICIENTS
C      B = VECTOR OF UNKNOWN COEFFICIENTS
C      BMIN = VECTOR OF MINIMUM VALUES OF B
C      BMAX = VECTOR OF MAXIMUM VALUES OF B
C      X = VECTOR OF THE INDEPENDENT VARIABLE DATA POINTS(1)
C      Y = VECTOR OF DEPENDENT VARIABLE
C      PH = LEAST SQUARES OBJECTIVE FUNCTION
C      Z = COMPUTED VALUES OF DEPENDENT VARIABLE
C      BV = CODE VECTOR: 1.0 FOR NUMERICAL DERIVATIVES
C
C (1) THIS PROGRAM IS CURRENTLY SET UP FOR ONE INDEPENDENT VARIABLE
C
C      DESCRIPTION OF OUTPUT PARAMETERS
C
C      ICON = THE NUMBER OF COEFFICIENTS NOT SATISFYING THE CONVERGENCE
C             CRITERION
C      B = THE FINAL VALUE OF THE REGRESSION COEFFICIENTS
C      YCAL = THE VALUE OF THE DEPENDENT VARIABLE CALCULATED FROM THE REGRESSION
C             COEFFICIENTS
C
C      DIMENSION P(2000),A(16,18),AC(16,18),FV(16),DV(16)
C      DIMENSION B(16),Z(250),Y(IDIM),BV(16),BMIN(16),BMAX(16)
C      COMMON X(500)
C      EXTERNAL FUNC
C      NI = 1
C      NO = 1
C      READ IN NUMBER OF DATA POINTS, UNKNOWNNS.
C      READ (NI,*) NN, KK
C      NN=IDIM
C      KK=NPAR
C011  FORMAT (8I10)
C      READ IN INITIAL GUESSES.
C      READ (NI,*) (B(J), J=1, KK)
C12  FORMAT(8E10.3)
C      READ IN LIMITS ON VARIABLES.
C      READ (NI,*) (BMIN(J), J=1, KK)
C      READ (NI,*) (BMAX(J), J=1, KK)
C      READ IN INDEPENDENT VARIABLES.
C      READ IN DEPENDENT VARIABLES.
C      READ (NI,*) (X(I), I=1, NN)
C      READ (NI,*) (Y(I), I=1, NN)

```

```

C 847 FORMAT(10F8.6)
C 851 FORMAT(10F8.4)
      FNU=0.0
      FLA=0.0
      TAU=0.0
      EPS=0.0
      PHMIN=0.0
      I=0
      KD=KK
      FV(1)=0.0
      DO 100 J=1, KK
        BV(J)=1
100  CONTINUE
      ICON=KK
      ITER = 0
      WRITE (IOUT,015)
015  FORMAT (1H1,10X,27HBSOLVE REGRESSION ALGORITHM )
C      WRITE(NO,018)
C18  FORMAT(' ',//,' RAW DATA ',//,12X,'X',14X,' Y ')
C      DO 701 J=1, NN
C701  WRITE(NO,017)X(J),Y(J)
      WRITE(NO,016)
016  FORMAT(' ',//,' INITIAL GUESSES    UPPER LIMITS    LOWER LIMITS
1')
      DO 700 J=1, KK
700  WRITE(NO,017)B(J),BMAX(J),BMIN(J)
017  FORMAT(3E17.3)
1050 DO 1099 ICONT=1,10
200  CALL BSOLVE(KK,B,NN,Z,Y,PH,FNU,FLA,TAU,EPS,PHMIN,I,ICON,FV,DV,BV,
      LBMIN,BMAX,P,DERIV,KD,A,AC,GAMM)
      ITER=ITER+1
      WRITE (NO,001) ICON, PH, ITER
001  FORMAT (/ ,2X,6HICON = ,I3,4X, 5HPH = ,E15.8,4X,
1 16HITERATION NO. = ,I3)
      IF (ICON) 10, 300, 1099
10  IF (ICON+1) 20, 60, 1099
20  IF (ICON+2) 30, 70, 1099
30  IF (ICON+3) 40, 80, 1099
40  IF (ICON+4) 50, 90, 1099
50  GO TO 95
1099 CONTINUE
      DO 1100 J=1, KK
1100 WRITE(1,018)J, B(J)
018  FORMAT(2X,I5,1PE15.8)
      WRITE(1,1110)
1110 FORMAT('ENTER "1" TO STOP ITERATIONS')
      READ(1,*) ISTOP
      IF(ISTOP.EQ.1) GO TO 1000
      GO TO 1050
60  WRITE (NO,004)
004  FORMAT (//,2X,32HNO FUNCTION IMPROVEMENT POSSIBLE )
      GO TO 300
70  WRITE (NO,005)
005  FORMAT (//,2X, 28HMORE UNKNOWNNS THAN FUNCTIONS)

```

```

      GO TO 300
80  WRITE (NO,006)
006  FORMAT (//,2X, 24HTOTAL VARIABLES ARE ZERO)
      GO TO 300
90  WRITE (NO,007)
007  FORMAT (//,2X,79HCORRECTIONS SATISFY CONVERGENCE REQUIREMENTS BUT
      LLAMDA FACTOR (FLA) STILL LARGE)
      GO TO 300
95  WRITE (NO,008)
008  FORMAT (//,2X, 20HTHIS IS NOT POSSIBLE)
      GO TO 300
300  WRITE (IOUT,002)
002  FORMAT (//,2X, 26HSOLUTIONS OF THE EQUATIONS)
      DO 400 J=1,KK
      WRITE (IOUT,003) J, B(J)
003  FORMAT (/,2X, 2HB(,I2,4H) = ,E16.8)
400  CONTINUE
C    WRITE(NO,65)
C65  FORMAT(//,9X, '      X      Y      YCAL'//)
      SUM2=0.0
      DO 63 IE=1,NN
      SUM2=SUM2+(Y(IE)-Z(IE))**2
C    WRITE(NO,66) IE,X(IE),Y(IE),Z(IE)
C66  FORMAT(5X,I2,3E12.4).
63  CONTINUE
      WRITE(NO,67)SUM2
67  FORMAT(//,'THE LEAST SQUARES OBJECTIVE FUNCTION = ',E16.6,//)
1000 RETURN
      END

```

12.12.17 Subroutine BSOLV

FTN4

```

SUBROUTINE BSOLVE (KK, B, NN, Z, Y, PH, FNU, FLA, TAU, EPS,
1      PHMIN, I, ICON, FV, DV, BV, BMIN, BMAX, P,
2      FUNC, DERIV, KD, A, AC, GAMM)
  DIMENSION B(10),Z(50),Y(50),BV(10),BMIN(10),BMAX(10)
  DIMENSION P(100),A(10,10),AC(10,10),X(25),FV(10),DV(10)
  K = KK
  N = NN
  KP1 = K + 1
  KP2 = KP1 + 1
  KBI1 = K*N
  KBI2 = KBI1 + K
  KZI = KBI2 + K
  IF( FNU .LE. 0. ) FNU = 10.0
  IF( FLA .LE. 0. ) FLA = 0.01
  IF( TAU .LE. 0. ) TAU = 0.001
  IF( EPS .LE. 0. ) EPS = 0.00002
  IF(PHMIN.LE.0.) PHMIN=0.
120  KE=0
130  DO 160 I1=1,K
160  IF( BV(I1) .NE. 0. ) KE = KE + 1
      IF( KE .GT. 0 ) GO TO 170
162  ICON = -3
163  GO TO 2120
170  IF( N .GE. KE ) GO TO 500
180  ICON= -2
190  GO TO 2120
500  I1 = 1
530  IF( I .GT. 0 ) GO TO 1530
550  DO 560 J1=1,K
      J2 = KBI1 + J1
      P(J2) = B(J1)
      J3 = KBI2 + J1
560  P(J3) = ABS(B(J1)) + 1.0E-02
      GO TO 1030
590  IF (PHMIN .GT. PH .AND. I .GT. 1) GO TO 625
      DO 620 J1=1,K
          N1 = (J1-1)*N
          IF( BV(J1) ) 601,605,605
601  CALL DERIV (Z, Y, Z, P(N1), FV, DV, J1, JTEST)
          IF( JTEST .NE. (-1) ) GO TO 620
          BV(J1) = 1.0
605  DO 606 J2=1,K
          J3 = KBI1 + J2
606  P(J3) = B(J2)
          J3 = KBI1 + J1
          J4 = KBI2 + J1
          DEN = 0.001*AMAX1(P(J4),ABS(P(J3)))
          IF (P(J3) + DEN .LE. BMAX(J1)) GO TO 55

```

```

        P(J3) = P(J3) - DEN
        DEN = - DEN
55  P(J3) = P(J3) + DEN
    GO TO 56
56  CALL FUNC      (K, P(KBI1+1), N, P(N1+1), FV)
    DO 610 J2=1,N
        JB = J2 + N1
    610 P(JB) = (P(JB) - Z(J2))/DEN
    620 CONTINUE
C   SET UP CORRECTION EQUATIONS
    625 DO 725 J1=1,K
        N1 = (J1-1)*N
        A(J1,KP1) = 0.
        IF( BV(J1) ) 630,692,630
    630 DO 640 J2=1,N
        N2 = N1 + J2
    640 A(J1,KP1) = A(J1,KP1) + P(N2)*(Y(J2)-Z(J2))
    650 DO 680 J2=1,K
    660 A(J1,J2)=0.
    665 N2 = (J2-1)*N
    670 DO 680 J3=1,N
    672 N3 = N1 + J3
    674 N4 = N2 + J3
    680 A(J1,J2)=A(J1,J2) + P(N3)*P(N4)
        IF(A(J1,J1).GT.1.E-20) GO TO 725
    692 DO 694 J2=1,KP1
    694  A(J1,J2) = 0.
    695  A(J1,J1) = 1.0
    725  CONTINUE
        GN = 0.
        DO 729 J1=1,K
    729  GN = GN + A(J1,KP1)**2
C   SCALE CORRECTION EQUATIONS
    DO 726 J1=1,K
    726  A(J1,KP2) = SQRT(A(J1,J1))
        DO 727 J1=1,K
        A(J1,KP1) = A(J1,KP1)/A(J1,KP2)
        DO 727 J2=1,K
    727  A(J1,J2) = A(J1,J2)/(A(J1,KP2)*A(J2,KP2))
    730  FL=FLA/FNU
        GO TO 810
    800  FL = FNU*FL
    810  DO 840 J1=1,K
    820  DO 830 J2=1,KP1
    830  AC(J1,J2)= A(J1,J2)
    840  AC(J1,J1)=AC(J1,J1) + FL
C   SOLVE CORRECTION EQUATIONS
    DO 930 L1=1,K
        L2=L1+1
        DO 910 L3=L2,KP1
    910  AC(L1,L3)=AC(L1,L3)/AC(L1,L1)
        DO 930 L3=1,K
        IF(L1-L3)920,930,920
    920  DO 925 L4=L2,KP1

```



```

925 AC(L3,L4)=AC(L3,L4)-AC(L1,L4)*AC(L3,L1)
930 CONTINUE
    DN = 0.
    DG = 0.
    DO 1028 J1=1,K
    AC(J1,KP2) = AC(J1,KP1)/A(J1,KP2)
    J2 = KBI1 + J1
    P(J2) = AMAX1(BMIN(J1),AMIN1(BMAX(J1),B(J1)+AC(J1,KP2)))
        DG = DG + AC(J1,KP2) * A(J1,KP1) * A(J1,KP2)
    DN = DN + AC(J1,KP2)*AC(J1,KP2)
1028 AC(J1,KP2)=P(J2)-B(J1)
    COSG = DG/SQRT (DN*GN)
    JGAM = 0
    IF( COSG ) 1100,1110,1110
1100 JGAM = 2
    COSG = - COSG
1110 CONTINUE
        COSG = AMIN1(COSG, 1.0)
    GAMM= ARCOS(COSG)*180./(3.14159265)
    IF( JGAM .GT. 0 ) GAMM = 180. - GAMM
1030 CALL FUNC      (K, P(KBI1+1), N, P(KZI+1), FV)
1500 PHI = 0.
    DO 1520 J1=1,N
    J2 = KZI + J1
1520 PHI=PHI+(P(J2)-Y(J1))**2
    IF(PHI.LT. 1.E-10) GO TO 3000
    IF( I .GT. 0 ) GO TO 1540
1521 ICON = K
    GO TO 2110
1540 IF( PHI .GE. PH ) GO TO 1530
C   EPSILON TEST
1200 ICON = 0
    DO 1220 J1=1,K
    J2=KBI1+J1
1220 IF( ABS(AC(J1,KP2))/(TAU + ABS(P(J2))) .GT. EPS ) ICON = ICON + 1
    IF( ICON .EQ. 0 ) GO TO 1400
C   GAMMA LAMBDA TEST
    IF (FL .GT. 1.0 .AND. GAMM .GT. 90.0) ICON = -1
    GO TO 2105
C   GAMMA EPSILON TEST
1400 IF (FL .GT. 1.0 .AND. GAMM .LE. 45.0) ICON = -4
    GO TO 2105
1530 IF( I1 - 2 ) 1531,1531,2310
1531 I1 = I1 + 1
    GO TO (530,590,800),I1
2310 IF( FL .LT. 1.0E+8 ) GO TO 800
1320 ICON = -1
2105 FLA = FL
    DO 2091 J2=1,K
    J3 = KBI1 + J2
2091 B(J2) = P(J3)
2110 DO 2050 J2=1,N
    J3 = KZI + J2
2050 Z(J2) = P(J3)

```

```
      PH = PHI
      I = I + 1
2120 RETURN
3000 ICON=0
      GO TO 2105
      END
      FUNCTION ARCOS(Z)
      X=Z
      KEY=0
      IF( X.LT. (-1.)) X=-1.
      IF( X.GT. 1.) X=1.
      IF( X.GE. (-1.) .AND. X .LT. 0.) KEY=1
      IF( X.LT. 0.) X=ABS(X)
      IF( X.EQ. 0.) GO TO 10
      ARCOS=ATAN (SQRT(1.-X*X)/X)
      IF( KEY .EQ. 1) ARCOS=3.14159265-ARCOS
      GO TO 999
10  ARCOS=1.5707963
999 RETURN
      END
```

12.12.18 Subroutine FUNC

FTN4

```

SUBROUTINE FUNC(KK,B,NN,Z,FV)
C
C ROUTINE TO DETERMINE THE FUNCTION VALUE FOR A GIVEN
C SET OF INPUT PARAMETERS, B, AND VALUES OF X
C
C X IN DEGREES 2*THETA
C
C IF X(500) ,< 0 , THEN DO NOT APPLY K-ALPHA DOUBLET CORRECTION
C OTHERWISE CONSIDER K-ALPHA K-ALPHA2 BROADENING
C
C DIMENSION Z(NN),B(KK),DELTH(2)
C DOUBLE PRECISION RLAM1, RLAM2,RL1,RL2,THETA1,THETA2,D(2)
C COMMON X(500)
C RLAM1=1.540562
C RLAM2=1.544390
C RAD=0.0174533
C DO 10 J=1,2
C   D(J)=RLAM1/(2.*SIN(B(8*(J-1)+3)* RAD/2.))
C   RL1=0.5*RLAM1/D(J)
C   RL2=0.5*RLAM2/D(J)
C   THETA1=DATAN(RL1/DSQRT(1.-RL1**2))
C   THETA2=DATAN(RL2/DSQRT(1.-RL2**2))
C   DELTH(J)=2.*(THETA2-THETA1)/RAD
C   IF(X(500).LT.0) DELTH(J)=0.
10 CONTINUE
DO 100 N=1,NN
Z(N)=0.
DO 50 K=1,KK,8
J=(K+7)/8
U=B(K+7)
IF(X(N).GT.B(K+2)) U=1.
DELX=X(N)-B(K+2)
P1=0.66667*B(K)/(1.+U*B(K+1)*DELX**2)**B(K+3)
P2=0.66667*B(K+4)*(EXP(-U*B(K+5)*DELX**2))**B(K+6)
DELX=DELX-DELTH(J)
P3=0.33333*B(K)/(1.+U*B(K+1)*DELX**2)**B(K+3)
P4=0.33333*B(K+4)*(EXP(-U*B(K+5)*DELX**2))**B(K+6)
Z(N)=Z(N)+P1+P2+P3+P4
50 CONTINUE
100 CONTINUE
RETURN
END

```

12.12.19 Subroutine DIST

FTN4

SUBROUTINE DIST(IANG,RINT,IDIM)

C

C

CHANGE ANGLE TO INTERPLANAR DISTANCE BY:

C

 $X=1/D=2*\sin(\text{THETA})/\text{LAMBDA}$

C

LAMBDA=1.5418 ANGSTROM

C

IANG=100*2*THETA

C

THIS ROUTINE ALSO PERFORMS APPROXIMATE ANGULAR CORRECTIONS
ON THE INTENSITY OF SUBTRACTED PROFILES

C

C

LET APPARENT INTENSITY=PURE INTENSITY*K(THETA)

C

WHERE K(THETA)=LORENZ-POLARIZATION *TEMP *SCATTERING FACTORS

C

C

TEMPORARY CHANGE 1983-03-03

C

X(K)=ANGLE (in Degrees 2*Theta)

C

DIMENSION IANG(IDIM),RINT(IDIM)

COMMON X(500)

RLAM=1.5418

RINMX=0.0

XINMX=0.0

XHAF=0.0

WRITE(1,10)

10 FORMAT('ENTER "1" TO APPLY ANGLE CORRECTION')

READ(1,*) ICOR

IF(ICOR.NE.1) GO TO 75

C

C

CORRECT INTENSITY

C

C

CALCULATE THE TEMPERATURE FACTOR CONSTANTS

C

ASSUMING CUBIC CRYSTALS OF PT-IR ALLOY

C

VALUES OF PHI FROM LINEAR APPROXIMATION OF

C

Cullity, Appendix 15.

C

ITEMP=0

TDEBY=257.5

TEMP=293.

X1=TDEBY/TEMP

IF(X1.LT.0.7.OR.X1.GT.1.0) GO TO 15

PHI=0.839-(X1-0.7)*0.203

A=77.5

RM1=1.15E4*TEMP/(TDEBY*TDEBY*A)*(PHI+X1/4.)

GO TO 20

15 WRITE(1,16)

16 FORMAT('***ERROR-TEMPERATURE EXCEEDS RANGE FOR TEMPERATURE'
1, ' FACTOR INTERPOLATION-- TEMP FACTOR SET=1.0')

ITEMP=1

RM1=0.

```

20 DO 50 K=1, IDIM
    TWOTH=(3.141592/180.)*FLOAT(IANG(K))/100.
    THETA=TWOTH/2.
C
C    CALCULATE THE RECIPROCAL INTERPLANAR DISTANCES, X
C
    X(K)=2.*SIN(THETA)/RLAM
C
C    CALCULATE THE LORENZ-POLARIZATION FACTOR
C
    RLPF=(1.0+(COS(TWOTH))**2)/(SIN(THETA)*SIN(THETA)*COS(THETA))
C
C    CALCULATE THE TEMPERATURE FACTOR
C
    TF=EXP(-2.*RM1*(X(K)/2.))**2)
    IF(ITEMP.EQ.1) TF=1.0
    RINT(K)=RINT(K)/(RLPF*TF)
C
C    CALCULATE THE SCATTERING FACTOR
C
    F=77.01-34.8*X(K)
    IF(X(K).GE.0.38.AND.X(K).LE.1.0) GO TO 40
30 WRITE(1,31)
31 FORMAT('**WARNING-RECIPROCAL LATTICE SPACING OUT OF'
1    , ' RANGE-')
40 RINT(K)=RINT(K)/(F*F)
C
C    RESCALE THE PEAK (ARBITRARILY BY 50000*)
C
    RINT(K)=RINT(K)*5.E4
C
    RINMX=AMAX1(RINMX, RINT(K))
C
    IF(RINMX.EQ.RINT(K)) XINMX=X(K)
C
    RIHAF=RINMX/2.
C
    IF(RINT(K).LE.RIHAF.AND.RINT(K-1).GE.RIHAF)
C
1    XHAF=X(K)
    X(K)=FLOAT(IANG(K))/100.
50 CONTINUE
C
C    LIST THE CORRECTED PEAK IF DESIRED
C
    WRITE(1,60)
60 FORMAT('ENTER "1" FOR A LIST OF THE CORRECTED PEAK')
    READ(1,*) ILIST
    IF(ILIST.NE.1) GO TO 81
    DO 70 K=1, IDIM
        WRITE(1,65) IANG(K), RINT(K)
65    FORMAT(2X, I5, 2X, F8.4)
70 CONTINUE
    GO TO 81
C
C    GENERATE THE RECIPROCAL SPACINGS IF NO CORRECTION IS REQUESTED
C
75 DO 80 K=1, IDIM
    THETA=(3.141592/180.)*FLOAT(IANG(K))/(100.*2.)

```

```
C      X(K)=2.*SIN(THETA)/RLAM
C      X(K)=FLOAT(IANG(K))/100.
C      RINMX=AMAX1(RINMX,RINT(K))
C      IF(RINMX.EQ.RINT(K)) XINMX=X(K)
C      RIHAF=RINMX/2.
C      IF(RINT(K).LE.RIHAF.AND.RINT(K-1).GE.RIHAF)
C      1  XHAF=X(K)
C      80 CONTINUE
C      81 CONTINUE
C      81 IF(XHAF.GT.1.E-6) GO TO 82
C      XHAF=(X(1)+XINMX)/2.
C      82 WRITE(1,83) RINMX,XINMX,XHAF
C      83 FORMAT(2X,'THE MAXIMUM PEAK HEIGHT IS: ',F8.2,
C      1 /,'AT RECIPROCAL SPACING: ',F8.4,' ANGSTROM**-1',
C      2 /,'THE HALF HEIGHT OF THE PEAK OCCURS AT: ',F8.4)
C      100 RETURN
C      END
```

12.12.20 Subroutine PROF

```

FTN4
SUBROUTINE PROF(HR,HI,GR,GI,FR,FI,NFOR,IOUT)
DOUBLE PRECISION HR(NFOR),HI(NFOR),GR(NFOR),GI(NFOR)
C
C PROGRAM TO DETERMINE THE PURE COEFFICIENTS,F, FROM
C THE OBSERVED COEFFS, H, AND THE MACHINE COEFFS, G
C
DOUBLE PRECISION DEN,FR(NFOR),FI(NFOR)
C
F0=H0/G0
C
DO 20 JP1=1,NFOR
DEN=GR(JP1)*GR(JP1) + GI(JP1)*GI(JP1)
FR(JP1)=(HR(JP1)*GR(JP1) +HI(JP1)*GI(JP1))/DEN
FI(JP1)=(HI(JP1)*GR(JP1) - HR(JP1)*GI(JP1))/DEN
20 CONTINUE
C
WRITE(IOUT,30)
30 FORMAT(/,20X,'** PURE PROFILE FOURIER COEFFICIENTS **',
& /,10X,'J',8X,'FR',8X,'FI',7X,'AMP',/)
DO 50 JP1=1,NFOR
J=JP1-1
AMP=(FR(JP1)*FR(JP1) + FI(JP1)*FI(JP1))**.5
WRITE(IOUT,40) J,FR(JP1),FI(JP1),AMP
40 FORMAT(6X,I5,3(2X,F8.3))
50 CONTINUE
RETURN
END

```

12.12.21 Subroutine ESTB

FTN4

SUBROUTINE ESTB(RINT, IANG, IDIM, NPAR, PARA, PARMN, PARMX)

C

C

C

ESTIMATE THE PARAMETERS FOR THE BEST FIT SAUCHY CURVE

DIMENSION PARA(NPAR), PARMN(NPAR)

DIMENSION RINT(1), IANG(1)

DIMENSION IPAR(2)

COMMON X(500)

C

C

C

C

C

C

C

C

C

C

C

C

C

Estimate the parameters for the best fit Modified
Voigt Profile $F = F_1 + F_2$

where

 $F_1 = \text{PARA}(1) / (1 + \text{PARA}(2) * U * (\text{ANG} - \text{PARA}(3))^{**2})^{**\text{PARA}(4)}$ $F_2 = \text{PARA}(5) * \text{EXP}(-\text{PARA}(6) * U * (\text{ANG} - \text{PARA}(3))^{**2})^{**\text{PARA}(7)}$ $U = 1.0$ if $X < \text{PARA}(3)$ $U = \text{PARA}(8)$ if $X > \text{PARA}(3)$

ASSUME:

 $\text{PARA}(1) = \text{PARA}(5) = (\text{PEAK HT}) / 2.$ $\text{PARA}(4) = \text{PARA}(7) = \text{PARA}(8) = 1.0$

IANHF=0

IANMX=0

NPEAK=NPAR/8

DO 10 I=1,NPAR

PARA(I)=1.

10 CONTINUE

IF(NPAR.GT.8) GO TO 30

DO 20 K=1,IDIM

PARA(1)=AMAX1(PARA(1),RINT(K))

IF(PARA(1).EQ.RINT(K)) IANMX=IANG(K)

RIHAF=PARA(1)/2.

IF(RINT(K).LE.RIHAF.AND.RINT(K-1).GE.RIHAF) IANHF=IANG(K)

20 CONTINUE

IF(IANHF.GT.0) GO TO 22

IANHF=(IANG(1)+IANMX)/2

22 PARA(1)=PARA(1)/2.

PARA(2)=ABS((FLOAT(IANMX-IANHF))/100.)**(-2)

PARA(3)=FLOAT(IANMX)/100.

PARA(5)=PARA(1)

PARA(6)=0.6931/(FLOAT(IANHF-IANMX)/100.)**2

GO TO 110

30 WRITE(1,35) NPEAK

35 FORMAT(/,2X,'THE PROGRAM WILL ATTEMPT TO FIND',I5,' PEAKS',

& /,5X,'ENTER THE INITIAL GUESSES FOR PEAK LOCATION',

& /,10X,'1 - The (111) Peaks of Pt and Ir

& /,10X,'2 - The (200) Peaks of Pt and Ir

& /,10X,'3 - Enter the initial guesses, deg 2*theta')


```

      READ(1,*) IGESS
      IF(IGESS.LT.1.OR.IGESS.GT.3) GO TO 30
      IF(IGESS.GT.2) GO TO 50
      IF(IGESS.GT.1) GO TO 40
      PARA(3)=39.79
      PARA(11)=40.71
      IF(NPEAK.LT.3) GO TO 60
      PARA(11)=40.25
      GO TO 60
40  PARA(3)=46.27
      PARA(11)=47.36
      GO TO 60
50  READ(1,*)(PARA(I),I=3,NPAR,8)
C
60  DO 80 I=1,NPEAK
      IPAR(I)=IFIX(PARA(3+8*(I-1))*100.)
      DO 70 K=1,IDIM
          IF(IPAR(I).GE.IANG(K).AND.IPAR(I).LE.IANG(K+1))
&      PARA(1+8*(I-1))=RINT(K)/2.
70  CONTINUE
      PARA(5+8*(I-1))=PARA(1+8*(I-1))
80  CONTINUE
C
110 DO 120 I=1,NPAR,8
      PARMN(I)=PARA(I)/100.
      PARMX(I)=PARA(I)*5.0
      PARMN(I+1)=0.001
      PARMX(I+1)=1000.
      PARMN(I+2)=PARA(I+2)*0.8
      PARMX(I+2)=PARA(I+2)*1.2
      PARMN(I+3)=0.5
      PARMX(I+3)=20.0
      PARMN(I+4)=PARMN(I)
      PARMX(I+4)=PARMX(I)
      PARMN(I+5)=PARA(I+5)/50.
      PARMX(I+5)=PARA(I+5)*50.
      PARMN(I+6)=0.5
      PARMX(I+6)=20.
      PARMN(I+7)=0.1
      PARMX(I+7)=1.5
120 CONTINUE
C
200 WRITE(1,220)
220  FORMAT('INITIAL GUESSES ARE: ',12X,'GUESS',10X,'MIN',10X,'MAX')
      DO 240 I=1,NPAR
          WRITE(1,230) I,PARA(I),PARMN(I),PARMX(I)
230  FORMAT(3X,I4,3(5X,1PE10.2))
240  CONTINUE
245 WRITE(1,250)
250  FORMAT('ENTER THE PARAMETER TO BE CHANGED')
      READ(1,*) JPAR
      IF(JPAR.LT.1) GO TO 999
      WRITE(1,260) JPAR
260  FORMAT('ENTER THE NEW PARAMETER, MIN, AND MAX FOR NO. ',I5)

```

```
      READ(1,*) PARA(JPAR),PARMN(JPAR),PARMX(JPAR)  
      GO TO 200  
999 RETURN  
      END
```

12.12.22 Subroutine READP

FTN4

SUBROUTINE READP(IDC,NAME,FR,FI,NFOR)

C

C

C

C

C

ROUTINE TO READ IN A SET OF FOURIER COEFFICIENTS FROM
A FILE (COEFS MUST BE STORED IN THE SAME FORMAT AS
GIVEN BY ROUTINE 'SAVE1')

DIMENSION NAME(5),IDCB(144),IBUF(30)

DOUBLE PRECISION FR(NFOR),FI(NFOR)

CALL OPEN (IDCB,IERR,NAME,0,NAME(4),NAME(5))

IF(IERR.LT.0) GO TO 100

KK=0

DO 50 K=1,NFOR

DO 10 I=1,30

IBUF(I)=2H

10 CONTINUE

KK=KK+1

CALL READF(IDC,IERR,IBUF,30,LEN)

IF(IERR.LT.0) GO TO 80

IF(LEN.EQ.-1) GO TO 100

CALL CODE

READ(IBUF,20) FR(KK),FI(KK)

20 FORMAT(9X,1PE12.5,4X,1PE12.5)

50 CONTINUE

55 CONTINUE

GO TO 100

80 WRITE(1,90) IERR

90 FORMAT(/,5X,'TROUBLE IN FMP CALL, ROUTINE READP. IERR= ',I5)

100 RETURN

END

12.12.23 Subroutine NURNG

```

SUBROUTINE NURNG(GR,GI, IDEL1, IDEL2, NFOR, IOUT)
C      ROUTINE TO DEVELOP A SET OF FOURIER COEFFS OVER
C      A BROAD RANGE OF 2THETA FROM A NARROW RANGE OF
C      ANGLES. THE NARROW RANGE IS NECESSARY FOR
C      NARROW PEAKS (EG. MACHINE PROFILES) TO PREVENT
C      ALIASSING. THE BROAD RANGE IS REQUIRED FOR
C      BROAD PEAKS
C      THE RELATIONSHIP IS GIVEN BY KLUG AND ALEXANDER
C
DOUBLE PRECISION GR(NFOR),GI(NFOR)
DIMENSION DUMR(125),DUMI(125)
IRATIO=IDEL1/IDEL2
RATIO=FLOAT(IDEL1)/FLOAT(IDEL2)
IF(ABS(FLOAT(IRATIO)-RATIO).GT.0.05) GO TO 90
C
DO 20 JP1=1,NFOR
  J=JP1-1
  JPP1=J/IRATIO+1
  FRAC=FLOAT(J)/RATIO - J/IRATIO
  DUMR(JP1)=GR(JPP1)+FRAC*(GR(JPP1+1)-GR(JPP1))
  DUMI(JP1)=GI(JPP1)+FRAC*(GI(JPP1+1)-GI(JPP1))
20 CONTINUE
C
WRITE(IOUT,22)
22 FORMAT(/,5X,'MACHINE FOURIER COEFFICIENTS FOR BROAD RANGE',/
& 7X,'J',11X,'GR',13X,'GI')
DO 30 JP1=1,NFOR
  J=JP1-1
  GR(JP1)=DUMR(JP1)/RATIO
  GI(JP1)=DUMI(JP1)/RATIO
  WRITE(IOUT,25) J,GR(JP1),GI(JP1)
25 FORMAT(5X,I5,2(5X,F10.5))
30 CONTINUE
GO TO 100
90 WRITE(1,95)
95 FORMAT('ERROR- IDEL1 IS NOT AN EVEN MULTIPLE OF IDEL2-'
& //5X,'** DO NOT BELIEVE THE PURE PROFILE, FR, AND FI**')
100 RETURN
END

```